

UNCLASSIFIED

|                                                                                                                                                                                                                             |
|-----------------------------------------------------------------------------------------------------------------------------------------------------------------------------------------------------------------------------|
|                                                                                                                                                                                                                             |
|                                                                                                                                                                                                                             |
|                                                                                                                                                                                                                             |
| AD NUMBER                                                                                                                                                                                                                   |
| AD283324                                                                                                                                                                                                                    |
| NEW LIMITATION CHANGE                                                                                                                                                                                                       |
| TO<br>Approved for public release, distribution unlimited                                                                                                                                                                   |
| FROM<br>Distribution authorized to U.S. Gov't. agencies and their contractors; Administrative/Operational Use; JUN 1962. Other requests shall be referred to Aeronautical Systems Division, Wright-Patterson AFB, OH 45433. |
| AUTHORITY                                                                                                                                                                                                                   |
| ASD ltr dtd 6 Apr 1966                                                                                                                                                                                                      |

THIS PAGE IS UNCLASSIFIED

**UNCLASSIFIED**

**AD 283 324**

*Reproduced  
by the*

**ARMED SERVICES TECHNICAL INFORMATION AGENCY  
ARLINGTON HALL STATION  
ARLINGTON 12, VIRGINIA**



**UNCLASSIFIED**

NOTICE: When government or other drawings, specifications or other data are used for any purpose other than in connection with a definitely related government procurement operation, the U. S. Government thereby incurs no responsibility, nor any obligation whatsoever; and the fact that the Government may have formulated, furnished, or in any way supplied the said drawings, specifications, or other data is not to be regarded by implication or otherwise as in any manner licensing the holder or any other person or corporation, or conveying any rights or permission to manufacture, use or sell any patented invention that may in any way be related thereto.

283 324

ASD-TDR-62-572

CATALOGED BY ASTIA  
AD NO. 283324

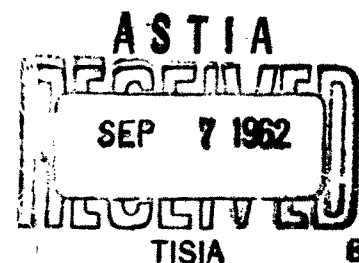
MECHANISMS OF REVERSIBLE AND IRREVERSIBLE LOSS OF  
MECHANICAL PROPERTIES OF ELASTOMERIC VULCANIZATES  
WHICH OCCUR AT ELEVATED TEMPERATURES

TECHNICAL DOCUMENTARY REPORT NO. ASD-TDR-62-572

June 1962

Directorate of Materials and Processes  
Aeronautical Systems Division  
Air Force Systems Command  
Wright-Patterson Air Force Base, Ohio

Project No. 7342, Task No. 734202



Prepared under Contract No. AF 33(616)-8298, SRI Project PRU-3659  
by the Stanford Research Institute, Menlo Park, California  
Thor L. Smith, author

NO OTS

**Best  
Available  
Copy**

## NOTICES

When Government drawings, specifications, or other data are used for any purpose other than in connection with a definitely related Government procurement operation, the United States Government thereby incurs no responsibility nor any obligation whatsoever; and the fact that the Government may have formulated, furnished, or in any way supplied the said drawings, specifications, or other data, is not to be regarded by implication or otherwise as in any manner licensing the holder or any other person or corporation, or conveying any rights or permission to manufacture, use, or sell any patented invention that may in any way be related thereto.

ASTIA release to OTS not authorized.

Qualified requesters may obtain copies of this report from the Armed Services Technical Information Agency, (ASTIA), Arlington Hall Station, Arlington 12, Virginia.

Copies of this report should not be returned to the Aeronautical Systems Division unless return is required by security considerations, contractual obligations, or notice on a specific document.

## FOREWORD

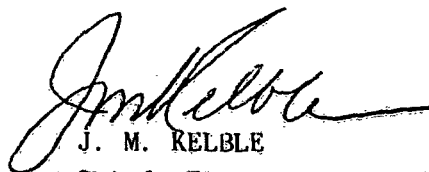
This report was prepared by Stanford Research Institute under USAF Contract No. AF 33(616)-8298. The contract was initiated under Project No. 7342, "Fundamental Research on Macromolecular Materials and Lubrication Phenomena," Task No. 734202, "Studies on the Structure-Property Relationships of Polymeric Materials." The work was administered by the Non-metallic Materials Laboratory, Directorate of Materials and Processes, Deputy Commander/Technology, Aeronautical Systems Division, with Lt. T. J. Dudek as project engineer. This report covers work conducted from 1 May 1961 to 30 April 1962.

The data in this report have resulted from the combined efforts of a large number of people. The author wishes to acknowledge the assistance of those who contributed a significant amount to the work. The stress relaxometer for studies of thermal stability was designed by Fred E. Littman, who also obtained the majority of the stress-relaxation data. The detailed design of the apparatus was made by A. James Aitken. Warren L. Dowler made significant contributions to the design of the high-temperature equipment for the Instron and to the development of the method for preparing and determining the dimensions of the ring-type specimens. He also had primary responsibility for setting up the machine methods for data processing, for checking such procedures, and for general supervision of the machine aspects of data reduction. The detailed design of the high-temperature equipment was ably carried out by John L. Smith. Rodney B. Beyer provided invaluable assistance in analyzing and preparing the Instron data for presentation in this report. A special acknowledgment is made of the contributions of Richard L. Moore, who conscientiously prepared the innumerable ring specimens and tested them with the Instron. In addition, he obtained all test data needed to evaluate the reliability of data obtained by the preparation and testing of ring specimens.

## ABSTRACT

Strength characteristics of five elastomeric gum vulcanizates were investigated over a wide range of evaluation conditions. Results from continuous and intermittent stress-relaxation evaluations made between 100 and 200°C showed that the thermal stabilities of the vulcanizates decrease in the following order: hydrofluorocarbon, resin-cured butyl, silicone, sulfur-cured butyl, and natural rubber. Tensile properties of each vulcanizate in the absence of thermal degradation were determined with an Instron tester at about 10 strain rates and 10 temperatures. Except for natural rubber, the ultimate tensile properties of each vulcanizate could be characterized by a time- and temperature-independent failure envelope which results from a plot of  $\log \sigma_b 273/T$  vs.  $\log \epsilon_b$ , where  $\sigma_b$  is the tensile strength and  $\epsilon_b$  is the ultimate strain. Envelopes for the different vulcanizates are essentially identical in shape; their relative displacements result from difference in degree of crosslinking and probably from differences in their chemical and physical structures. No fundamental differences seem to exist in the strength characteristics of the various vulcanizates provided they are compared in corresponding temperature and physical states. Stress-strain curves for natural rubber were analyzed to separate time and finite-strain effects. At temperatures between -20 and 100°C, the stress-strain data were found unexpectedly to be time independent although they are temperature dependent.

This technical documentary report has been reviewed and is approved.



J. M. KELBLE

Chief, Elastomers and Coatings Branch  
Nonmetallic Materials Laboratory

## CONTENTS

---

|     |                                                                                                |    |
|-----|------------------------------------------------------------------------------------------------|----|
| I   | INTRODUCTION . . . . .                                                                         | 1  |
| II  | BACKGROUND INFORMATION . . . . .                                                               | 3  |
|     | A. Irreversible Changes in Tensile Properties . . . . .                                        | 4  |
|     | B. Ultimate Tensile Properties in the Absence of Degradation Effects . . . . .                 | 5  |
|     | C. Molecular Theories of Rupture . . . . .                                                     | 10 |
|     | D. Special Problems Associated with Understanding Ultimate Tensile Properties . . . . .        | 11 |
| III | IRREVERSIBLE CHANGES IN TENSILE PROPERTIES OF GUM VULCANIZATES (THERMAL STABILITIES) . . . . . | 13 |
|     | A. Discussion of Experimental Method and Results . . . . .                                     | 13 |
|     | 1. Vulcanizate of Natural Rubber . . . . .                                                     | 15 |
|     | 2. Butyl Vulcanizate (Sulfur) . . . . .                                                        | 16 |
|     | 3. Butyl Vulcanizate (Resin) . . . . .                                                         | 17 |
|     | 4. Silicone Vulcanizate . . . . .                                                              | 21 |
|     | 5. Viton B Vulcanizate . . . . .                                                               | 22 |
|     | 6. Stillman Rubber SR-251-70 (Viton A) . . . . .                                               | 23 |
|     | B. Comparison of Stability of Vulcanizates . . . . .                                           | 25 |
| IV  | CONSTANT STRAIN RATE TENSILE PROPERTIES OF GUM VULCANIZATES . . . . .                          | 27 |
|     | A. Experimental Method . . . . .                                                               | 27 |
|     | B. Method for Data Reduction . . . . .                                                         | 29 |
|     | C. Rate and Temperature Dependence of Stress-Strain Curves of Natural Rubber . . . . .         | 30 |
|     | 1. Background Information . . . . .                                                            | 30 |
|     | 2. Results from Analysis of Curves . . . . .                                                   | 33 |
|     | 3. Stress-Temperature Coefficient . . . . .                                                    | 49 |
|     | D. Ultimate Tensile Properties of Vulcanizates Other Than Natural Rubber . . . . .             | 53 |
|     | 1. Failure Envelopes . . . . .                                                                 | 53 |
|     | 2. Time-Temperature Reduction of Ultimate Property Data . . . . .                              | 58 |
|     | E. Ultimate Tensile Properties of Natural Rubber . . . . .                                     | 74 |
|     | 1. Failure Envelope . . . . .                                                                  | 74 |
|     | 2. Temperature and Rate Dependence of Ultimate Properties . . . . .                            | 76 |
|     | F. Comparison of Ultimate Tensile Properties of Vulcanizates . . . . .                         | 77 |
| V   | CONCLUSIONS . . . . .                                                                          | 97 |

CONTENTS

|                     |                                                                                                      |     |
|---------------------|------------------------------------------------------------------------------------------------------|-----|
| <i>APPENDIX I</i>   | COMPOSITION AND CHARACTERISTICS OF GUM VULCANIZATES USED FOR STUDY . . . . .                         | 101 |
|                     | A. Composition and Storage of Vulcanizates . . . . .                                                 | 103 |
|                     | B. Degree of Crosslinking and Percent Sol in Vulcanizates . . . . .                                  | 103 |
|                     | C. Glass Temperatures and Expansion Coefficients of Vulcanizates . . . . .                           | 105 |
| <i>APPENDIX II</i>  | DESCRIPTION OF STRESS RELAXOMETER AND EXPERIMENTAL PROCEDURE . . . . .                               | 115 |
|                     | A. Constant Temperature Air Bath . . . . .                                                           | 117 |
|                     | B. Stress Relaxometer . . . . .                                                                      | 120 |
|                     | C. Experimental Procedure . . . . .                                                                  | 120 |
| <i>APPENDIX III</i> | TEMPERATURE CONTROL EQUIPMENT FOR INSTRON TESTER . . . . .                                           | 125 |
| <i>APPENDIX IV</i>  | PREPARATION AND EVALUATION OF RING-TYPE SPECIMENS FOR OBTAINING TENSILE STRESS-STRAIN DATA . . . . . | 137 |
|                     | A. General Discussion of Testing Method . . . . .                                                    | 139 |
|                     | B. Evaluation of Data Obtained by Testing Ring Specimens . . . . .                                   | 145 |
|                     | 1. Preparation and Dimensions of Rings . . . . .                                                     | 146 |
|                     | 2. Slippage of Rings During Test . . . . .                                                           | 150 |
|                     | 3. Ultimate Tensile Properties . . . . .                                                             | 152 |
|                     | 4. Stress-Strain Values Prior to Rupture . . . . .                                                   | 156 |
|                     | C. Summary Remarks . . . . .                                                                         | 158 |
| <i>APPENDIX V</i>   | TABULATION OF ULTIMATE TENSILE PROPERTIES OF GUM VULCANIZATES . . . . .                              | 159 |
| REFERENCES          | . . . . .                                                                                            | 167 |

## ILLUSTRATIONS

|         |                                                                                                                                                                                         |    |
|---------|-----------------------------------------------------------------------------------------------------------------------------------------------------------------------------------------|----|
| Fig. 1  | Illustrative Example of a Tensile Failure Envelope.<br>Data for a SBR Gum Vulcanizate . . . . .                                                                                         | 9  |
| Fig. 2  | Continuous and Intermittent Stress-Relaxation Results<br>on Natural Rubber Gum Vulcanizate. . . . .                                                                                     | 15 |
| Fig. 3  | Continuous and Intermittent Stress-Relaxation Results on<br>Butyl-Sulfur Gum Vulcanizate (Compare with Fig. 4) . . . . .                                                                | 16 |
| Fig. 4  | Additional Continuous and Intermittent Stress-Relaxation<br>Results on Butyl-Sulfur Gum Vulcanizate (Compare with Fig. 3). . . . .                                                      | 17 |
| Fig. 5  | Continuous Stress-Relaxation Results on Butyl-Resin Gum Vulcanizate. . . . .                                                                                                            | 18 |
| Fig. 6  | Continuous and Intermittent Stress-Relaxation Results on<br>Butyl-Resin Gum Vulcanizate (Compare with Fig. 7). . . . .                                                                  | 19 |
| Fig. 7  | Additional Continuous and Intermittent Stress Relaxation<br>Results on Butyl-Resin Gum Vulcanizate (Compare with Fig. 6) . . . . .                                                      | 21 |
| Fig. 8  | Continuous Stress-Relaxation Results on Silicone Gum<br>Vulcanizate at 200°C . . . . .                                                                                                  | 22 |
| Fig. 9  | Continuous and Intermittent Stress-Relaxation Results on<br>Silicone Gum Vulcanizate . . . . .                                                                                          | 23 |
| Fig. 10 | Continuous and Intermittent Stress-Relaxation Results on<br>Viton B Gum Vulcanizate. . . . .                                                                                            | 24 |
| Fig. 11 | Continuous and Intermittent Stress-Relaxation Results on<br>Stillman Hubber SR-251-70 (Viton A Containing Carbon Black). . . . .                                                        | 24 |
| Fig. 12 | Tensile Stress-Strain Data for Natural Rubber at 100°C Plotted<br>as $\log \sigma_{273/T}$ vs $\log t$ for Various Fixed Values of Strain . . . . .                                     | 34 |
| Fig. 13 | Tensile Stress-Strain Data for Natural Rubber at -20°C Plotted<br>as $\log \sigma_{273/T}$ vs $\log t$ for Various Fixed Values of Strain . . . . .                                     | 36 |
| Fig. 14 | Tensile Stress-Strain Data for Natural Rubber at -45°C Plotted<br>as $\log \sigma_{273/T}$ vs $\log t$ for Various Fixed Values of Strain . . . . .                                     | 37 |
| Fig. 15 | Isochronal Stress-Strain Curves for Natural Rubber at 100° and -45°C . . . . .                                                                                                          | 38 |
| Fig. 16 | Plot of True Stress $\lambda_c \sigma_c$ Against Strain $\epsilon_c$ for Natural Rubber at<br>100°C (Values of Stress and Strain Based on Dimensions of<br>Specimen at 100°C) . . . . . | 40 |
| Fig. 17 | Plot of $\sigma_c$ vs $\lambda_c - \lambda_c^{-2}$ for Natural Rubber at 100°C . . . . .                                                                                                | 41 |
| Fig. 18 | Plot of Stress-Strain Data for Natural Rubber at 100°C<br>to Evaluate the Constants in the Mooney-Rivlin Equation. . . . .                                                              | 42 |
| Fig. 19 | Plots of $\log g(\epsilon)$ vs Temperature for Natural Rubber at<br>Constant Strain Values Between 0.10 and 2.0. . . . .                                                                | 45 |
| Fig. 20 | Plots of $\log g(\epsilon)$ vs Temperature for Natural Rubber at<br>Constant Strain Values Between 3.0 and 6.0 . . . . .                                                                | 46 |
| Fig. 21 | Plots of $\log g(\epsilon)$ vs $\log \lambda$ for Natural Rubber at Different<br>Temperatures Between -45 and 100°C . . . . .                                                           | 47 |

ILLUSTRATIONS

|         |                                                                                                                                          |    |
|---------|------------------------------------------------------------------------------------------------------------------------------------------|----|
| Fig. 22 | Plots to determine Stress-Temperature Coefficient for Natural Rubber at Various Strains . . . . .                                        | 52 |
| Fig. 23 | Failure Envelope for Butyl Gum Vulcanizate (Sulfur) . . . . .                                                                            | 54 |
| Fig. 24 | Failure Envelope for Butyl Gum Vulcanizate (Resin). . . . .                                                                              | 55 |
| Fig. 25 | Failure Envelope for Viton B Gum Vulcanizate. . . . .                                                                                    | 56 |
| Fig. 26 | Failure Envelope for Silicone Gum Vulcanizate . . . . .                                                                                  | 57 |
| Fig. 27 | Temperature Dependence of $\log a_T$ for Butyl Gum Vulcanizate (Sulfur). . . . .                                                         | 60 |
| Fig. 28 | Plot of $\log \sigma_b 273/T$ vs $\log t_b/a_T$ for Butyl Gum Vulcanizate (Sulfur). . . . .                                              | 61 |
| Fig. 29 | Plot of $\log \epsilon_b$ vs $\log t_b/a_T$ for Butyl Gum Vulcanizate (Sulfur). . . . .                                                  | 62 |
| Fig. 30 | Temperature Dependence of $\log a_T$ for Butyl Gum Vulcanizate (Resin) . . . . .                                                         | 64 |
| Fig. 31 | Plot of $\log \sigma_b 273/T$ vs $\log t_b/a_T$ for Butyl Gum Vulcanizate (Resin) . . . . .                                              | 65 |
| Fig. 32 | Plot of $\log \epsilon_b$ vs $\log t_b/a_T$ for Butyl Gum Vulcanizate (Resin) . . . . .                                                  | 66 |
| Fig. 33 | Temperature Dependence of $\log a_T$ for Viton B Gum Vulcanizate . . . . .                                                               | 67 |
| Fig. 34 | Plot of $\log \sigma_b 273/T$ vs $\log t_b/a_T$ for Viton B Gum Vulcanizate . . . . .                                                    | 69 |
| Fig. 35 | Plot of $\log \epsilon_b$ vs $\log t_b/a_T$ for Viton B Gum Vulcanizate . . . . .                                                        | 69 |
| Fig. 36 | Temperature Dependence of $\log a_T$ for Silicone Gum Vulcanizate . . . . .                                                              | 70 |
| Fig. 37 | Plot of $\log a_T$ vs $1/T$ for Silicone Gum Vulcanizate. . . . .                                                                        | 70 |
| Fig. 38 | Plot of $\log \sigma_b 273/T$ vs $\log t_b/a_T$ for Silicone Gum Vulcanizate . . . . .                                                   | 72 |
| Fig. 39 | Plot of $\log \epsilon_b$ vs $\log t_b/a_T$ for Silicone Gum Vulcanizate . . . . .                                                       | 75 |
| Fig. 40 | Ultimate Properties of Natural Rubber Plotted as $\log \sigma_b 273/T$ vs $\log \epsilon_b$ . . . . .                                    | 75 |
| Fig. 41 | Dependence of Tensile Strength of Natural Rubber on Time-to-Break at Temperatures Between 10 and 100°C. . . . .                          | 78 |
| Fig. 42 | Dependence of Tensile Strength of Natural Rubber on Time-to-Break at Temperatures Between -5 and -55°C. . . . .                          | 79 |
| Fig. 43 | Dependence of Ultimate Strain of Natural Rubber on Time-to-Break at Temperatures Between 10 and 100°C. . . . .                           | 80 |
| Fig. 44 | Dependence of Ultimate Strain of Natural Rubber on Time-to-Break at Temperatures Between -5 and -55°C. . . . .                           | 81 |
| Fig. 45 | Dependence of Tensile Strength of Natural Rubber on Temperature at Four Strain Rates Between 0.0102 and 10.2 min <sup>-1</sup> . . . . . | 82 |
| Fig. 46 | Dependence of Ultimate Strain of Natural Rubber on Temperature at Four Strain Rates Between 0.0102 and 10.2 min <sup>-1</sup> . . . . .  | 83 |
| Fig. 47 | Replot of Curves Shown in Fig. 45 . . . . .                                                                                              | 84 |

ILLUSTRATIONS

|      |       |                                                                                                                                         |     |
|------|-------|-----------------------------------------------------------------------------------------------------------------------------------------|-----|
| Fig. | 48    | Replot of Curves Shown in Fig. 46 . . . . .                                                                                             | 85  |
| Fig. | 49    | Comparison of Failure Envelopes for the<br>Five Vulcanizates Studied . . . . .                                                          | 86  |
| Fig. | 50    | Superposition of the Failure Envelopes for<br>the Five Vulcanizates Studied . . . . .                                                   | 88  |
| Fig. | 51    | Double Logarithmic Plot Showing Variation of Tensile Strength<br>with the Equilibrium Modulus for Six Vulcanizates . . . . .            | 90  |
| Fig. | 52    | Linear Plot Showing Variation of Tensile Strength<br>with Equilibrium Modulus for Six Vulcanizates . . . . .                            | 91  |
| Fig. | 53    | Comparison of the Shapes of Curves which Show the<br>Variation of Tensile Strength with Time-to-Break. . . . .                          | 92  |
| Fig. | 54    | Comparison of the Shapes of Curves which Show the<br>Variation of Ultimate Strain with Time-to-Break . . . . .                          | 94  |
| Fig. | I-1   | Temperature Dependence of Specific Volume of<br>Natural Rubber Gum Vulcanizate. . . . .                                                 | 106 |
| Fig. | I-2   | Temperature Dependence of Specific Volume of<br>Viton B Gum Vulcanizate . . . . .                                                       | 107 |
| Fig. | I-3   | Temperature Dependence of Specific Volume of<br>Butyl-Resin Gum Vulcanizate . . . . .                                                   | 108 |
| Fig. | I-4   | Temperature Dependence of Specific Volume of<br>Butyl-Sulfur Gum Vulcanizate. . . . .                                                   | 109 |
| Fig. | I-5   | Temperature Dependence of Specific Volume of<br>Silicone Gum Vulcanizate. . . . .                                                       | 110 |
| Fig. | II-1  | Variation in Equilibrium Temperature of Air Bath<br>with Continuous Heater Voltage. . . . .                                             | 118 |
| Fig. | II-2  | Schematic Diagram of the Heating and Control Circuits<br>for Constant Temperature Air Bath . . . . .                                    | 119 |
| Fig. | II-3  | Diagram of Stress Relaxometer Including Air Bath. . . . .                                                                               | 121 |
| Fig. | II-4  | Clamps to Hold Test Specimens . . . . .                                                                                                 | 122 |
| Fig. | II-5  | Illustrative Data Showing Continuous and Intermittent<br>Stress-Relaxation Behavior Observed at 50% Elongation<br>and at 160°C. . . . . | 123 |
| Fig. | III 1 | High-Temperature Cabinet on Instron Tester. . . . .                                                                                     | 128 |
| Fig. | III-2 | Interior View of High-Temperature Cabinet<br>on Instron Tester . . . . .                                                                | 129 |
| Fig. | III-3 | High-Temperature Instron Cabinet with<br>Front Panel Removed . . . . .                                                                  | 130 |
| Fig. | III-4 | High-Temperature Instron Cabinet with Front Panel<br>Removed and Crosshead in Lowest Position. . . . .                                  | 131 |
| Fig. | III-5 | High-Temperature Box for Use with High-Temperature<br>Instron Cabinet . . . . .                                                         | 133 |
| Fig. | III-6 | High-Temperature Box Connected to High-Temperature<br>Instron Cabinet . . . . .                                                         | 134 |
| Fig. | IV-1  | Sketch of Ring-Specimen Stretched over Supporting Hooks . . . . .                                                                       | 140 |
| Fig. | IV-2  | Adjustable and Fixed Cutters for Cutting Ring Specimens . . . . .                                                                       | 147 |
| Fig. | IV-3  | Variation with Time of Distance Between Bench Marks on<br>Ring Specimen . . . . .                                                       | 151 |
| Fig. | IV-4  | Variation with Time of Extension Ratio ( $\epsilon + 1$ ) Obtained<br>from Bench Marks on Dumbbell-Shaped Specimen. . . . .             | 154 |

## TABLES

|       |   |                                                                                              |    |
|-------|---|----------------------------------------------------------------------------------------------|----|
| Table | 1 | Comparison of Thermal Stability of Vulcanizates . . . . .                                    | 25 |
| Table | 2 | Values of the 1-Minute Constant-Strain-Rate Modulus for Natural Rubber Vulcanizate . . . . . | 44 |
| Table | 3 | Values of $g(\epsilon)$ for Natural Rubber Vulcanizate . . . . .                             | 45 |

### APPENDICES

|       |      |                                                                                                                                                            |     |
|-------|------|------------------------------------------------------------------------------------------------------------------------------------------------------------|-----|
| Table | I-1  | Compounding Formulas of Gum Vulcanizates. . . . .                                                                                                          | 104 |
| Table | I-2  | Degree of Crosslinking and Weight Percent Sol in Gum Vulcanizates . . . . .                                                                                | 105 |
| Table | I-3  | Glass Temperatures and Expansion Coefficients of Vulcanizates . . . . .                                                                                    | 111 |
| Table | IV-1 | Average Values and Percent Standard Deviation (% S.D.) of Various Quantities Used to Characterize Dimensions of Rings in Various Series Studied . . . . .  | 148 |
| Table | IV-2 | Strain Rate in Ring Specimens Tested at Constant Crosshead Speeds . . . . .                                                                                | 152 |
| Table | IV-3 | Average Values of Tensile Strength (psi) and Ultimate Strain and Percent Standard Deviation. Tests Made 5.0 Inches/Minute Crosshead Speed . . . . .        | 153 |
| Table | IV-4 | Ultimate Tensile Properties Obtained by Testing Dumbbell-Shaped Specimens . . . . .                                                                        | 155 |
| Table | IV-5 | Effect of Strain Rate on Ultimate Tensile Properties . . . . .                                                                                             | 155 |
| Table | IV-6 | Average Values of Stress $\sigma$ (psi) and Percent Standard Deviation at Various Values of Strain. Tests Made 5.0 Inches/Minute Crosshead Speed . . . . . | 157 |
| Table | V-1  | Ultimate Tensile Properties for Butyl Gum Vulcanizate (Sulfur) . . . . .                                                                                   | 162 |
| Table | V-2  | Ultimate Tensile Properties for Butyl Gum Vulcanizate (Resin) . . . . .                                                                                    | 163 |
| Table | V-3  | Ultimate Tensile Properties for Viton B Gum Vulcanizate . . . . .                                                                                          | 164 |
| Table | V-4  | Ultimate Tensile Properties for Silicone Gum Vulcanizate . . . . .                                                                                         | 165 |
| Table | V-5  | Ultimate Tensile Properties for Natural Rubber Gum Vulcanizate . . . . .                                                                                   | 166 |

## I INTRODUCTION

Certain elastomers now commercially available are relatively stable at temperatures up to 200-300°C, but at such temperatures they have poor strength characteristics. This deficiency can result from reversible and irreversible changes in mechanical properties, but the molecular mechanisms associated with these changes are not well understood.

Previous studies of reversible changes have provided only fragmentary information about the basic factors which determine strength. In fact, few data are available which show in a satisfactory manner the effect of test conditions on strength characteristics. As a result, the current molecular theories, based on limited and perhaps erroneous data, are quite crude; at best, they give only a qualitative description of certain factors which affect strength properties. Other factors which may be quite important have not been considered. Consequently, the molecular theories are of limited use for predicting and correlating the properties of various elastomers observed under different test conditions.

Although studies have been made of the irreversible changes in mechanical properties of elastomers at elevated temperatures, quantitative information about the stability of certain elastomers of current interest is not available.

The primary objection of this program was to determine basic factors which affect the strength characteristics of elastomers, especially those elastomers for use at elevated temperatures, and to relate such factors to molecular characteristics. A secondary objective was to study the irreversible changes in properties effected by elevated temperatures.

Because systematic and detailed data suitable for comparing the properties of different types of elastomers were not available, five elastomers were selected and tested to obtain such data. As the complex interactions between filler and polymer in a filled elastomer complicate the

interpretation of results, only gum vulcanizates were studied. These were gum vulcanizates\* of natural rubber, silicone, a hydrofluorocarbon (Viton B), and butyl; both a sulfur-cured and a resin-cured butyl were included.

Each vulcanizate was characterized (1) by determining dilatometrically its glass temperature and thermal expansion coefficients both above and below the glass temperature; (2) by determining its sol fraction; and (3) by measuring its equilibrium modulus which is proportional to the number of effective polymer chains per unit volume.

The chemical stabilities of the vulcanizates were studied by measuring the so-called continuous and intermittent stress-relaxation properties at elevated temperatures. Such data were needed not only to show the relative stabilities of the vulcanizates and the changes in network structure which occur at elevated temperatures but also to suggest the highest temperatures at which tensile properties could be measured without the results being affected significantly by irreversible changes in properties during the test period.

Primary emphasis was placed on determining and analyzing tensile stress-strain data. Such data were obtained on each vulcanizate at about 10 strain rates and 10 temperatures. Detailed analyses were made of the tensile strength and ultimate elongation data to determine the similarities and differences among the vulcanizates, as well as the key factors which affect the observed properties. For the natural rubber vulcanizate, a detailed analysis was also made of the stress-strain curves observed prior to rupture.

---

\* These materials are commonly called gum vulcanizates, but they do contain either 2.5 or 5 parts of some filler, as given in Appendix I.

## II BACKGROUND INFORMATION

The state of stress throughout a material subjected to a homogeneous deformation can be represented by a point in an orthogonal coordinate system whose axes are the principal stresses  $\sigma_1$ ,  $\sigma_2$ , and  $\sigma_3$ ; the corresponding state of strain can be represented by a point in a similar coordinate system whose axes are the principal strains  $\epsilon_1$ ,  $\epsilon_2$ , and  $\epsilon_3$ . By measurement of the principal stresses and strains which exist at rupture, a point in the principal stress space is obtained along with a point in the principal strain space. If the values of the stresses and strains at rupture are independent of test conditions, a failure surface<sup>1,3</sup> in the stress space and a corresponding one in the strain space can be obtained by making measurements under a variety of stress fields. In practice, however, the state of stress and that of strain at rupture depend on the temperature and on the stress-strain-time history of a test specimen. By keeping certain of the test conditions constant, it should be possible to determine failure surfaces for elastomers; different failure surfaces would be obtained, however, for each chosen set of test conditions.

Essentially no work has been done to determine failure surfaces for polymers. Most studies of failure have employed uniaxial tensile tests and tear tests, although some have employed conditions which approach that of triaxial tension. Consequently, the difficulties associated with the determination of meaningful failure surface are not known. Studies to determine failure surfaces must be made, however, before general criteria can be established for predicting the conditions under which failure will result in a specimen subjected to arbitrary test conditions. At present, the mode of failure (distortion, dilatation, or a combination of these) under various test conditions is not known. Failure in both distortion and dilatation should be considered, because under the high local stresses which rupture molecular chains the dilatational properties may be highly significant, even though under similar test conditions involving small stresses such properties have little effect on the observed behavior.

A knowledge of the failure surfaces for elastomers would be of value in several ways, provided the effects of temperature and experimental

time-scale on the surfaces are precisely known. This information would be of value in designing items to be fabricated from elastomeric materials, in providing a complete phenomenological description of the strength characteristics of elastomers, and in providing a sound starting point for the development of molecular theories. However, among the many rheological properties of elastomers, the strength or ultimate properties are undoubtedly the least understood and the most difficult to describe phenomenologically and to relate to molecular structure. Before ultimate properties can be understood adequately, a clear understanding is required of the various rheological characteristics of an elastomer at all deformations prior to rupture. Thus, the germane rheological properties include linear and non-linear viscoelastic phenomena in both distortion and dilatation. Because such information will result only from extensive work by many investigators, it is necessary at present to focus attention on restricted aspects of the over-all problem.

For various reasons, it is appropriate now to limit our attention to the tensile properties of elastomers. Such properties can conveniently be divided between those associated with irreversible (chemical) changes, and those associated with reversible changes; the latter result from variations in such factors as temperature and stress-strain-time history. After some information has been obtained about the effects of such factors on tensile properties, studies can be more readily made of the properties of elastomers under more complex stress fields.

#### A. IRREVERSIBLE CHANGES IN TENSILE PROPERTIES

Irreversible changes in mechanical properties can result from one or more of the following chemical changes at elevated temperatures: (1) a rupture of primary valence bonds producing a decrease in the degree of crosslinking (a decrease in the number of effective network chains); (2) a formation of primary valence bonds such that the degree of crosslinking is increased; (3) a rearrangement of primary valence bonds without a net change in the number of effective network chains; and (4) a change in the number and type of chemical groups without a concomitant change in the geometrical nature of the three-dimensional polymeric network. (Irreversible changes resulting from the presence of filler particles are not considered here as the discussion is limited to gum vulcanizates.)

In general, primary valence bonds are both broken and formed in a specimen at elevated temperatures. The net increase or decrease in the

number of effective network chains can be determined by stretching periodically a specimen to some elongation and measuring the retractive force. Between each measurement, the specimen is kept in its undeformed state. If the observed force (stress) values are known to characterize the material in the absence of viscous relaxation effects, then the change in force can be related to the net change in the number of effective network chains by use of the well-known equation from the kinetic theory of rubberlike elasticity. For such an analysis to be valid, the number of bonds broken or formed during the time required to make the measurement must be negligible compared with the changes which occur while the specimen is undeformed.

The number of network chains broken can be obtained by measuring stress of a specimen subjected continuously to a fixed elongation. An analysis of such data, along with those obtained from the intermittent measurements, gives not only the total number of effective chains existing at any time but also the ratio of the number of chains broken to the number formed. This analysis is possible because when bonds are formed in a specimen subjected continuously to a fixed deformation, no change in stress occurs because the network chains are formed in an unstressed state. But when bonds are formed in an undeformed specimen, the resulting chains will contribute to the modulus which is determined intermittently. This method for determining the number of bonds broken and formed was developed by Tobolsky<sup>4</sup> and is based on what are commonly called continuous and intermittent stress-relaxation measurements.

Chemical reactions which do not produce either a change in the number of effective chains or a rearrangement of junction points can normally be detected only by employing appropriate chemical analytical techniques. Such chemical reactions, however, are usually unimportant because they do not affect mechanical properties, although they may be precursors to reactions which modify the number of effective chains.

#### B. ULTIMATE TENSILE PROPERTIES IN THE ABSENCE OF DEGRADATION EFFECTS

Although all vulcanizates of current interest undergo chemical changes when stored for prolonged periods at elevated temperatures, such changes are not primarily responsible for the marked decrease in tensile strength and ultimate elongation which is commonly observed in vulcanizates at

elevated temperatures. These changes, which may be termed a reversible loss of mechanical properties, are related in general to several factors: (1) a decrease with increasing temperature of internal viscous effects or of specific interactions between chains; (2) the inability of the vulcanizate to crystallize during extension when its temperature is sufficiently high; and (3) a decrease in bonding between a reinforcing filler, if present, and the network chains.

At temperatures in the vicinity of the glass temperature  $T_g$ , the internal viscosity of an elastomer is sufficiently high so that long-range changes in the conformations of polymer chains cannot occur. Only short molecular segments and side chains, or groups attached to the backbone of network chains, can undergo rearrangements. As the temperature is raised progressively, the internal viscosity decreases and long range rearrangements of polymer chains can occur with increasing rapidity. The increased chain mobility effects a decrease in modulus, e.g., the 10-second relaxation modulus changes from a value of about  $10^{10.5}$  dynes/cm<sup>2</sup> (typical of polymers in their glassy state) to about  $10^7$  dynes/cm<sup>2</sup> (typical of a lightly cross-linked rubber). The lower value represents the equilibrium modulus and is determined by the degree of crosslinking. The kinetic theory of rubberlike elasticity predicts that the equilibrium modulus should be directly proportional to the absolute temperature as well as to the number of effective network chains per unit volume.

For many amorphous polymers, the temperature dependence of the internal viscosity over the temperature range  $T_g < T < T_g + 100$  is a near-universal function of  $T - T_g$ . The equation which gives this dependence, proposed by Williams, Landel, and Ferry<sup>5</sup> (WLF), is

$$\log a_T = - \frac{C_1(T - T_g)}{C_2 + T - T_g}$$

where  $C_1$  and  $C_2$  are near-universal constants and  $a_T = \eta T_g / \eta T$  where  $\eta$  and  $\eta_g$  are the viscosities at  $T$  and  $T_g$ , expressed in °K, respectively. At elevated temperatures, this equation may become inapplicable because of the importance of specific forces between chain segments. When this occurs,  $\log a_T$  often varies linearly with the reciprocal of the absolute temperature. In general, however, the WLF equation can be used to interrelate the effects of time and temperature on the mechanical properties

of amorphous polymers over the temperature range  $T_g < T < T_g + 100$ . (Actually, this equation is often applicable at temperatures considerably higher than  $T_g + 100$ .) When molecular motions occur which are not coordinated with the motions of the backbone of polymer chains, e.g., motions of side chains about the main polymer chain, the temperature dependence of such molecular mechanisms are different from that given by the WLF equation.

From certain points of view, it might be expected that when a rubber is deformed slowly at a temperature of  $T_g + 100$ , the deformation would occur under equilibrium, or near-equilibrium, conditions. In other words, the observed values of stress and strain would be independent of time. Such behavior is not always observed, however, and to obtain equilibrium stress-strain values, the test must often be conducted at considerably higher temperatures or special techniques must be used to obtain equilibrium results at the lower temperature. This difficulty in obtaining equilibrium results is caused by certain types of chain interactions whose exact nature is not clearly understood.

Like the modulus, the tensile strength and elongation at break of elastomers depend on both the temperature and testing rate. The tensile strength may change by a factor of 100 or so as the test temperature or the testing rate is varied over a wide range. In the vicinity of  $T_g$ , the ultimate elongation is of the order of a few percent (provided necking or cold drawing of the specimen does not occur) but as the test temperature is increased, the elongation increases markedly and passes through a maximum<sup>6-10</sup>. It has been shown previously<sup>6,7,10</sup> that for certain rubbers, such as SBR gum vulcanizates and certain highly filled elastomeric materials, these variations in the ultimate properties are caused by changes in the internal viscosity. (As is discussed later in this report, such behavior is found--at least over some range of test conditions--for the elastomers tested as part of the present study, with the exception of the natural rubber vulcanizate.)

The ultimate tensile properties of rubbers which crystallize upon extension are considerably more complex than those which remain amorphous until rupture occurs. The crystallites act to reinforce the rubber, and thus under many test conditions the tensile strength and often the ultimate elongation are considerably greater than are found if crystallization does not occur. Because crystallization is a complex time- and temperature-dependent phenomenon, the quantitative interpretation of the variation of the ultimate properties with testing temperature and rate is quite complex.

In considering strength characteristics, it is desirable to classify elastomers into those which do not crystallize under any test condition and those which crystallize when stretched under certain conditions. Elastomers in each of these classifications can be subdivided to include those in which specific interchain forces are absent (do not affect mechanical properties) and those in which interchain forces have an appreciable effect on their mechanical properties.

Those elastomers which do not crystallize and in which specific interchain forces are unimportant exhibit strength properties which are currently the best understood. For example, the effects of strain rate and temperature on their tensile strength ( $\sigma_b$ ) and corresponding ultimate strain ( $\epsilon_b$ ) can be interrelated by the use of the WLF equation in somewhat the same manner as used to interrelate the effects of time and temperature on the stress-relaxation modulus (or other small-deformation time-dependent mechanical properties). Such interrelation was found in a study<sup>6</sup> of an SBR gum vulcanizate whose ultimate properties were determined at numerous strain rates at temperatures between 93.3 and -67.8°C. Curves resulting from plots of  $\log \sigma_b T_0/T$  vs.  $-\log \dot{\epsilon}$  at different temperatures were shifted along the  $-\log \dot{\epsilon}$  axis to effect superposition. Values of the shift factor  $\log a_T$  obtained from superposing both types of data were in agreement and these values were in agreement with the WLF equation. This behavior showed that the variations in  $\sigma_b$  and  $\epsilon_b$  with strain rate and temperature were the result of internal viscous friction and its dependence on temperature. (Later considerations<sup>11</sup> indicate that the use of plots of  $\log \sigma_b T_0/T$  and of  $\epsilon_b$  against  $\log t_b$ , where  $t_b$  is the time-to-rupture under conditions of constant strain rate, has a more theoretical basis than plots of these quantities against  $-\log \dot{\epsilon}$ .)

If time-temperature reduction is applicable for interrelating  $\sigma_b$  and  $\epsilon_b$  data determined at different strain rates and temperatures, then the data must yield a single curve on a plot of  $\log \sigma_b T_0/T$  vs.  $\log \epsilon_b$ . The resulting curve is called the tensile failure envelope<sup>11</sup>. For illustration, the failure envelope for the SBR gum vulcanizate is shown in Fig. 1. (The values of the tensile strengths are somewhat in error as the stress-strain curves, determined by testing ring-type specimens, were not extrapolated beyond the rupture point; the need for this extrapolation is discussed in Appendix IV.)

As either the strain rate is increased or the test temperature is decreased, the rupture point moves counterclockwise along the curve. From

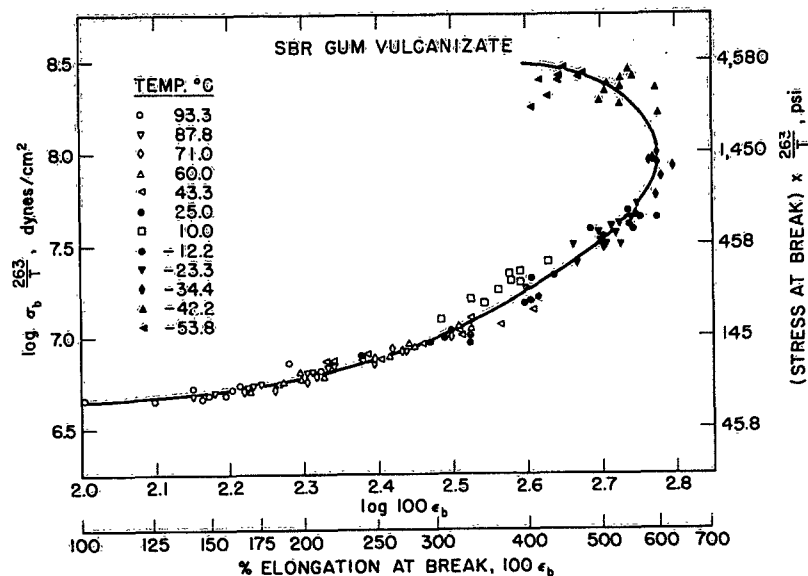


FIG. 1 ILLUSTRATIVE EXAMPLE OF A TENSILE FAILURE ENVELOPE. DATA FOR A SBR GUM VULCANIZATE

the limited data now available, the failure envelope appears<sup>11</sup> to be a material characteristic which is independent of the stress-strain-time history prior to failure. Thus, to compare the strength characteristics of different elastomers, it is desirable to determine and compare their failure envelopes. If such comparison methods are not employed and comparisons are based on only a few values of the ultimate properties of different elastomers, misleading conclusions may be reached about relations between properties and molecular characteristics.

For certain elastomers, time-temperature reduction is not applicable for interrelating ultimate property data determined under various test conditions at different temperatures, or at least the method may be applicable only to data determined within some limited range of test conditions. Thus, the ultimate tensile properties of such elastomers cannot be characterized in detail by the failure envelope. However, even the knowledge that such characteristics exist is of considerable value. Such behavior shows that prior to failure the molecular processes which determine the values of ultimate properties are of a different type from those which control the failure of elastomers whose ultimate properties define a characteristic failure envelope.

If specific interchain associations exist in an elastomer, its properties will be different from those of an elastomer whose network structure is similar except for the absence of chain association. However, as the testing temperature is increased, the two elastomers will be found to have similar ultimate properties when the temperature is sufficiently high so that all secondary bonds caused by chain association have been eliminated. An example of such behavior has been reported by Gul<sup>12</sup> who studied several nitrile rubbers which contained different amounts of acrylonitrile but which were crosslinked to the same extent.

### C. MOLECULAR THEORIES OF RUPTURE

Molecular theories of the tensile strength of elastomers have been reviewed by F. Bueche<sup>13</sup>. Theories concerned with the tensile strength as observed in the absence of viscous effects have been proposed by various investigators. The theory of A.M. Bueche<sup>14</sup> does not consider the molecular mechanism in detail but instead involves a consideration of the shape of the stress-strain curve immediately prior to rupture and the kinetics of bond rupture. The theories of Taylor and Darin<sup>15</sup> and of F. Bueche<sup>16</sup> consider the molecular mechanism of rupture and how the tensile strength should vary with the molecular weight of network chains. (The theory of Taylor and Darin has been investigated and extended by Epstein and Smith<sup>17</sup>.) When measured under conditions such that the internal viscous forces contribute to the stress, the tensile strength is found to be higher than when measured at elevated temperatures or at low strain rates. For data obtained under such conditions, F. Bueche<sup>18</sup> has presented a theory which predicts how the tensile strength should vary with temperature and the experimental time-scale.

Although the various molecular theories have clarified certain aspects of a difficult subject, they are of limited applicability and describe only in an approximate manner the relations between molecular structure and the tensile strength. A major difficulty in evaluating the molecular theories results from the lack of reliable ultimate property data. For example, even though stress-relaxation effects in an elastomer are quite small during tests made to determine ultimate properties, these effects can have a relatively large effect on the observed ultimate properties, as illustrated by the data in Fig. 1. Thus, most data used to test the theories which ignore viscous effects are probably

incorrect, and their use may have led to erroneous conclusions about the validity of the theories.

A major deficiency of the present molecular theories is that they do not explicitly consider the ultimate elongation. In general, as already mentioned, the ultimate elongation of elastomers passes through a maximum as either the test temperature is decreased or as the strain rate is increased. Thus, theories are needed which are at least consistent with this experimental fact, and preferably, which relate directly the observed phenomenon to specific molecular structure and processes. Because of the deficiencies of the current theories, they will not be considered further in this report.

#### D. SPECIAL PROBLEMS ASSOCIATED WITH UNDERSTANDING ULTIMATE TENSILE PROPERTIES

Although this report is concerned primarily with the properties of gum vulcanizates, it seems appropriate to mention certain special problems which are associated with understanding the ultimate tensile properties of filled polymers, crystalline polymers, and polymers which crystallize when deformed. Such problems exist, for example, because (1) the strain on a microscopic scale throughout a deformed specimen of such materials is not homogeneous; and (2) the materials, which originally may be isotropic, often become anisotropic when deformed. The latter arises because in specimens subjected to stress (1) vacuoles may form around filler particles, (2) crystallites originally present may become oriented, and (3) crystallites may be formed in an oriented condition.

Special experimental problems are encountered in studying ultimate properties (these are considered in detail in reference 2). For example, values of ultimate properties are not nearly as reproducible as are values of mechanical properties measured prior to rupture. The degree of reproducibility depends on the type of polymer, the test conditions, and the uniformity of the material (minor variations in structure and in the number of possible flaws throughout a single batch of material may cause a wide variation in observed values of the ultimate properties). In addition, the results may depend on the size of the test specimen, on the condition of the surface, and on the chemical and physical nature of the environment surrounding the test specimen. Also, under certain test conditions, necking of a specimen, which represents a type of failure,

may occur. When this phenomenon occurs, a temperature gradient may exist at the neck (apparently, however, this has not been conclusively demonstrated) and the strain throughout the specimen is not uniform. Under certain other conditions, the temperature of the specimen may increase significantly because of the work done on a specimen during a test.

### III IRREVERSIBLE CHANGES IN TENSILE PROPERTIES OF GUM VULCANIZATES (THERMAL STABILITIES)

The thermal stabilities of the five gum vulcanizates and of a Viton A containing carbon black (SR-251-70) were evaluated by measuring their continuous and intermittent stress-relaxation properties at elevated temperatures. The compositions and characteristics of the vulcanizates are given in Appendix I. The experimental method and the results for each vulcanizate are presented below, along with a brief discussion of the relative stabilities of the materials.

#### A. DISCUSSION OF EXPERIMENTAL METHOD AND RESULTS

The apparatus for the stress-relaxation measurements is described in Appendix II. To make measurements, the thermostatically controlled air bath and the lower portion of the relaxometer (contained in the air bath) were brought to the desired temperature. Then, the relaxometer was removed from the air bath and two test specimens placed in the apparatus. (The specimens were strips about 0.25 inch in width and about 5 inches long.) One specimen was stretched a predetermined amount and the relaxometer was then replaced in the air bath; the other specimen was left unstretched. From the results of tests mentioned in Section C of Appendix II, it appears that between 15 and 30 minutes are required before the specimen and the surrounding air reach the desired temperature. Because chemical degradation often occurred during the time required to attain thermal equilibrium, the values of the retractive force in stretched specimens at "zero time" are somewhat uncertain.

To obtain values of the zero-time retractive force  $f(0)$  for use in analyzing the data discussed subsequently, the following procedure was employed. The logarithm of the retractive force  $f(t)$  was plotted against time, and the resulting curve was extrapolated to zero time to obtain the best value of  $f(0)$ . In making this extrapolation, little weight was given to values of the retractive force measured during the first 15-30 minutes because this period was required for the specimen to reach the desired

temperature. A similar type of extrapolation was also made to obtain a value of  $f(0)$  to use in analyzing data obtained by stretching specimens intermittently during a test.

Because of the complexity of data obtained on specimens undergoing a temperature increase, certain of the values obtained for  $f(0)$  by extrapolation are not highly reliable, especially when the retractive force was observed to change rapidly with time. The change in retractive force during the initial portion of a test is the composite of three effects: (1) an increase in force caused by the effect of a temperature increase on the equilibrium modulus; (2) a decrease in force caused by viscous relaxation; and (3) a decrease in force caused by the rupture of chemical bonds. The effect which predominates is determined by the nature of the vulcanizate being tested and by the test conditions. In analyzing the data, examples were found which seemed to show the predomination of each effect.

The results from the continuous and intermittent stress-relaxation tests are discussed and presented graphically later in this section. The results are presented primarily as plots of  $f(t)/f(0)$  vs. log time, and individual values of  $f(0)$  are tabulated on the figures. In some instances, certain  $f(0)$  values obtained from continuous and intermittent tests made simultaneously, from duplicate tests, and from tests conducted at several temperatures on the same vulcanizate do not agree precisely or do not vary with the test temperature in the expected manner. Although this disagreement is caused in part by the uncertainty caused by the extrapolation method used to obtain  $f(0)$ , it is also caused by two facts: (1) the cross-sectional area of each test specimen was not precisely the same; and (2) the elongation to which a specimen was subjected was not measured with high precision. No effort was devoted to measuring precisely the elongation and cross-sectional area of specimens because under the test conditions employed the rate of degradation of a specimen is independent, or sensibly independent, of the applied elongation. Further, in analyzing continuous and intermittent stress-relaxation results in the conventional manner, the stress need not be known but only the force or the force ratio  $f(t)/f(0)$ .

Although the majority of measurements were made on specimens stretched 50%, some were made at 25% strain. As exceptions, the natural rubber vulcanizate was tested at 100% strain and one test was made on the silicone gum vulcanizate at 100% strain; this latter was made at 200°C. It was necessary to make measurements at these relatively low strains to prevent

specimens from breaking during a test. Although specimens stretched intermittently showed a greater tendency to break than those held at a fixed elongation, specimens at a fixed elongation occasionally broke during a test. However, only one specimen broke when held at 50% strain, although a number ruptured when stretched intermittently to this strain.

#### 1. VULCANIZATE OF NATURAL RUBBER

Continuous and intermittent measurements were made at 100% strain at 100 and 150°C, and the results are shown in Fig. 2. The specimen stretched intermittently at 150°C broke after one hour, although at 100°C the specimen did not rupture.

At 150°C, the vulcanizate degraded rapidly as shown by the curves in Fig. 2. Also, the surface of the vulcanizate oxidized to a high degree as indicated by a dark glossy layer over the surface of the specimen at the conclusion of the test. This layer was coherent although brittle,

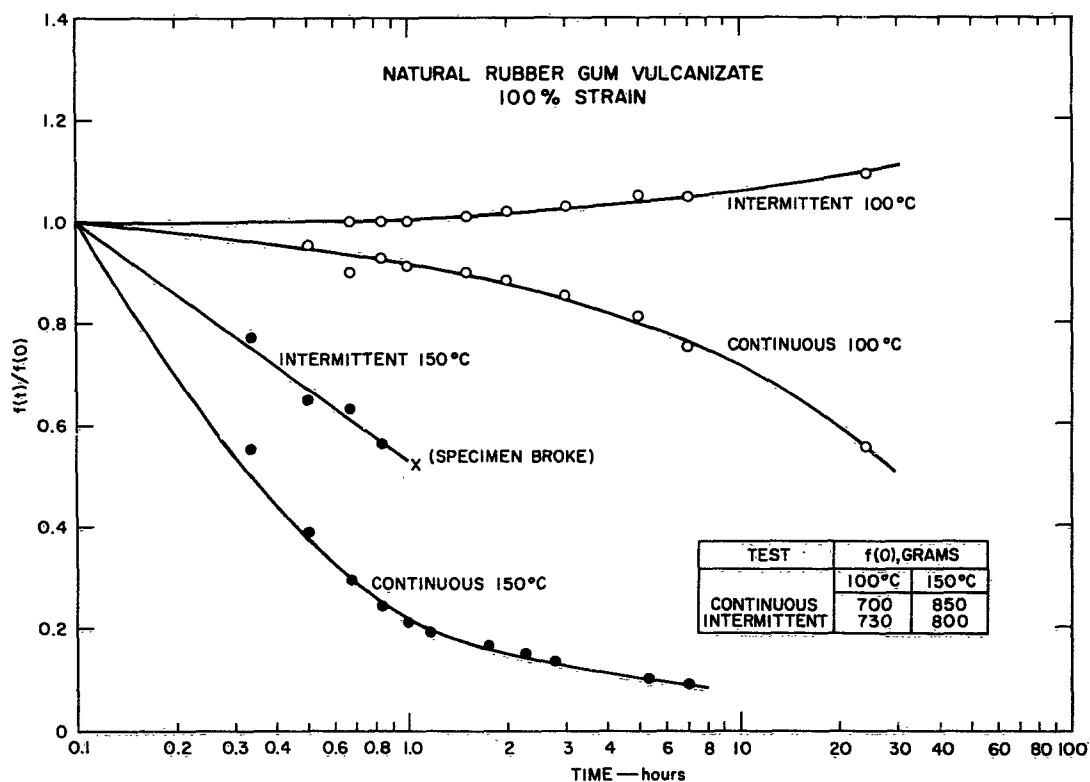


FIG. 2 CONTINUOUS AND INTERMITTENT STRESS-RELAXATION RESULTS ON NATURAL RUBBER GUM VULCANIZATE

and underneath the layer the vulcanizate appeared to be unchanged. However, the force measurements showed that considerable degradation must have occurred throughout the specimen.

## 2. BUTYL VULCANIZATE (SULFUR)

Measurements were made on this vulcanizate at 25 and 50% strain at both 100 and 150°C. The results are shown in Fig. 3. At both 100 and 150°C, the specimen subjected intermittently to 50% strain broke after about 10 minutes, and thus only the results from intermittent tests made at 25% strain are shown. Within experimental error, the results from the continuous tests made at 25% and 50% strain are in agreement. A comparison of the curves in Fig. 3 with those in Fig. 2 shows that the two vulcanizates behave qualitatively in a similar manner, although the butyl vulcanizate seems somewhat more stable at 150°C than the natural rubber vulcanizate. It does appear, however, at 100°C in the unstretched

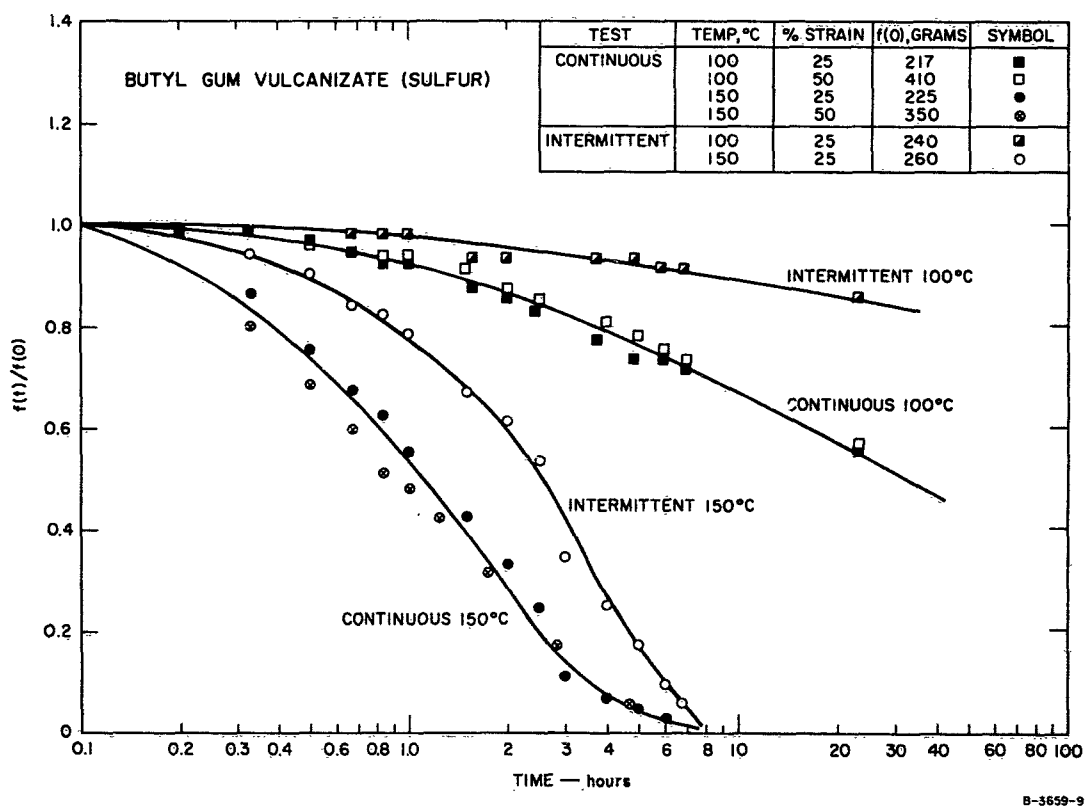


FIG. 3 CONTINUOUS AND INTERMITTENT STRESS-RELAXATION RESULTS ON BUTYL-SULFUR GUM VULCANIZATE (Compare with Fig. 4)

condition, that natural rubber gradually becomes somewhat harder but that the butyl vulcanizate becomes somewhat softer.

Later in the program, another set of measurements were made on the butyl vulcanizate at 100°C and at 25% strain. These tests were continued for 120 hours and the results, which are in close agreement with those shown in Fig. 3, are shown in Fig. 4.

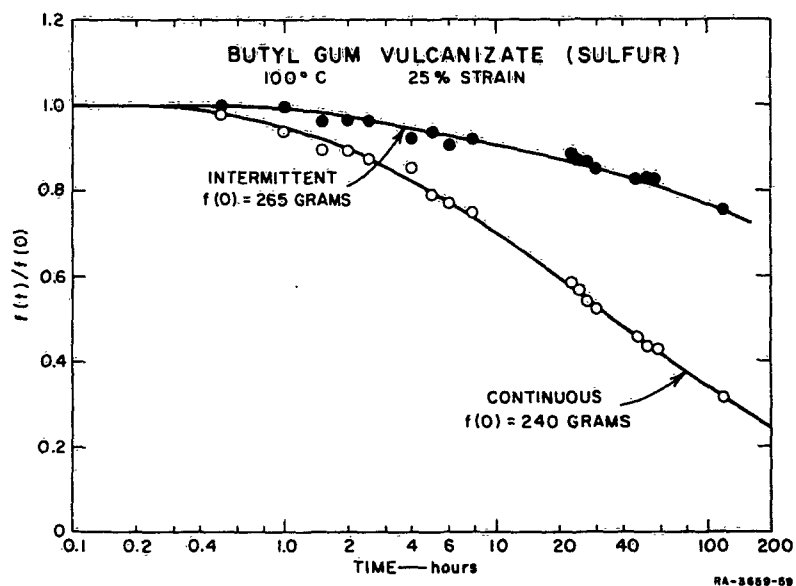


FIG. 4 ADDITIONAL CONTINUOUS AND INTERMITTENT STRESS-RELAXATION RESULTS ON BUTYL-SULFUR GUM VULCANIZATE (Compare with Fig. 3)

### 3. BUTYL VULCANIZATE (RESIN)

Measurements were made on this vulcanizate at 100°, 150°, and 200°C. At 100° and 150°C, tests were made at strains of 25 and 50%, but at 200°C, tests were made only at 25% strain. Specimens stretched intermittently to 50% strain tended to break during an experiment even at 100 and 150°C. However, two sets of intermittent data were obtained at 50% strain at 150°C and one set at 100°C

The results from some of the continuous measurements (those shown in Fig. 6) are also shown in Fig. 5, where they are plotted as  $\log f(t)$  vs. time. On this type of plot, results obtained at different strains

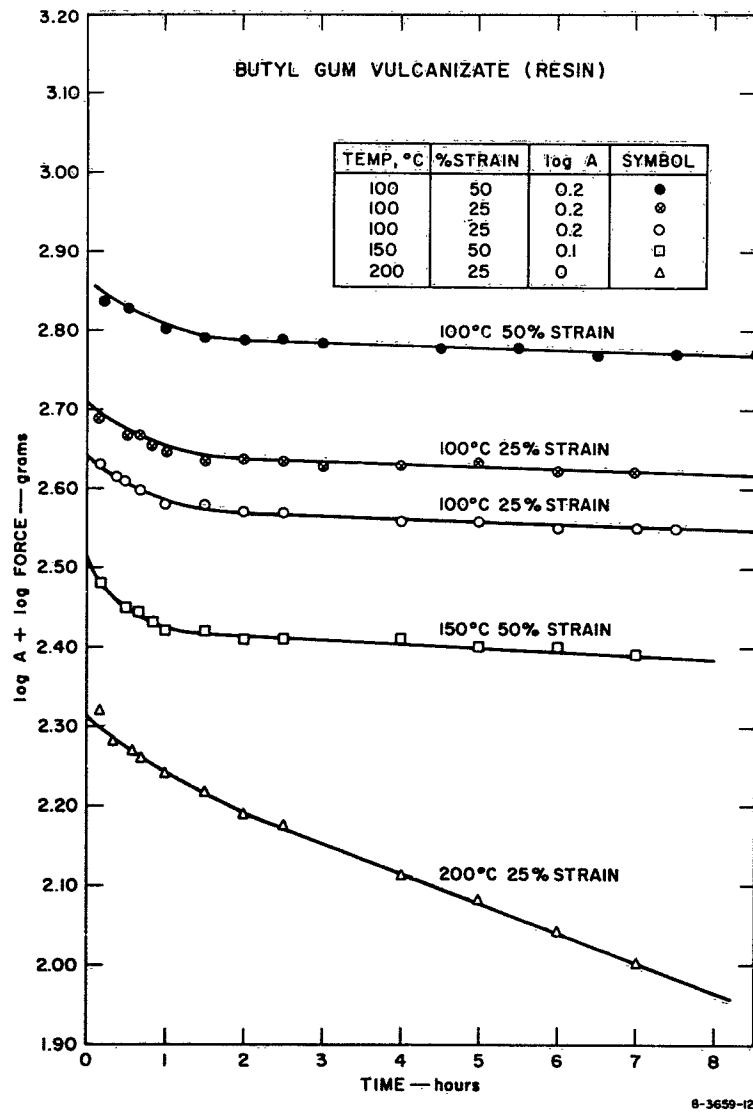
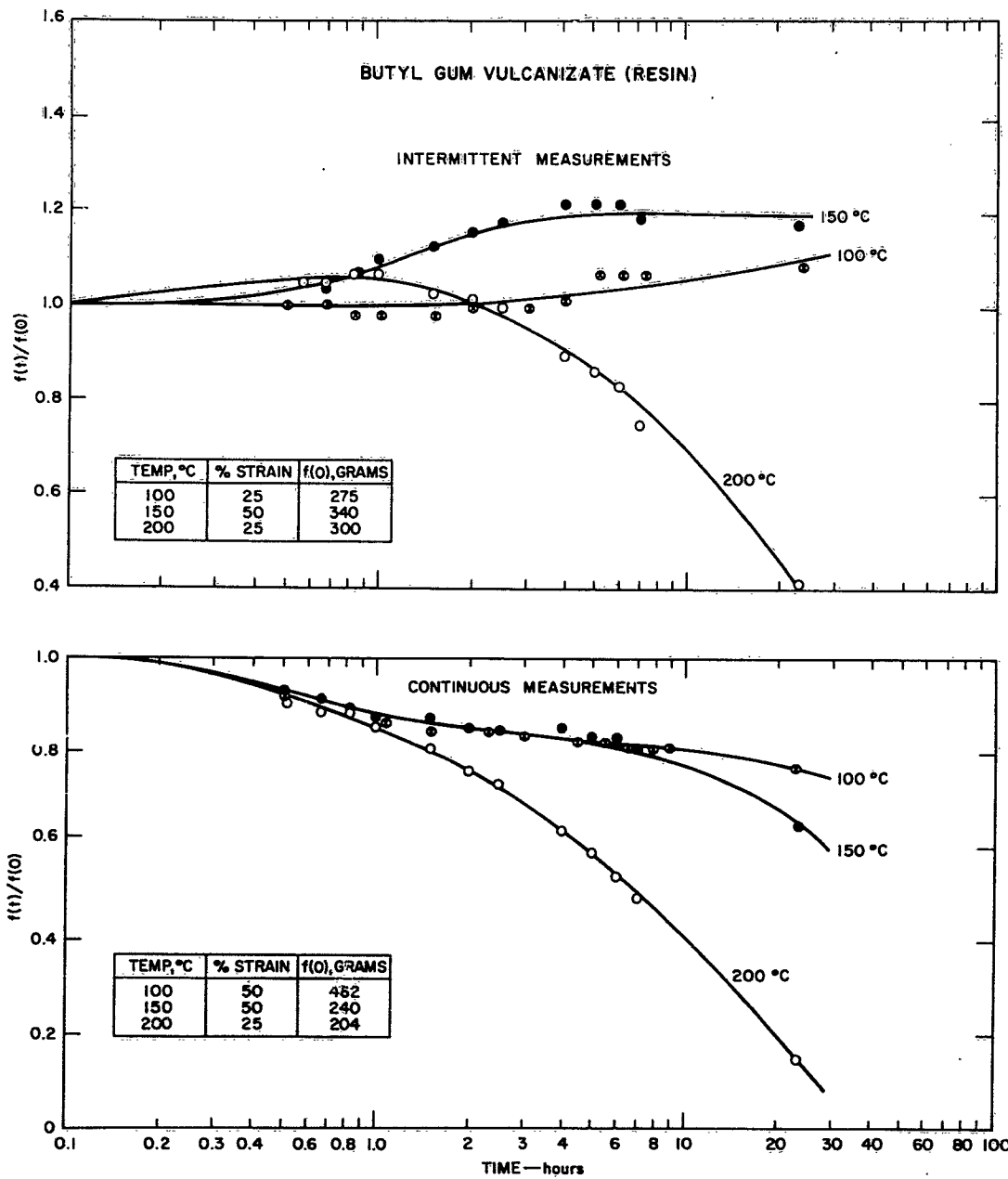


FIG. 5 CONTINUOUS STRESS-RELAXATION RESULTS ON BUTYL-RESIN GUM VULCANIZATE



C-3659-16

FIG. 6 CONTINUOUS AND INTERMITTENT STRESS-RELAXATION RESULTS ON BUTYL-RESIN GUM VULCANIZATE (Compare with Fig. 7)

should give parallel curves, provided the rate of bond rupture is independent of the applied strain. Thus, the curves in Fig. 5 representing the results at 100°C at 25 and 50% strain have been drawn parallel; it is seen that the curves fit the data points closely. Two tests were made at 25% strain at 100°C, and the duplicate results are shown in Fig. 5. Although the curves are parallel, they are displaced by about 0.07 logarithmic unit. This displacement may have been caused by the specimens either being stretched slightly different amounts or having slightly different cross-sectional areas.

The results from the continuous and intermittent tests are shown in Fig. 6 as plots of  $f(t)/f(0)$  vs. log time. At 100 and 150°C, only the results from the continuous tests made at 50% strain are shown because the results at 25% strain are identical with those at 50% strain, provided that the appropriate values of  $f(0)$  are selected. The results from all intermittent tests, in which specimen rupture did not occur, are shown.

Additional tests were made at 50% strain and at 100 and 150°C. These tests were continued for about 100 hours and the results are shown in Fig. 7. The curves in Figs. 6 and 7 show that the rate of degradation in specimens stretched continuously is the same at 100 and 150°C during the first 6 hours. Thereafter, the rate of degradation is higher at 150 than at 100°C. The data in the two figures are in essential agreement, except that the curves in Fig. 7 from the continuous measurements lie somewhat higher than those in Fig. 6. This disagreement results only from the values selected for  $f(0)$ ; by the proper selections, the curves in Figs. 6 and 7 could have been made to agree quite closely.

The results from the intermittent measurements at 100 and 150°C show that the elevated temperatures produce additional crosslinking, although at 150°C degradation begins to predominate after about 6 hours, as shown in Fig. 7. At 200°C, it appears that some crosslinking occurred during the first hour, but then degradation began and continued until the termination of the test.

The continuous stress-relaxation results confirm the expected behavior which is that a butyl-resin vulcanizate has better stability at elevated temperatures than a butyl-sulfur vulcanizate.

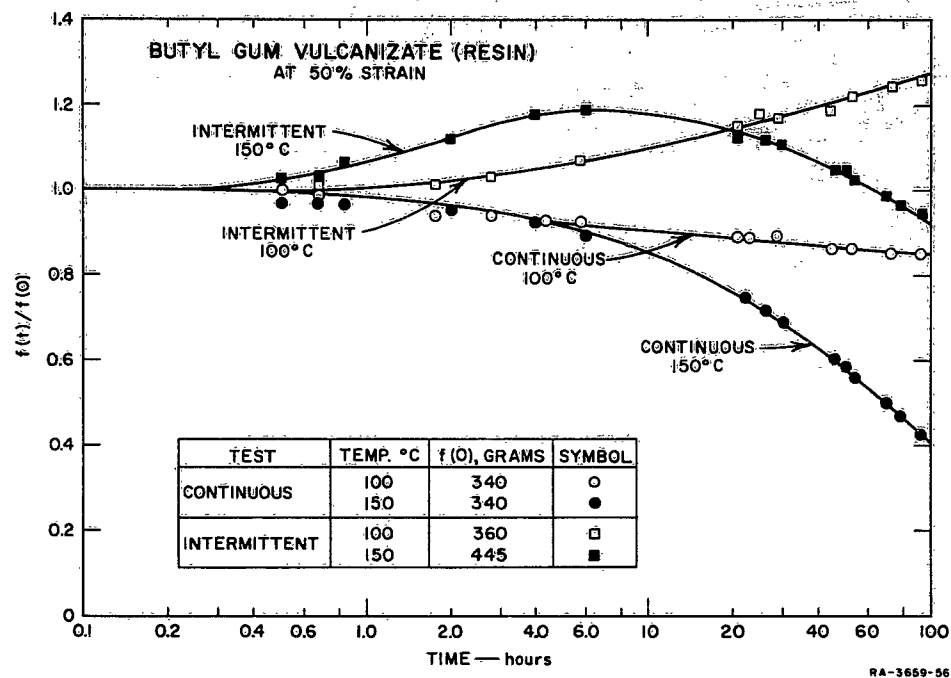


FIG. 7 ADDITIONAL CONTINUOUS AND INTERMITTENT STRESS RELAXATION RESULTS ON BUTYL-RESIN GUM VULCANIZATE (Compare with Fig. 6)

#### 4. SILICONE VULCANIZATE

Silicone gum vulcanizate was studied at 100, 150, and 200°C at a strain of 50%. In addition, measurements were made at strains of 25, 50, and 100% at 200°C. The results at 200°C from the continuous stress-relaxation tests are shown in Fig. 8 by a plot of  $\log f(t)$  vs. time. The curves through the points from the tests at the three strains are drawn parallel; this behavior indicates, as mentioned previously, that the rate of degradation is independent of the applied strain.

The values obtained for  $f(0)$  are shown by the tabulation at the bottom of Fig. 8 to be quite reliable. This conclusion results from the observation that  $(1 + \epsilon)f(0)/\epsilon$ , where  $\epsilon$  is the applied strain, is constant within a few percent. For many elastomers, the true tensile stress, i.e., the stress based on the cross-sectional area of a stressed specimen, is directly proportional to the strain for strains up to about 1.0, provided the stress-strain data represent equilibrium behavior. When no volume change accompanies extension, the true stress equals  $(1 + \epsilon)f(0)/A_0$ ,

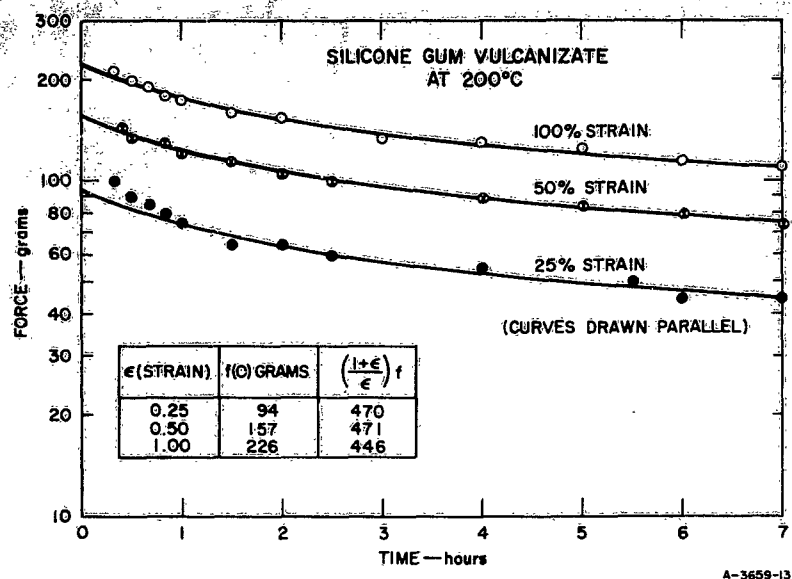


FIG. 8 CONTINUOUS STRESS-RELAXATION RESULTS ON SILICONE GUM VULCANIZATE AT 200°C

where  $A_0$  is the initial cross-sectional area of a specimen. Thus, the quantity  $(1 + \epsilon)f(0)/\epsilon$  should be a constant, independent of strain; this is shown to be true by the tabulated data in Fig. 8.

The continuous and intermittent stress-relaxation results obtained at 100, 150, and 200°C are shown in Fig. 9. Results of the intermittent measurements at 100°C are not shown because the changes observed were small. The results at the other temperatures show that the stress increases quite appreciably with time, although it appears that at 150°C the stress initially decreases somewhat and then increases. Under a continuously applied strain at 200°C, the stress decreases with time at about the same rate as shown in Fig. 6 for the butyl-resin vulcanizate.

#### 5. VITON B VULCANIZATE

Tests were made on the gum vulcanizate of Viton B at 100, 150, and 200°C at 50% strain, and the results are shown in Fig. 10. The continuous stress-relaxation results show that the rates of degradation at 100 and 150°C are nearly the same. On the other hand, the results from the intermittent measurements show that the stress increases with time at 150 and 200°C at about the same rate. The data at 200°C suggest that the stress first decreases somewhat with time before it increases. Before

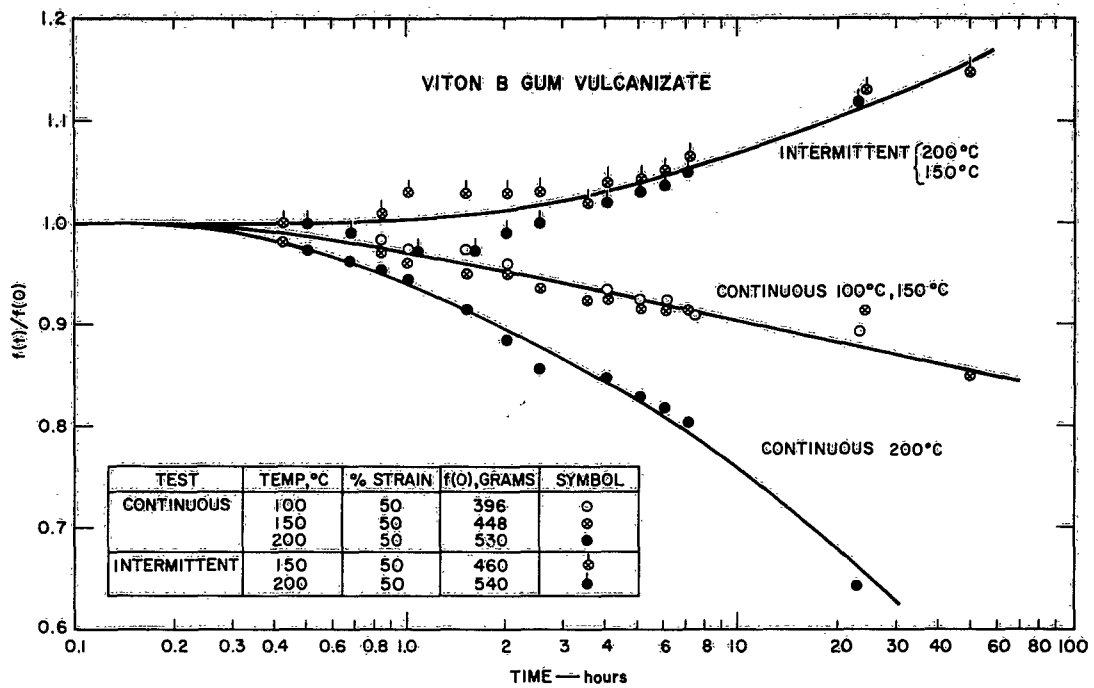


FIG. 10 CONTINUOUS AND INTERMITTENT STRESS-RELAXATION RESULTS ON VITON B GUM VULCANIZATE

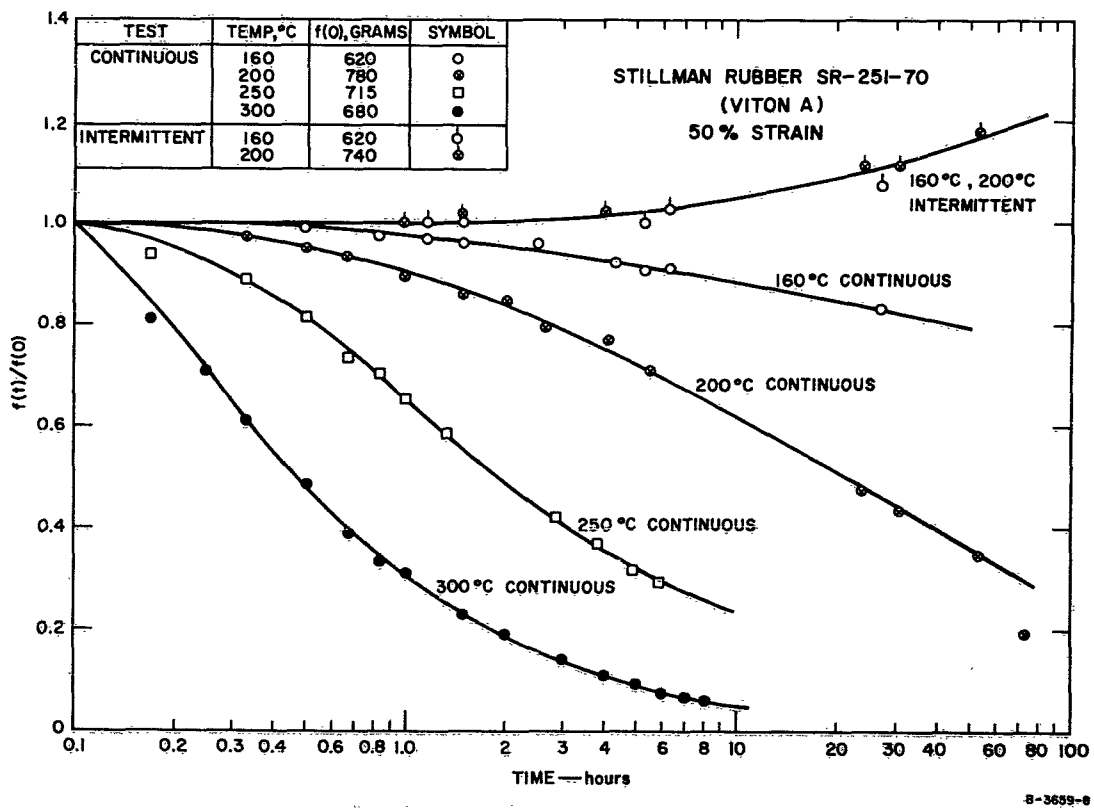


FIG. 11 CONTINUOUS AND INTERMITTENT STRESS-RELAXATION RESULTS ON STILLMAN RUBBER SR-251-70 (Viton A Containing Carbon Black)

Stillman rubber. The results, perhaps, are too few to allow firm conclusions to be drawn at this time.

## B. COMPARISON OF STABILITY OF VULCANIZATES

From the data obtained thus far, a qualitative, or semi-quantitative comparison can be made which indicates the relative stability of the various vulcanizates. To make this comparison, results obtained from continuous measurements at 150°C were used, except 160°C data for the Stillman rubber were used. The time required for the initial force to decrease by 30% (the time at which  $f(t)/f(0)$  equals 0.7) was noted or was obtained by extrapolation; these times are given in Table 1.

The results show that the Viton vulcanizates are by far the most stable of those tested and that the butyl-resin and silicone vulcanizates are the next most stable materials. Because long extrapolations were required to estimate the hours required for the initial force applied to the Viton vulcanizates to decrease 30% at 150°C, the hours given in Table 1 for these materials are probably not very precise. A range of time is given for the butyl-resin because the curves in Figs. 6 and 7 are displaced somewhat. However, it is believed that the curve in Fig. 7 is the most reliable of the two and thus the value of 29 hours is preferable.

The stability of silicone rubber has been reported<sup>19</sup> to depend markedly on relative humidity and on traces of catalyst in the rubber. It also has been found<sup>19</sup> that vulcanizates cured with benzoyl peroxide, like the one tested in the present study, are considerably less stable than those cured by radiation. In view of such factors, as well as other uncertainties, it is not possible to make a general statement comparing the relative stability of butyl-resin and silicone vulcanizates.

The data presented in this report have not been analyzed in detail and have not been compared

Table 1  
COMPARISON OF THERMAL STABILITY  
OF VULCANIZATES  
(Hours required at 150°C for stress  
in specimens subjected to fixed  
elongation to decrease 30%)

| GUM VULCANIZATE     | HOURS  |
|---------------------|--------|
| Natural             | 0.2    |
| Butyl (Sulfur)      | 0.6    |
| Butyl (Resin)       | 18-29* |
| Silicone            | 6      |
| Stillman (Viton A)§ | 700†   |
| Viton B             | 2000†  |

\* Value depends on whether data in Fig. 6 or Fig. 7 are used.

† Estimated by extrapolation of short-time test data.

§ The vulcanizate tested contained carbon black.

critically with those data available in the literature. Before such analyses and comparisons are warranted, additional tests should be conducted under improved and better defined experimental conditions. For example, the specimens tested were relatively thick (ca 0.07 in.) and thus their equilibration during the tests with oxygen in the surrounding gas might be sufficiently slow to cause the rates of degradation to be diffusion controlled. Thus, some caution is warranted in interpreting the rate data presented at this time. However, the data show that all vulcanizates undergo appreciable degradation when in a strained condition at 150°C, and also that the Viton vulcanizates are considerably more stable than the other materials tested.

## IV CONSTANT STRAIN RATE TENSILE PROPERTIES OF GUM VULCANIZATES

Tensile stress-strain curves for the five vulcanizates being studied were determined at about 10 temperatures over a wide range and at about 10 strain rates at each temperature. The primary purpose of this work was to characterize the ultimate tensile properties of the vulcanizates; a secondary purpose was to study their large deformation viscoelastic properties.

This section presents a detailed analysis of the stress-strain curves of natural rubber. (The analysis of the curves of the four other vulcanizates will constitute part of the work to be performed on a subsequent program.) In addition, the ultimate tensile properties of the five vulcanizates are discussed and compared.

### A. EXPERIMENTAL METHOD

Tensile stress-strain data were obtained by testing ring-type specimens with the Instron tester. The method for preparing and testing such specimens is given in Appendix IV along with the results of a detailed study made to evaluate the reliability of data obtained by testing rings. In addition, the temperature control equipment for use with the Instron is described in Appendix III.

For the study discussed in this section, rings were cut from sheets of the various vulcanizates using the adjustable cutter described in Appendix IV. To obtain the dimensions of a ring, the weights of the ring and the disc from the center of the ring were determined, along with the thickness of the disc. From these quantities and the density of the rubber (obtained by the hydrostatic-weighing technique), the outside and inside diameters and the cross-sectional area of a ring were calculated.

The weights of the rings varied somewhat. For example, for the natural rubber, the weights ranged from about 0.29 to 0.35 gram. Some of this variation occurred because the thicknesses of the rubber sheets were not the same; in fact, the sheets had a slight taper. The measured thicknesses of discs varied from about 0.074 to 0.076 inch, although

several were thicker than 0.080 inch. The precision of the thickness measurement is high, as described in Appendix IV, and is about 0.3%; thus, the variation observed in the thickness is real.

Another reason for the variation in ring weight is a variation in the outside and inside diameters of the rings; the calculated outside diameter of the rings of natural rubber varied from about 1.36 to 1.38 inches and the inside diameter from about 1.23 to 1.24 inches. However, even these small variations are sufficient to cause more than an 18% variation in the weights of the rings. As a result of variations in rubber thickness and ring diameters, the cross-sectional areas of the rings varied from about 0.0046 to 0.0053 sq in., or about 14%.

The variation in the diameters of the natural rubber rings was probably caused by changes in the sharpness of the cutter, although the cutter was sharpened periodically. Also, after a certain number of rings were cut, a change was made in the design of the cutter, and this may have caused a small difference in the dimensions of rings cut after the change. Although the weights of rings of the other vulcanizates have not been carefully inspected, it is likely that similar variations occurred.

Rings were tested by placing them over hooks attached to the load cell and to the movable crosshead of the Instron. The hooks were lubricated with silicone grease, except that at low test temperatures a DC-200 fluid was used. Even though the results presented in Appendix IV show that a lubricant is not needed, the lubricant was used to insure that the ring would slip freely around the hooks during a test. Exactly ten minutes after a ring was placed over the hooks, the test was begun. This period was sufficient for the temperature of the specimen to reach that of the surrounding air. This procedure also insured that a specimen was not maintained at an elevated temperature for a period sufficiently long to cause appreciable degradation prior to the beginning of a test.

Specimens were tested at about 8 to 10 crosshead speeds at a number of temperatures. The crosshead speeds ranged from 0.02 to 20 inches per minute and these speeds gave strain rates\* between about 0.0098 and

---

\* The strain rate  $\dot{\epsilon}$  is related to the crosshead speed (XHS) by the equation

$$\dot{\epsilon} = \frac{2(XHS)}{\pi D_a}$$

where  $D_a$  is the average diameter of a ring; for the tests discussed in this report, the rings had a  $D_a$  of about 1.30 inches.

9.8 min<sup>-1</sup>. The test temperature ranged in general from one somewhat above the glass temperature of a vulcanizate up to a temperature somewhat below that at which chemical degradation might be expected to occur during the test period. Upper temperatures were selected by considering the stress-relaxation data presented in Section III.

## B. METHOD FOR DATA REDUCTION

Because of the labor involved in reducing data obtained from the testing of rings, machine methods were employed as much as possible. Approximately 40-50 points were read from each Instron trace by means of a Bensen-Lehner Oscar Model K connected to an IBM keypunch. In addition, the weight of each ring and the weight of the center disc were recorded on an IBM card along with the thickness of the disc, the density of the rubber, and the test conditions, *i.e.*, temperature, chart speed, cross-head speed, etc. These cards were then processed through a Burroughs 220 computer.

The program for the computer was prepared so that the dimensions and cross-sectional area of each ring were computed. Next, the stress and strain corresponding to each point read from an Instron trace were computed. As discussed in the next section, it is necessary to know, at a series of fixed values of strain, the stresses which were obtained from tests conducted at different strain rates. The input data to the computer included the desired strain values; the stresses at these strains were obtained by the computer by making linear interpolations between the appropriate data already calculated. The elapsed times required during a tensile test to reach these stress values were also calculated.

Although the computer calculates and prints out a variety of quantities, the key quantities for present purposes are as follows: the prescribed values of strain; the corresponding values of  $\log \sigma / 273/T$ , where  $\sigma$  is the stress and  $T$  is the test temperature in °K; and values of  $\log t$ , where  $t$  is the time to reach the stress.

The computer treated the ultimate property data in a special manner. The strain at rupture was calculated from the crosshead displacement at rupture and the inside diameter of a ring. (All other values of strain were based on the average diameter of a ring.) To obtain a value of the tensile strength (stress at rupture) the computer performed a numerical

extrapolation of the final portion of each Instron curve; the need for this extrapolation is discussed in Appendix IV. The extrapolation was made by fitting about 10-15 stress-strain values preceding rupture to a polynomial using a least-squares method. From this polynomial, the stress corresponding to the computed strain at rupture was calculated. The values of interest relating to each rupture point were tabulated.

The program also computed other quantities such as isochronal stress-strain values at different prescribed values of time. (However, such data provided by the computer were not used in the analyses discussed in this report.) Selected output data were recorded on punch cards, in addition to being tabulated, so that they could be processed by an automatic plotter if desired. Of the results presented in this report, the automatic plotter was used only to prepare the failure envelopes discussed in Section IV-D.

### C. RATE AND TEMPERATURE DEPENDENCE OF STRESS-STRAIN CURVES OF NATURAL RUBBER

#### 1. BACKGROUND INFORMATION

A method for analyzing stress-strain curves has been developed recently and evaluated<sup>20</sup> by analyzing stress-strain curves which were measured on an SBR gum vulcanizate by testing ring specimens at numerous strain rates at each of 10 temperatures between -42.8 and 93.3°C. As the results are not generally available (they are currently in publication), the method will be described briefly, along with the main conclusions.

For representing mechanical properties within the range of small (or infinitesimal) strain, equations provided by the theory of linear viscoelasticity are applicable. Although these equations are not generally applicable to represent large-deformation time-dependent mechanical properties, empirical modifications of these equations can sometimes be used. For example, some years ago Guth, Wack, and Anthony<sup>21</sup> showed that the stress-relaxation properties of certain elastomers, as determined at large tensile deformations, can be represented by an equation of the form,  $\sigma(\lambda, t) = \Gamma(\lambda)E(t)$  where  $\sigma(\lambda, t)$  is the stress which depends on the time,  $t$ , and on the extension ratio,  $\lambda$ , ( $\lambda - 1 = \epsilon$ , where  $\epsilon$  is the tensile strain);  $\Gamma(\lambda)$  is some function of  $\lambda$  and approaches  $\lambda - 1$  as the strain approaches zero; and  $E(t)$  is the ordinary stress-relaxation modulus which

depends only on the time. Accordingly, the time and strain dependence of the stress are separable. This type of behavior was likewise noted at about the same time by Tobolsky and coworkers.<sup>22</sup>

Another example of nonlinear viscoelastic behavior is illustrated by tensile stress-strain curves of elastomers determined at constant rates of elongation. Such curves are nonlinear except when the test is conducted under equilibrium conditions over an exceedingly small range of strain. Provided the elastomer does not crystallize or degrade during a test, the nonlinear dependence of stress on strain occurs for two reasons: (1) under most test conditions, relaxation of stress takes place continuously throughout a test; and (2) even in the absence of stress relaxation, the stress-strain curve is nonlinear, as is well known and is predicted by the statistical theory of rubberlike elasticity. If crystallization occurs during a test, as is true when natural rubber is tested to rupture under most conditions, the shape of the stress-strain curve is modified.

A method for separating inherent nonlinear effects from those caused by stress relaxation was developed<sup>20</sup> by first considering a linear viscoelastic material. To represent the properties of such a material, a generalized Maxwell model, which is characterized by the relaxation spectrum,  $H(\tau)$ , and the equilibrium modulus,  $E_e$ , was employed. (Actually, the Boltzman superposition equation could have been used equally well.) If this model in its relaxed state at zero time is subjected to a strain which increases linearly with time, the resulting strain- and time-dependent stress,  $\sigma(\epsilon, t)$ , is given by the equation<sup>23</sup>

$$\sigma(\epsilon, t) = E_e \dot{\epsilon} t + \dot{\epsilon} \int_{-\infty}^{\infty} \tau H(\tau) (1 - e^{-t/\tau}) d \ln \tau \quad (1)$$

where  $\dot{\epsilon}$  is the strain rate and  $\tau$  the relaxation time. As pointed out previously,<sup>24</sup> Eq. (1) shows that  $\sigma(\epsilon, t)/\dot{\epsilon}$  is a function of time only. Consequently, stress-strain curves measured at different strain rates will superpose to yield a single composite curve on a plot of  $\log \sigma/\dot{\epsilon}$  vs.  $\log t$ , provided the data are sensibly linear viscoelastic. Also, the slope of a stress-strain curve evaluated at  $t = \epsilon/\dot{\epsilon}$  equals the stress-relaxation modulus  $E(t)$ . This interrelation results from differentiating Eq. (1) with respect to  $\epsilon$  which gives the equation:

$$\frac{d\sigma}{d\epsilon} = \frac{1}{\dot{\epsilon}} \frac{d\sigma}{dt} = E_e + \int_{-\infty}^{\infty} H(\tau) e^{-t/\tau} d \ln \tau \quad (2)$$

It was found empirically that Eq. (1) was suitable for representing stress-strain curves of polyisobutylene<sup>24</sup> and SBR<sup>25</sup> at strains up to about 100% provided the stress was replaced by the true stress, *i.e.*, the force divided by the cross-sectional area of the stressed specimen. For elastomers, the true stress equals  $\lambda\sigma$ . However, this method of treating stress-strain curves was considered unsatisfactory in two respects: (1) data at elongations greater than 100% could not be analyzed; and (2) no satisfactory test was provided to assure that the data were being analyzed in a rigorous manner. What was needed was a method which shows when and how the time dependence can be separated from the inherent nonlinear effects.

A rigorous method was developed by first replacing  $\dot{\epsilon}$  in Eq. (1) by  $\epsilon/t$  and then rearranging the equation to obtain the following:

$$\frac{\sigma(\epsilon, t)}{\epsilon} = E_e + \frac{1}{t} \int_{-\infty}^{\infty} \tau H(\tau) (1 - e^{-t/\tau}) d \ln \tau \quad (3)$$

The ratio  $\sigma(\epsilon, t)/\epsilon$ , which is a function of time alone, was called the constant-strain-rate modulus,  $F(t)$ . This modulus can be shown in a straightforward manner to be related to the stress-relaxation modulus by the equation:

$$E(t) = F(t) \left[ 1 + \frac{d \log F(t)}{d \log t} \right] \quad (4)$$

Because  $d \log F(t)/d \log t$  is a nonpositive number which normally lies between about 0 and -0.67, it follows that  $3E(t) > F(t) \geq E(t)$ . Also,  $F(t)$  varies with time in quantitatively the same manner as  $E(t)$  and can be readily converted into  $E(t)$  by using Eq. (4).

Before applying Eqs. (3) and (4) to data obtained at finite strains, it is necessary to assume that  $F(t)$  at a given temperature can be represented by an equation of the form:

$$F(t) = \frac{g(\epsilon)\sigma(\epsilon, t)}{\epsilon} \quad (5a)$$

$$\log F(t) = \log \frac{g(\epsilon)}{\epsilon} + \log \sigma(\epsilon, t) \quad (5b)$$

where  $g(\epsilon)$  is some function of the strain and approaches unity as the strain goes to zero. It is reasonable, even in the absence of direct verification, to assume that Eq. (5) will apply to data obtained on certain elastomers because of the work of Cath and coworkers.<sup>21</sup>

To test the applicability of Eq. (5), stress-strain curves at a number of strain rates must be available. The procedure consists of first selecting a number of strains and then noting the stress obtained at each strain rate at each of the selected values of strain. The times required to reach each of the stress values are calculated from the values of the strain and the strain rates employed. Finally, plots are made of  $\log \sigma$  vs.  $\log t$  where the points for each curve represent data at a fixed strain. If the curves which represent the constant strain data are parallel, this indicates that the function  $g(\epsilon)$  exists and is independent of time over the range covered by the data. In other words, the data can be represented by Eq. (5). If  $g(\epsilon)$  is found to be independent of time, then it must also be independent of temperature, at least over a restricted range, provided the time and temperature effects are caused solely by internal viscosity effects. On the other hand, if a temperature change effects a change in the physical state of the material (e.g., changes resulting from crystallization or from the formation or disruption of units or clusters held together by hydrogen bonds), then, at various temperatures, though  $g(\epsilon)$  may be independent of time over an extended range, it may be dependent on temperature.

## 2. RESULTS FROM ANALYSIS OF CURVES

Figure 12 shows plots of  $\log \sigma 273/T$  vs.  $\log t$  for various fixed strain values lying between 0.1 and 5.5. The data for these plots were obtained from stress-strain curves measured at 100°C and at crosshead speeds between 0.02 and 20 inches per minute. At all values of strain and over about three decades of time, it is seen that the points define quite precisely lines of zero slope. (Essentially no point lies more than 0.05 logarithmic unit from a line and most lie considerably closer

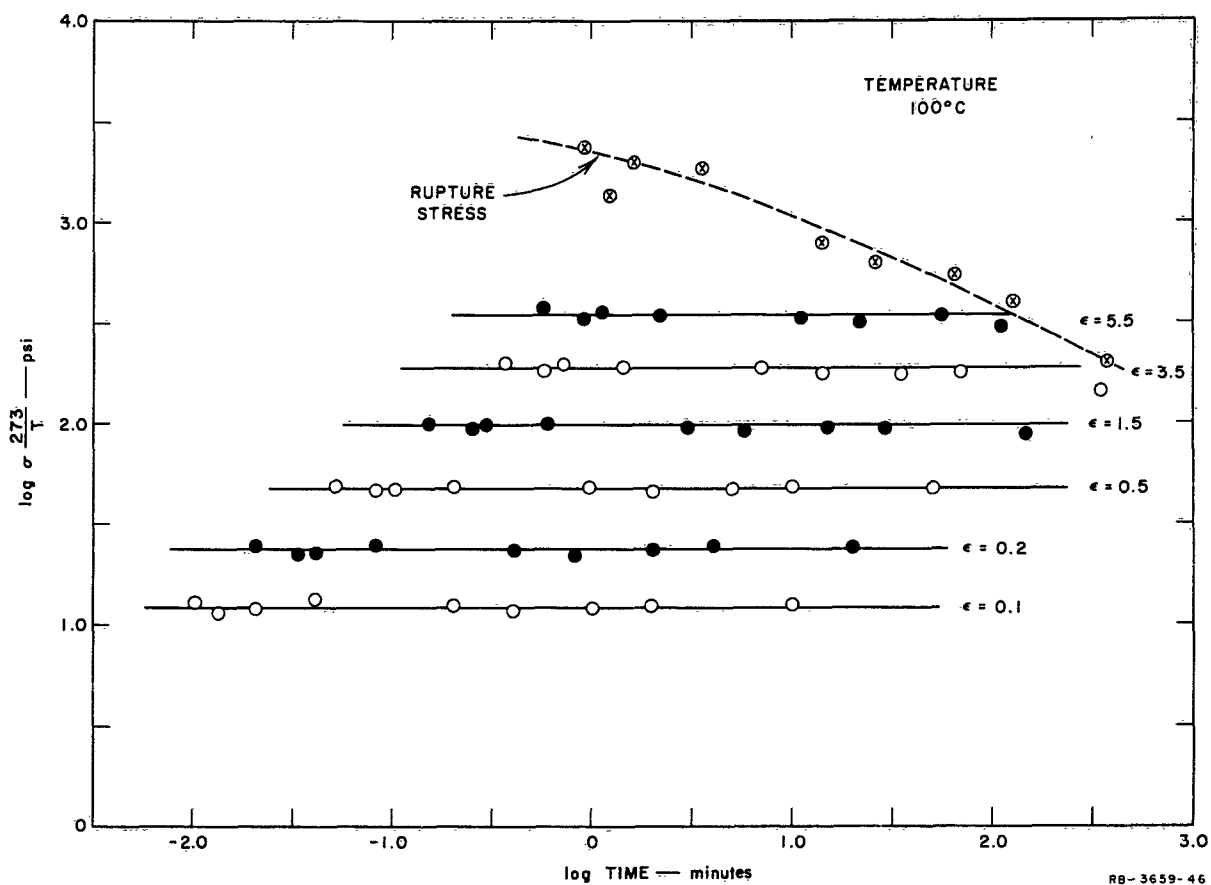


FIG. 12 TENSILE STRESS-STRAIN DATA FOR NATURAL RUBBER AT 100°C PLOTTED AS  $\log \sigma \frac{273}{T}$  vs.  $\log t$  FOR VARIOUS FIXED VALUES OF STRAIN

to the lines; an 0.05 logarithmic unit represents a 12% error.) This indicates that the data represent equilibrium or quasi-equilibrium behavior.

Plots similar to those shown in Fig. 12 were also prepared from data determined at 80, 60, 40, 25, 10, -5, -20, -35, and -45°C. Rather surprisingly, it was found at all temperatures between 100 and -20°C that all lines had zero slope, even though the strains ranged up to about 7. For further illustration of this interesting behavior, Fig. 13 shows the results at -20°C. Although the data are not shown, at short values of time at -35°C, the lines curved upward somewhat, indicating viscous effects. However at -45°C, relaxation of stress definitely occurred throughout the tests, as shown by the solid curves in Fig. 14 where the lines at all strains have been drawn parallel. Because the data can be fitted by parallel curves, it can be concluded that the effects of time and finite strain are separable and that the data can be represented by Eq. (5).

The fact that the plots of  $\log \sigma 273/T$  vs.  $\log t$  yield lines of zero slope at temperatures between 100 and -20°C suggests that the observed stress-strain curves represent equilibrium behavior. However, as shown by the subsequent analysis, the data represent only quasi-equilibrium behavior, at least for elongations greater than 100%.

To analyze the results further, values of stress were read at 1 minute ( $\log t = 0$ ) from the lines at different strains. These isochronal data were then used to prepare plots of  $\log \sigma$  vs.  $\log \epsilon$  using data obtained at each test temperature. For illustration, Fig. 15 shows the curves representing the -45 and 100°C data. If the strain function  $g(\epsilon)$ , given in Eq. (5), is independent of temperature, then curves like those in Fig. 15 must be parallel. Although the curves in Fig. 15 are sensibly parallel at low strains, they are nonparallel at high strains. Over the range in which the curves are parallel, the vertical distance between the curves equals the difference between the logarithms of the modulus  $F(1)$  at the two temperatures, as can be seen from Eq. (5b). (Actually, as discussed in Section IV-C-3, the temperature factor  $273/T$  may not be correct for reducing the stress to a common reference temperature, although the error introduced by its use is small.)

The evaluation of  $g(\epsilon)$  at various temperatures requires a knowledge of the modulus at each temperature. To evaluate the modulus at 100°C and to obtain information about the shape of the stress-strain curve, various plots were made of the 100°C data.

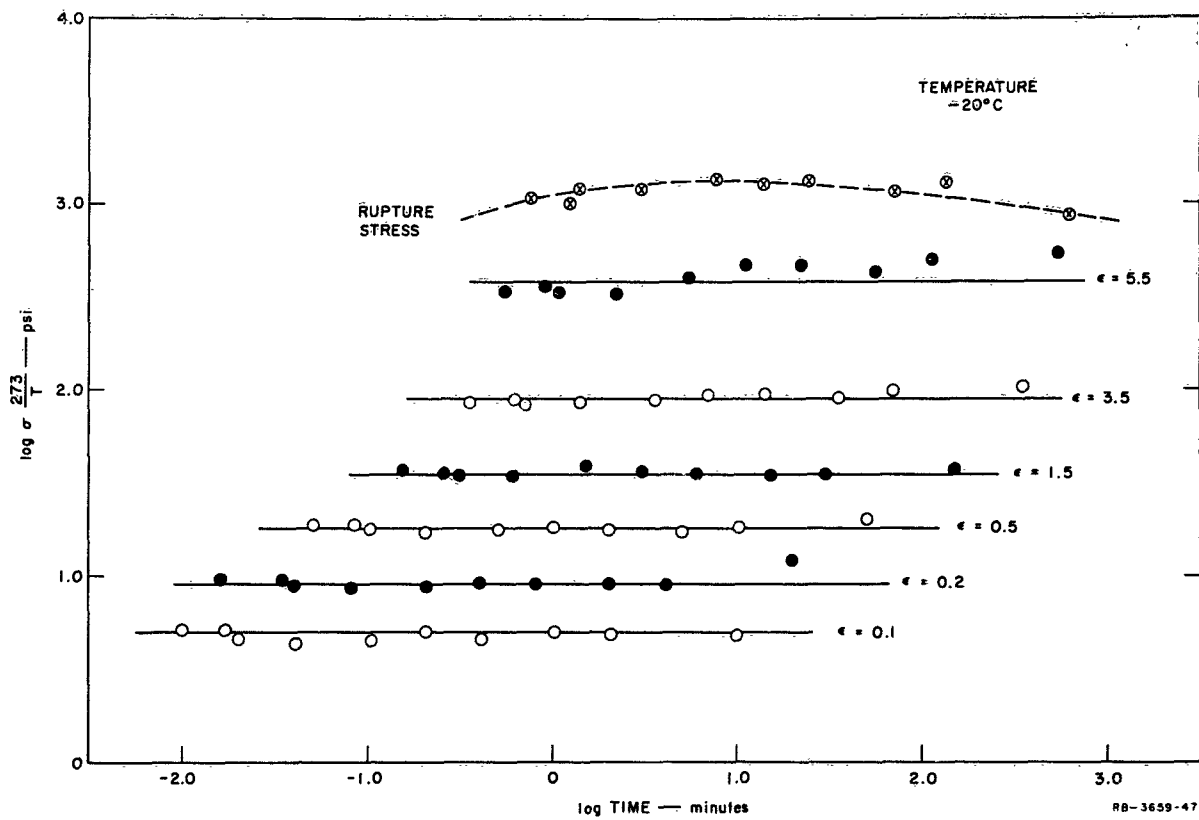


FIG. 13 TENSILE STRESS-STRAIN DATA FOR NATURAL RUBBER AT  $-20^{\circ}\text{C}$  PLOTTED AS  $\log \sigma \frac{273}{T}$  vs.  $\log t$  FOR VARIOUS FIXED VALUES OF STRAIN

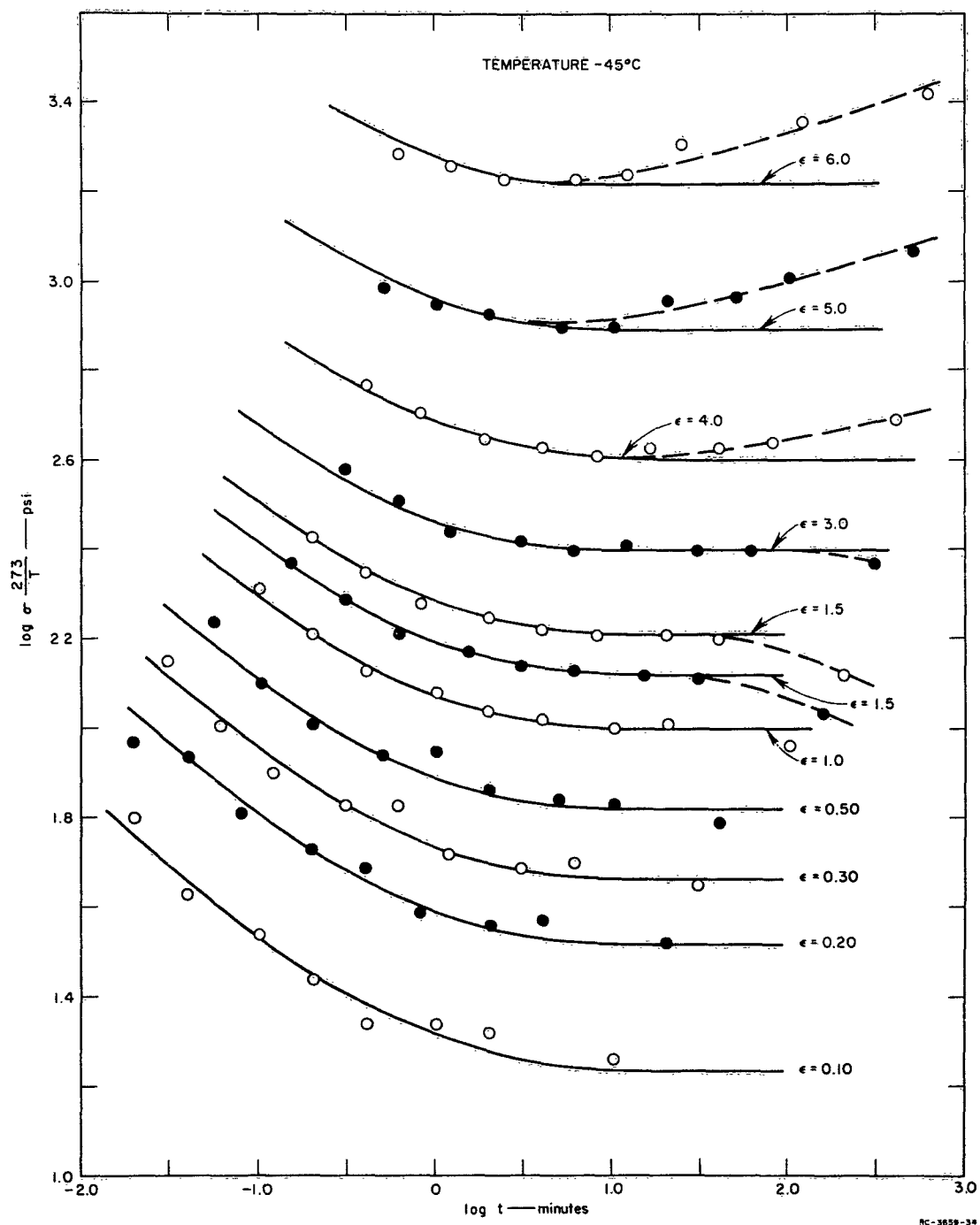


FIG. 14 TENSILE STRESS-STRAIN DATA FOR NATURAL RUBBER AT -45°C PLOTTED AS  $\log \sigma \frac{273}{T}$  vs.  $\log t$  FOR VARIOUS FIXED VALUES OF STRAIN

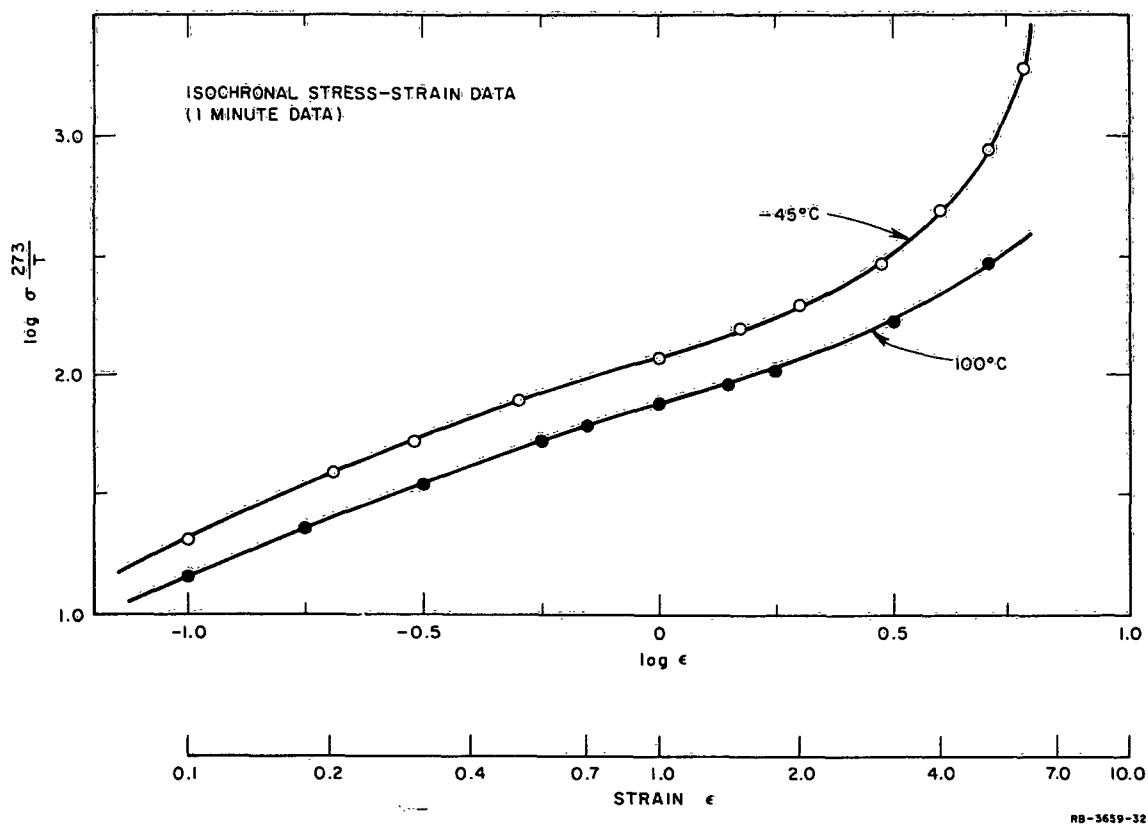


FIG. 15 ISOCHRONAL STRESS-STRAIN CURVES FOR NATURAL RUBBER AT  $100^{\circ}$  AND  $-45^{\circ}\text{C}$

In making plots to analyze the stress-strain behavior at  $100^{\circ}\text{C}$ , specially corrected values of  $\sigma$  and  $\epsilon$  were used. As used throughout this report,  $\sigma$  at any temperature is defined as the force divided by the cross-sectional area of the specimen at  $25^{\circ}\text{C}$ . Also,  $\epsilon$  at any temperature is the strain defined as  $\Delta l/l_0$  where  $\Delta l$  is the increase in length of the specimen and  $l_0$  is the length of the unstretched specimen at  $25^{\circ}\text{C}$ . Strictly speaking, however, values of stress and strain should be based on the dimensions of the specimen at the test temperature. It can be readily shown that  $\sigma$  and  $\epsilon$  can be converted into values based on the correct dimensions by the equations

$$\sigma_c = \frac{\sigma}{1 + \frac{2}{3} \alpha (T - T_0)} \quad (6)$$

$$\epsilon_c = \frac{\epsilon}{1 + \frac{\alpha}{3} (T - T_0)} \quad (7)$$

where  $\sigma_c$  and  $\epsilon_c$  are the corrected values of stress and strain,  $\alpha$  is the coefficient of cubical expansion of the material,  $T$  is the test temperature, and  $T_0$  is the temperature at which the dimensions of the specimen are measured.

For the natural rubber gum vulcanizate, it was found, as discussed in Appendix I, that  $\alpha = 5.9 \times 10^{-4} \text{ } ^\circ\text{C}^{-1}$ . Thus, Eqs. (6) and (7) show that at  $100^\circ\text{C}$ ,  $(\sigma_c/\sigma) = 1.030$  and  $(\epsilon_c/\epsilon) = 1.015$ . Accordingly, a 3% error is introduced in the stress and a 1.5% error in the strain by basing  $\sigma$  and  $\epsilon$  on the dimensions of a specimen at  $25^\circ\text{C}$ .

To evaluate the modulus at  $100^\circ\text{C}$ , a plot was first made of  $\lambda_c \sigma_c$  vs.  $\epsilon_c$ , as shown in Fig. 16. (Data used in preparing the plot were obtained from the lines in Fig. 12; thus each point in Fig. 16 represents average data obtained from a number of separate tests.) The quantity,  $\lambda_c \sigma_c$ , is the stress based on the actual cross-sectional area of a specimen, and for most elastomers, this quantity is directly proportional to the strain for strains up to about 0.6 to 1.0. Figure 16 shows that the points at elongations up to about 60% are defined by a straight line quite accurately. The slope corresponds to a Young's modulus,  $E$ , of 189 psi. If a plot had been made of  $\lambda \sigma$  vs.  $\epsilon$ , a modulus of 194 psi would have been obtained.

According to the kinetic theory of rubberlike elasticity, the equilibrium tensile stress-strain curve is given by the equation

$$\sigma = G \left( \lambda - \frac{1}{\lambda^2} \right) \quad (8)$$

where  $G$  is the shear modulus which equals  $E/3$ . Figure 17 shows that a plot of  $\sigma_c$  vs.  $\lambda_c - \lambda_c^{-2}$  defines a reasonably good straight line for small values of  $\lambda_c$  and the slope of this line gives  $G = 61.5$  psi or  $E = 184.5$  psi, which is in fair agreement with the value of 189 psi obtained from the plot in Fig. 16.

The Mooney-Rivlin equation for the large deformation tensile properties of a rubber is as follows:

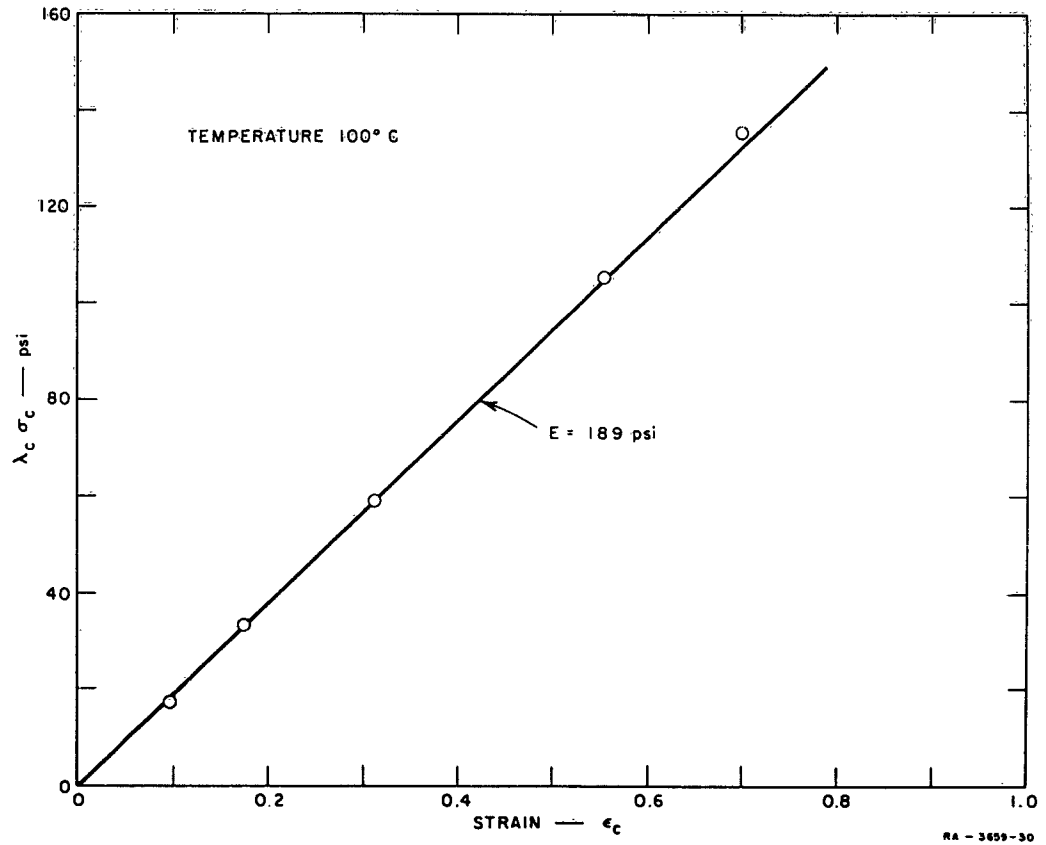


FIG. 16 PLOT OF TRUE STRESS  $\lambda_c \sigma_c$  AGAINST STRAIN  $\epsilon_c$  FOR NATURAL RUBBER AT 100°C (Values of Stress and Strain Based on Dimensions of Specimen at 100°C)

$$\sigma = 2G_1 \left( \lambda - \frac{1}{\lambda^2} \right) + 2G_2 \left( 1 - \frac{1}{\lambda^3} \right) \quad (9)$$

To evaluate the constants  $G_1$  and  $G_2$ , Eq. (9) is rearranged to give

$$\frac{\sigma}{\lambda - \lambda^{-2}} = 2G_1 + \frac{2G_2}{\lambda} \quad (10)$$

Thus, a plot of  $\sigma/(\lambda - \lambda^{-2})$  vs.  $\lambda^{-1}$  should yield a straight line whose slope is  $2G_2$  and whose intercept at  $\lambda^{-1} = 0$  is  $2G_1$ . In order for Eqs. (9) and (10) to be consistent with classical elasticity theory, the quantity  $(2G_1 + 2G_2)$  must equal the shear modulus  $G$ . Thus, in preparing the plot

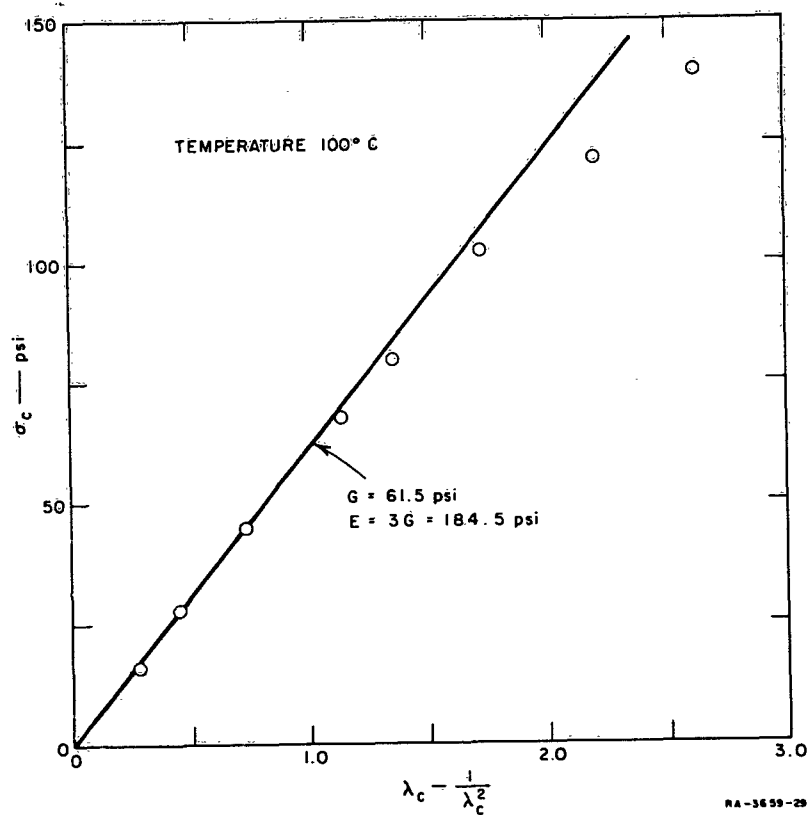


FIG. 17 PLOT OF  $\sigma_c$  vs.  $\lambda_c - \lambda_c^{-2}$  FOR NATURAL RUBBER AT 100°C

indicated by Eq. (10), the shear modulus is the quantity to be plotted at  $\lambda = 1$ .

Figure 18 shows a plot made to evaluate  $C_1$  and  $C_2$ . Because the shear modulus is known rather precisely from the plot in Fig. 16, the line in Fig. 18 has been drawn through the value of the shear modulus at  $\lambda = 1$ . From the slope and intercept of the line, it is found that  $2C_1 = 52.9 \text{ psi}$  ( $3.65 \times 10^6 \text{ dynes/cm}^2$ ) and  $2C_2 = 10.1 \text{ psi}$  ( $0.70 \times 10^6 \text{ dynes/cm}^2$ ).

There has been some discussion recently about the meaning of the  $C_2$  term, especially since its existence is not predicted by molecular theories. It has been suggested<sup>26</sup> that some fraction, if not all, of  $C_2$  may be caused by nonequilibrium effects and that if true equilibrium data were available,  $C_2$  would be close to zero, if not actually zero.

The limited data of Ciferri and Flory<sup>26</sup> on natural rubber shows that  $C_1/C_2$  increases as the test temperature is increased. For example, they

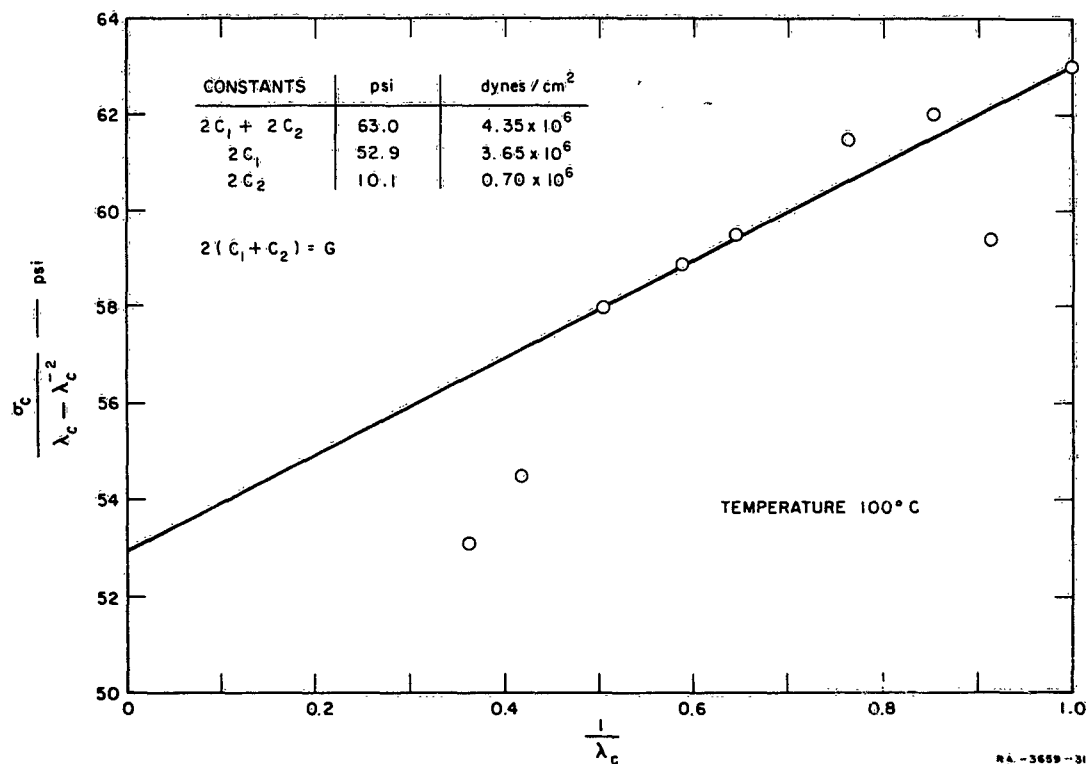


FIG. 18 PLOT OF STRESS-STRAIN DATA FOR NATURAL RUBBER AT 100°C TO EVALUATE THE CONSTANTS IN THE MOONEY-RIVLIN EQUATION

report that for one sample of natural rubber  $C_1/C_2$  is 1.20 at 34°C and is 1.34 at 59°C; data apparently were not determined at higher temperatures. Our results show that  $C_1/C_2$  is 5.2 at 100°C; hence, the contribution of  $C_2$  to the shear modulus is much less than observed by Ciferri and Flory. A further analysis of factors which affect  $C_2$  is planned as part of a subsequent program.

The strain function  $g(\epsilon)$  can be calculated according to Eq. (5) from stress-strain data and the modulus. The modulus at 100°C was found to be 189 psi, provided stress and strain data are based on the dimensions of a specimen at this temperature. Because values of stress and strain at all other temperatures were not corrected for the changes in dimensions effected by temperature and because such changes are relatively small, the subsequent analysis is conducted by using 194 psi for the modulus at 100°C; this value was obtained by basing the stress-strain data on the room temperature dimensions of a specimen.

As discussed in Section IV-C-3, equilibrium values of the stress at fixed values of the strain depend approximately on the absolute temperature according to the equation

$$\sigma = \sigma_0 \left( \frac{T}{T_0} \right)^{0.7} \quad (11)$$

where  $\sigma_0$  is the stress at a reference temperature  $T_0$  and  $\sigma$  is the stress at temperature  $T$ . Actually, at low strains the exponent is 0.87 but this decreases with increasing strain; a value of 0.7 is used here for convenience. The use of  $\sigma(273/T)$  for the temperature-reduced stress, as in Figs. 12-15, is somewhat incorrect; a better quantity would have been  $\sigma(273/T)^{0.7}$ . However, the use of  $\sigma(273/T)$  does not introduce any errors in the conclusions drawn thus far, and for the subsequent analysis, except for the analysis of tensile strength data, the somewhat better measure of temperature dependence is used. (Actually, the difference between  $(273/T)$  and  $(273/T)^{0.7}$  is relatively unimportant.)

For the evaluation of  $\log g(\epsilon)$  by using Eq. (5b), values of the modulus  $F$  are needed at the various temperatures. It was decided to use  $F(1,T)$  which is the 1-minute modulus at temperature  $T$ . After careful examination of the data, it was decided that values of  $F$  at all temperatures between 10 and 100°C are given accurately by the equation

$$F(1,T) = 194 \left( \frac{T}{373} \right)^{0.7} \quad (12)$$

where 194 is the modulus at 373°K (100°C).

However, to obtain  $F(1,T)$  at temperatures below 10°C, the 1-minute isothermal stress-strain curves, like those shown in Fig. 15, were shifted along the ordinate to effect superposition. In effecting superposition, greatest weight was given to points at values of  $\epsilon$  less than 1. From the shift distances relative to the curve at 10°C, values of  $F(1,T)$  were calculated, after subtracting in an appropriate manner the factor  $\log(273/T)$ . The resulting values\* as well as those for temperatures between 10 and 100°C are given in Table 2.

\* It should be emphasized that the moduli  $E$  and  $F$  are identical, provided stress and strain data are time independent, as shown in Figs. 12 and 13. If the data are time dependent, the  $F$  and  $E$  are related according to Eq. (4).

Computed values of  $\log g(\epsilon)$  are given in Table 3 and are plotted against temperature in Figs. 19 and 20. These figures show that  $g(\epsilon)$  is sensibly independent of temperature for strains of 1.0 and less, but it is definitely temperature dependent for all strains greater than 1.0. Figure 21 was constructed to show how  $\log g(\epsilon)$  varies with  $\log \lambda$  at five selected temperatures between  $-45$  and  $100^\circ\text{C}$ . The values of  $\log g(\epsilon)$  used in this figure were obtained from the solid lines in Figs. 19 and 20 and thus they are smoothed or average values.

Table 2

VALUES OF THE 1-MINUTE CONSTANT-STRAIN-RATE MODULUS FOR NATURAL RUBBER VULCANIZATE

| TEMPERATURE<br>( $^\circ\text{C}$ ) | $\log F(1)$        | $F(1)$ |
|-------------------------------------|--------------------|--------|
| 100                                 | 2.288              | 194    |
| 80                                  | 2.271              | 187    |
| 60                                  | 2.254              | 180    |
| 40                                  | 2.235              | 172    |
| 25                                  | 2.218              | 165    |
| 10                                  | 2.204              | 160    |
| -5 <sup>†</sup>                     | 2.151 <sup>†</sup> | 142    |
| -20                                 | 2.186              | 154    |
| -35                                 | 2.179              | 151    |
| -45                                 | 2.261              | 182    |

<sup>†</sup> For various reasons, it appears that  $F(1)$  at  $-5^\circ\text{C}$  may be slightly low; however, for computational purposes, the value given in the table was used.

The dotted line of unit slope in Fig. 21 is that which would result if  $\lambda\sigma$  is directly proportional to  $\epsilon$ . The values of  $\log \epsilon$  are seen to lie slightly below this line even for relatively small values of strain. This deviation may be surprising because the plot in Fig. 16 indicates that  $\lambda\sigma$  at  $100^\circ\text{C}$  is directly proportional to  $\epsilon$  for strains up to about 0.6. However, values of  $\log g(\epsilon)$  are average values obtained from Fig. 19, and the use of such values produces the apparent anomaly. Thus, it is possible that very precise data might show that  $g(\epsilon)$  is slightly temperature dependent over the entire range of strain.

In the study made previously<sup>20</sup> of an SBR gum vulcanizate, it was found that  $g(\epsilon)$  over the entire range of strain was independent of temperature (as well as independent of time) at all temperatures between  $-34.4$  and  $93.3^\circ\text{C}$ . At temperatures below  $-34.4^\circ\text{C}$  and for strains greater than unity,  $g(\epsilon)$  was temperature dependent in somewhat the same way as shown in Fig. 21 for natural rubber.

The results presented thus far show some interesting and perhaps surprising aspects about the large deformation properties of natural rubber. On the one hand, the plots of  $\log \sigma - 273/T$  vs.  $\log t$  at fixed values of strain and at temperatures between  $-20$  and  $100^\circ\text{C}$  yield lines of zero slope. This fact by itself implies that the data represent equilibrium stress-strain behavior. On the other hand, for values of  $\epsilon$  greater than 1,  $g(\epsilon)$  is found to depend on temperature. If the temperature dependence of stress-strain data is determined only by internal

Table 3  
VALUES OF  $\log g(\epsilon)$  FOR NATURAL RUBBER VULCANIZATE

| $\epsilon$ | $\log \lambda$ | $\log g(\epsilon)$ AT INDICATED TEMPERATURE °C |      |      |       |      |       |       |       |       |       |
|------------|----------------|------------------------------------------------|------|------|-------|------|-------|-------|-------|-------|-------|
|            |                | 100°                                           | 80°  | 60°  | 40°   | 25°  | 10°   | -5°   | -20°  | -35°  | -45°  |
| 0.1        | 0.041          | 0.07                                           | 0.06 | 0.05 | 0.095 | 0.03 | 0.07  | 0.06  | 0.02  | 0.05  | 0.03  |
| 0.25       | 0.097          | 0.11                                           | 0.10 | 0.09 | 0.10  | 0.11 | 0.10  | 0.08  | 0.09  | 0.08  | 0.08  |
| 0.50       | 0.176          | 0.18                                           | 0.18 | 0.17 | 0.17  | 0.19 | 0.17  | 0.16  | 0.16  | 0.16  | 0.15  |
| 0.75       | 0.243          | 0.23                                           | 0.24 | 0.23 | 0.23  | 0.25 | 0.22  | 0.22  | 0.23  | 0.23  | 0.22  |
| 1.0        | 0.301          | 0.28                                           | 0.28 | 0.27 | 0.28  | 0.29 | 0.26  | 0.27  | 0.29  | 0.26  | 0.27  |
| 1.5        | 0.398          | 0.35                                           | 0.37 | 0.34 | 0.35  | 0.36 | 0.32  | 0.34  | 0.35  | 0.34  | 0.32  |
| 2.0        | 0.477          | 0.40                                           | 0.41 | 0.38 | 0.40  | 0.39 | 0.37  | 0.37  | 0.38  | 0.36  | 0.36  |
| 3.0        | 0.602          | 0.43                                           | 0.43 | 0.41 | 0.42  | 0.40 | 0.40  | 0.37  | 0.36  | 0.34  | 0.36  |
| 4.0        | 0.699          | 0.42                                           | 0.41 | 0.40 | 0.40  | 0.30 | 0.29  | 0.28  | 0.26  | 0.42  | 0.25  |
| 5.0        | 0.778          | 0.39                                           | 0.38 | 0.34 | 0.34  | 0.30 | 0.13  | 0.13  | 0.098 | 0.058 | 0.08  |
| 6.0        | 0.845          | 0.32                                           | 0.31 | 0.24 | 0.23  | 0.18 | -0.07 | -0.26 | --    | --    | -0.16 |

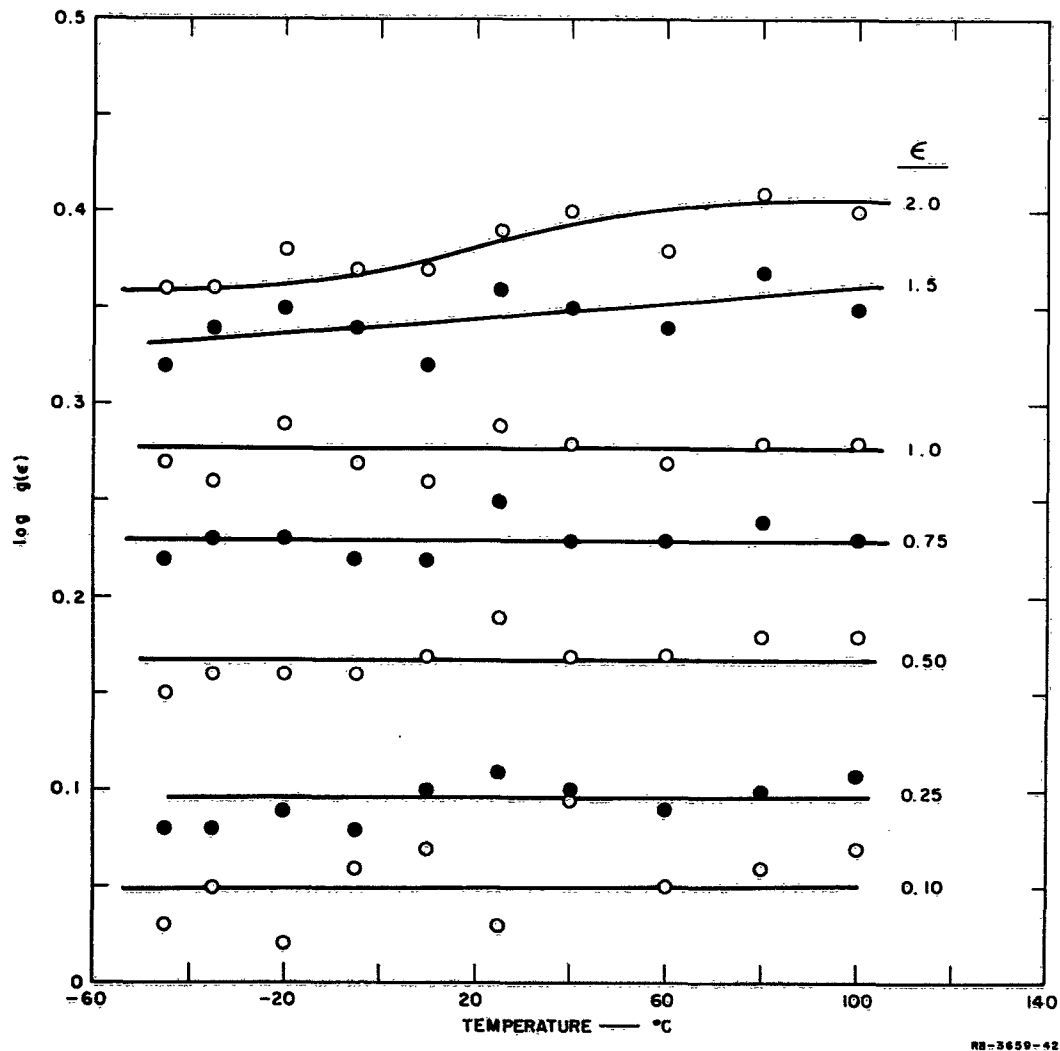


FIG. 19 PLOTS OF  $\log g(\epsilon)$  vs. TEMPERATURE FOR NATURAL RUBBER AT CONSTANT STRAIN VALUES BETWEEN 0.10 AND 2.0

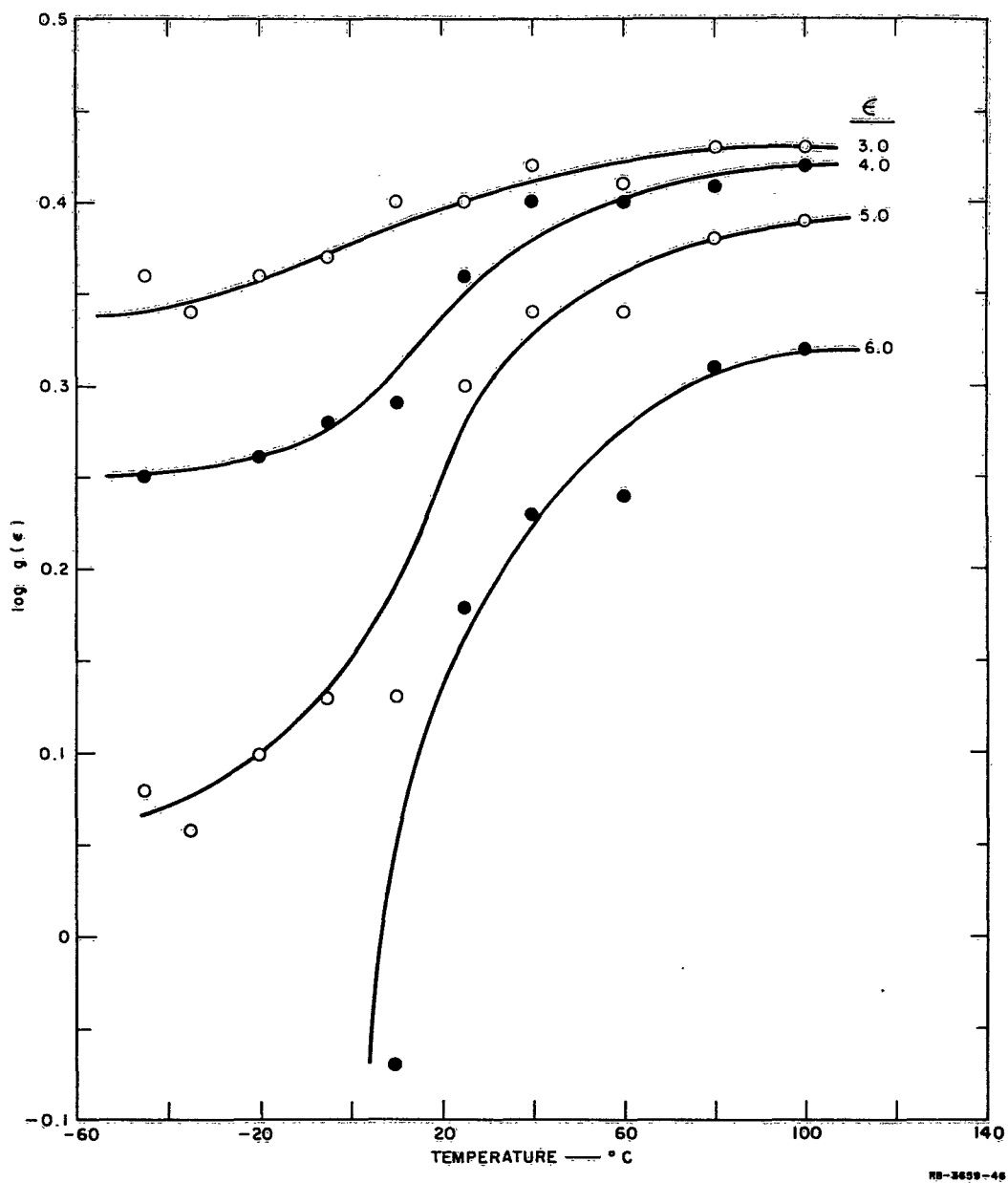


FIG. 20 PLOTS OF  $\log g(\epsilon)$  vs. TEMPERATURE FOR NATURAL RUBBER AT CONSTANT STRAIN VALUES BETWEEN 3.0 AND 6.0

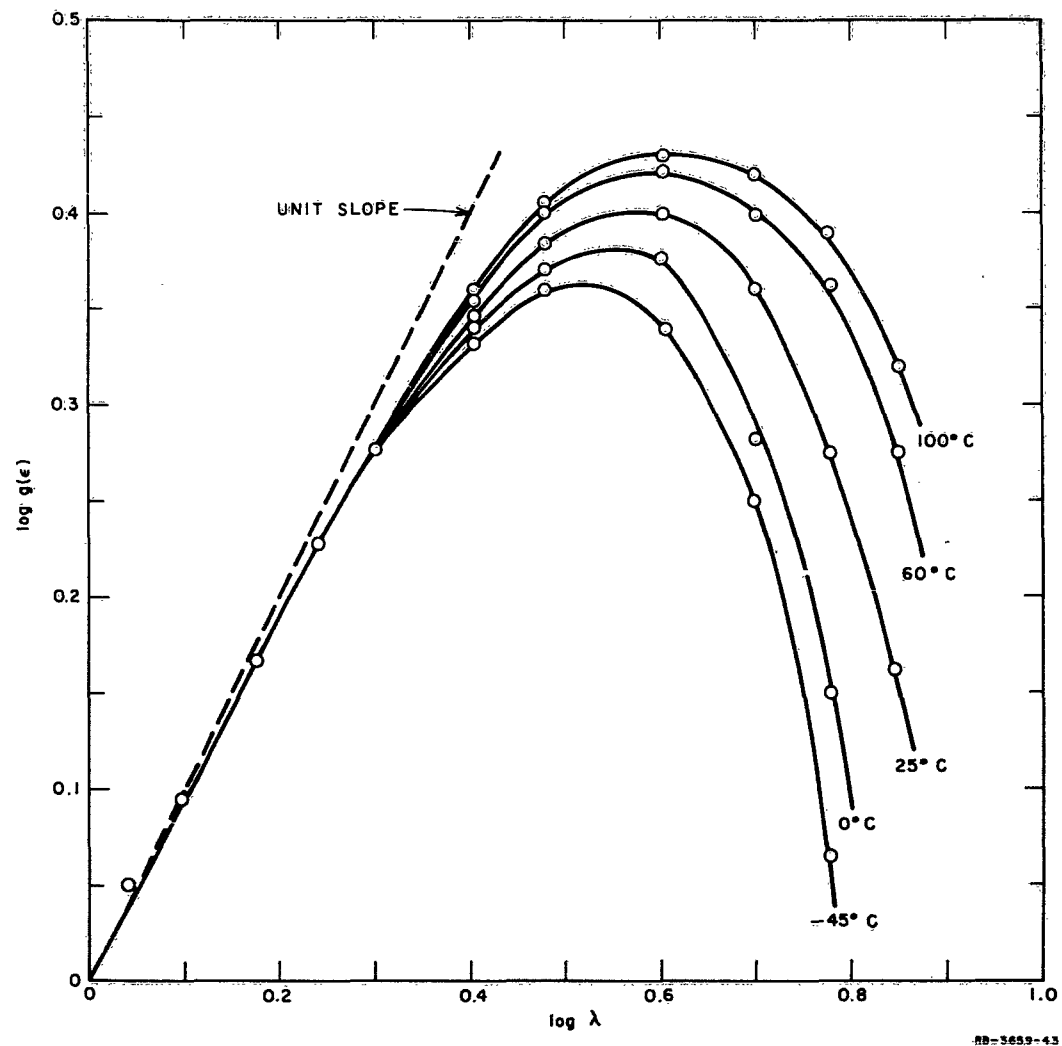


FIG. 21 PLOTS OF  $\log g(\epsilon)$  vs.  $\log \lambda$  FOR NATURAL RUBBER AT DIFFERENT TEMPERATURES BETWEEN  $-45$  AND  $100^\circ\text{C}$

viscosity, then time and temperature dependence must occur together. That is, if a mechanical property is dependent on time at temperature  $T$ , then within some temperature range  $T \pm \Delta T$ , that property must be temperature dependent if it is evaluated at a fixed value of time.

The large deformation properties of natural rubber are undoubtedly controlled largely by stress-induced crystallization.<sup>27</sup> However, at any temperature above about  $-20^{\circ}\text{C}$ , the degree of crystallization must depend primarily on the strain and the temperature (at least over the three decades of time covered by the present test method); otherwise quasi-equilibrium stress-strain behavior would not have been observed. In other words, the rate of stress-induced crystallization at the various strain values must be rapid compared with all rates at which specimens were stretched. However, the degree of crystallization at different values of strain must depend on the test temperature, otherwise  $g(\epsilon)$  would not have been found to be temperature dependent. If these statements about the crystallization phenomenon are correct, then it is quite likely that crystallization does not begin until the strain is reached at which  $g(\epsilon)$  becomes temperature dependent, i.e., about 100% elongation, as shown in Fig. 21. This conclusion is in essential agreement with the conclusions of Wood and Roth.<sup>27</sup>

It should not be generally inferred that crystallization is the sole cause for  $g(\epsilon)$  to be temperature dependent, especially since  $g(\epsilon)$  for SBR was found<sup>20</sup> to be temperature dependent at low temperatures. Because the stress-strain data for SBR were dependent on both time and temperature at all test temperatures below  $87.8^{\circ}\text{C}$ , this behavior shows that for SBR the nature of the dependence of stress on strain, time, and temperature is entirely different from that for the natural rubber vulcanizate.

For natural rubber, at temperatures between  $-20$  and  $100^{\circ}\text{C}$  and for elongations less than about 100%,  $g(\epsilon)$  is sensibly independent of temperature as well as time. Likewise, in this temperature range, the modulus (based on small deformation properties) is independent of time and temperature, except for the temperature factor  $T^{0.7}$  which arises from thermodynamic considerations.\* This behavior is in agreement with the well-known fact that hysteresis for natural rubber is low over an

---

\* As discussed in the following section, the factor appears to be  $T^{0.87}$  for strains less than 150%.

extended temperature range. It is also in agreement with the reported temperature dependence of the 10-minute stress-relaxation modulus evaluated at low strains (see p. 77 of Tobolsky's book.<sup>4</sup>) This modulus does not start to increase toward its glassy value until a temperature of about  $-40^{\circ}\text{C}$  is reached.

At temperatures of  $-35^{\circ}\text{C}$  and below, the internal viscosity of natural rubber influences the stress-strain properties, as indicated by the curvature in the plots of  $\log \sigma 273/T$  vs.  $\log t$  (see Fig. 14 which shows data at  $-45^{\circ}$ ). However, the points in Fig. 14 define parallel lines, which indicates that time and finite strain effects are separable, and thus crystallization apparently does not complicate the viscoelastic properties at this temperature. Figure 14 shows, however, that at long times and large values of  $\epsilon$ , some of the experimental values of stress lie above the solid lines. Although this behavior is probably caused by a crystallization rate effect, it may possibly be due to errors in the data.

Stress-strain curves determined at  $-55^{\circ}\text{C}$  could not be analyzed because of their odd shapes. Such data probably resulted from minor fluctuations in the temperature during the tests and also from some necking of the specimens. The latter phenomenon is deduced to have occurred in some instances because the stress-strain curves passed through a maximum at relatively low values of strain.

### 3. STRESS-TEMPERATURE COEFFICIENT

The classical theory of rubberlike elasticity is based on the premise that the internal energy of rubber depends only on its temperature and volume and not on its state of deformation. From this premise and from thermodynamic considerations, it follows that the retractive force in a specimen held at a fixed extension ratio is directly proportional to the absolute temperature.

Recently, Flory and coworkers<sup>28,29</sup> have considered the changes in internal energy that accompany the extension of real rubbers and have shown how this change can be derived from force-temperature data. They have shown that the fraction of the total retractive force which results from internal energy changes is given by

$$\frac{f_e}{f} = -T \left( \frac{\partial \ln f/T}{\partial T} \right)_{P,L} = \frac{\alpha T}{(\lambda^3 - 1)} \quad (13)$$

where  $f_e$  is the force resulting from the change in internal energy,  $f$  is the total retractive force, and  $\alpha$  is the coefficient of cubical expansion. The partial derivative in the brackets is evaluated at constant pressure and at constant length. To obtain the experimental data needed to evaluate  $f_e/f$ , the usual method employed is to maintain a specimen at some fixed length  $L$  and measure the retractive force as a function of temperature.

Although it was not mentioned by the authors,<sup>29</sup> Eq. (13) can be integrated under certain conditions to provide an equation which is more suitable for use in evaluating  $f_e/f$  from experimental data. To perform this integration, it is necessary to assume that  $f_e/f$ ,  $\alpha$ , and  $\lambda$  are independent of temperature. Over the range of temperature normally covered and for present purposes, these assumptions are valid to a high degree. Actually,  $f_e/f$  must be slightly temperature dependent, but it is unlikely that data of sufficient precision to show this dependence can be obtained. Also, for experiments made on a specimen maintained at constant length,  $\lambda$  must depend on temperature as  $\lambda$  is defined as the length of the stretched specimen at temperature  $T$  divided by the length of the unstretched specimen at the same temperature. However, because the term in Eq. (13) which contains  $\lambda$  is small compared with the main term, the error caused by neglecting the temperature dependence of  $\lambda$  is insignificant, except where  $\lambda$  is only slightly greater than unity.

Integration of Eq. (13), subject to the assumptions mentioned, leads to the following:

$$\frac{T}{2.303} \left( \frac{\alpha}{\lambda^3 - 1} \right) + \log f = \left( 1 - \frac{f_e}{f} \right) \log T + K \quad (14)$$

where  $K$  is the integration constant. Thus, a plot of the left side of Eq. (14) against  $\log T$  should yield a straight line whose slope equals  $(f - f_e)/f$ . Also, if data are obtained at different extensions, plots suggested by Eq. (14) should give a series of parallel lines, provided  $f_e/f$  is independent of extension. As shown by the data in Reference 29,  $f_e/f$  for certain polymers is sensibly independent of extension. This behavior is to be expected over certain ranges of extension ratio as long as special changes do not occur in the properties of the rubber, e.g., those caused by crystallization, dewetting of rubber from solid filler particles, etc.

From plots like those shown in Figs. 12 and 13, values of the stress were obtained at different strains and temperatures. These data are not as precise as those normally desired for use in evaluating  $f_e/f$ . The lack of precision is believed to result primarily from the relatively poor accuracy with which the cross-sectional areas of the specimens could be measured. However, each stress value is an average obtained from testing about 9 specimens.

Figure 22 shows stress-temperature data at strains between 0.50 and 3.0 plotted as suggested by Eq. (14). From stress-temperature data for natural rubber published by Wood and Roth<sup>27</sup>, Ciferri, Hoeve, and Flory<sup>29</sup> obtained  $f_e/f = 0.13 \pm 0.02$ . A cursory examination of the data of Wood and Roth<sup>27</sup> shows that this value applies only at small strains, i.e., approximately 50% and less. Because the data in Fig. 22 are not as precise as desired, the lines through the points at strains of 0.5, 1.0, and 1.5 have been drawn parallel and with a slope which corresponds to  $f_e/f = 0.13$ . The points are seen to lie quite close to the lines drawn. However, at strains greater than 1.5, lines of progressively decreasing slopes were drawn and these give values for  $f_e/f$  of 0.38, 0.48, and 0.57 at strains of 2.0, 2.5, and 3.0 respectively.

The above values for  $f_e/f$  are quite speculative and possibly are completely erroneous. The results of Wood and Roth<sup>27</sup> indicate that  $f_e/f$  should be zero at about 100% strain and should be negative at larger strains. The present results may be caused by (1) the use of stress values which are not equilibrium ones; (2) different degrees of crystallinity at the different temperatures, especially at the larger elongations; and (3) the presence of 5 parts of zinc oxide in the vulcanizate. Of these reasons, the second is most likely the correct one. Wood and Roth<sup>27</sup> conducted their experiments (on a vulcanizate without filler) in a manner such that data obtained at strains less than 150% were reversible. (They postulated that crystallization did not occur during tests made at strains less than 150%.) At strains between 150 and 500%, they encountered experimental difficulties but attempted to obtain data under as near reversible conditions as possible. In any event, the present results (Fig. 22) at strains above about 50% cannot now be interpreted and probably have little or no thermodynamic significance.

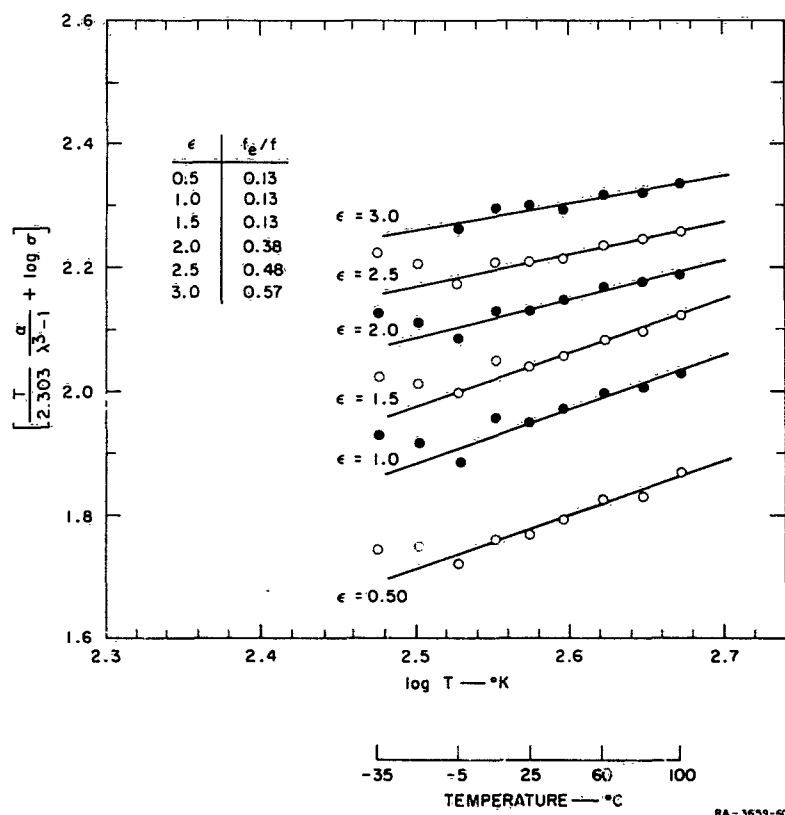


FIG. 22 PLOTS TO DETERMINE STRESS-TEMPERATURE COEFFICIENT FOR NATURAL RUBBER AT VARIOUS STRAINS

#### D. ULTIMATE TENSILE PROPERTIES OF VULCANIZATES OTHER THAN NATURAL RUBBER

In this section, an analysis is presented of the tensile strength ( $\sigma_b$ ) and the ultimate strain ( $\epsilon_b$ ) of the gum vulcanizates of butyl (sulfur cure), butyl (resin formulation), Viton B, and silicone. Because the ultimate tensile properties of the natural rubber vulcanizate varied with strain rate and temperature in a manner quite different from the other vulcanizates studied, the ultimate tensile properties of natural rubber are discussed separately in Section IV-E.

Ultimate tensile properties were measured on each vulcanizate at 9-11 temperatures and at 10 strain rates at nearly all temperatures; the results are tabulated in Appendix V. Although the stress-strain curves prior to rupture have not been analyzed in detail, the ones obtained at the highest test temperature for each vulcanizate have been examined by making plots of  $\log \sigma$  vs.  $\log t$ , like those shown for natural rubber in Fig. 12. For each vulcanizate, the plots yielded lines of zero slope. This behavior implies that little or no chemical degradation occurred during the test periods.

The ultimate property data were first analyzed in terms of the characteristic failure envelope. Subsequently, the time and temperature dependence were investigated by applying standard reduction procedures.

##### 1. FAILURE ENVELOPES

As mentioned in Section II-B, values of the tensile strength and ultimate strain determined at various strain rates and temperatures must define a single curve on a plot of  $\log \sigma_b T_0/T$  vs.  $\log \epsilon_b$  if time-temperature superposition is applicable to reduce the data to a single reference temperature. The resulting curve is called the failure envelope.

Some of the important aspects of the failure envelope have been presented previously.<sup>30,7,11</sup> For example, it has been shown<sup>30,7</sup> that delayed rupture is to be expected of a specimen subjected to either a constant strain or a constant stress provided either the constant strain or the constant stress exceed some critical value. It has also been shown<sup>11</sup> that the failure envelope obtained from ultimate property data determined under constant strain conditions is identical with the one obtained from data determined at constant strain rates. Thus, it appears

that the failure envelope is a material characteristic which is independent of the stress-strain-time history of a specimen. Further, in order for values of  $\sigma_b$  and  $\epsilon_b$  determined at different temperatures to superpose to yield a single failure envelope, it has been shown<sup>11</sup> that values of  $\sigma_b$  must be multiplied by the factor  $T_0/T$ ; otherwise a smooth continuous curve will not result. (This behavior can also be seen qualitatively by examining carefully the points on the failure envelopes discussed subsequently.)

The failure envelopes for the butyl-sulfur, butyl-resin, Viton B, and silicone vulcanizates are shown in Figs. 23-26. For each of the vulcanizates, the ultimate property data define quite precisely the

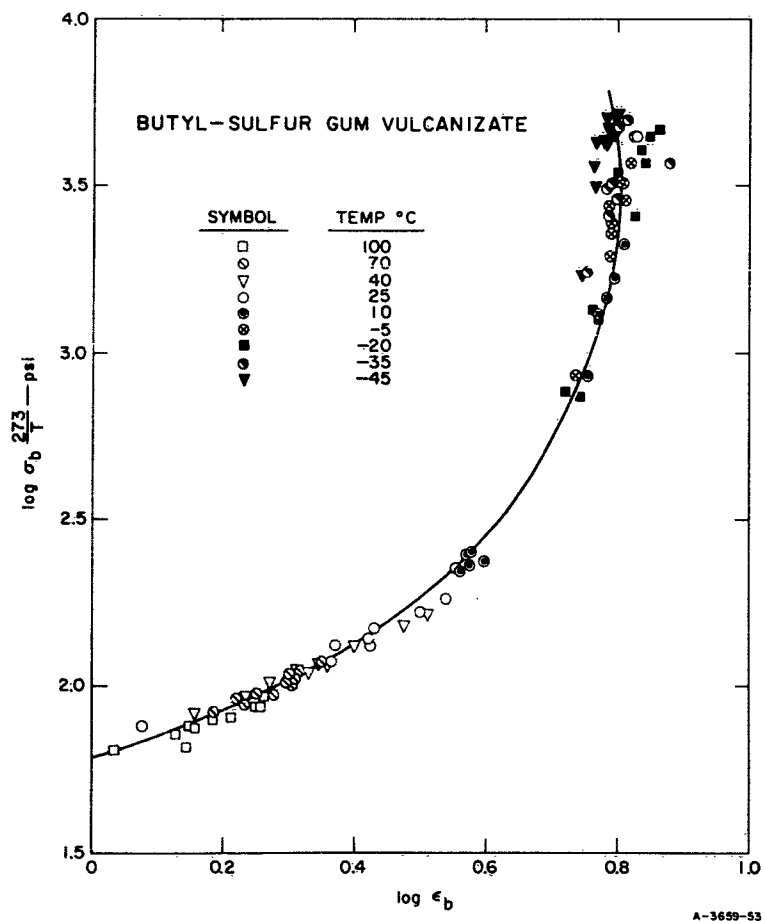


FIG. 23 FAILURE ENVELOPE FOR BUTYL GUM VULCANIZATE (Sulfur)

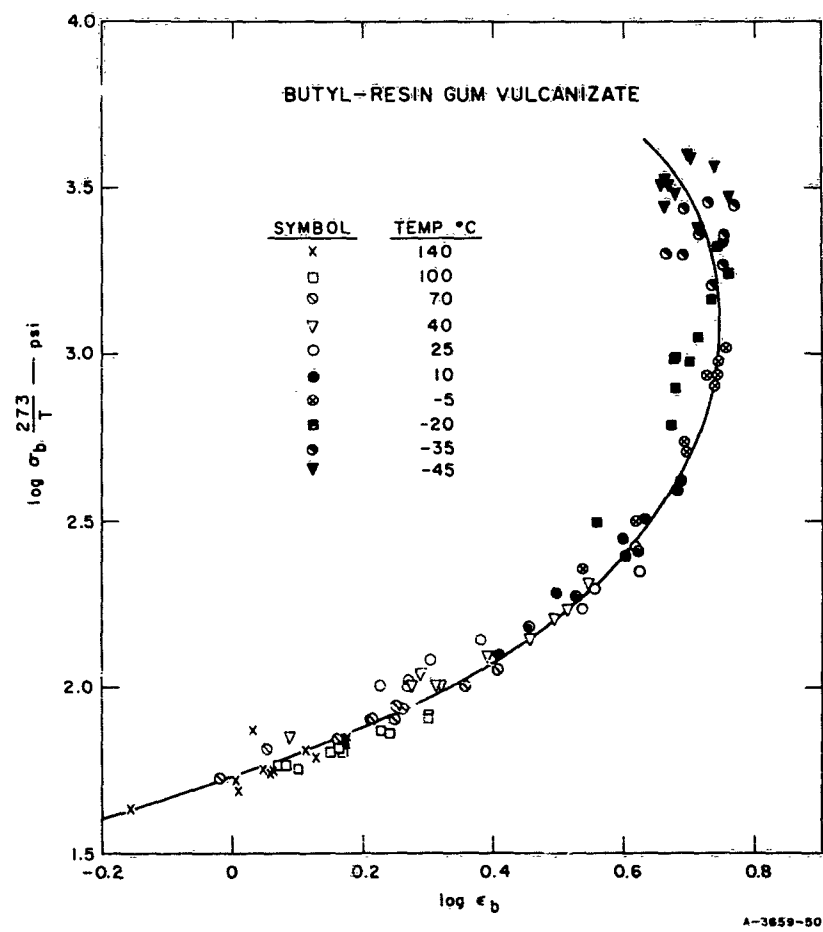


FIG. 24 FAILURE ENVELOPE FOR BUTYL GUM VULCANIZATE (Resin)

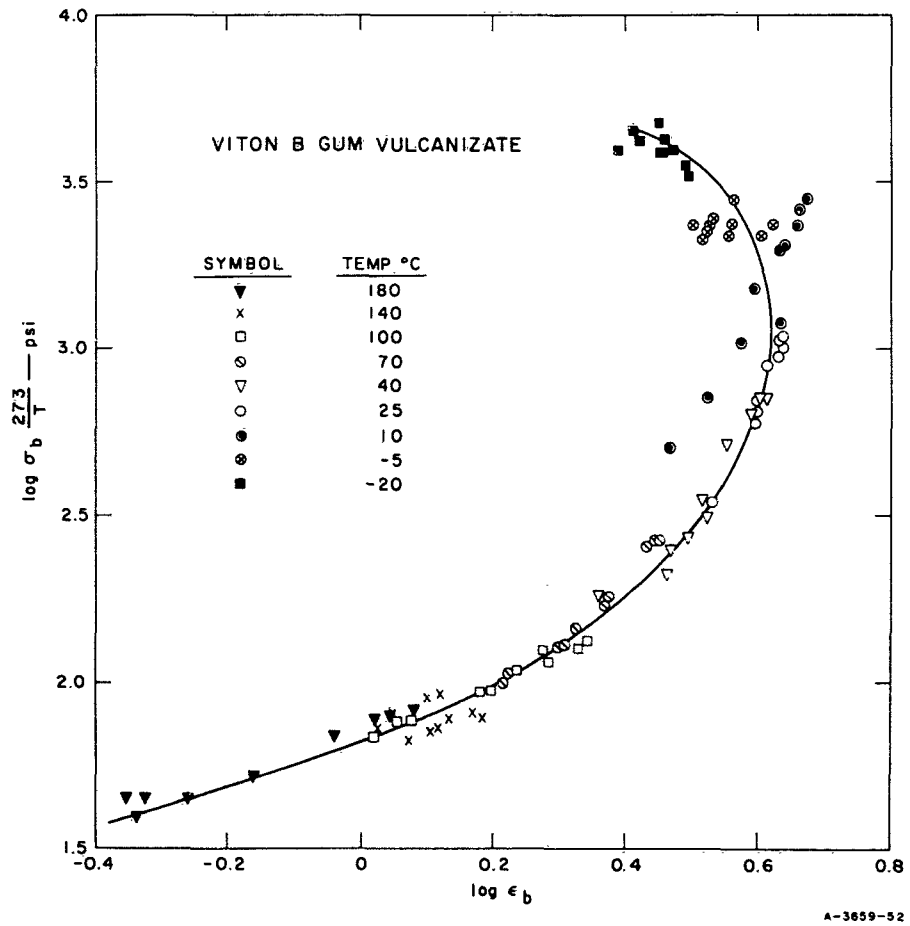


FIG. 25 FAILURE ENVELOPE FOR VITON B GUM VULCANIZATE

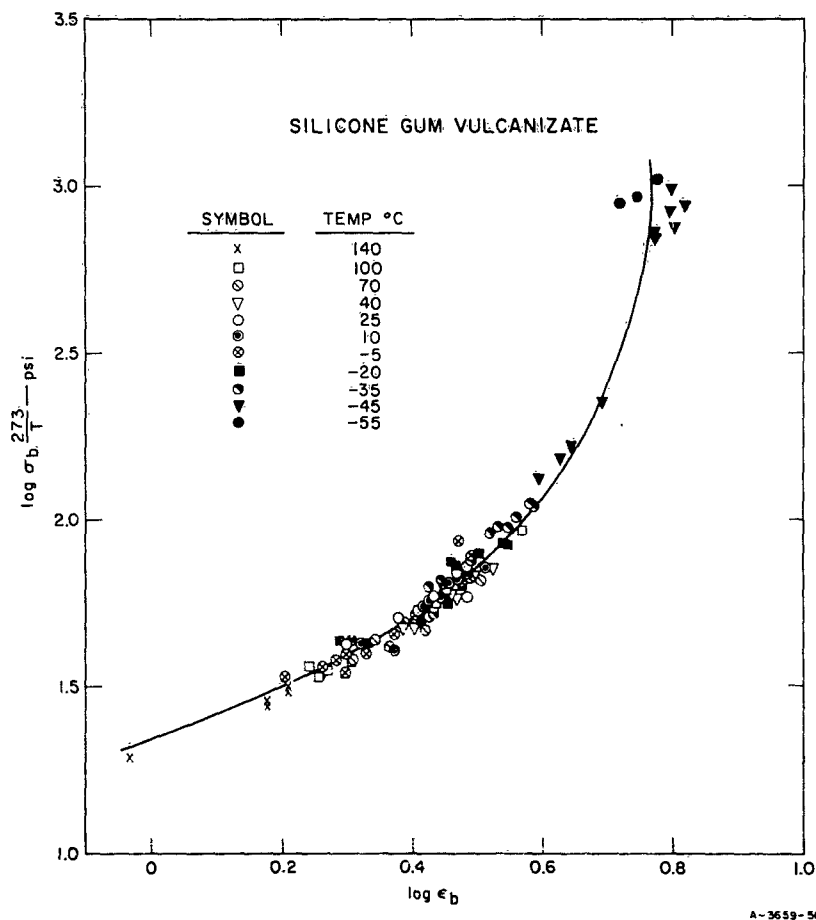


FIG. 26 FAILURE ENVELOPE FOR SILICONE GUM VULCANIZATE

failure envelopes shown. This precision is quite apparent if we note that by arbitrarily adjusting values of either  $\log \sigma_b \frac{273}{T}$  or  $\log \epsilon_b$  by 0.05 unit (a 0.05 logarithmic unit corresponds to a 12% change) essentially all of the points can be moved onto the lines. As ultimate property data are normally considered to show considerable scatter, a 12% variation in either  $\sigma_b$  or  $\epsilon_b$  seems quite small. Actually, most of the points lie even closer to the lines, especially those determined at all except the lowest two or three temperatures.

All observed values for the ultimate properties are shown in Figs. 23-26 except for values determined on the silicone vulcanizate at  $-65^\circ\text{C}$  and for values at four strain rates at  $-55^\circ\text{C}$ . These points were omitted because they showed considerable scatter; however, considerable

scatter is expected of data which represent ultimate properties as the glassy-like state is approached. In general, the scatter of data increases as the failure envelope is traversed counter-clockwise; as the envelope turns back towards low values of  $\epsilon_b$  at low temperatures or high strain rates, the data are often quite poor. This behavior can result from necking of the specimen, crystallization during or before a test, and heating of the specimen during a test.

## 2. TIME-TEMPERATURE REDUCTION OF ULTIMATE PROPERTY DATA

As already mentioned, if time-temperature reduction is applicable to ultimate property data, then the data must define a characteristic failure envelope. However, because data define a failure envelope, it does not follow that time-temperature reduction is applicable. In other words, data may vary somewhat erratically with strain rate and temperature, yet the values of the ultimate properties can all lie on a single failure envelope.

To analyze the time and temperature dependence of  $\sigma_b$  and  $\epsilon_b$  for the vulcanizates now being considered, data at each test temperature were first plotted as  $\log \sigma_b 273/T$  vs.  $\log t_b$  and  $\log \epsilon_b$  vs.  $\log t_b$ , where  $t_b$  is the time-to-break and equals  $\epsilon_b/\dot{\epsilon}$  where  $\dot{\epsilon}$  is the strain rate. Then, the plots representing results at different temperatures were shifted along the  $\log t_b$  axis to effect superposition. The shift distance required to superpose a curve at temperature  $T$  with a curve at a reference temperature  $T_0$  equals  $\log a_T$ . If time-temperature reduction is applicable, it is expected that the same values of  $\log a_T$  should result from superposition of both  $\sigma_b$  and  $\epsilon_b$  data. Further, it is expected that  $\log a_T$  should depend on temperature in the manner predicted by the WLF equation, at least for temperatures up to about  $T_g + 100$  or  $T_g + 150$ .

For present purposes, the WLF equation<sup>5</sup> in the following form was used:

$$\log a_T = - \frac{8.86(T - T_g)}{101.6 + T - T_g} \quad (15)$$

where 8.86 and 101.6 are the so-called universal constants and  $T_g$  is the standard reference temperature which for many amorphous polymers is approximately equal to  $T_g + 50$ . Actually, the constants in Eq. (15) depend somewhat on the nature of the polymer, and if precise values of

$\log a_T$  are available, constants characteristic of a given polymer can be obtained and they can be related<sup>31</sup> to the fractional free volume of the polymer and to the thermal expansion coefficient of the free volume. However, for many purposes, it is satisfactory to use the universal constants and to consider  $T_s$  as an adjustable parameter. This approach is normally quite satisfactory unless precise values of  $a_T$  are available and such cannot be expected to result from the superposition of ultimate property data. (For a general discussion of the temperature dependence of linear viscoelastic properties and the WLF equation, Chapter 11 of Ferry's book<sup>31</sup> should be consulted.)

In the previous work<sup>6,10</sup> done to superpose ultimate property data, the data were plotted against  $-\log \dot{\epsilon}$  and these curves at different temperatures shifted to effect superposition. From a certain viewpoint,<sup>11</sup> it seems that ultimate property values should be plotted against  $\log t_b$  and that such plots should be used to evaluate the applicability of time-temperature reduction. However, it has not been shown which type of plot is the most satisfactory from a practical standpoint. In analyzing the present data, only plots of the data against  $\log t_b$  were used; ideally, plots of the data against  $-\log \dot{\epsilon}$  should have been tested.

*Butyl Gum Vulcanizate (Sulfur).* In considering the ultimate property data for this vulcanizate, it appeared that somewhat more reliable values for the shift factor  $a_T$  could be obtained from plots of  $\log \sigma_b$   $273/T$  vs.  $\log t_b$  than from plots of  $\log \epsilon_b$  vs.  $\log t_b$ . Thus, the present analysis is based on the tensile strength data.

Values of  $\log \sigma_b$   $273/T$  at temperatures between 25 and 100°C were shifted along the  $\log t_b$  axis and relatively good superposition was obtained. Likewise, values at the five temperatures between 10 and -45°C could be superposed provided, at each temperature, only the results at the lower strain rates (higher values of  $t_b$ ) were considered. However, the curve at 10°C could not be superposed with the one at 25°C. In order to make the composite curve constructed from the data at the four highest temperatures extend to form a continuous curve with the composite curve obtained from the data at the five lowest temperatures, it was necessary to displace the two curves by about four decades along the  $\log t_b$  axis.

When plotted against temperature, the values of  $\log a_T$  at the four highest temperatures yielded a smooth curve; likewise values of  $\log a_T$

at the five lowest temperatures yielded a smooth curve. Although each of these curves has the shape predicted by the WLF equation, a single curve of the expected shape could not be obtained when all values of  $a_T$  were referred to the same reference temperatures. Thus, a standard reference temperature of 248°K (-23°C) was chosen and an arbitrary discontinuity of 4.1 logarithmic units in  $\log a_T$  was introduced, as shown in Fig. 27.

The present analysis seems to show that the vulcanizate behaves as if  $T_s = 248^\circ\text{K}$ ; this value is reasonable because, if  $T_g$  is 50°C below  $T_s$ ,  $T_g$  should equal -73°C. This value for  $T_g$  agrees satisfactorily with -68°C obtained from the dilatometric data discussed in Appendix I. However, the analysis shows that the nature of the vulcanizate changes markedly between temperatures of 25 and -10°C. This change is probably caused by the occurrence of crystallization during tests—at least during some of the tests—at temperatures between 10 and -45°C.

Values of  $\log a_T$  from the curves in Fig. 27 were used to construct the reduced plots shown in Figs. 28 and 29. (It should be noted that  $\sigma_b$  has been reduced to 273°K whereas  $a_T$  equals unity at 248°K.) These figures

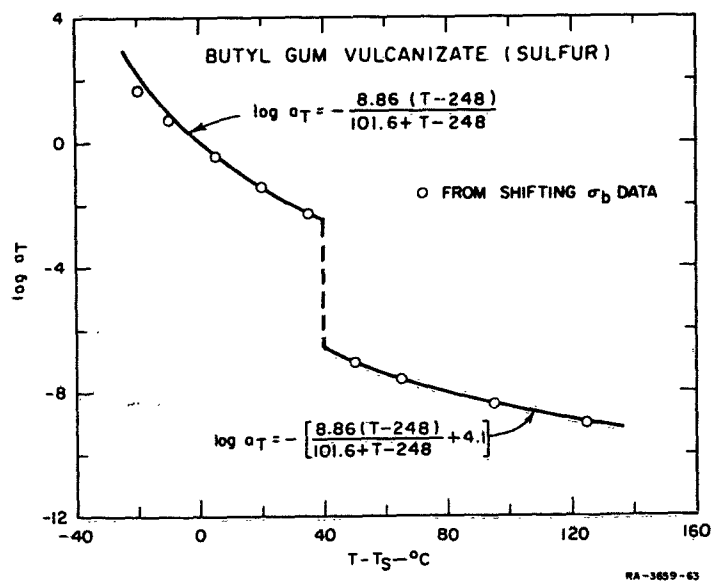


FIG. 27 TEMPERATURE DEPENDENCE OF  $\log a_T$  FOR BUTYL GUM VULCANIZATE (Sulfur)

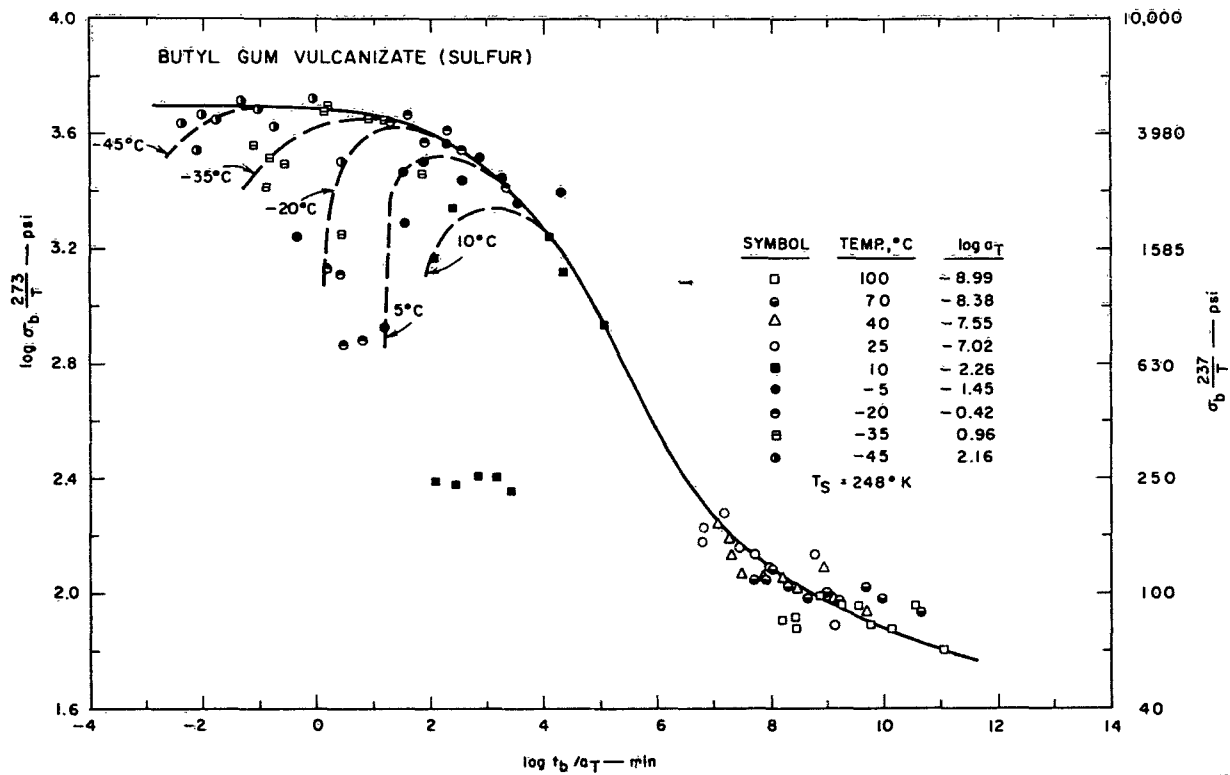


FIG. 28 PLOT OF  $\log \sigma_b \frac{273}{T}$  vs.  $\log t_b/a_T$  FOR BUTYL GUM VULCANIZATE (Sulfur)

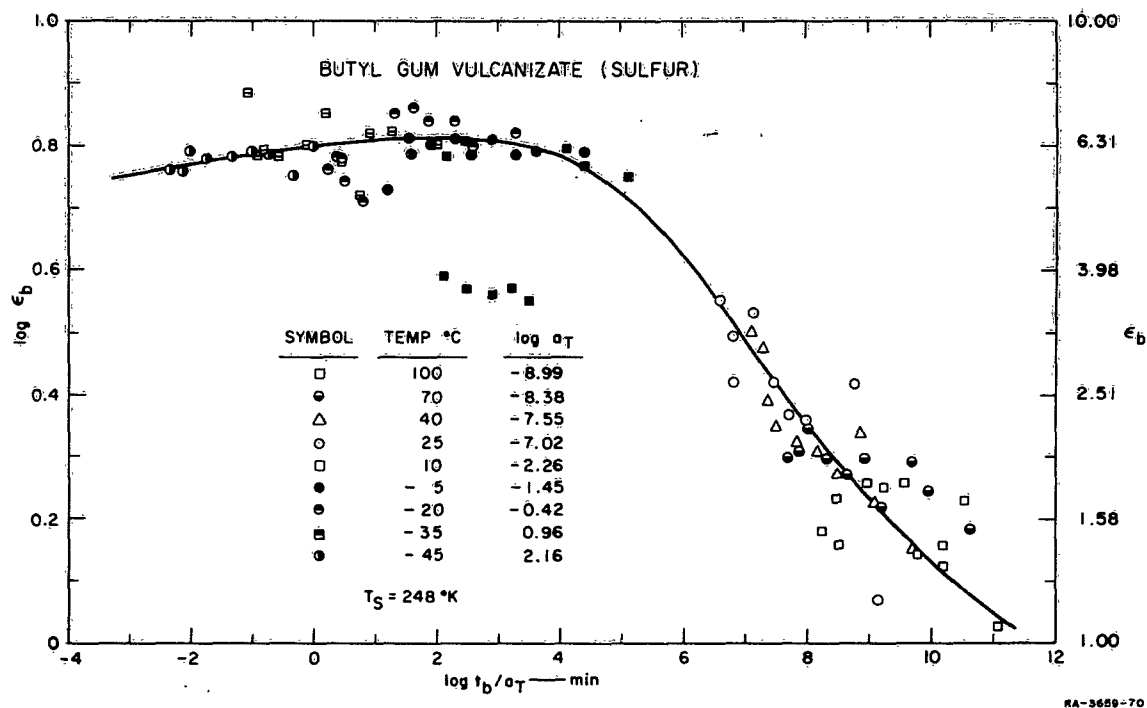


FIG. 29 PLOT OF  $\log \epsilon_b$  vs.  $\log t_b/a_T$  FOR BUTYL GUM VULCANIZATE (Sulfur)

show that values of  $\sigma_b$  and  $\epsilon_b$  at 25°C do not overlap those at 10°C. This behavior shows why it was not possible to apply time-temperature reduction in the normal manner. Figure 28 shows that at the lowest temperatures only the values of  $\sigma_b$  observed at the larger values of  $t_b$  lie along the solid line; the other values lie approximately along the dotted lines drawn for each temperature. On the other hand, Fig. 29 shows that most of the  $\epsilon_b$  values at the lowest temperatures lie quite close to the solid line.

Now let us compare the results shown by Figs. 27-29 with the failure envelope shown in Fig. 23. The plot in Fig. 23 shows that all values of the ultimate properties lie quite close to the line which is the failure envelope. However, it is quite apparent from Figs. 27-29 that time-temperature superposition is not applicable to reduce all data observed at temperatures between 10 and -45°C. Phenomenologically, this behavior can be explained by observing that values of  $\epsilon_b$  at temperatures between 10 and -45°C are relatively constant. Thus, even if values of  $\sigma_b$  vary considerably and in a random manner, they still will lie close to the failure envelope.

It is interesting to note that the points along the failure envelope form two groups: those whose values of  $\log \epsilon_b$  are less than 0.6 and those whose values are greater than about 0.8. However, half of the points from data obtained at 10°C form part of the lower group while the other half form part of the higher group. Those that are part of the lower group correspond to the five points in Figs. 28 and 29 (solid squares) which lie far below the lines drawn. Thus, it might be concluded that relatively little crystallization occurred during the tests conducted to determine these values. Also, the maxima in the dotted lines (Fig. 28) at the various temperatures probably occur because the amount of crystallization increases as the time-to-break increases; the decrease in tensile strength to the right of a maximum probably occurs for the same reasons that the tensile strength of a completely amorphous elastomer decreases with increasing time-to-break.

The results from the analysis are tentative and further studies will be required to determine more clearly the conditions under which crystallization occur and the effect of crystallization on the ultimate tensile properties. The reduced plots in Figs. 28 and 29 represent primarily a convenient method for showing all of the data; they cannot be used to interrelate quantitatively the effect of strain rate and temperature, except over certain restricted ranges of these variables.

*Butyl Gum Vulcanizate (Resin).* Superposition of the ultimate property data for this vulcanizate gave the values of  $\log a_T$  shown in Fig. 30. At the highest three temperatures (70, 100, and 140°C), values of  $\log a_T$  obtained by shifting the  $\epsilon_b$  data are considerably different from those obtained from shifting the  $\sigma_b$  data. However, at these temperatures, the slopes of plots of  $\log \sigma_b$ ,  $273/T$  vs.  $\log t_b$  and  $\log \epsilon_b$  vs.  $\log t_b$  were quite small; this, along with the normal scatter in ultimate property data, prevented an accurate evaluation of  $\log a_T$ . At the other temperatures, values obtained from shifting the  $\sigma_b$  data are in fair agreement with those obtained from shifting  $\epsilon_b$  data, although the agreement is not as good as desirable.

The values of  $\log a_T$  can be fitted, as shown in Fig. 30, by the WLF equation with  $T_s = 269^\circ\text{K}$ . This equation represents values of  $\log a_T$  obtained from the  $\epsilon_b$  data reasonably well, although values obtained from the  $\sigma_b$  data lie quite close to the dotted straight line. Because the WLF equation often is not applicable to data at temperatures greater than about  $T_s + 50$ , it is not known whether the solid or the dotted line is more reliable.

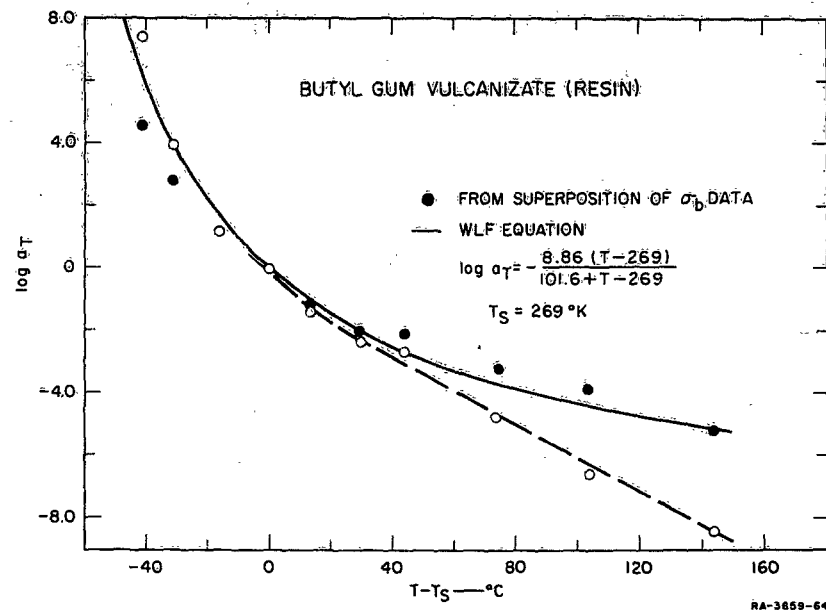


FIG. 30 TEMPERATURE DEPENDENCE OF  $\log a_T$  FOR BUTYL GUM VULCANIZATE (Resin)

The value  $T_s = 269^\circ\text{K} (-4^\circ\text{C})$  suggests that  $T_g$  is approximately  $-54^\circ\text{C}$ , which is  $11^\circ\text{C}$  higher than the value  $-65^\circ\text{C}$  obtained dilatometrically (Appendix I). However, by selecting  $T_s = 259^\circ\text{K}$  (which corresponds to  $T_g = -64^\circ\text{C}$ ), the WLF equation would fit the data shown by the solid circles in Fig. 30 as well as or perhaps better than by using  $T_s = 269^\circ\text{K}$ .

The reduced plots shown in Figs. 31 and 32 were constructed by using values of  $\log a_T$  predicted by the WLF equation with  $T_s = 269^\circ\text{K}$ . In these figures, values of  $t_b$  are reduced to  $269^\circ\text{K}$  but the values of  $\sigma_b$  in Fig. 31 are reduced to  $273^\circ\text{K}$ .

Although the points scatter about the lines drawn in Figs. 31 and 32, there is no gross evidence of inapplicability of time-temperature superposition. This behavior contrasts to that found for the butyl-sulfur vulcanizate. In other words, if crystallization occurred during any test, it did not affect to a significant extent values of  $\sigma_b$  and  $\epsilon_b$ .

*Viton B Gum Vulcanizate.* Of the vulcanizates studied during the current program, the ultimate properties of Viton B were found to be the most amenable to time-temperature superposition. Values of  $\log a_T$  obtained by

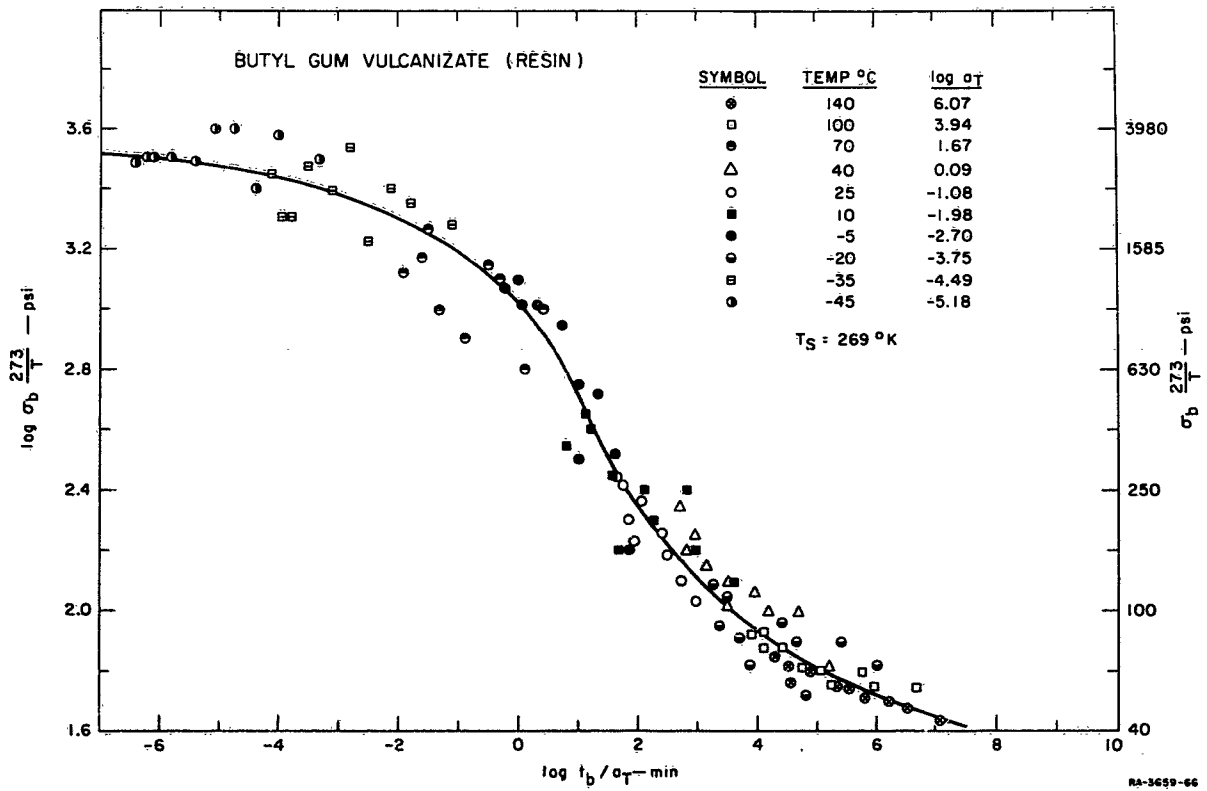


FIG. 31 PLOT OF  $\log \sigma_b \frac{273}{T}$  vs.  $\log t_b/a_T$  FOR BUTYL GUM VULCANIZATE (Resin)

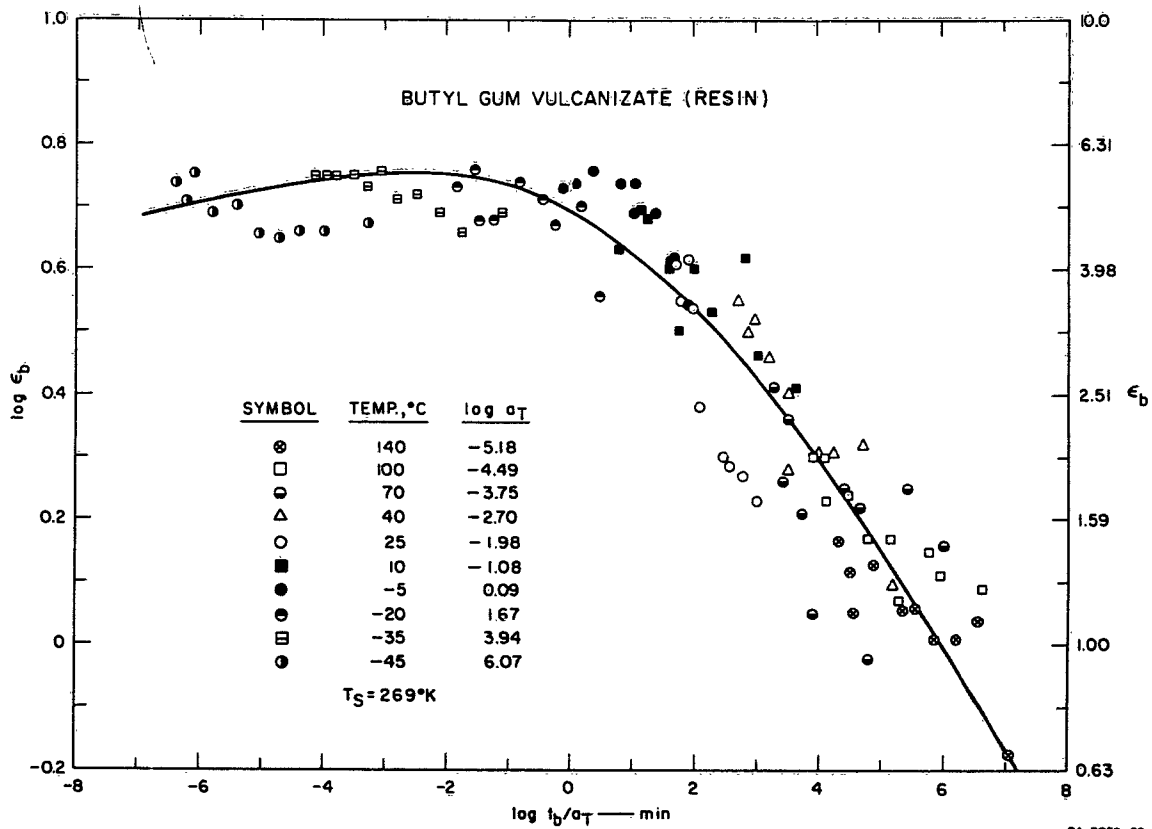


FIG. 32 PLOT OF  $\log \epsilon_b$  vs.  $\log t_b/a_T$  FOR BUTYL GUM VULCANIZATE (Resin)

shifting the  $\sigma_b$  data were in close agreement with those obtained from the  $\epsilon_b$  data. Thus, the averages of the two values are shown in Fig. 33 plotted against  $T - T_g$ , where  $T_g = 313^\circ\text{K}$  ( $40^\circ\text{C}$ ). The points are seen to lie on the solid line which represents the WLF equation with  $T_g = 313^\circ\text{K}$ . This close agreement exists even for the point obtained from data determined at  $180^\circ\text{C}$ .

The value of  $T_g$  obtained for Viton B seems somewhat high; it predicts a  $T_g$  of  $-10^\circ\text{C}$  which can be compared to a value of  $-37^\circ\text{C}$  obtained dilatometrically (Appendix I). This apparent discrepancy is presently of little concern, although it is of interest. As already mentioned, the constants 8.86 and 101.6 used in the WLF equation are the so-called universal values. The values of these constants have been found<sup>31</sup> to vary with the nature of the polymer. In the present study, the universal values are used and  $T_g$  is considered to be an adjustable parameter. By taking  $T_g = T_g + 50$ , or any other convenient value, new constants can be derived so that

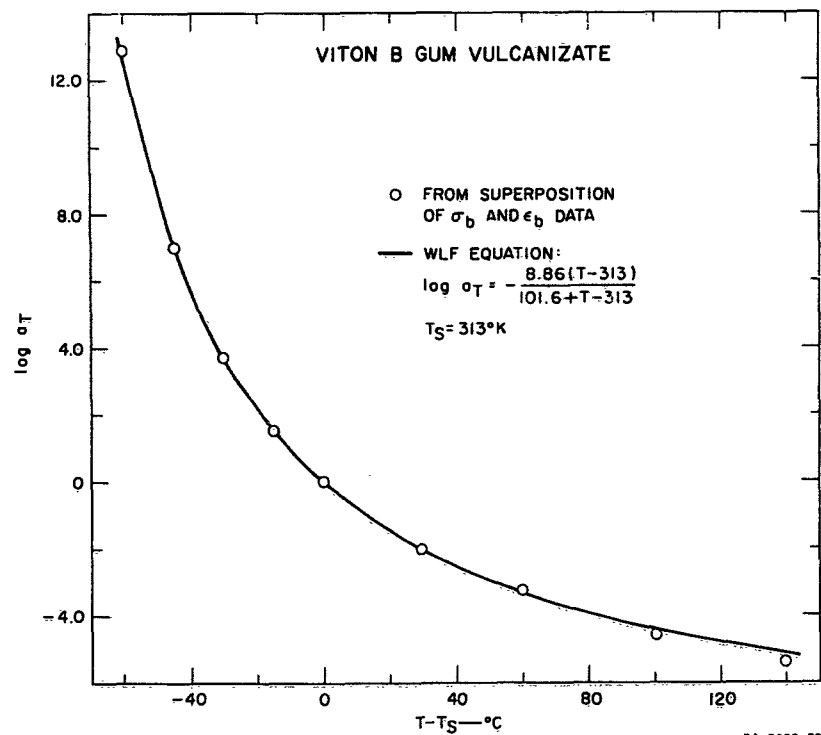


FIG. 33 TEMPERATURE DEPENDENCE OF  $\log a_T$  FOR VITON B GUM VULCANIZATE

experimental values of  $\log a_T$  fit the WLF equation. These constants can then be related to the fractional free volume at the reference temperature and to the coefficient of thermal expansion of the free volume. Because the physical properties of fluorinated materials are often found to be quite different than predicted by applying theories which are applicable to other types of materials, it is quite possible that the universal constants for the WLF equation do not apply to Viton B. If this is true, however, it appears that by choosing  $T_g$  properly, the universal constants provide an equation which represents quite accurately experimental values of  $\log a_T$ , as seen in Fig. 33.

Values of  $a_T$  given by the WLF equation (Fig. 33) were used to construct the reduced plots shown in Figs. 34 and 35. These figures show that the majority of the points lie quite close to the lines drawn. Actually, data obtained at 10°C do not fit closely the failure envelope shown in Fig. 25. (This behavior suggests that the data are in error, although no error could be found by checking the original Instron traces.) The same points which do not lie on the failure envelope are seen to lie some distance from the curves in Figs. 34 and 35. In addition, values of  $\epsilon_b$  observed at 140°C scatter about the curve in Fig. 35. If these points along with values of  $\sigma_b$  and  $\epsilon_b$  obtained at 10°C are excluded, essentially all remaining points are seen to lie quite close to the composite curves.

*Silicone Gum Vulcanizate.* Values of  $\log a_T$  obtained from superposing the ultimate property data are shown in Fig. 36 plotted against  $T - T_g$ . Data at -45, -55, and -65°C could not be superposed because they undoubtedly were affected by the occurrence of crystallization during tests at these temperatures. However, except at -45°C, crude estimates were made of  $\log a_T$ .

The WLF equation should not be expected to fit the values for  $a_T$  because measurements were made many degrees above  $T_g$  which for silicone<sup>32</sup> is about -120°C. However, the curve shown in Fig. 36 is predicted by the WLF equation with  $T_g = 203^\circ\text{K}$  which corresponds to  $T_g = -120^\circ\text{C}$  if  $T_g = T_g + 50$ . It is seen that this equation does not fit the experimental values.

Over a temperature range of about -20 to 100°C, the experimental values of  $\log a_T$  vary linearly with  $1/T$ , as shown in Fig. 37. The slope of the line gives an activation energy of 6.85 kcal. This value can be compared

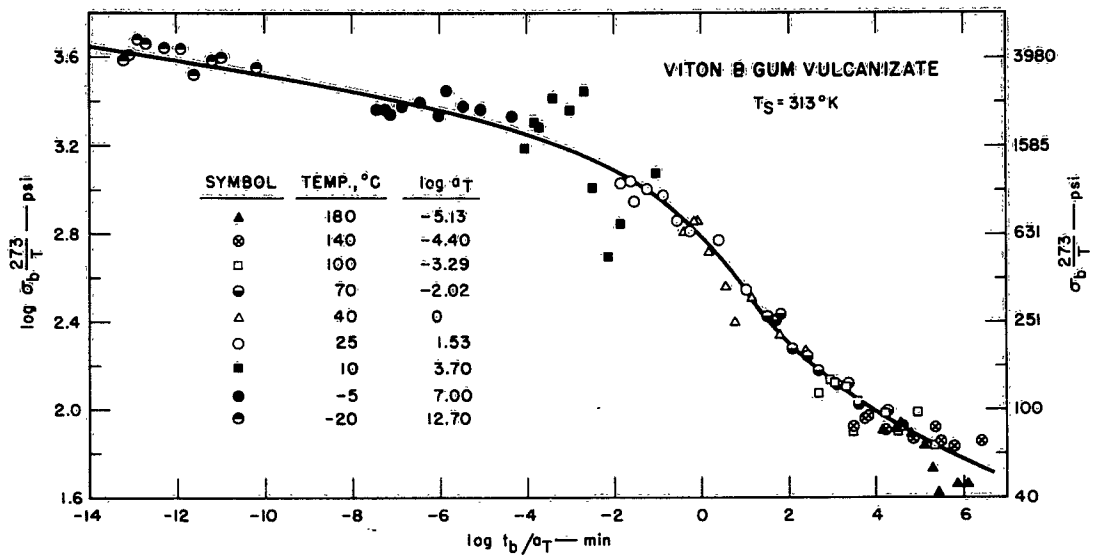


FIG. 34 PLOT OF  $\log \sigma_b \frac{273}{T}$  vs.  $\log t_b/a_T$  FOR VITON B GUM VULCANIZATE

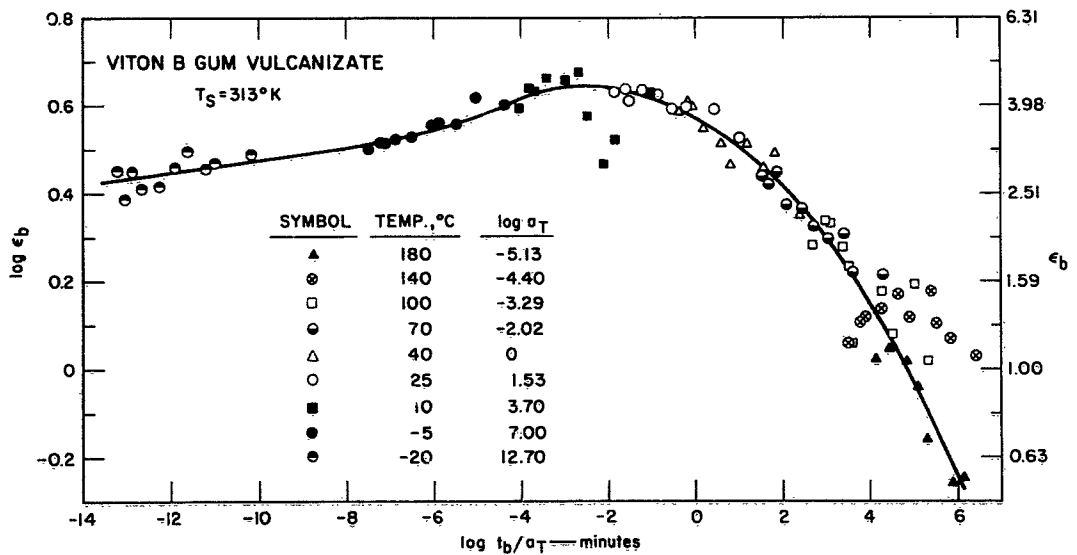


FIG. 35 PLOT OF  $\log \epsilon_b$  vs.  $\log t_b/a_T$  FOR VITON B GUM VULCANIZATE

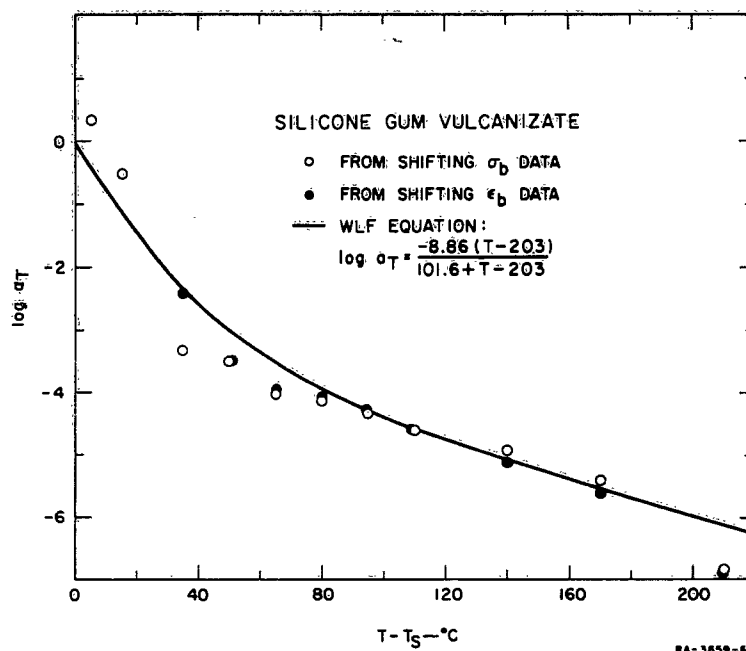


FIG. 36 TEMPERATURE DEPENDENCE OF  $\log a_T$  FOR SILICONE GUM VULCANIZATE

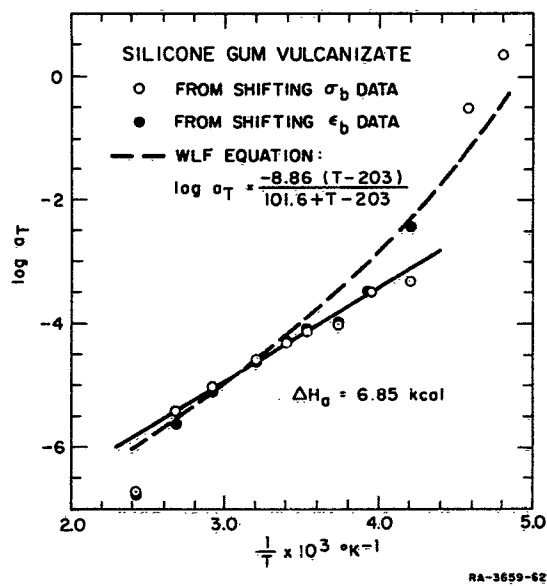


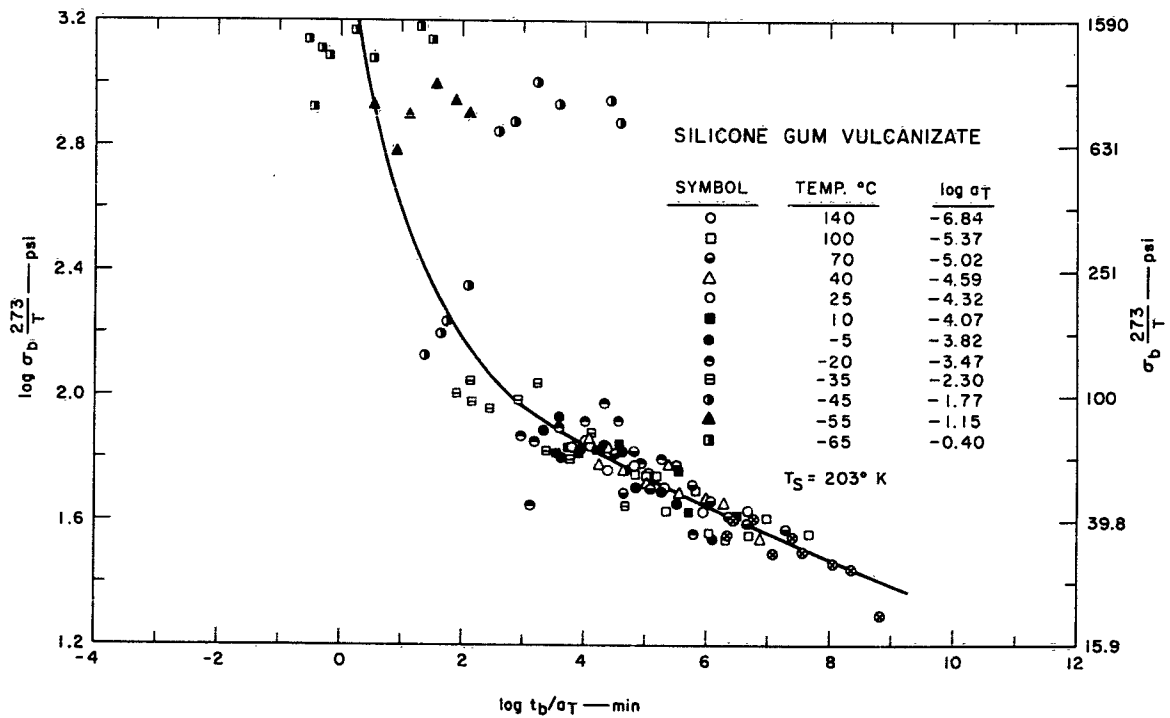
FIG. 37 PLOT OF  $\log a_T$  vs.  $1/T$  FOR SILICONE GUM VULCANIZATE

with 3.65 kcal obtained by Plazek, Dannhauser, and Ferry<sup>33</sup> on a noncross-linked silicone polymer whose  $\bar{M}_w = 4.1 \times 10^5$ . These workers measured viscosities by the falling ball method at temperatures between -43 and 141°C and they found that the activation energy was constant from -21 to 141°C. The present data give a constant activation energy over a similar temperature range, although the activation energy is lower than for the uncrosslinked silicone polymer.

For constructing the reduced plots, values of  $\log a_T$  were read from the solid line in Fig. 37 at temperatures between -20 and 100°C. At lower temperatures, values were obtained from the dotted line, and at 140°C, the experimental value was used. The resulting reduced plots are shown in Figs. 38 and 39.

Most of the data obtained at temperatures between -20 and 140°C are seen in Figs. 38 and 39 to lie reasonably close to the lines drawn. The data at lower temperatures scatter considerably. At -45°C, values of  $\epsilon_b$  are not shown as they would lie considerably above the solid lines. (Values of  $\log \epsilon_b$  ranged from about 0.60 to 0.82) It is interesting, however, that all points shown in Fig. 26 lie quite close to the failure envelope, although some of the data at -55°C and all data at -65°C have been omitted.

The erratic behavior at temperatures below -20°C are attributed to the occurrence of crystallization during the tests. Various studies<sup>32,34-37</sup> have been made of the crystallization of silicone rubbers and the results of these studies are in general agreement with the present observations. For example, Ohlberg, Alexander, and Warrick<sup>34</sup> studied a silicone, which contained 17% by volume of a fine silica filler, and reported that in its undeformed state no crystallization occurred at temperatures above about -55°C. However, at 320% strain, crystallization occurred at temperatures below about -27°C. Other work<sup>35,36</sup> has shown that a significant increase in tensile strength occurs when crystallization occurs. Thus, the increase in tensile strength and the marked decrease in ultimate strain found at low temperatures (Figs. 38 and 39) are consistent with previous work and are the result of crystallization.



RA-3659-65

FIG. 38 PLOT OF  $\log \sigma_b \frac{273}{T}$  vs.  $\log t_b/a_T$  FOR SILICONE GUM VULCANIZATE

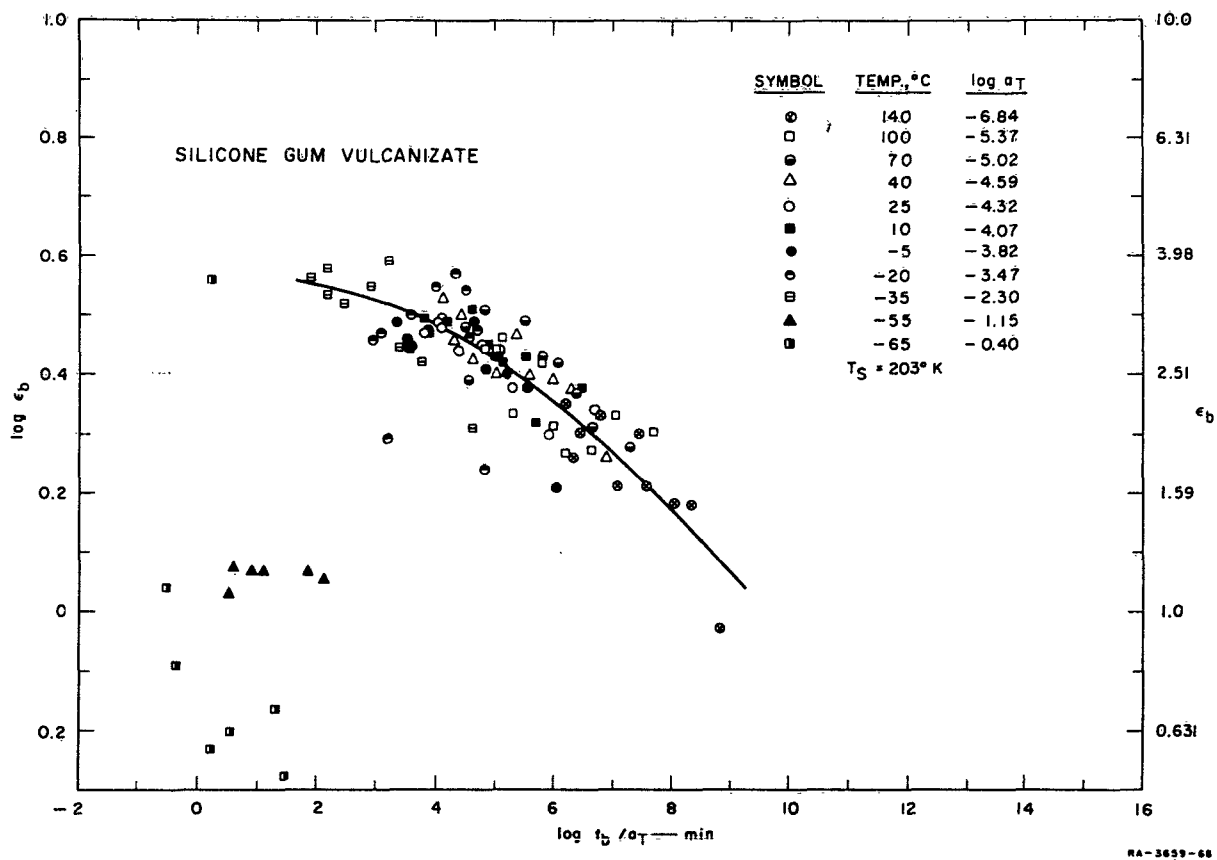


FIG. 39 PLOT OF  $\log \epsilon_b$  vs.  $\log t_b/a_T$  FOR SILICONE GUM VULCANIZATE

## E. ULTIMATE TENSILE PROPERTIES OF NATURAL RUBBER

Natural rubber vulcanizate is quite different from the other vulcanizates studied in that its tensile strength and ultimate strain remain high over a wide range of temperature. This difference probably results from the ability of natural rubber to crystallize readily under strain and at relatively high temperatures. Because of this known characteristic, it was expected that the ultimate tensile properties of natural rubber would not define a failure envelope and that time-temperature superposition would not be applicable to reduce such data.

### 1. FAILURE ENVELOPE

The ultimate property data of natural rubber are tabulated in Appendix V and are shown in Fig. 40 plotted as  $\log \sigma_b 273/T$  vs.  $\log \epsilon_b$ . The dotted lines show approximately the variation of the ultimate properties with strain rate at various temperatures between  $-45$  and  $80^\circ\text{C}$ . Along any one of these lines, a point tends to move upward as the strain rate is increased.

The solid lines in Fig. 40 are drawn through the points determined at the temperature extremes, *i.e.*,  $100$  and  $-55^\circ\text{C}$ . It is quite likely that these lines (especially the one through the  $100^\circ\text{C}$  data) represent the extremes of a characteristic failure envelope which would result if crystallization did not exert a controlling effect on failure at any temperature and strain rate. If the two solid lines are connected by a smooth curve, the over-all curve has the shape expected of a failure envelope which characterizes the properties of an elastomer like SBR (Fig. 1) and Viton B (Fig. 25) for which the internal viscosity controls the rate and temperature dependence of the ultimate properties.

The curve which represents the  $100^\circ\text{C}$  data shows an exceptionally large variation of the ultimate properties with strain rate. The tensile strength increases by a factor greater than 10 and the ultimate strain by a factor of nearly 2.5. That this variation is not caused by chemical degradation during the tests at this elevated temperature can be seen from the plots in Fig. 12. If degradation occurred, the lines in Fig. 12 would not have zero slope over the three decades of time which were covered.

To determine whether or not internal viscosity controls the variation of the ultimate properties of the natural rubber at high temperatures and

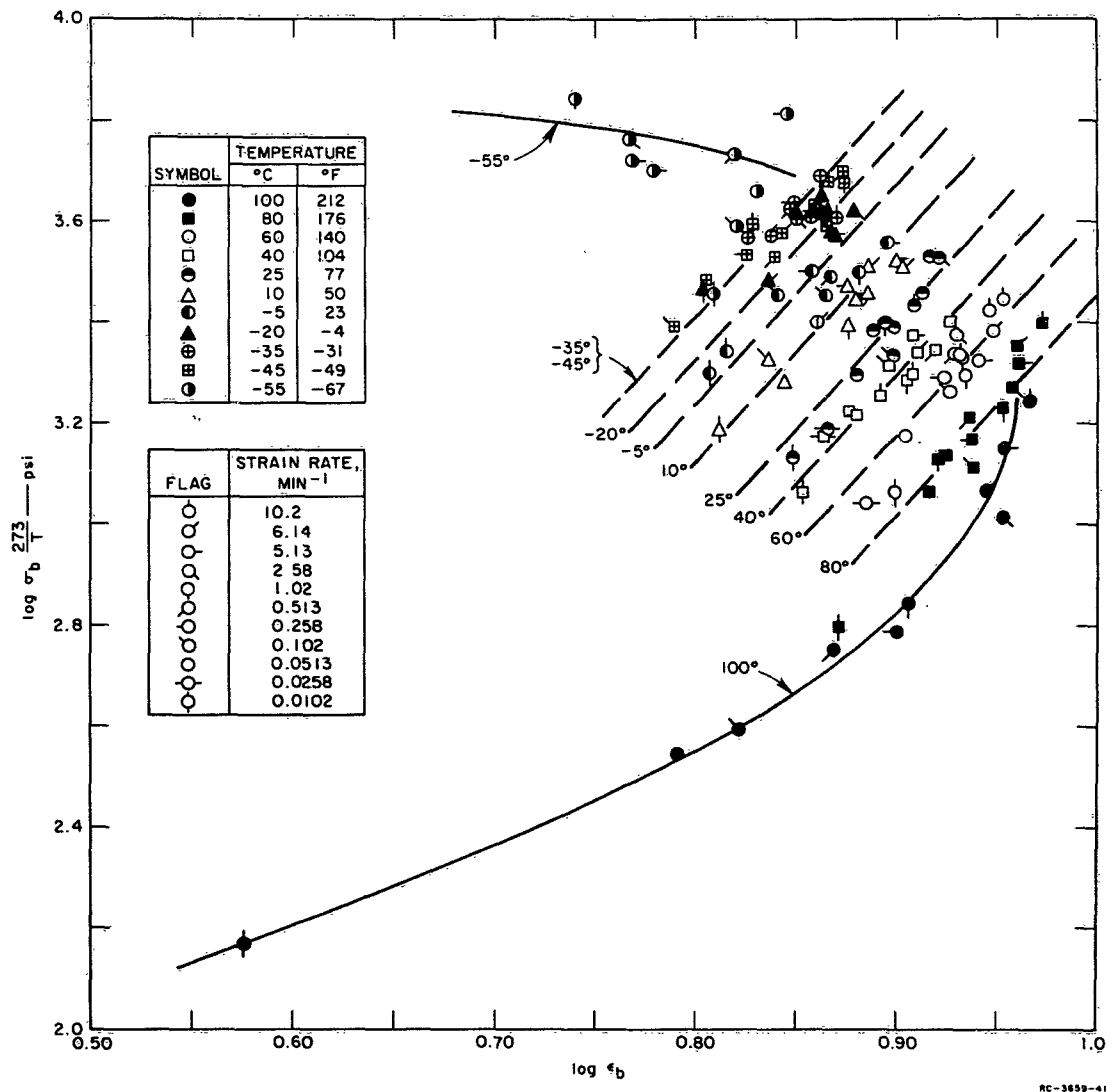


FIG. 40 ULTIMATE PROPERTIES OF NATURAL RUBBER PLOTTED AS  $\log \sigma_b \frac{273}{T}$  vs.  $\log \epsilon_b$

low rates, data at various strain rates are needed at temperatures above 100°C. Such tests would have to be made at sufficiently rapid strain rates so that thermal degradation would not occur during any of the tests. Such tests could probably be made at temperatures up to 120°C provided the tests required no more than perhaps 5-10 minutes. If the resulting data were found to fall on the solid curve in Fig. 12, such behavior would show that the curve represents a portion of the characteristic failure envelope for natural rubber.

Although further analysis of the data now available is needed along with additional data at elevated temperatures, some concluding, but somewhat speculative, remarks can be made about the meaning of the results shown by Fig. 40. The solid lines may be the extremes of a characteristic failure envelope. The area covered by the dotted lines results from the occurrence of crystallization prior to rupture. Further, if the degree of crystallinity depends only on the temperature and the strain and not on the strain rate, then the progressive displacement of the dotted line with temperature can be explained. (It may also be necessary to assume that the degree of crystallization does not change appreciably as the strain increases from about 6.3 to 9.0.) The possible explanation is that each dotted line is like a segment of the failure envelope of a different material and for each material the ultimate properties are controlled by viscous effects. This latter statement seems reasonable because the rupture point moves upward along any one of the lines as the strain rate is increased, as is expected. That this behavior is generally true can be seen from Fig. 40 or from the data tabulated in Table V-5. The data in the table show that at all temperatures, with the possible exception of -45°C, both  $\sigma_b$  and  $\epsilon_b$  increase with increasing strain rate. (The results at -45°C are not too reliable because of the occurrence of temperature fluctuations during some of the tests and because certain stress-strain curves appear to show that necking occurred.)

## 2. TEMPERATURE AND RATE DEPENDENCE OF ULTIMATE PROPERTIES

The ultimate property data were discussed above in relation to a plot of  $\log \sigma_b$ ,  $273/T$  vs.  $\log \epsilon_b$ . Although such a plot is perhaps the best single method for presenting ultimate property data, it does not show clearly and directly how the ultimate properties vary with temperature, strain rate, and time-to-rupture  $t_b$ .

Figures 41 and 42 show plots of  $\log \sigma_b$ ,  $273/T$  vs.  $\log t_b$  and Figs. 43 and 44 show plots of  $\log \sigma_b$  vs.  $\log t_b$ . (The quantity  $A$  is used along the ordinates to displace the curves so that they do not overlap.) The points are seen to lie rather close to the curves drawn, and consequently most of the data appears to be rather precise. Values of  $\epsilon_b$  appear to be exceptionally precise, as indicated by the fact that the majority of the points do not deviate from the lines by more than 0.01-0.02 logarithmic unit (this deviation corresponds to about 2.5-5.0%.)

Values of  $\sigma_b$  appear to be less accurately known than those for  $\epsilon_b$ . This difference is probably due to the rapid increase of the stress along a stress-strain curve immediately prior to rupture. Also, values of  $\sigma_b$  were obtained by extrapolating the Instron traces beyond the observed rupture point as explained in Appendix IV. Because of the high curvature immediately prior to rupture, the extrapolation is probably not highly reliable. Nevertheless, only a few of the  $\sigma_b$  values fall further than 0.05 logarithmic unit (12%) from the curves drawn.

Figures 41 and 42 show that at all temperatures  $\sigma_b$  increases with the strain rate (decreases with the time-to-break). The same behavior is observed for  $\epsilon_b$ , as shown in Figs. 43 and 44, with the exception of data at  $-55^\circ\text{C}$ . At this temperature,  $\epsilon_b$  appears to pass through a maximum with increasing rate. Such behavior is not unexpected as it must occur at some temperature because  $\epsilon_b$  in the glassy state is low.

Because many of the curves at different temperatures have similar shapes, it might appear that some of them could be shifted along the  $\log t_b$  axis to effect superposition. A close inspection, however, shows that superposition cannot be effected; in fact, Fig. 40 shows conclusively that the data are not amenable to time-temperature superposition.

Figures 45 and 46 show the temperature dependence of the  $\sigma_b$  and  $\epsilon_b$  data determined at four strain rates. The same curves are shown in Figs. 47 and 48 without the points and without the  $A$  factor. These latter figures show quite clearly that only a relatively small change occurs in  $\sigma_b$  and  $\epsilon_b$  over most of the temperature range.

#### F. COMPARISON OF ULTIMATE TENSILE PROPERTIES OF VULCANIZATES

The failure envelopes for the five vulcanizates discussed in this report are compared in Fig. 49. The curve for natural rubber represents

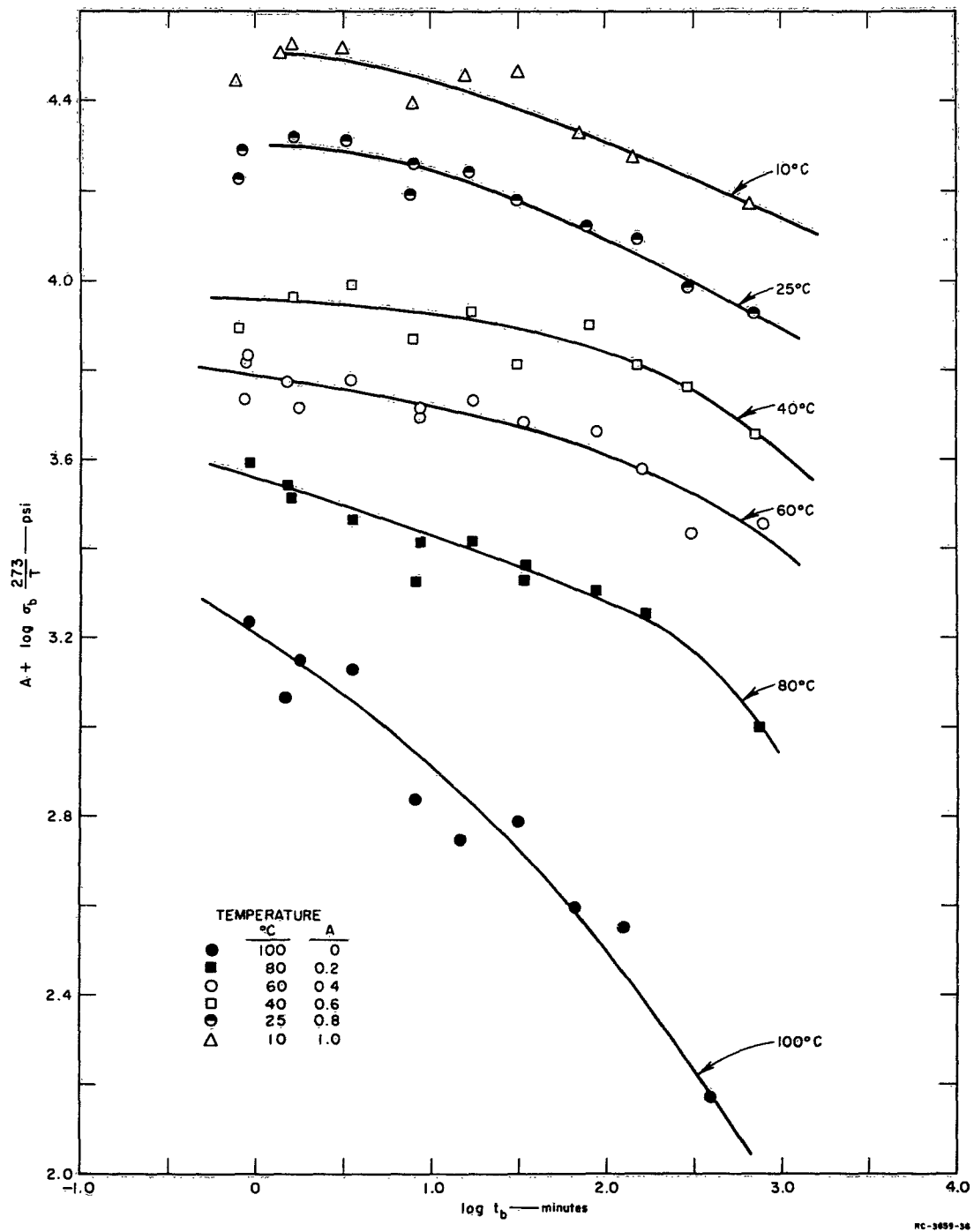


FIG. 41 DEPENDENCE OF TENSILE STRENGTH OF NATURAL RUBBER ON TIME-TO-BREAK AT TEMPERATURES BETWEEN 10 AND 100°C

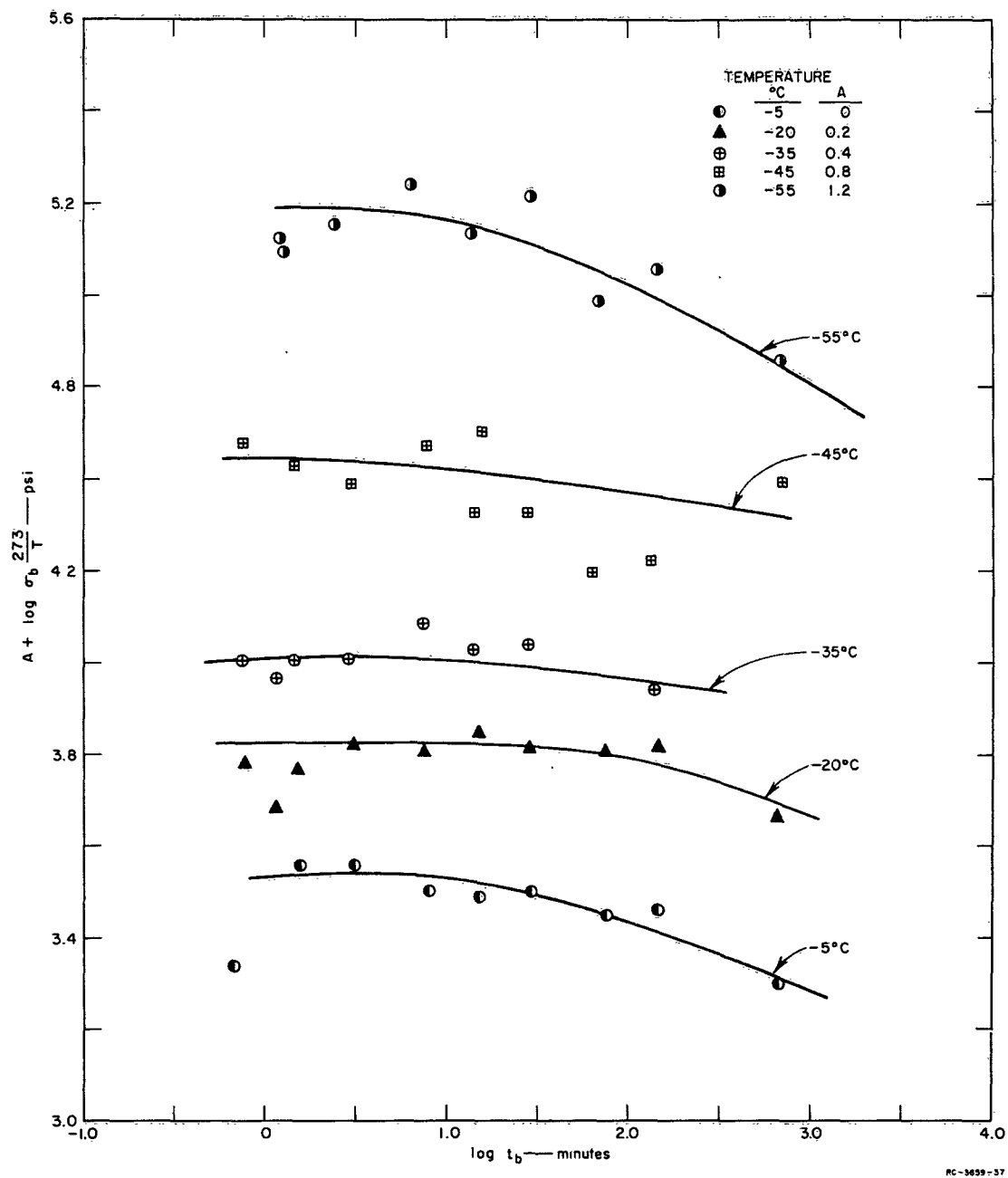


FIG. 42 DEPENDENCE OF TENSILE STRENGTH OF NATURAL RUBBER ON TIME-TO-BREAK AT TEMPERATURES BETWEEN  $-5$  AND  $-55^{\circ}\text{C}$

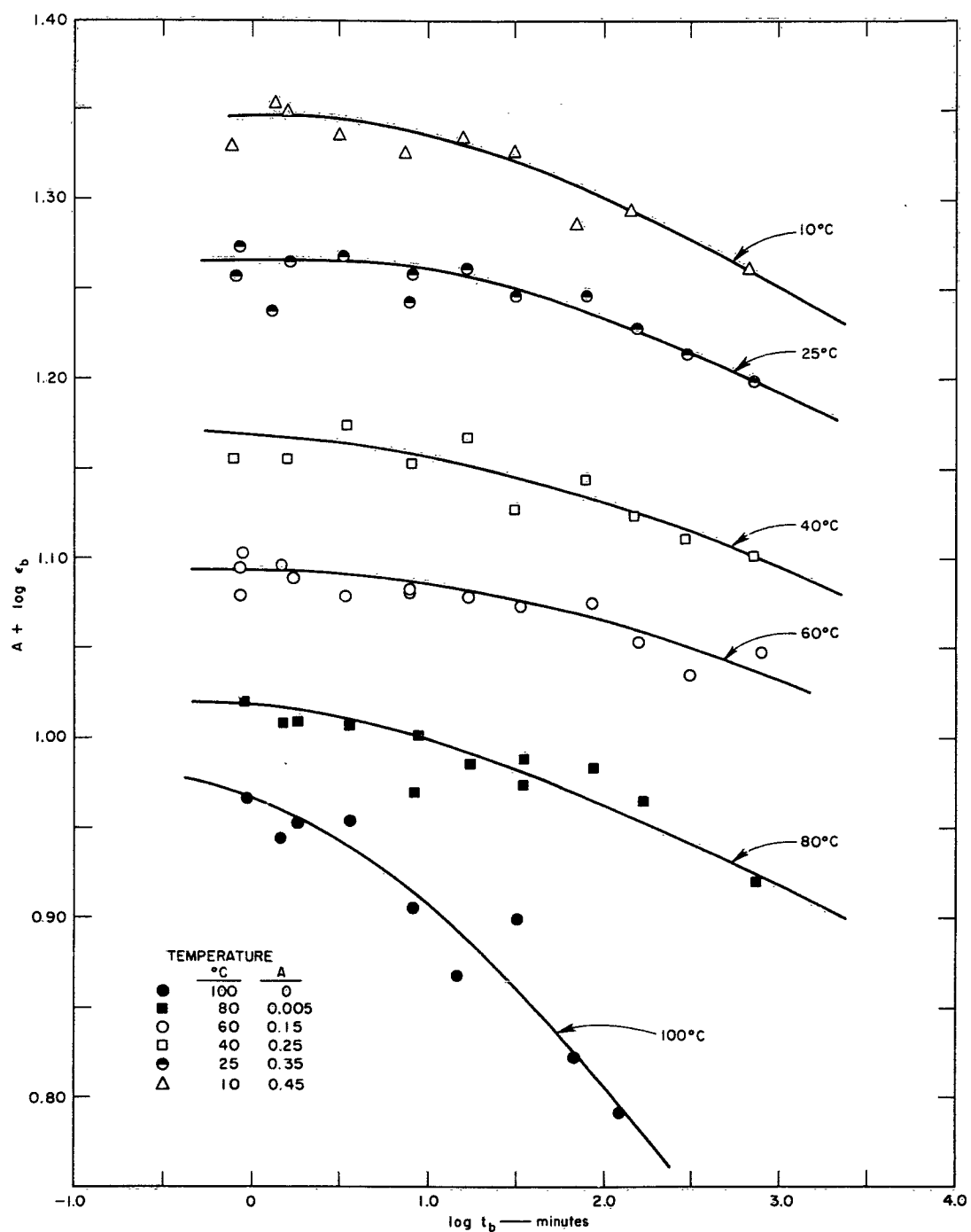


FIG. 43 DEPENDENCE OF ULTIMATE STRAIN OF NATURAL RUBBER ON TIME-TO-BREAK AT TEMPERATURES BETWEEN 10 AND 100°C

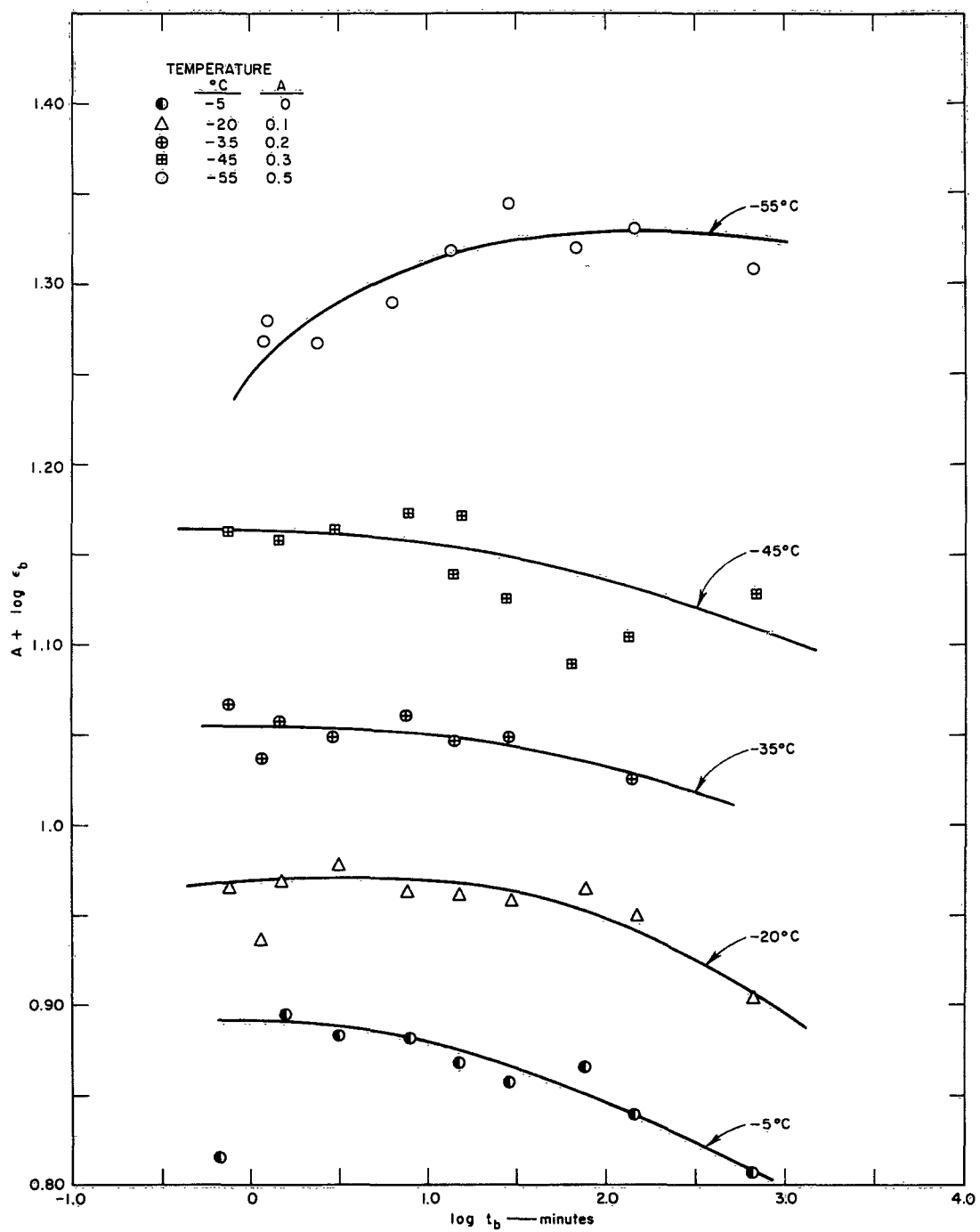


FIG. 44 DEPENDENCE OF ULTIMATE STRAIN OF NATURAL RUBBER ON TIME-TO-BREAK AT TEMPERATURES BETWEEN  $-5$  AND  $-55^{\circ}\text{C}$

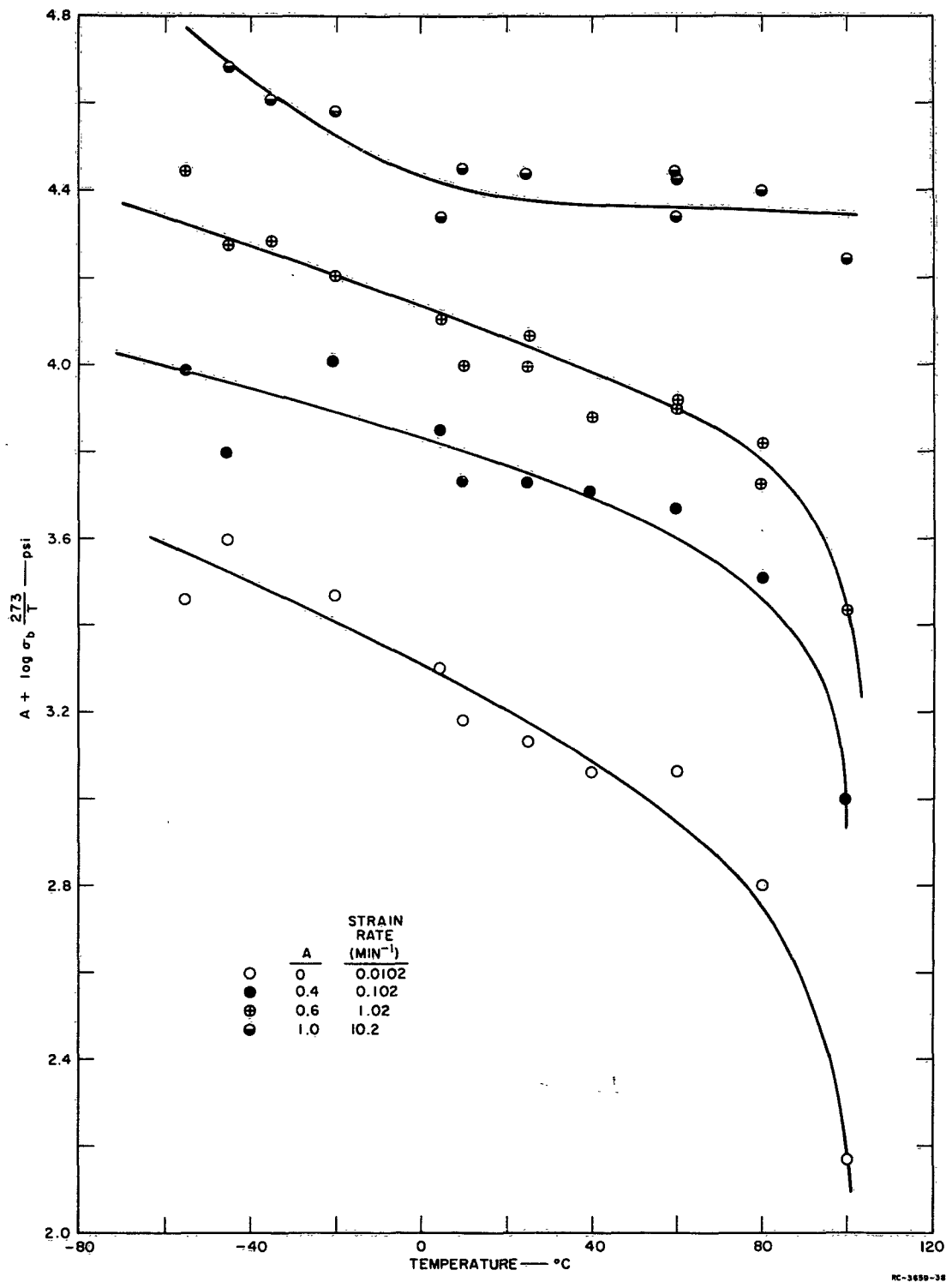


FIG. 45 DEPENDENCE OF TENSILE STRENGTH OF NATURAL RUBBER ON TEMPERATURE AT FOUR STRAIN RATES BETWEEN 0.0102 AND 10.2 MIN<sup>-1</sup>

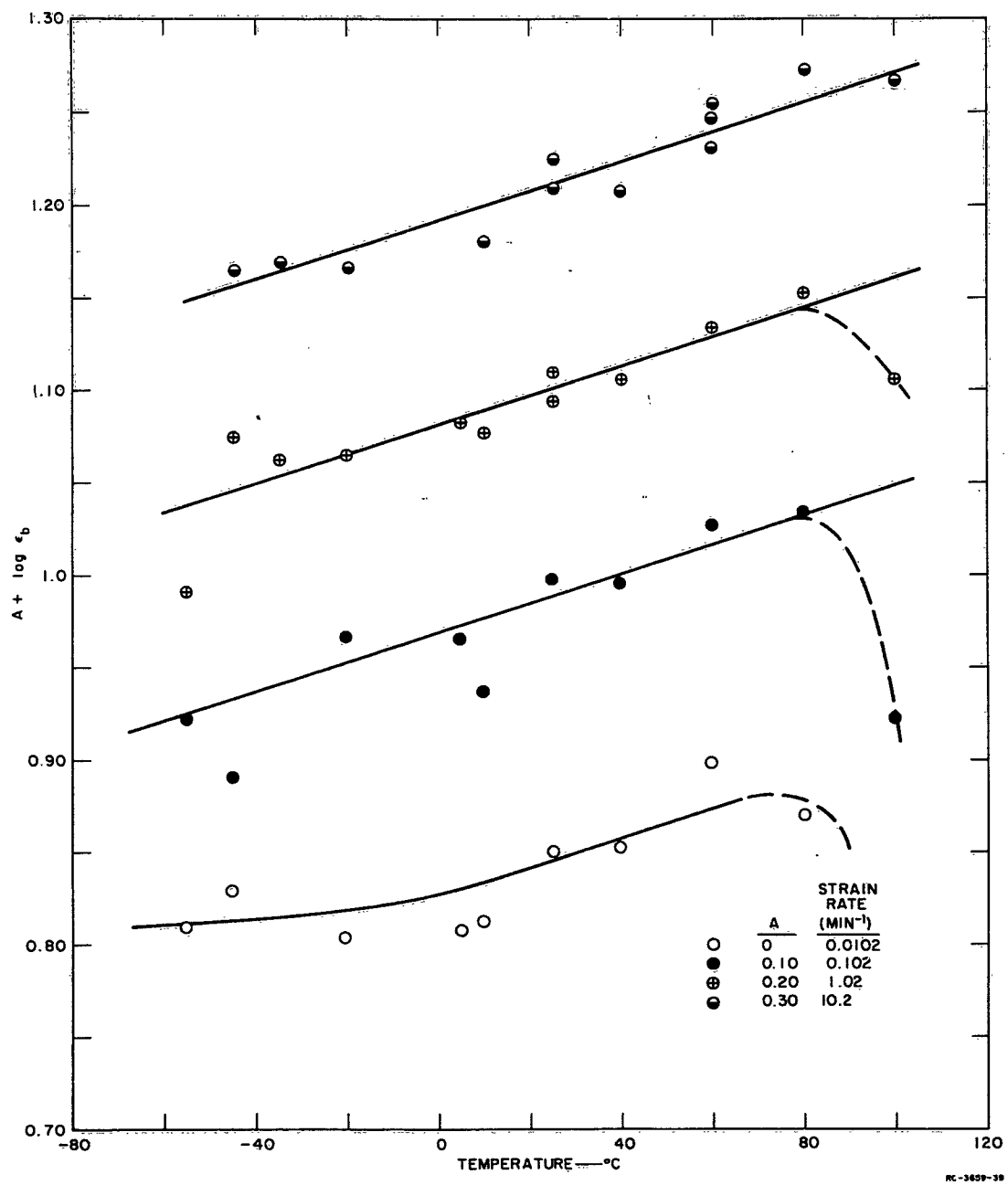


FIG. 46 DEPENDENCE OF ULTIMATE STRAIN OF NATURAL RUBBER ON TEMPERATURE AT FOUR STRAIN RATES BETWEEN 0.0102 AND 10.2 MIN<sup>-1</sup>

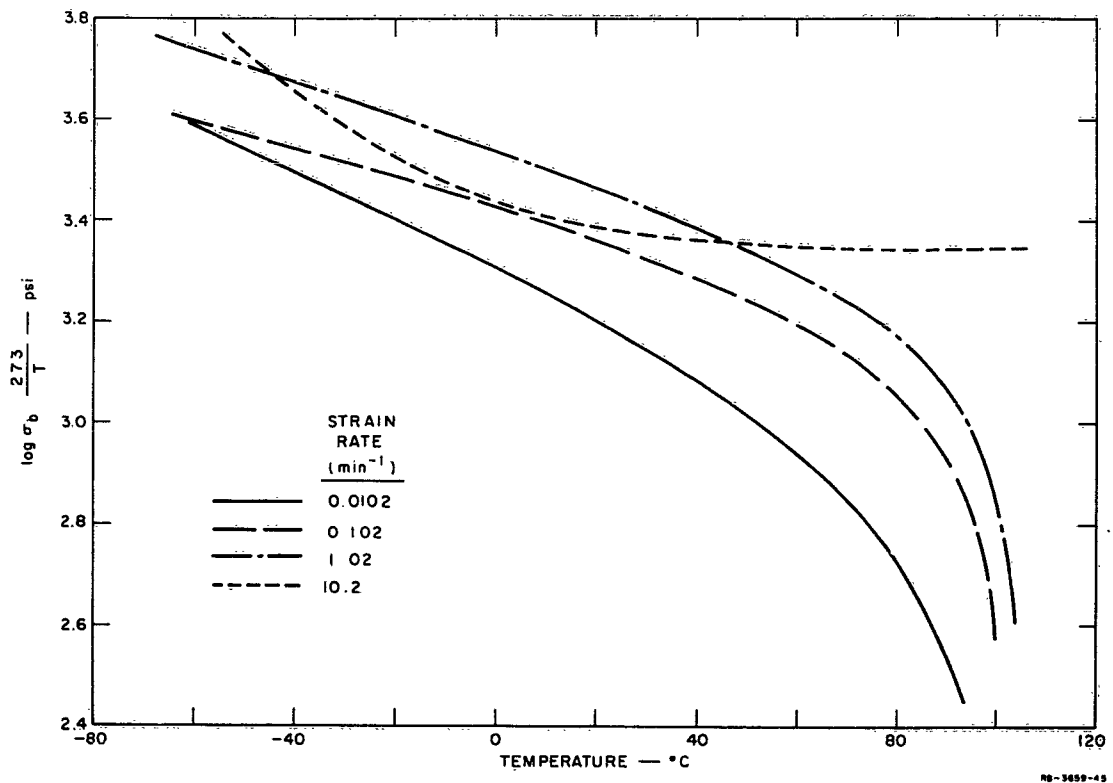


FIG. 47 REPLOT OF CURVES SHOWN IN FIG. 45

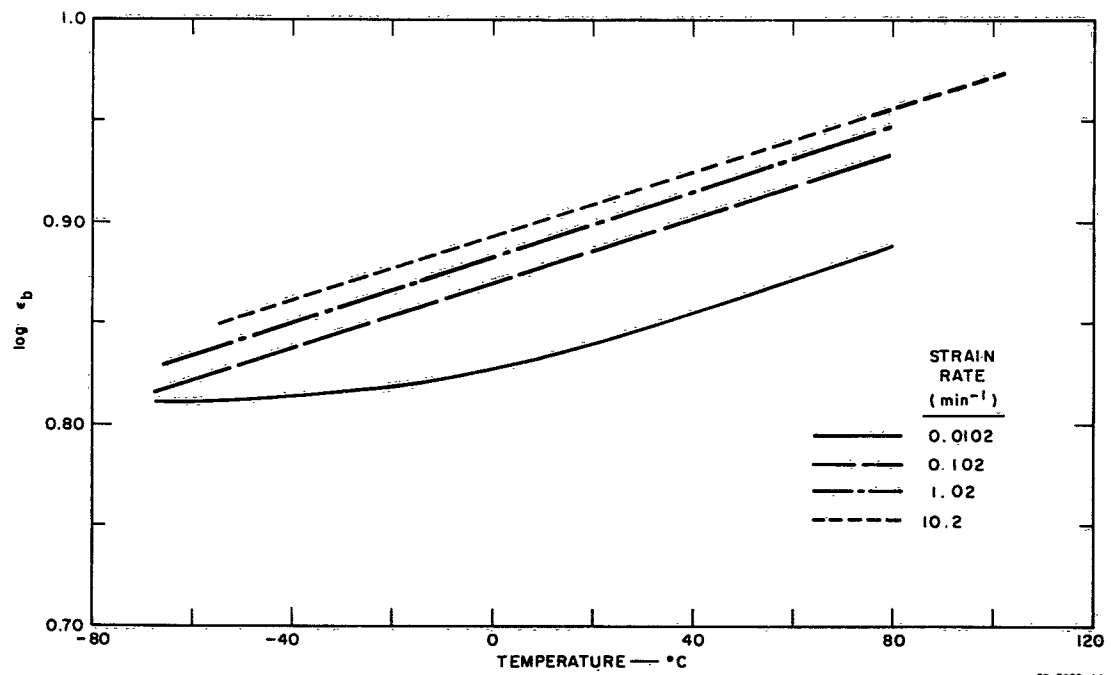


FIG. 48 REPLOT OF CURVES SHOWN IN FIG. 46

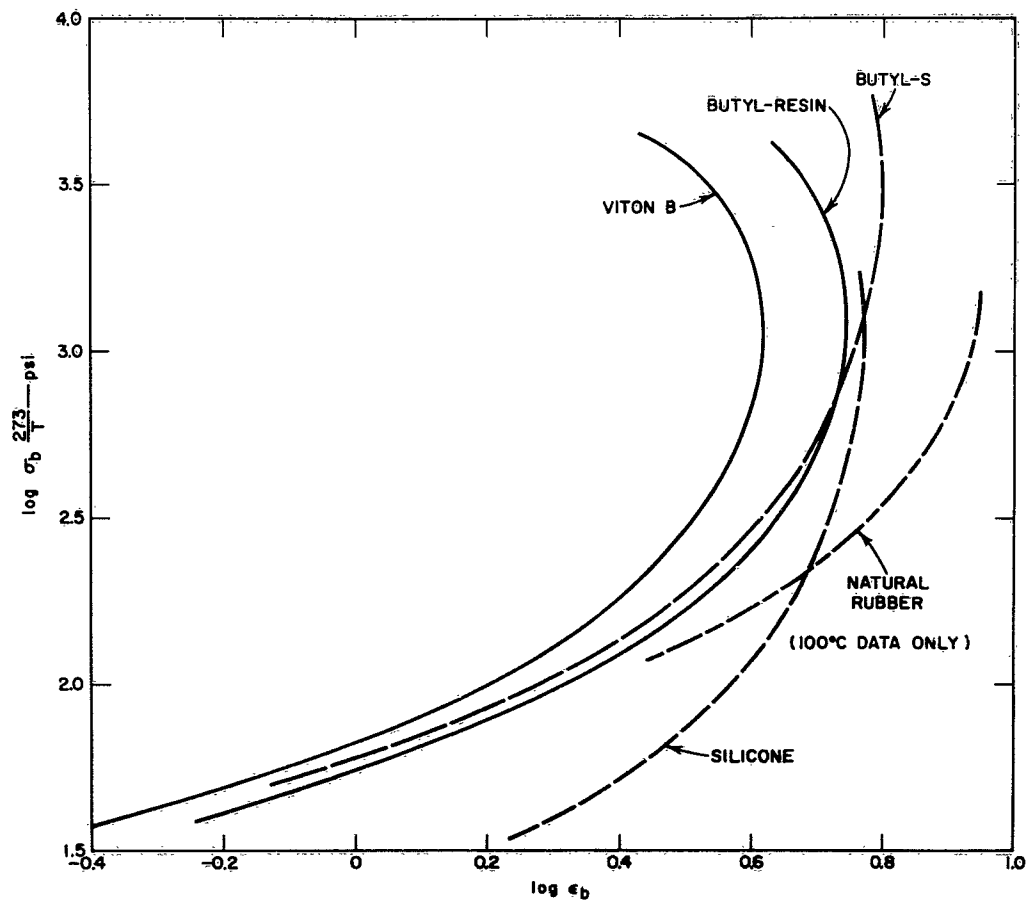


FIG. 49 COMPARISON OF FAILURE ENVELOPES FOR THE FIVE VULCANIZATES STUDIED

only data obtained at 100°C. Although the failure envelopes show that the vulcanizates have different ultimate properties, these differences are relatively small, especially as it is usually claimed that such vulcanizates have grossly different properties.

To analyze and compare further the ultimate properties of the vulcanizates, the failure envelopes in Fig. 49 were shifted vertically and horizontally to effect superposition. Rather surprisingly, it was found that all failure envelopes have the same shape except in the region of high tensile strength. The superposed curves are shown in Fig. 50 along with values of the shift factors  $\log A$  and  $\log B$ .

In superposing the failure envelopes, the curve for Viton B was not shifted and the envelopes for the other vulcanizates were superposed on that for Viton B. Thus  $\log A$  equals  $\log \sigma_b / (\sigma_b)_v$  where  $\sigma_b$  is the tensile strength for any one of the vulcanizates and  $(\sigma_b)_v$  is the value for Viton B. Likewise,  $\log B$  equals  $\log \epsilon_b / (\epsilon_b)_v$  where  $\epsilon_b$  is the ultimate strain for any vulcanizate and  $(\epsilon_b)_v$  is the ultimate strain for Viton B. Thus, values of  $A$  and  $B$  give the relative ultimate properties of the vulcanizates when they are compared in corresponding states.

To date it appears that no reliable data have been published which show the effect of the degree of crosslinking on the ultimate tensile properties. This statement is made because other investigators have not considered the wide variation in ultimate properties effected by a change in temperature and strain rate. As the results of the present study show, this variation continues to occur even after the stress-strain curves prior to rupture represent equilibrium or quasi-equilibrium properties. Thus, the effect of extent of crosslinking on the ultimate properties can be determined reliably only by considering the properties of vulcanizates when they are compared in corresponding states.

To determine precisely the effect of the degree of crosslinking on ultimate properties, failure envelopes should be determined for one type of vulcanizate which has been crosslinked to different amounts. However, because the failure envelopes for all of the vulcanizates used in the present study have the same shape, it is interesting to assume that the different positions of the envelopes in Fig. 49 are caused solely by the differences in the degree of crosslinking. If this assumption is correct, then it should be possible to relate values of  $A$  and  $B$  to degree of crosslinking.

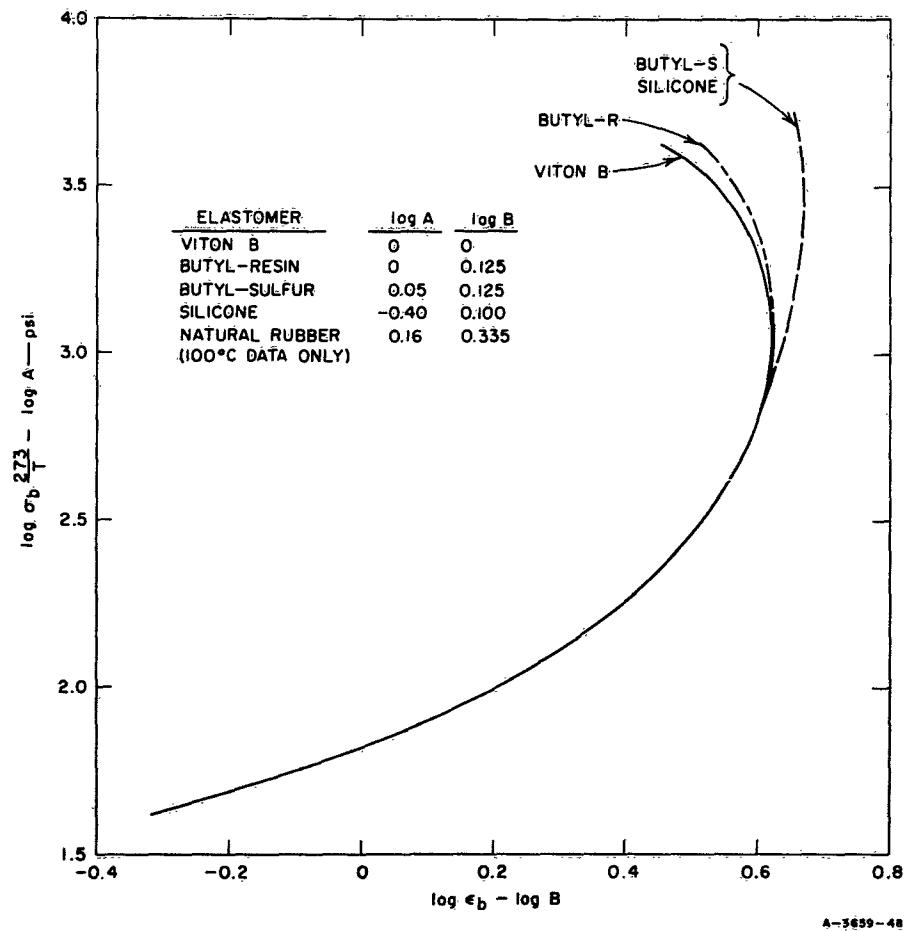


FIG. 50 SUPERPOSITION OF THE FAILURE ENVELOPES FOR THE FIVE VULCANIZATES STUDIED

Because the number of effective network chains in a vulcanizate is directly proportional to its equilibrium modulus, this quantity can be used as a measure of degree of crosslinking. Values of the equilibrium modulus for each vulcanizate are given in Table I-2 of Appendix I. Figure 51 shows a plot of  $\log E_{298}/T$  vs.  $\log A$  where  $E$  is the equilibrium modulus at temperature  $T$  and  $A$  is the shift factor tabulated in Fig. 50; the same data are shown on linear coordinates in Fig. 52. A line of unit slope has been drawn through the points in Fig. 51, and this line fits the data quite well. To obtain data on the point labelled SBR, the failure envelope for SBR (Fig. 1) was superposed with the curve in Fig. 50. The failure envelope for SBR has a somewhat different shape than the one in Fig. 50 and thus only an estimate could be made of  $\log A$  and  $\log B$  by superposing the two curves. The difference in shape may result partially because values of  $\sigma_b$  for SBR are somewhat in error as they were obtained by testing ring specimens and the stress-strain curves were not extrapolated beyond the observed rupture point to obtain correct values of  $\sigma_b$ . The modulus for SBR was obtained from data reported previously.<sup>20</sup> The results given in Figs. 51 and 52 show that the tensile strength of a vulcanizate is directly proportional to its equilibrium modulus.

An attempt was made to correlate  $B$ , which equals  $\epsilon_b/(\epsilon_b)_v$ , with the equilibrium modulus, but the data were scattered considerably and no trend was apparent. However, with the exception of the value for the silicone vulcanizate, values of  $B$  seemed to be nearly independent of the modulus. Such behavior, however, may not be correct and may have been found only because the modulus values for the vulcanizates (except for silicone) varied only from 105 to 155 psi. Because the ultimate properties of a vulcanizate should depend to some extent on the chemical nature of its network chains, it may be that such differences are reflected in values of  $B$ .

To compare the shapes of the curves which show the time-dependence of the ultimate properties of the vulcanizates, plots of  $\log \sigma_b$  vs.  $\log t_b/a_T$  (Figs. 28, 31, 34, 38) were shifted along the reduced-time axis so that the curves crossed at or near their inflection points. The resulting plots are shown in Fig. 53 along with the amount each curve was shifted. Because the curves for the butyl-sulfur and the silicone vulcanizates are affected by crystallization, it is not appropriate to state specifically the reduced temperature for each curve in Fig. 53. For example, the reduced time-scale in Fig. 28 for butyl-sulfur is somewhat

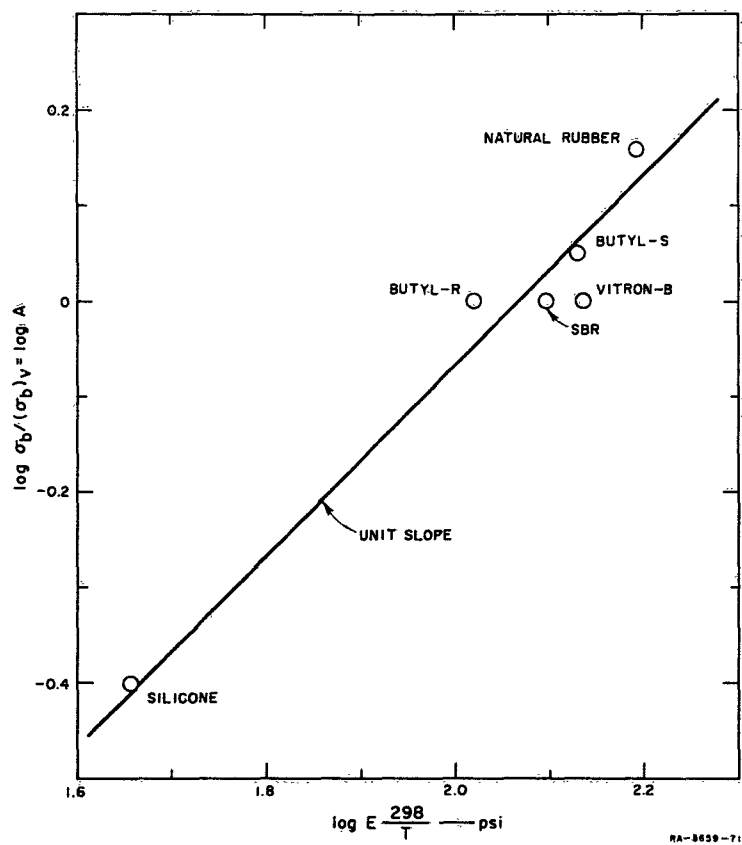


FIG. 51 DOUBLE LOGARITHMIC PLOT SHOWING VARIATION OF TENSILE STRENGTH WITH THE EQUILIBRIUM MODULUS FOR SIX VULCANIZATES

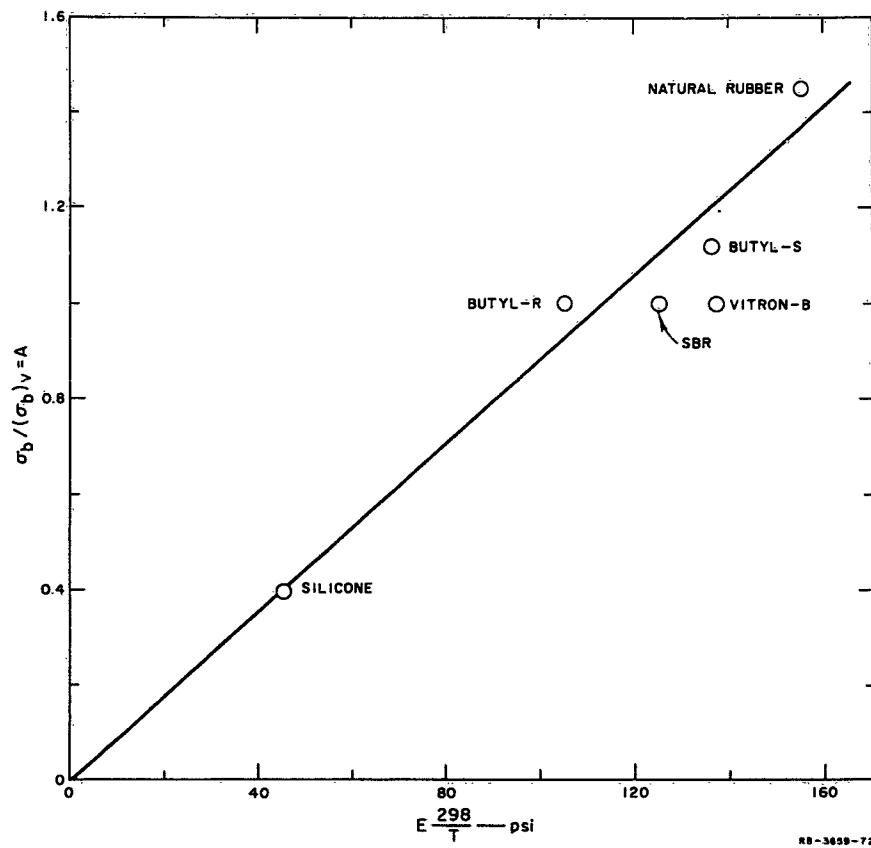
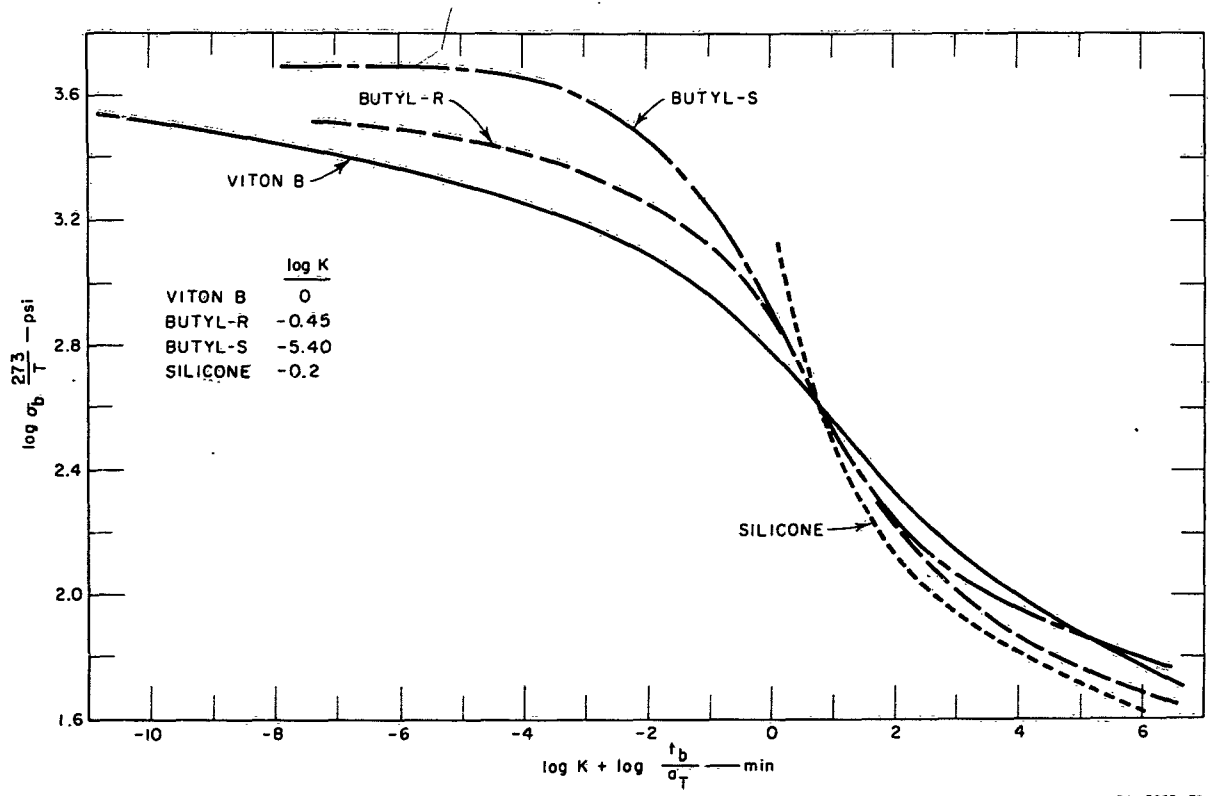


FIG. 52 LINEAR PLOT SHOWING VARIATION OF TENSILE STRENGTH WITH EQUILIBRIUM MODULUS FOR SIX VULCANIZATES



RA-3659-73

FIG. 53 COMPARISON OF THE SHAPES OF CURVES WHICH SHOW THE VARIATION OF TENSILE STRENGTH WITH TIME-TO-BREAK

arbitrary due to the method used to obtain  $a_T$  values. The figure is shown primarily to indicate certain similarities and differences among the vulcanizates. Except for the butyl-sulfur and the silicone vulcanizates at short times (low temperatures) where the tensile strengths for both are affected in a complex manner by crystallization, the curves are relatively similar, as might be expected from the close similarity of the failure envelopes. However, some of the difference at long reduced-times may result from the different degrees of crosslinking of the vulcanizates.

Figure 54 compares the shapes of the curves which show the time-dependence of  $\log \epsilon_b$ . The values used for  $\log K$  were the same as those used in Fig. 53. Again, at long times the curves are quite similar except the one for silicone. This difference may result from silicone being lightly crosslinked compared to the other vulcanizates, as seen by the data in Figs. 51 and 52.

The comparisons made in this section enable certain statements to be made about the effect of molecular structure on the ultimate tensile properties of different vulcanizates. In the past such comparisons could not be made with any degree of certainty because the ultimate properties of vulcanizates were not characterized by failure envelopes. Because ultimate properties depend on temperature and strain rate, it is necessary to eliminate effects caused by these experimental variables before the ultimate properties of different vulcanizates are compared. As the failure envelope is independent of temperatures and strain rate, differences in the failure envelopes for various vulcanizates are caused only by differences in their structures.

As shown in Fig. 50, the failure envelopes for the various vulcanizates have the same shape, but their locations on the  $\log \sigma_b, 273/T - \log \epsilon_b$  coordinates are different (see Fig. 49). Thus, the quantities  $A = \sigma_b / (\sigma_b)_v$  and  $B = \epsilon_b / (\epsilon_b)_v$ , which give the differences among the vulcanizates, are the ones to be related to structure. At present, the relation of these quantities to structure is somewhat ambiguous because the vulcanizates not only are different chemically but also are crosslinked to different degrees. The results shown in Figs. 51 and 52 strongly suggest, but do not prove, that the tensile strength is proportional to the number of effective polymer chains per unit volume of vulcanizate. This result is certainly reasonable because the modulus of a vulcanizate depends in the same way on the number

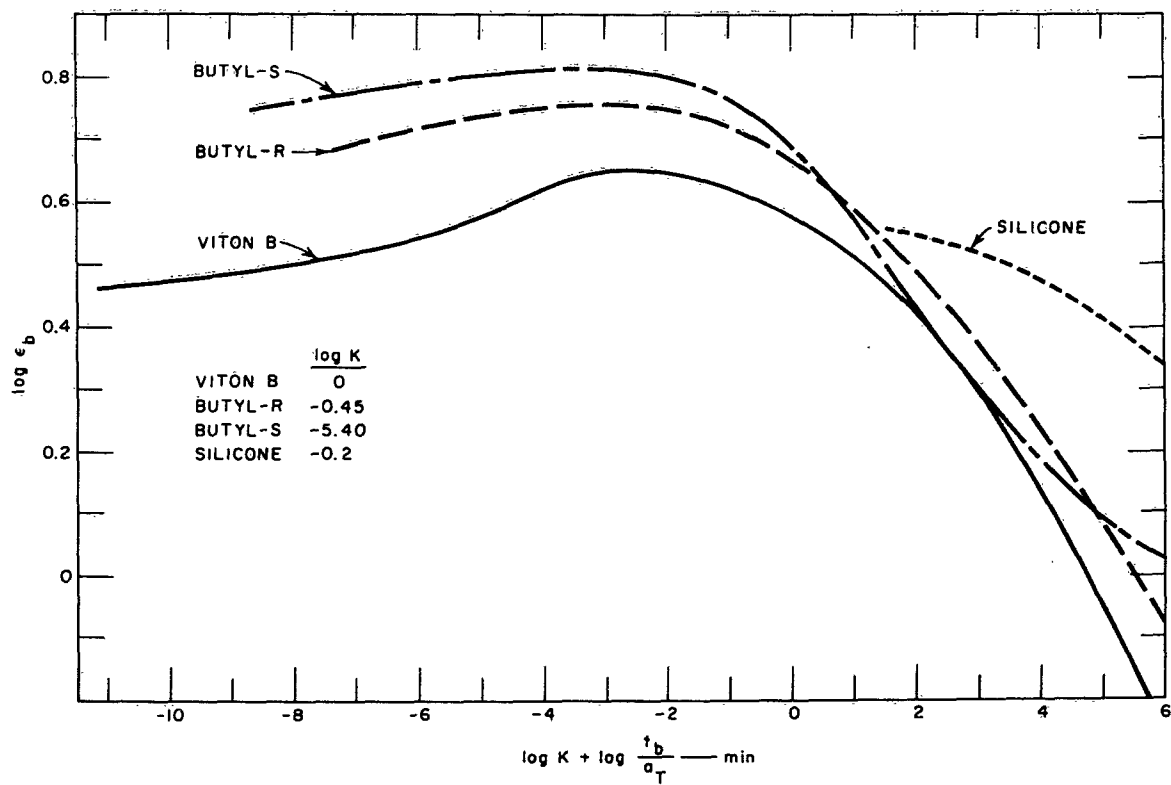


FIG. 54 COMPARISON OF THE SHAPES OF CURVES WHICH SHOW THE VARIATION OF ULTIMATE STRAIN WITH TIME-TO-BREAK

of effective chains. Thus, it is possible that the quantity  $B = \epsilon_b / (\epsilon_b)_v$  shows, at least to some degree, the effect of the different chemical natures of the vulcanizates. On the other hand, it is quite possible that a failure envelope is essentially independent of the chemical nature of the polymer and depends primarily on network topology.

One fact that the present work shows quite conclusively is that from a molecular viewpoint no gross differences exist in the basic ultimate properties of the vulcanizates studied. The relatively large differences that are commonly reported (for example, between silicone and other common vulcanizates) are found by comparing the properties observed when the vulcanizates are not in corresponding states; i.e., when they are either in different temperature states or in different physical states resulting from crystallization.

## V CONCLUSIONS

A study has been made of factors which affect the strength of gum vulcanizates of natural rubber, butyl (both sulfur cured and resin cured), silicone, and a hydrofluorocarbon (Viton B). To evaluate their thermal stabilities, measurements were made of the continuous and so-called intermittent stress-relaxation properties at temperatures between 100 and 200°C. Mechanical properties in the absence of chemical degradation were studied by measuring with the Instron tester stress-strain curves at numerous strain rates (crosshead speeds from 0.02 to 20 inches per minute) at about 10 temperatures. Analysis of the data leads to the following conclusions.

1. The continuous stress-relaxation data show that, of the vulcanizates studied, Viton B has by far the best thermal stability. The stabilities of the other vulcanizates in order of decreasing stability are: resin-cured butyl, silicone, sulfur-cured butyl, and natural rubber. However, even for Viton B at 100°C, a 10% decrease in modulus occurs during the first 10-20 hours at this temperature.

2. The modulus of Viton B and silicone vulcanizates, as determined by intermittent stress-relaxation measurements, increases at 150 and 200°C; for the resin-cured butyl at 150°C, the modulus passes through a maximum during the first ten hours. The modulus for the sulfur-cured butyl decreases at 100 and 150°C, for natural rubber the modulus decreases rapidly at 150°C but increases slightly at 100°C.

3. The ultimate tensile properties, determined in the absence of thermal degradation, of each vulcanizate except natural rubber could be characterized by a failure envelope which results from a plot of  $\log \sigma_b \cdot 273/T$  vs.  $\log \epsilon_b$ , where  $\sigma_b$  is the tensile strength and  $\epsilon_b$  is the ultimate strain. As such an envelope is independent of temperature and time (strain rate), it can in principle be related to network topology and the chemical and physical nature of a vulcanizate. The envelopes for the vulcanizates were essentially identical in shape and thus they could be superposed by shifting along the ordinate and abscissa. (The failure envelope for natural rubber resulting from ultimate properties determined at 100°C could also be superposed on the envelopes which

characterize the other vulcanizates.) The shift distances give the relative tensile strengths and relative ultimate elongations of the vulcanizates when they are in corresponding temperature and physical states. These relative values are determined by differences in the degree of crosslinking of the vulcanizates and probably by differences in their chemical and physical structure. Although it was not possible to determine the relative importance of these two effects, it was tentatively concluded that the tensile strength of a vulcanizate is directly proportional to the degree of crosslinking.

4. The high tensile strength and high ultimate strain for natural rubber over a wide temperature range was attributed to its unique ability to crystallize rapidly when subjected to stress. The ultimate property data determined at each test temperature defined (in an approximate manner) a line which is similar to a segment of a failure envelope. With decreasing test temperature, the segment shifted toward higher tensile strength and lower ultimate strain. Thus, natural rubber behaved as if a different material were being tested at each temperature. Such behavior is reasonable if the conclusions drawn about crystallization (see item 7 below) are correct. However, at temperatures of about 100°C and higher, it appears that the ultimate tensile properties can be characterized by a failure envelope which is independent of temperature and time.

5. The dependence of the ultimate tensile properties on temperature and time-to-break, for all vulcanizates except natural rubber, were analyzed by superposition methods. For Viton B and resin-cured butyl vulcanizates, all values of  $\sigma_b$  and  $\epsilon_b$  could be superposed to yield composite curves which depend on the reduced time-to-break; the superposition of the data for Viton B was particularly good. For the other vulcanizates, the analysis indicated that crystallization occurred during tests conducted at the lower temperatures. However, at temperatures at which crystallization apparently did not occur, the data could be superposed in a reasonably satisfactory manner. The results of this analysis showed that, in the absence of crystallization, the increase in  $\sigma_b$  and  $\epsilon_b$  with increasing strain rate and decreasing temperature is caused by the internal viscosity.

6. The results of the present study strongly suggest that no basic differences exist in the ultimate tensile properties of the vulcanizates. The differences normally reported result from comparing properties obtained by testing vulcanizates not in corresponding temperature and

physical states or by testing vulcanizates crosslinked to different degrees. Corresponding temperature states for different vulcanizates normally occur at approximately equal values of  $T - T_g$ . Different physical states can result from crystallization, or from differences in the uniformity of the distribution of junction sites in the three dimensional molecular network.

7. Stress-strain curves for natural rubber were analyzed by a method which shows whether or not finite strain effects can be separated from time effects. Over an extended temperature range (about  $-35$  to  $100^\circ\text{C}$ ), it was found that the curves for natural rubber are temperature dependent but are independent of time (strain rate) over the three decades covered at each temperature. This behavior can occur if the rate of crystallization is rapid compared with the strain rate and if the amount of crystallization depends only on temperature and the magnitude of the strain. However, at  $-45^\circ\text{C}$ , the curves were found to depend on time, although time and temperature effects could be separated for the most part.

*APPENDIX I*

**COMPOSITION AND CHARACTERISTICS OF  
GUM VULCANIZATES USED FOR STUDY**

## APPENDIX I

### COMPOSITION AND CHARACTERISTICS OF GUM VULCANIZATES USED FOR STUDY

#### A. COMPOSITION AND STORAGE OF VULCANIZATES

The gum vulcanizates were prepared at Wright-Patterson Air Force Base. The compounding formulas and cure conditions are given in Table I-1. To minimize changes in the properties of the vulcanizates, sheets were stored in sealed polyethylene bags in a refrigerator prior to use.

The chemical nature of the gum stocks are generally well-known, at least qualitatively, with the possible exception of Viton B. This material is manufactured by the Elastomer Chemicals Department of E. I. duPont de Nemours & Company, Inc. Viton B is a fluorinated hydrocarbon elastomer somewhat similar to Viton A which is a copolymer of hexafluoropropylene and vinylidene fluoride.

#### B. DEGREE OF CROSSLINKING AND PERCENT SOL IN VULCANIZATES

The moles of active network chains per unit volume ( $\nu_e$ ) were calculated for each vulcanizate from the measured value of the equilibrium tensile modulus. Modulus values were obtained from stress-strain curves determined at various strain rates and at the highest temperature at which tests were made. The curves obtained at the various strain rates were analyzed by plotting  $\log \sigma$  vs  $\log t$  for different fixed values of the strain, as discussed in Section IV-C. These plots yielded parallel lines of zero slope. Values of stress obtained from the lines were plotted as  $\lambda\sigma$  vs  $\epsilon$ . The plots gave straight lines for strains up to about 0.75 and the slope of such a plot was taken as the modulus. The values obtained are given in Table I-2 along with reduced values of the modulus,  $E/298/T$ . Values of  $\nu_e = 3E/RT$ , are also given in the table; for the butyl-sulfur, Viton B, and natural rubber vulcanizates the values of  $\nu_e$  are nearly the same, whereas those for the butyl-resin and silicone vulcanizates are lower by factors of about 1.3 and 3, respectively.

Table I-1  
COMPOUNDING FORMULAS OF GUM VULCANIZATES

|                                                                               |  |              |
|-------------------------------------------------------------------------------|--|--------------|
| <b>A. Natural Rubber</b>                                                      |  | <i>Parts</i> |
| Smoked Sheet                                                                  |  | 100          |
| Zinc Oxide                                                                    |  | 5            |
| Sulfur                                                                        |  | 2.5          |
| Stearic Acid                                                                  |  | 0.5          |
| Captax (2-mercaptobenzothiazole)                                              |  | 1.0          |
| PBNA                                                                          |  | 0.5          |
| Cured 20 minutes at 290°F.                                                    |  |              |
| <b>B. Silicone</b>                                                            |  |              |
| SE 30 ( G.E. - polydimethylsiloxane)                                          |  | 100          |
| Cab-O-Sil (silica)                                                            |  | 5            |
| Benzoyl Peroxide                                                              |  | 0.6          |
| Press cured 20 minutes at 260°F.                                              |  |              |
| Post cured 6 hours at 400°F (air oven).                                       |  |              |
| <b>C. Viton B</b>                                                             |  |              |
| Viton B                                                                       |  | 100          |
| MgO (Maglite K)                                                               |  | 5            |
| Ethylenediamine Carbamate (DIAK 2)                                            |  | 1            |
| Press cured 30 minutes at 320°F and cooled under pressure to prevent blowing. |  |              |
| Post cured 24 hours at 400°F (air oven).                                      |  |              |
| <b>D. Butyl-Resin</b>                                                         |  |              |
| Butyl 218                                                                     |  | 100          |
| ZnO                                                                           |  | 2.5          |
| Stearic Acid                                                                  |  | 0.5          |
| SP-1055 Resin (Brominated Phenol-Aldehyde resin)                              |  | 12.0         |
| Cured 70 minutes at 320°F.                                                    |  |              |
| <b>E. Butyl-Sulfur</b>                                                        |  |              |
| Butyl 218                                                                     |  | 100          |
| ZnO                                                                           |  | 2.5          |
| Stearic Acid                                                                  |  | 0.5          |
| Tuex (Tetramethylthiuram disulfide)                                           |  | 2.0          |
| Captax (2-mercaptobenzothiazole)                                              |  | 1.0          |
| Sulfur                                                                        |  | 1.5          |
| PBNA (phenyl B-naphthylamine)                                                 |  | 0.5          |
| Cured 60 minutes at 320°F.                                                    |  |              |

To determine the percent sol in the vulcanizates, samples were extracted for 4 days in Soxhlet extractors with benzene at its normal boiling point. Some extractions were also made with carbon tetrachloride and a Freon solvent. Subsequent to the extractions, the swollen samples

were dried under vacuum until constant weights were obtained. The percent sol was calculated from the initial and final weight of a specimen and the values considered to be most reliable are given in Table I-2.

Table I-2  
DEGREE OF CROSSLINKING AND WEIGHT PERCENT SOL  
IN GUM VULCANIZATES

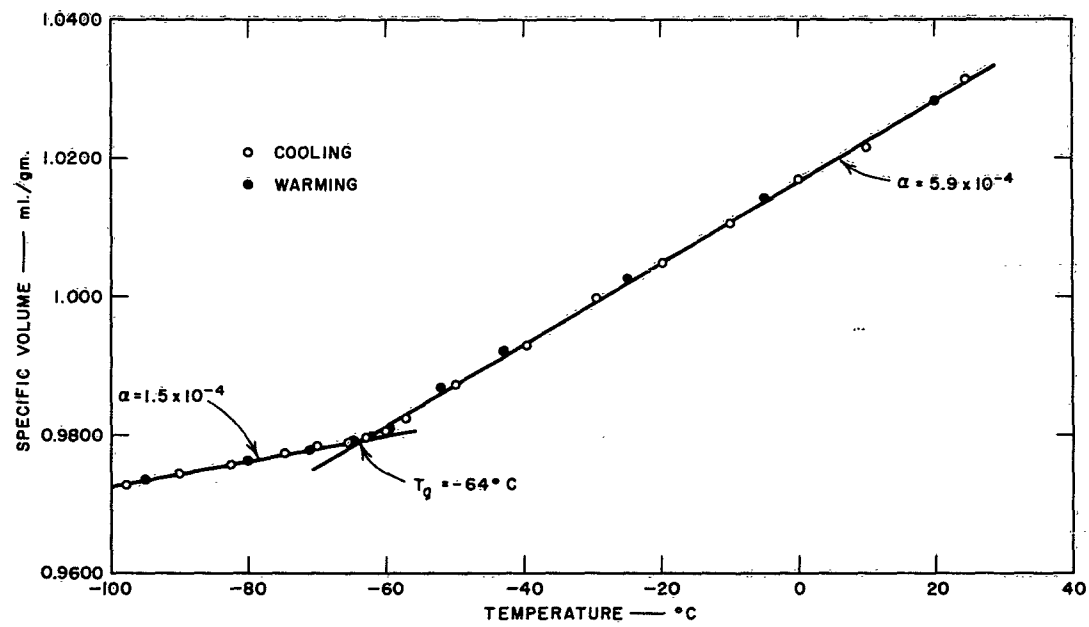
| VULCANIZATE    | EQUILIBRIUM VALUES OF TENSILE MODULUS, $E$ (psi) | $F_{298/T}$ (psi) | $\nu_e \times 10^3$ (mole/cm <sup>3</sup> ) | WT. % SOL |
|----------------|--------------------------------------------------|-------------------|---------------------------------------------|-----------|
| Silicone       | 62.9 at 140°C                                    | 45.3              | 3.78                                        | 11        |
| Butyl-Resin    | 132 at 100°C                                     | 105               | 8.76                                        | 5         |
| Butyl-Sulfur   | 170 at 100°C                                     | 136               | 11.3                                        | 5         |
| Viton B        | 208 at 180°C                                     | 137               | 11.4                                        | 1.7       |
| Natural Rubber | 194 at 100°C                                     | 155               | 12.9                                        | 4         |

The results of the extraction tests show that the percent sol in each vulcanizate except the silicone is low, i.e., 5% or less. For the silicone, however, the percent sol was 11%. From the amount of sol and values of  $\nu_e$ , values of the molecular weight between junction points in the vulcanizates can be calculated if desired. However, because such data are of less value than  $\nu_e$ , they are not tabulated.

#### C. GLASS TEMPERATURE AND EXPANSION COEFFICIENTS OF VULCANIZATES

Values of the glass temperature and expansion coefficients for each vulcanizate were measured. For each vulcanizate except Viton B, a glass dilatometer was used. The dilatometer and the procedure are described briefly elsewhere.<sup>38</sup> Data for the Viton B were obtained by a hydrostatic weighing method which is also described elsewhere.<sup>39</sup> The results are shown in Figs. I-1 to I-5 and are summarized in Table I-3.

Absolute ethanol was used as the confining fluid for measurements made on natural rubber, butyl-resin, and silicone vulcanizates. When the silicone vulcanizate was immersed in ethanol at room temperature, the weight of the vulcanizate was found to increase by about 4%. However, the weight gain was less than that observed upon immersing the silicone vulcanizate in a number of other organic liquids. Dow-Corning silicone fluid No. 330 was used for measurements made on the butyl-sulfur vulcanizate, and iso-octane was the liquid used in studying Viton B by the hydrostatic weighing method.



C-3739-2

FIG. 1-1 TEMPERATURE DEPENDENCE OF SPECIFIC VOLUME OF NATURAL RUBBER GUM VULCANIZATE

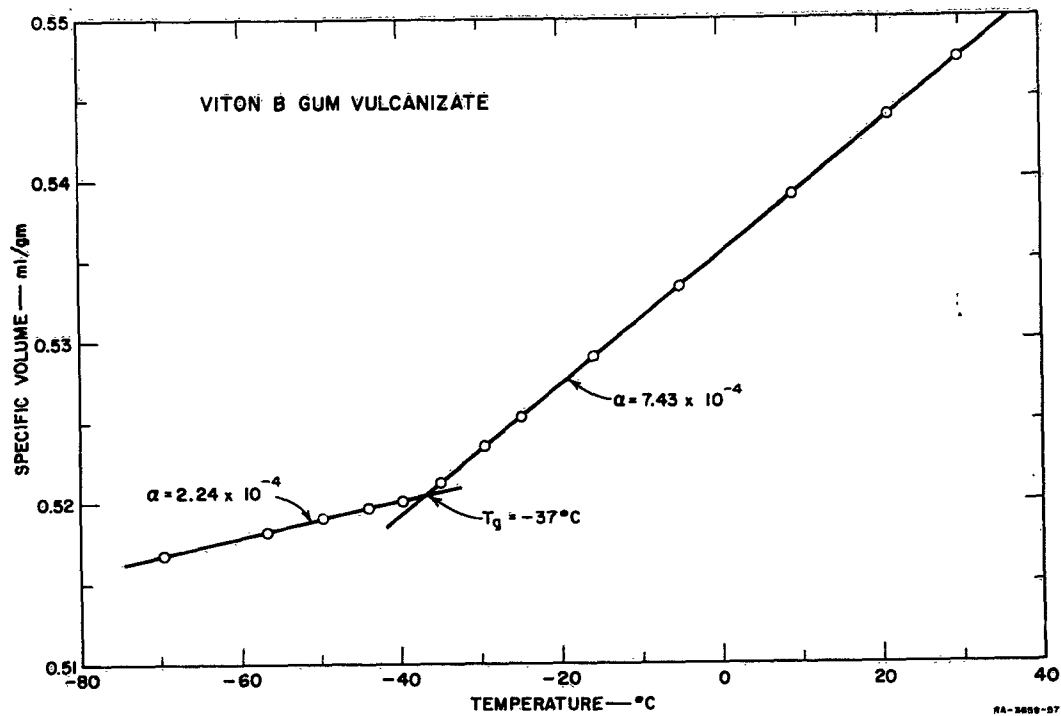


FIG. 1-2 TEMPERATURE DEPENDENCE OF SPECIFIC VOLUME OF VITON B GUM VULCANIZATE

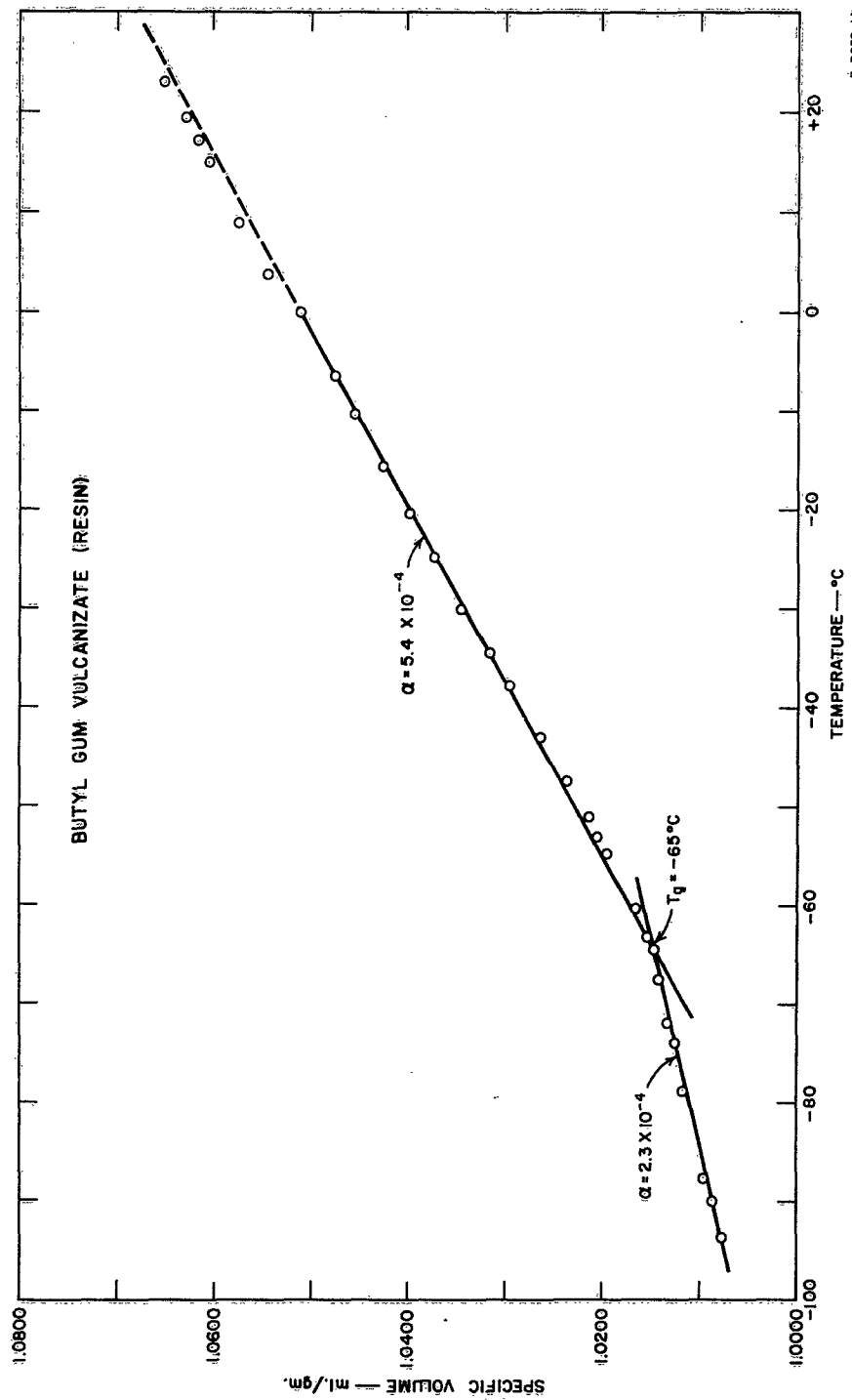


FIG. 1-3 TEMPERATURE DEPENDENCE OF SPECIFIC VOLUME OF BUTYL-RESIN GUM VULCANIZATE

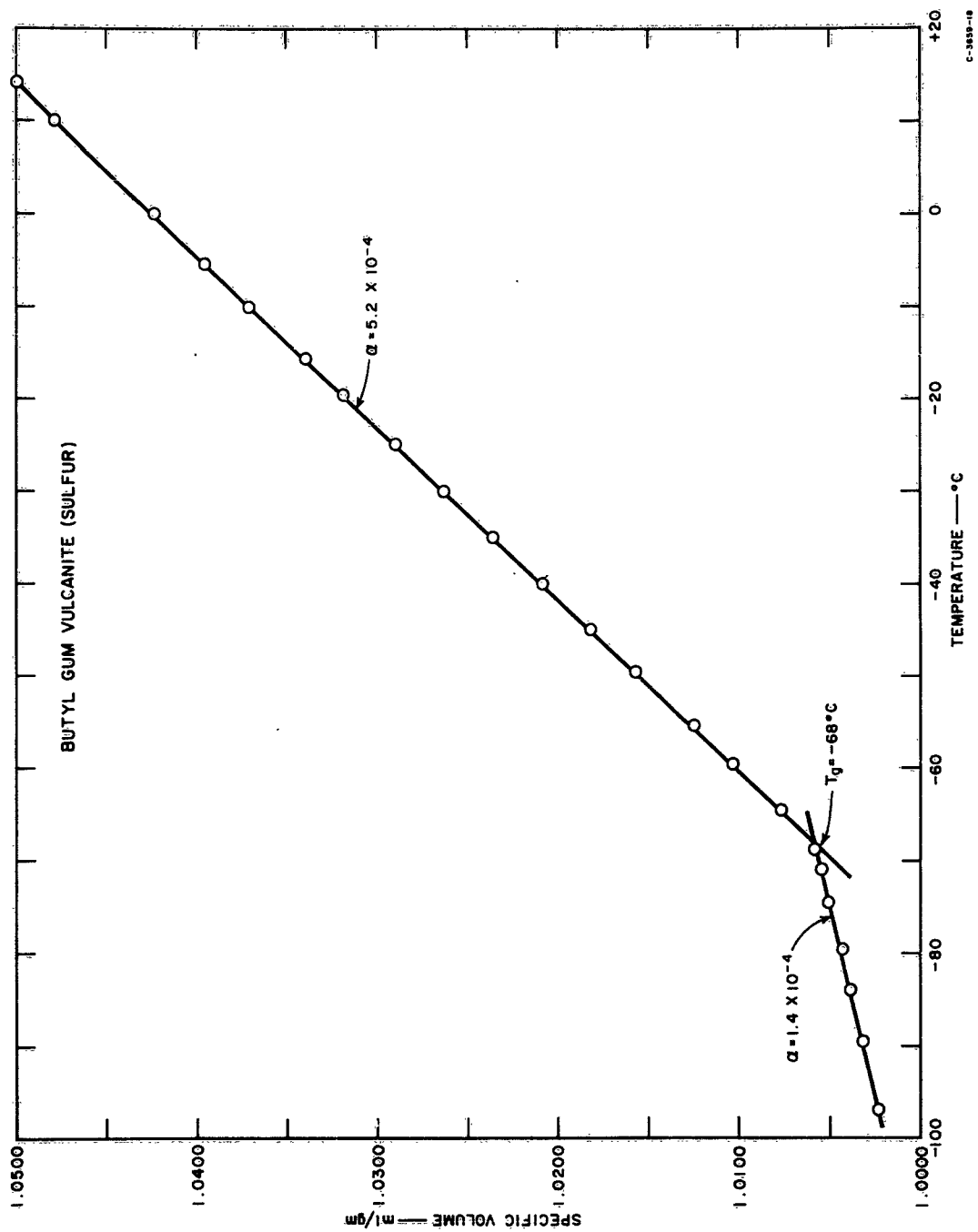


FIG. 1-4 TEMPERATURE DEPENDENCE OF SPECIFIC VOLUME OF BUTYL-SULFUR GUM VULCANIZATE

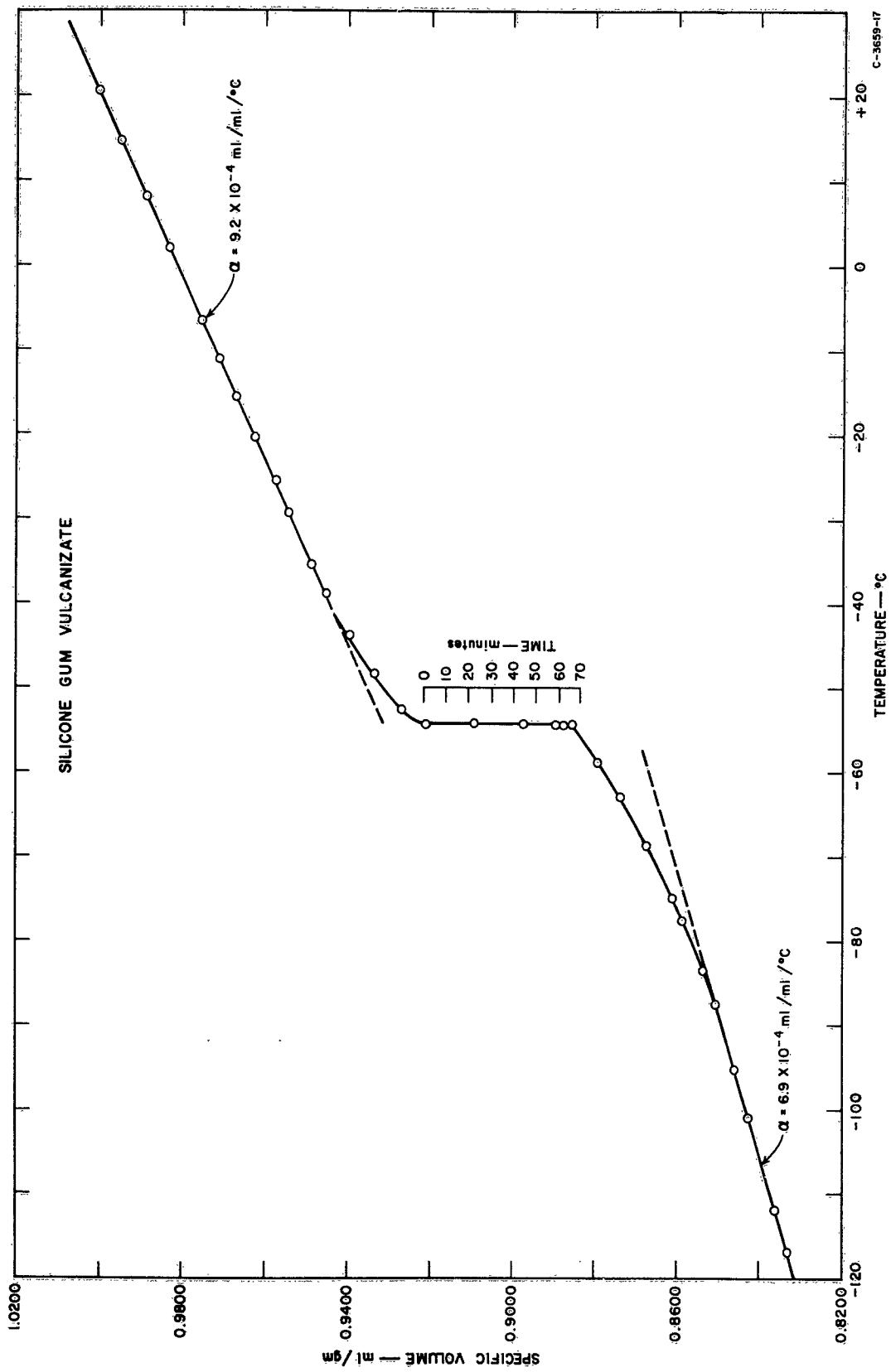


FIG. 1-5 TEMPERATURE DEPENDENCE OF SPECIFIC VOLUME OF SILICONE GUM VULCANIZATE

C-3659-17

The results obtained on the natural rubber vulcanizate are shown in Fig. I-1. Measurements were made by both cooling and warming the specimen in the dilatometer. Good agreement was obtained between the two measurements. The value observed for  $T_g$  is  $-64^\circ\text{C}$ , which is in agreement with literature values. Although  $T_g$  for unvulcanized natural rubber<sup>40</sup> is  $-72^\circ\text{C}$ , the addition of sulfur for vulcanization increases this value. The present vulcanizate contains 2.5 parts of sulfur per hundred parts of rubber. According to data of Payne,<sup>41</sup> this amount of sulfur should increase  $T_g$  by about  $7^\circ\text{C}$ ; thus, this increase gives a  $T_g$  of  $-65^\circ\text{C}$ , which is in close agreement with the present experimental value of  $-64^\circ\text{C}$ . Also, Bekkedahl and Wood<sup>42</sup> report that  $T_g$  for a vulcanizate which contains 4 parts of sulfur is  $-62^\circ\text{C}$ .

The values found for the coefficients of cubical expansion of the natural rubber vulcanizate above and below its  $T_g$  (Table I-3) are somewhat less than literature values.<sup>41</sup> However, the present vulcanizate contained 5 parts of zinc oxide filler per hundred parts of rubber (see Table I-1). As the filler should decrease the expansion coefficients somewhat, the values found are probably reliable. On the other hand, values observed for expansion coefficients below  $T_g$  on the vulcanizates in the present study are not as precise as those observed above  $T_g$ . This lesser precision results from the low values of the expansion coefficients and the corrections that need to be applied for the expansion of the confining fluid.

Table I-3  
GLASS TEMPERATURES AND EXPANSION COEFFICIENTS  
OF VULCANIZATES

| VULCANIZATE    | $\alpha \times 10^4, \text{ ml/ml}/^\circ\text{C}$ |                                        |             |                  | $T_g, ^\circ\text{C}$ |                   |
|----------------|----------------------------------------------------|----------------------------------------|-------------|------------------|-----------------------|-------------------|
|                | Above $T_g$                                        |                                        | Below $T_g$ |                  | Obs.                  | Lit.              |
|                | Obs.                                               | Lit.                                   | Obs.        | Lit.             |                       |                   |
| Viton B        | 7.43                                               | --                                     | 2.24        | --               | -37                   | --                |
| Natural Rubber | 5.9                                                | 6.5 <sup>1,2</sup>                     | 1.5         | 2.0 <sup>1</sup> | -64                   | -65 <sup>*</sup>  |
| Butyl-Resin    | 5.4                                                | --                                     | 2.3         | --               | -65                   | --                |
| Butyl-Sulfur   | 5.2                                                | 5.7 <sup>3</sup>                       | 1.4         | --               | -68                   | -69 <sup>4</sup>  |
| Silicone       | 9.2                                                | 10.5 <sup>5</sup><br>12.0 <sup>6</sup> | --          | 2.7 <sup>6</sup> | --                    | -123 <sup>6</sup> |
|                | 6.9 <sup>†</sup>                                   | 5.4 <sup>6</sup>                       |             |                  |                       |                   |

\* For vulcanizate containing 2.5 parts of sulfur; value estimated from literature data, as discussed in text.

† Above  $T_g$  but below crystallization point.

<sup>1</sup> N. Bekkedahl, *J. Research National Bureau of Standards* 13, 411 (1934).

<sup>2</sup> N. Bekkedahl and L. A. Wood, *Ind. Eng. Chem.* 33, 381 (1941).

<sup>3</sup> N. Bekkedahl, *J. Research National Bureau of Standards* 43, 145 (1959).

<sup>4</sup> C. E. Weir, National Bureau of Standards, unpublished results presented by L. A. Wood in "Physical Chemistry of Synthetic Rubbers," *Synthetic Rubber*, edited by G. S. Whitby, John Wiley and Sons, Inc., New York, 1954.

<sup>5</sup> This value is for a silicone (Dow Corning 330) and was obtained from the Dow-Corning Co.

<sup>6</sup> C. E. Weir, W. H. Leser, and L. A. Wood, *J. Research National Bureau of Standards* 44, 367 (1950).

The results on Viton B (Fig. I-2) show that  $T_g$  is about  $-37^\circ\text{C}$ . No search has been made of the literature to see if other workers have reported a value for  $T_g$ .

Volume-temperature data on the butyl-resin and butyl-sulfur vulcanizates are shown in Figs. I-3 and I-4. These vulcanizates have glass temperatures of  $-65$  and  $-68^\circ\text{C}$ , respectively. These values are in agreement with a literature value of  $-69^\circ\text{C}$  (see Table I-3). The difference between the observed and literature values of the expansion coefficient for the butyl-sulfur vulcanizate may be caused by the present vulcanizate containing 2.5 parts of zinc oxide filler, although it may reflect an experimental error.

The results on the silicone vulcanizate are shown in Fig. I-5. The sharp drop in the curve at  $-54^\circ\text{C}$  is caused by crystallization. In conducting the experiment, the specimen was cooled in the normal manner to about  $-54^\circ\text{C}$ . Then, the specimen was held at this temperature for about 70 minutes and, during this period, the points shown in Fig. I-5 were obtained. The specimen was then cooled to  $-100^\circ\text{C}$ . The temperature at which crystallization was observed is essentially identical with that reported by Ohlberg, Alexander, and Warrick.<sup>34</sup>

A study has been made by Weir, Leser, and Wood<sup>32</sup> of crystallization and of glass temperatures of unfilled unvulcanized silicone rubbers and of filled vulcanized silicone rubbers. The composition and manner of preparation of the filled vulcanized materials were not precisely known. However, these workers report that silicone rubber has a  $T_g$  of  $-123^\circ\text{C}$  with a maximum estimated uncertainty of  $\pm 5^\circ\text{C}$ . They also report that  $T_g$  seems to be unaffected by the presence of filler or by vulcanization. They found that crystallization invariably begins in the vicinity of  $-60^\circ\text{C}$ , in reasonable agreement with the present results and those of other workers.<sup>34</sup>

The value found for the expansion coefficient above the crystallization point was  $9.2 \times 10^{-4}$ . This value can be compared to  $12 \times 10^{-4}$  obtained by Weir *et al.*<sup>32</sup> on unfilled unvulcanized silicone rubber, and to  $8.12 \times 10^{-4}$  obtained by Polmanteer and Hunter<sup>36</sup> who used mercury as the confining fluid. They<sup>36</sup> obtained  $9.44 \times 10^{-4}$  when *n*-propyl alcohol was the confining fluid. Also, for Dow-Corning silicone fluid No. 330, a value of  $10.5 \times 10^{-4}$  has been reported by the Dow-Corning Company.

The present value of  $6.9 \times 10^{-4}$  for the expansion coefficient below the crystallization point can be compared with  $5.4 \times 10^{-4}$  reported<sup>32</sup> for an unfilled unvulcanized silicone rubber. This same rubber is reported<sup>32</sup> to have an expansion coefficient below the glass temperature of  $2.7 \times 10^{-4}$

*APPENDIX II*

**DESCRIPTION OF STRESS RELAXOMETER AND  
EXPERIMENTAL PROCEDURE**

## APPENDIX II

### DESCRIPTION OF STRESS RELAXOMETER AND EXPERIMENTAL PROCEDURE

A stress relaxometer is a device for measuring the time-dependent force necessary to maintain a sample at some fixed elongation at a constant temperature. The stress-relaxation modulus, as ordinarily defined, equals the stress (force per unit cross-sectional area of the unstretched specimen) divided by the strain; the strain is held constant during a test. To measure the so-called intermittent stress-relaxation modulus, a specimen is maintained in its unstretched state except that periodically it is stretched to some prescribed elongation and the retractive force measured; the ratio of this stress to strain is the intermittent stress-relaxation modulus.

To measure the continuous and intermittent stress-relaxation moduli at temperatures above ambient, a stress relaxometer was designed and built which consists of two functional parts: (1) an air bath whose temperature can be controlled at any temperature between ambient and about 350°C; and (2) a twin relaxometer which holds two specimens so that the continuous and intermittent moduli can be measured simultaneously.

#### A. CONSTANT TEMPERATURE AIR BATH

The air bath consists essentially of a heavy-wall (1 inch thick) aluminum vessel whose inside diameter is 6 inches and whose length is 12 inches. A removable, insulated lid for the vessel supports the actual relaxometer. The aluminum vessel is surrounded by a Glascol heating mantle, which in turn has an aluminum shell lending rigidity to the heating mantle. The mantle has two 500-watt heaters which are connected in series so that the maximum input is 250 watts at 110 volts. This heating circuit is adequate to produce temperatures in excess of 350°C in the air bath; the temperature is controlled roughly by varying the input voltage with a Powerstat transformer. Equilibrium temperatures for given input voltages are shown in Fig. II-1.

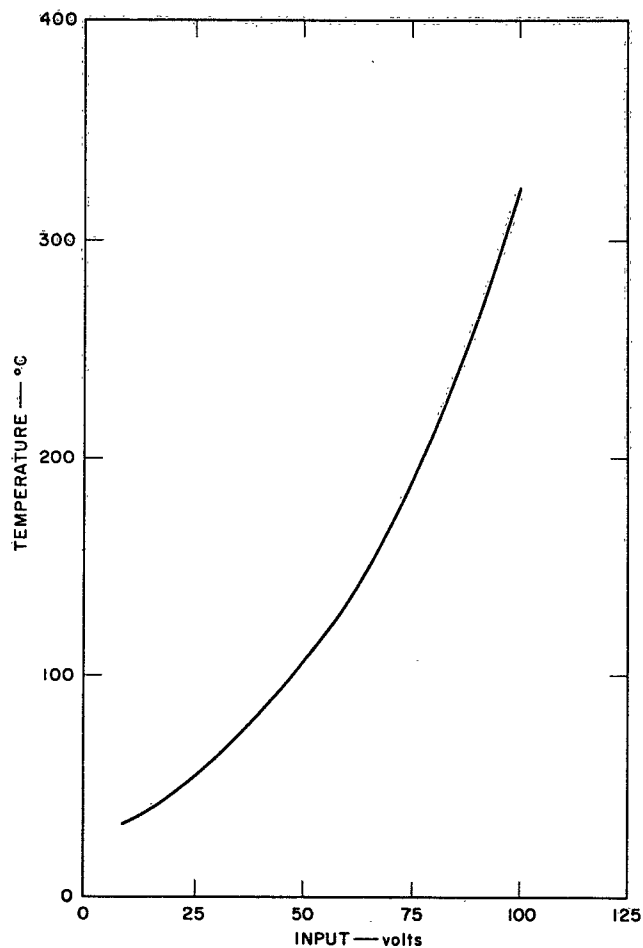


FIG. II-1 VARIATION IN EQUILIBRIUM TEMPERATURE OF AIR BATH WITH CONTINUOUS HEATER VOLTAGE

Precise temperature control is achieved by an auxiliary heater consisting of 12 feet of heating tape wound around the aluminum cylinder. The input voltage to this heater is also controlled by a Powerstat transformer, and the heater is activated in an on-off fashion by a Blue M Microtrol\* thermostat whose sensing element is located in the wall of the aluminum vessel. This type of thermostat, which is hydraulically actuated, was chosen in preference to the more sensitive mercury regulators because the latter tend to become unreliable near the upper end of the desired temperature range. The thermostat, which is equipped with a snap-action

\* Blue M Engineering Co., 2312 South Main St., Los Angeles, California

microswitch, carries no current, but activates a Thyatron-controlled mercury switch in a relay. A schematic diagram of the heating and control circuit is shown in Fig. II-2.

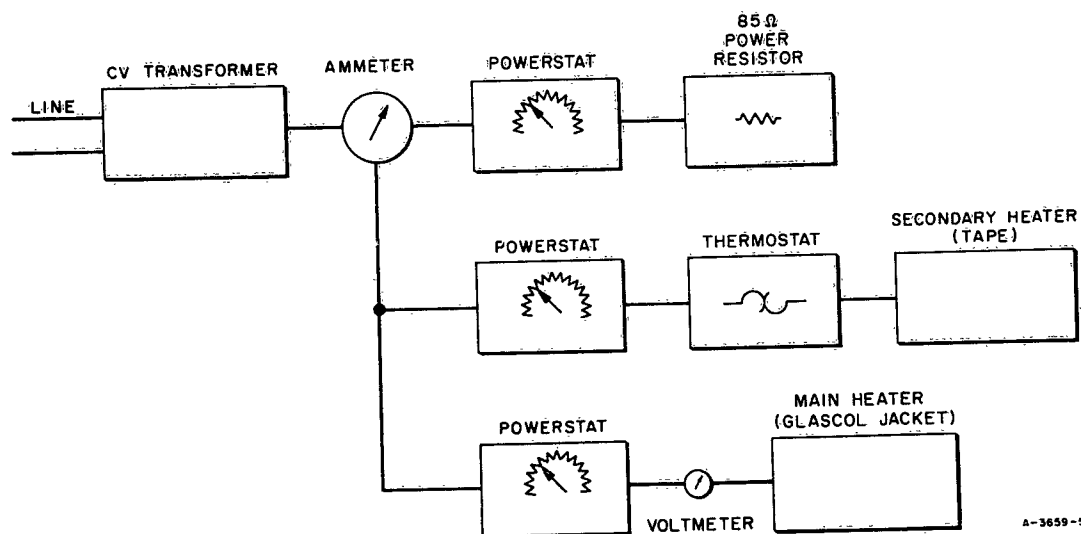


FIG. II-2 SCHEMATIC DIAGRAM OF THE HEATING AND CONTROL CIRCUITS FOR CONSTANT TEMPERATURE AIR BATH

A thermometer well in the heavy-wall aluminum vessel allows the use of a precision thermometer or thermocouple to record the "body" temperature. An iron-constantan thermocouple is used for temperature measurement and the output of the thermocouple is recorded on a 1-mv full scale Brown recorder. Since the output of the thermocouple is about 0.05 mv per degree C, each degree corresponds to five chart divisions. A zero suppression circuit containing a mercury cell was used to keep the output on the recorder scale at various temperatures. A thermocouple junction can also be placed in the airspace near the test specimens to measure the air temperature.

To control the atmosphere around the test specimens and to provide better heat exchange between the walls of the heated aluminum vessel and the samples, air (or an inert gas) is bled into the system. The gas enters near the bottom of the vessel containing the relaxometer after passing through a heat exchanger which consists of about 15 feet of 5/16-inch aluminum tubing imbedded in a recess cut in the outside

wall of the vessel, as illustrated in Fig. II-3. The flow of air is controlled by a needle valve in conjunction with a pressure regulator, and the flow is monitored by a rotometer. Gas flows of the order of 5 liters/minute give adequate mixing of the gas in the relaxometer chamber.

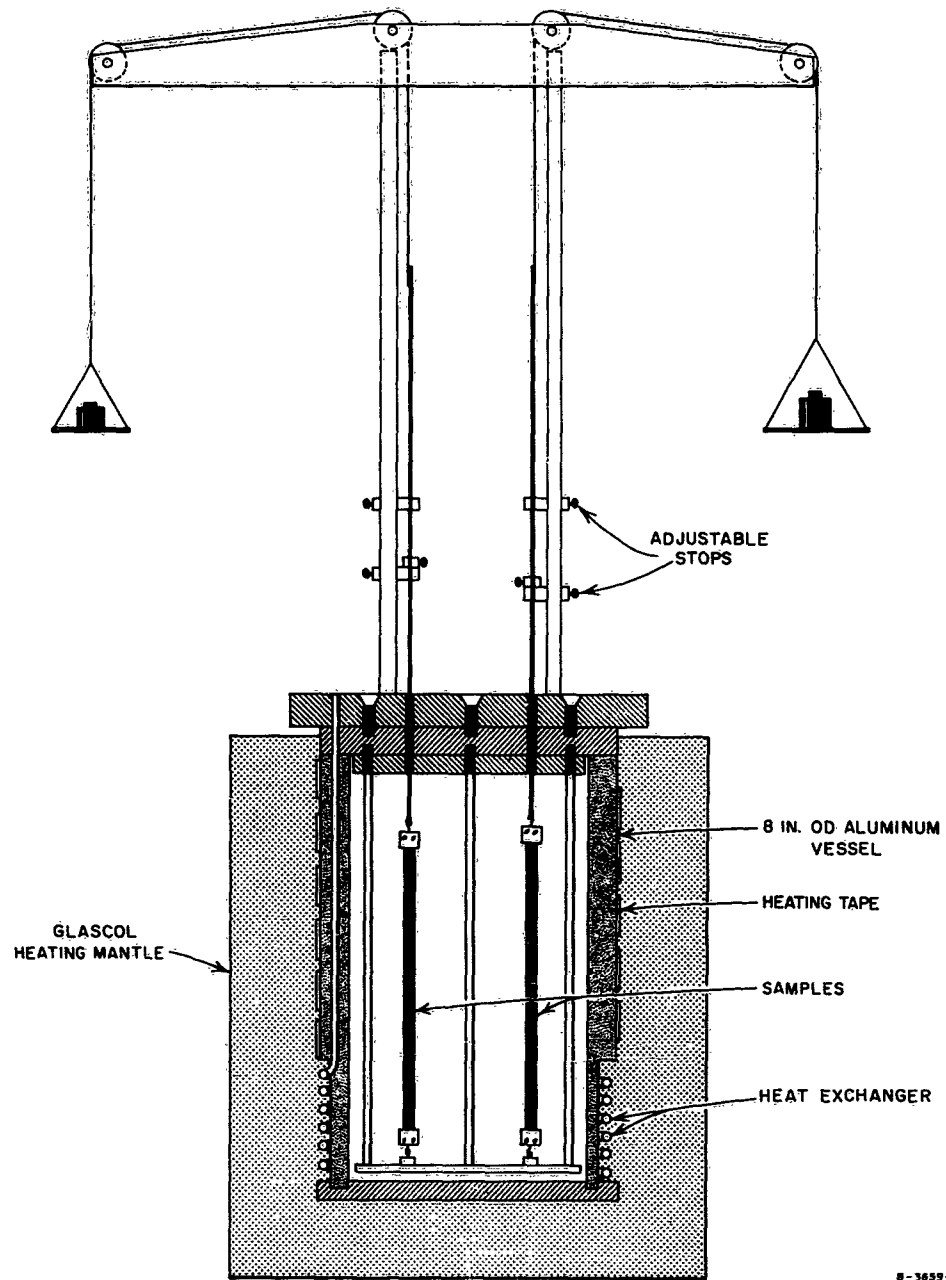
#### B. STRESS RELAXOMETER

A schematic diagram of the stress relaxometer including the heating mantle is shown in Fig. II-3. Rectangularly shaped test specimens are secured in clamps which are designed (Fig. II-4) so that the pull is against a clamped portion. The lower clamp is held rigidly against the frame of the relaxometer, and the upper clamp is connected to a rod which protrudes through the lid of the relaxometer. The rod is connected to a weighing pan by means of a nylon line and a set of pulleys. Adjustable stops (shown in Fig. II-3) permit the fixing of the rod in any position thus maintaining constant elongation in a specimen. The force necessary to just lift the stop on the rod from its rest position can be determined at given intervals by placing weights on the pan. The setup is a twin arrangement which allows measurements to be made simultaneously of the continuous and intermittent stress-relaxation moduli.

#### C. EXPERIMENTAL PROCEDURE

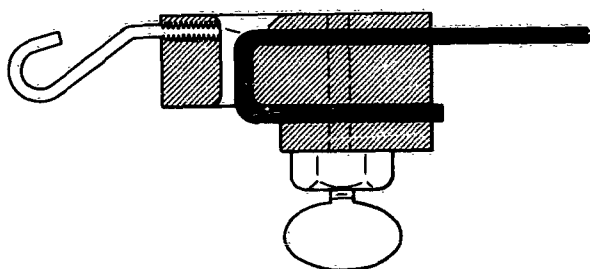
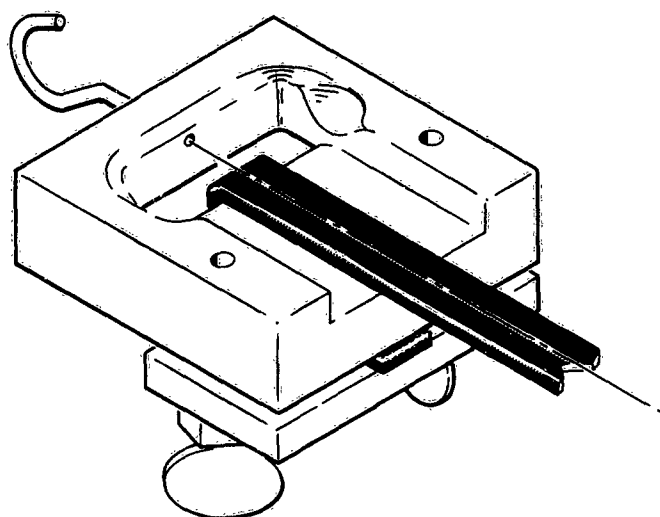
The following description of the first test run serves to illustrate the procedure followed and the necessity for minor modifications of the apparatus which were subsequently made. The assembled relaxometer was brought to 160°C by choosing the proper voltage from the chart shown in Fig. II-1 and by setting the thermostatically controlled auxiliary heater to 10°C higher than the equilibrium temperature chosen from the chart. The apparatus was allowed to equilibrate overnight with a stream of air passing through it at a constant rate. A constant voltage transformer (Fig. II-2), loaded to at least 75% of its rated capacity, is used to assist in maintaining long time temperature stability.

Rubber specimens (Stillman SR-251-70 which is a Viton A vulcanizate containing carbon black), consisting of strips, 0.075 × 0.25 × 5.0 inches, were clamped in such a way as to leave a 2-inch length between bench marks placed on the specimens near to the clamps. The relaxometer was lifted out of the air bath and the clamps holding the specimens were hooked into place. One specimen was then stretched to an elongation of



8-3659-4

FIG. II-3 DIAGRAM OF STRESS RELAXOMETER INCLUDING AIR BATH



A-3659-3

FIG. II-4 CLAMPS TO HOLD TEST SPECIMENS

50% and the stops were appropriately set. The other specimen was inserted but in its unstretched state. The apparatus was reassembled and two thermocouples introduced through a glass tube in the center of the lid in such a manner that their positions were approximately opposite the center of the samples. One thermocouple was connected to a direct reading meter to obtain the temperature to the nearest degree. The other was connected to the 1-mv Brown recorder to give a record of the temperature fluctuations during the run. As shown in Fig. II-5, almost an hour elapsed before the apparatus returned to thermal equilibrium. This delay was caused primarily by the large amount of heat required to reheat the metal parts in the relaxometer and the specimen clamps.

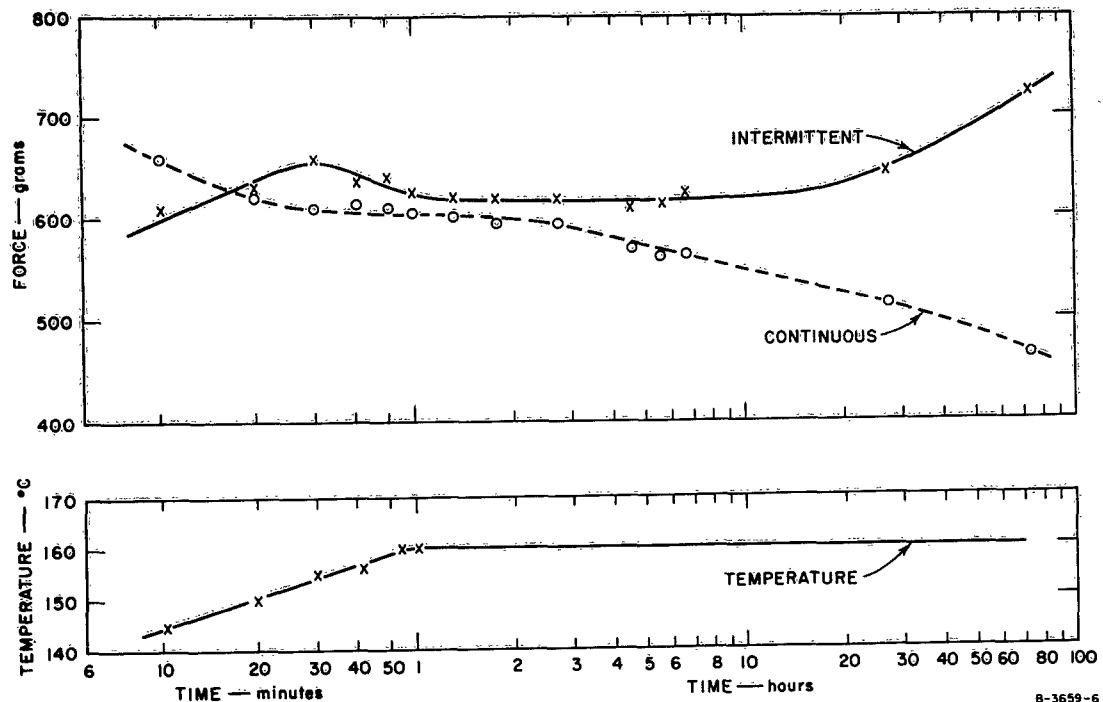


FIG. II-5 ILLUSTRATIVE DATA SHOWING CONTINUOUS AND INTERMITTENT STRESS-RELAXATION BEHAVIOR OBSERVED AT 50% ELONGATION AND AT 160°C

The force necessary to lift the stop off its support was determined at intervals; this force could be determined to within about 5-10 grams. At the same times that these measurements were made, the force required to stretch the other specimen 50% was determined. This latter specimen was allowed to recover after a force measurement was made.

The results obtained during a 72-hour period are shown in Fig. II-5. Because about one hour was required for the temperature of the air bath to reach 160°C after the specimens were inserted, only the force measurements subsequent to one hour are meaningful. Figure II-5 shows that the force required to maintain 50% elongation in a specimen decreased from about 600 grams (70.5 psi) to 460 grams (54.0 psi). On the other hand, the force required to stretch a specimen intermittently to 50% remained relatively constant for about 10 hours and then it slowly increased.

To decrease the delay in achieving the desired temperature in the apparatus, the weight of metal was reduced by replacing the solid metal base of the relaxometer with a base consisting of concentric metal rings and by replacing the relatively large metal clamps with smaller ones.

These changes effected a marked reduction in the time required to re-establish thermal equilibrium after the relaxometer was replaced in the air bath. For example, it was found that when the original temperature of the air bath was 250°C, the temperature returned in 10 minutes to within 10°C of the original value and in 20 minutes to within several degrees. On the other hand, when the original air temperature was 100°C, the air temperature returned to within a degree or so of this temperature within 10 minutes.

During the period required to re-establish thermal equilibrium, the temperature of a test specimen is of necessity less than that of the surrounding air. A test was conducted to determine the magnitude of this thermal lag. The test consisted of embedding a fine thermocouple in a test specimen and comparing the temperature of the thermocouple with that of the surrounding air. When the original temperature of the air bath was 250°C, it was found that after 10 minutes the temperature of the test specimen was about 10°C below the air temperature and after 20 minutes it was about 3°C below the air temperature.

From the tests conducted, it was concluded that under the most unfavorable test conditions (temperatures of 250°C and above) a test specimen attains the desired temperature within 30 minutes after the relaxometer is returned to the air bath. However, when tests are conducted at temperatures below 250°C, this delay period is reduced; at 100°C, the period is about 10-15 minutes.

*APPENDIX III*

**TEMPERATURE CONTROL EQUIPMENT FOR INSTRON TESTER**

### Appendix III

#### TEMPERATURE CONTROL EQUIPMENT FOR INSTRON TESTER

In order to obtain stress-strain data over a wide temperature range, it was necessary to construct a special temperature-conditioning cabinet which can be mounted and used on the Instron tester for conducting tests at temperatures up to 300°C. An auxiliary box to supply thermostatically controlled air to this cabinet was also constructed.

The temperature-conditioning cabinet is similar to one previously built at the Institute for use over the temperature range -75 to 100°C. (The earlier cabinet, described elsewhere,<sup>42</sup> would not withstand temperatures much in excess of 100°C.) Figure III-1 shows a front view of the cabinet mounted on the Instron. The upper portion of the front panel is a door which has a window, a light, and two armholes for inserting and removing test specimens. The upper portion of the cabinet with the door open is shown in Fig. III-2.

The construction of the cabinet, with the front panel removed, is shown in Fig. III-3. As shown by the photograph, each side of the cabinet consists of three panels, the two outer panels being attached to the top of the cabinet. The innermost pair of panels is attached to the bottom of the cabinet, which is mounted on the movable crosshead of the Instron. The center pair of panels is free to slide between the inner and outer panels as the crosshead moves down and up. The position of the panels when the crosshead is in its lowest position is shown in Fig. III-4. A metal track is mounted on the inner and outer edges of the movable panels and these tracks fit in grooves on the inside of the back and front panels of the cabinet. Likewise, tracks are mounted on the outer surfaces of the movable panels and these tracks slide in grooves cut in the adjacent panels. To assure that the center panels move down in the desired manner, appropriately designed stops have been incorporated into the design of the cabinet.



FIG. III-1 HIGH-TEMPERATURE CABINET ON INSTRON TESTER

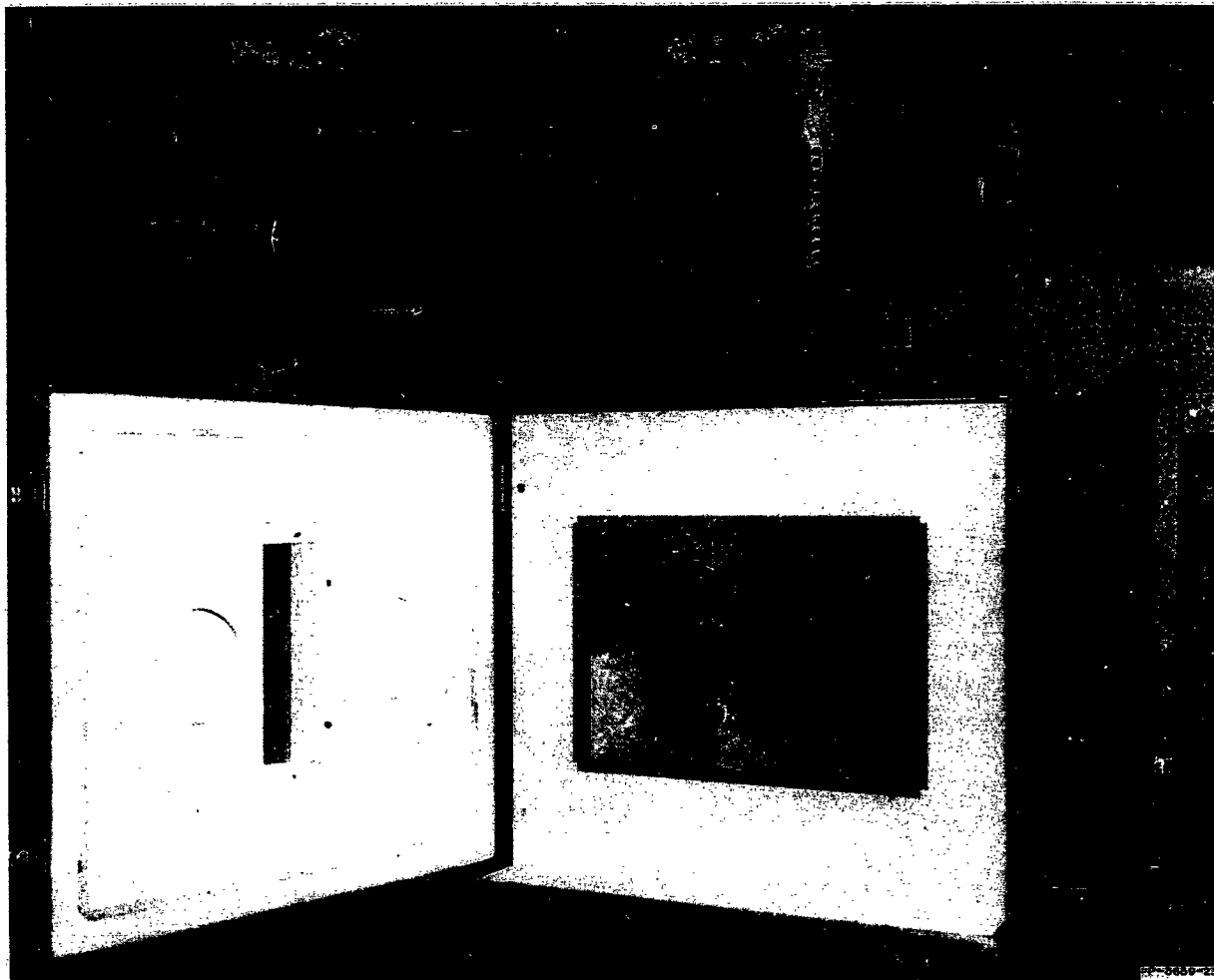


FIG. III-2 INTERIOR VIEW OF HIGH-TEMPERATURE CABINET  
ON INSTRON TESTER

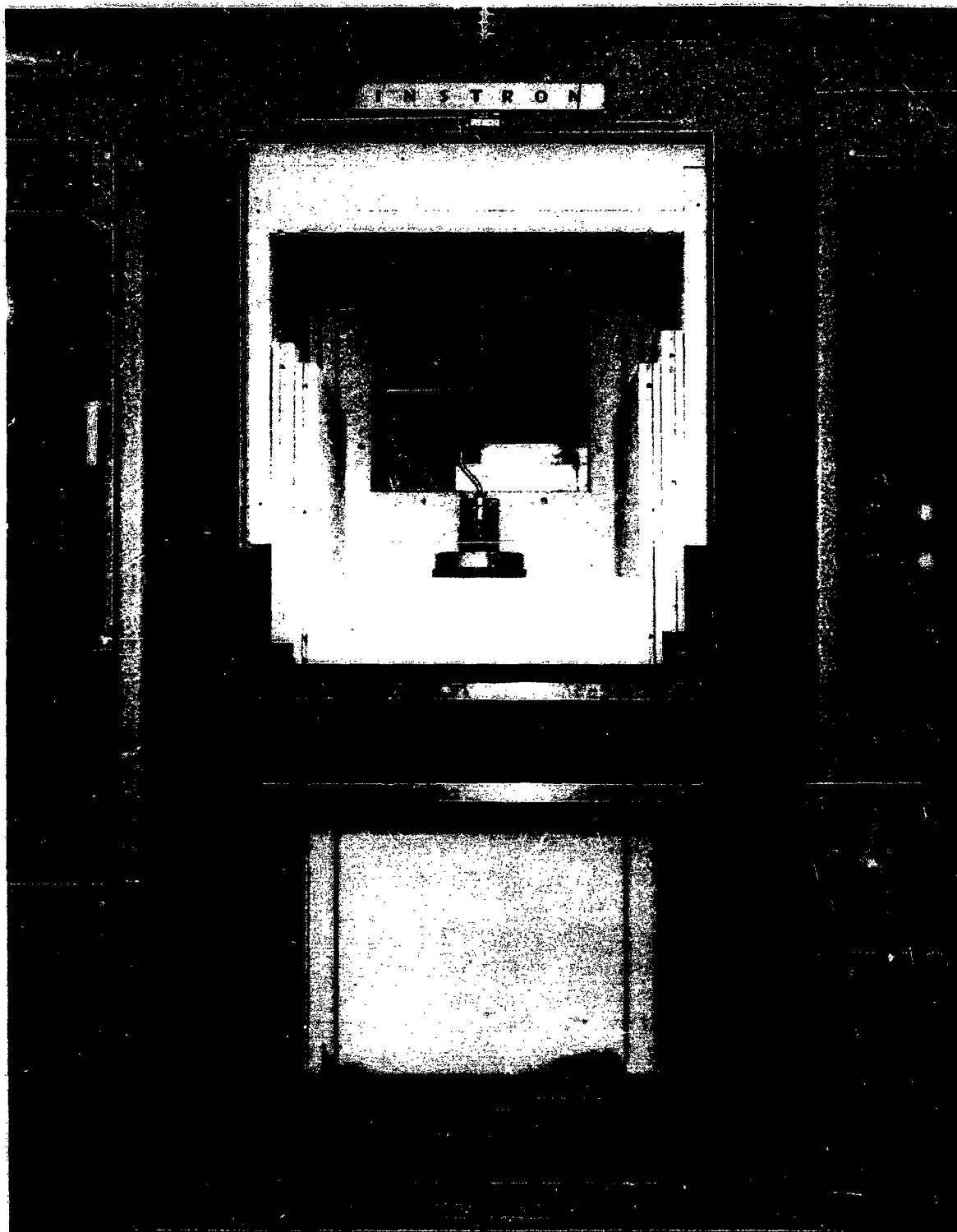


FIG. III-3 HIGH-TEMPERATURE INSTRON CABINET WITH FRONT PANEL REMOVED

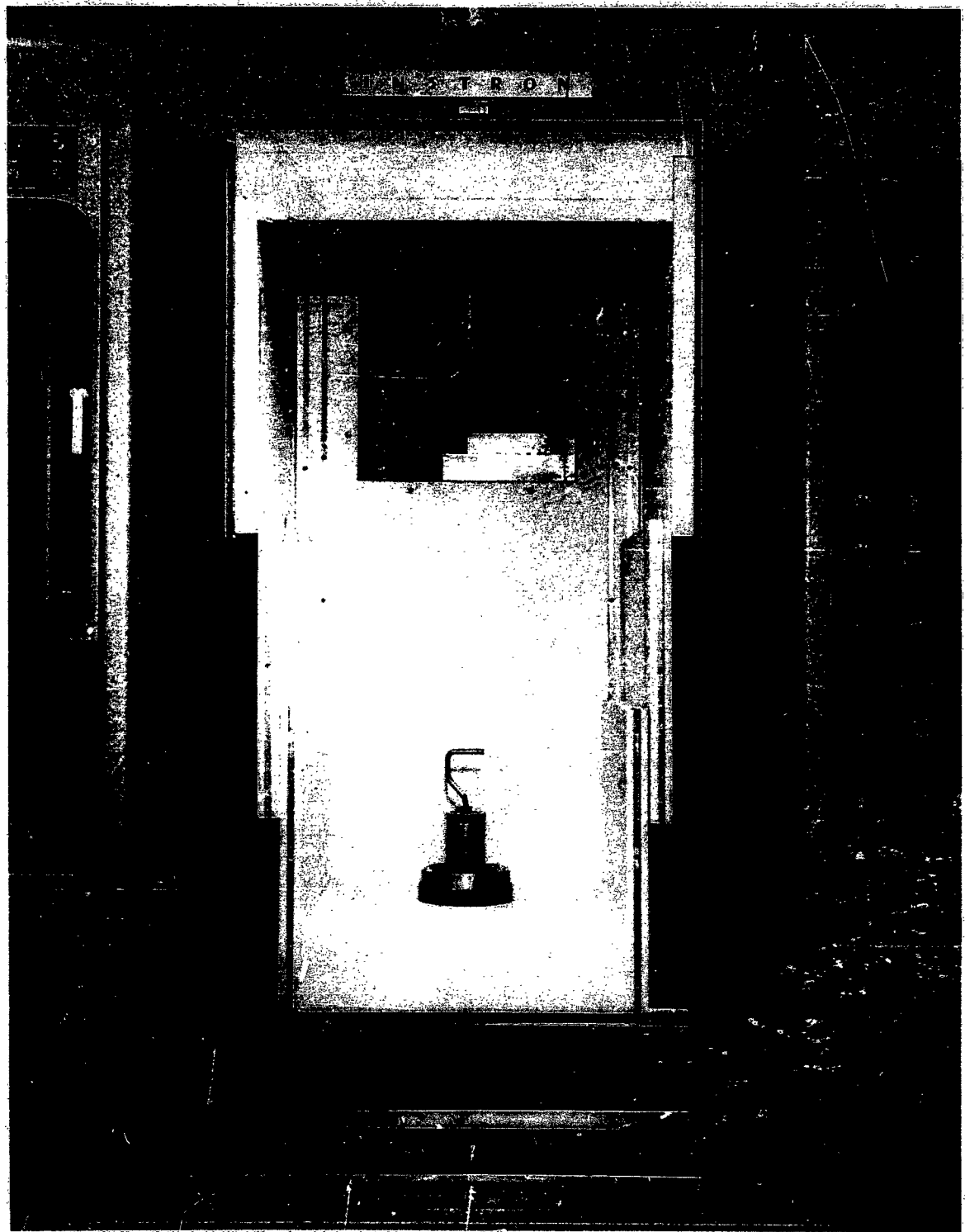


FIG. III-4 HIGH-TEMPERATURE INSTRON CABINET WITH FRONT PANEL REMOVED AND CROSSHEAD IN LOWEST POSITION

The exterior of the cabinet is sheet metal. The top and bottom of the cabinet, as well as the back panel and the bottom portion of the front panel, are constructed of two 1-inch-thick pieces of Marinite (a Johns Mansville insulation board) with 2 inches of thermobestos insulation between the pieces of Marinite. The side panels are made of 1-inch Marinite, and the cabinet door of three 1-inch pieces of Marinite. The window in the front of the cabinet has three panes of glass; the inner pane is Vycor and the outer two are window glass.

To maintain the load cell at room temperature, it is raised 12 inches above the top of the Instron and rests on a heavy piece of metal pipe; a number of  $\frac{3}{8}$ -inch holes were drilled through the wall of the pipe, as can be seen in Fig. III-1. Glass wool for insulation is placed at the top and bottom of the pipe. As an added precaution, a stream of air is blown into the metal pipe across the extension rod which connects the load cell to the sample hook on the inside of the cabinet. The extension rod was made from several ceramic standoff insulators which are 4 inches long and 1 inch in diameter. These insulators were threaded and fastened together by this means. Marinite and glass wool are placed, in a suitable manner, in the cylindrical hole which passes through the top of the cabinet.

To heat the cabinet, constant-temperature air is circulated continuously through it from an auxiliary temperature box, shown in Fig. III-5. The metal duct, seen on the side of the box in Fig. III-5, is inserted into the hole in the back panel of the cabinet mounted on the Instron. The box in its normal operating position is shown in Fig. III-6.

The outer surfaces of the auxiliary temperature box are constructed from two 1-inch-thick pieces of Marinite separated by 2 inches of thermobestos insulation. Sheet metal is used on the exterior. The box is divided into two compartments. One compartment contains electrical heaters, two blowers, and appropriate baffles and thermoregulators. The other compartment contains the motors attached to the blowers located inside the heated compartment. The blowers and associated motors were selected to withstand elevated temperatures.

One blower is employed to circulate air within the heated compartment and the other circulates the air through the cabinet mounted on the Instron.

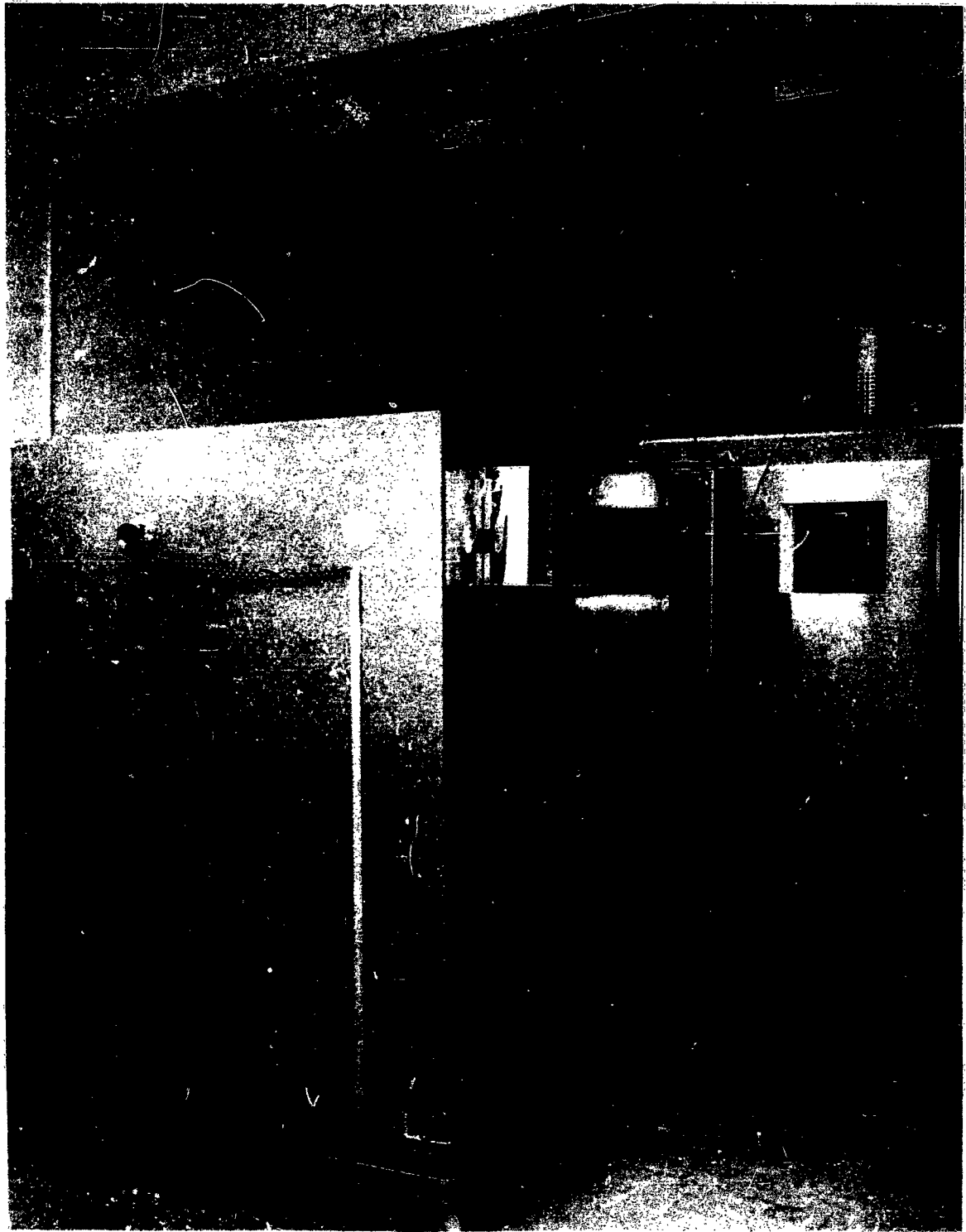


FIG. III-5 HIGH-TEMPERATURE BOX FOR USE WITH HIGH-TEMPERATURE INSTRON CABINET

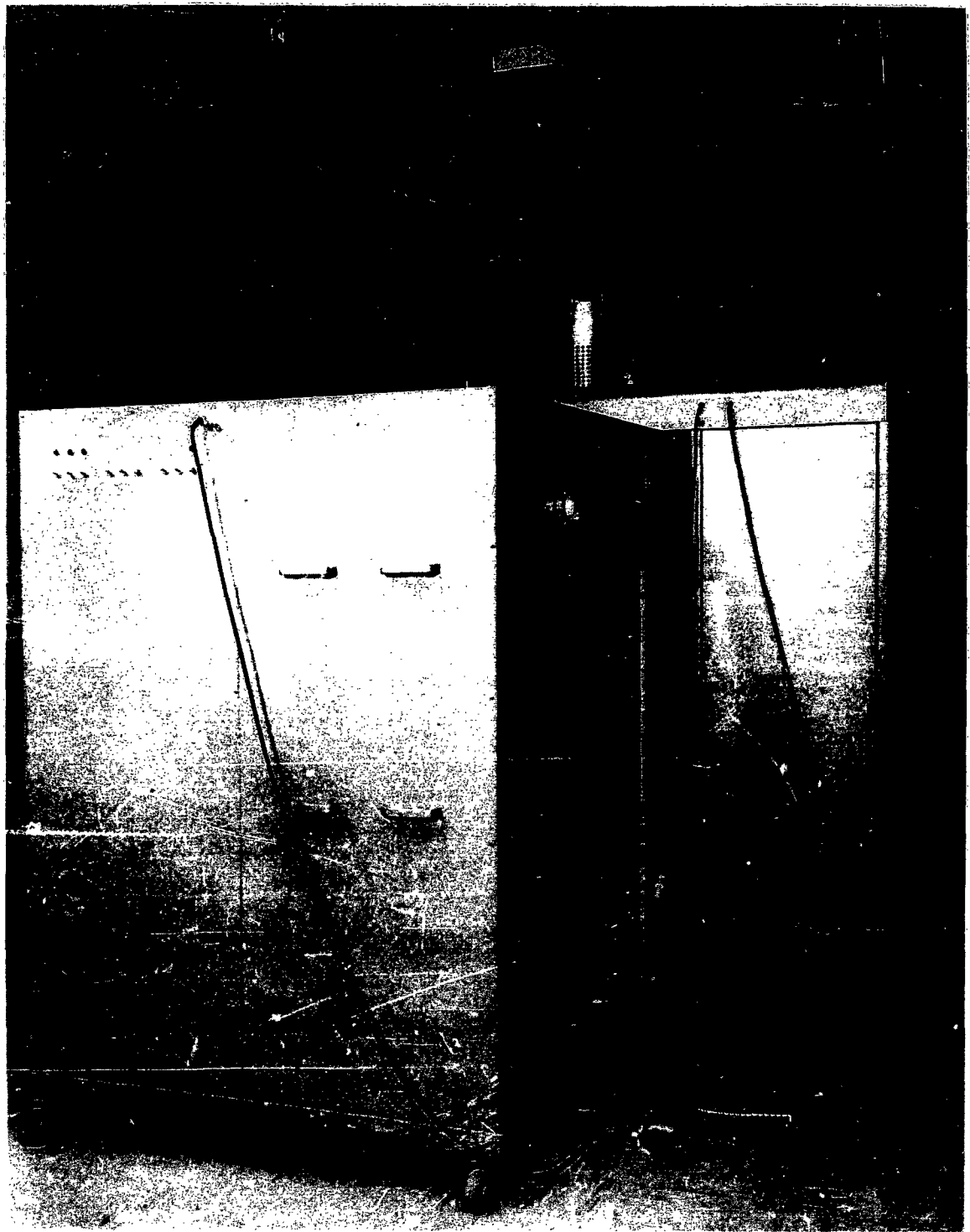


FIG. III-6 HIGH-TEMPERATURE BOX CONNECTED TO HIGH-TEMPERATURE INSTRON CABINET

The temperature in the box is controlled by an Aminco bimetallic thermostat which activates a selected number of heaters in the box. (Another thermostat is mounted in the box and used as a safety high-temperature cut-out switch.) The other heaters are operated continuously when the box is being used.

Tests made with thermocouples at various positions in the cabinet mounted on the Instron showed that the temperature at a fixed position can be controlled to about  $\pm 1^{\circ}\text{C}$  when the temperature is between about 100 and  $300^{\circ}\text{C}$ . To make tests at temperatures between about  $100^{\circ}\text{C}$  and  $-75^{\circ}\text{C}$ , another auxiliary temperature box equipped with heaters and a two-stage compressor was used in place of the special high-temperature box. With this other temperature box, the temperature in the cabinet on the Instron can be controlled to about  $\pm 0.5^{\circ}\text{C}$  at temperatures between 100 and  $-40^{\circ}\text{C}$ ; at temperatures below  $-40$ , the temperature could be controlled to about  $\pm 1^{\circ}\text{C}$ . Subsequent to obtaining the data presented in this report, some minor modifications were made in the equipment; it is believed now that the temperature can be controlled to about  $\pm 0.5^{\circ}\text{C}$  at all temperatures below  $100^{\circ}\text{C}$ .

*APPENDIX IV*

**PREPARATION AND EVALUATION OF RING-TYPE SPECIMENS  
FOR OBTAINING TENSILE STRESS-STRAIN DATA**

## APPENDIX IV

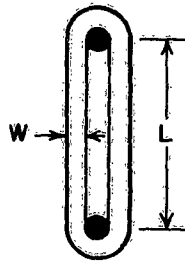
### PREPARATION AND EVALUATION OF RING-TYPE SPECIMENS FOR OBTAINING TENSILE STRESS-STRAIN DATA

Valuable information about the basic properties of vulcanizates can be obtained from tensile stress-strain curves, provided that the curves are measured over a wide range of testing conditions and the data are accurate. An objective of the present work was to obtain basic information not only about the ultimate tensile properties of selected vulcanizates but also about their viscoelastic properties under large tensile deformation. Before vulcanizates could be tested at various strain rates and temperatures, it seemed highly desirable to consider and carefully evaluate methods for obtaining such data.

#### A. GENERAL DISCUSSION OF TESTING METHOD

Although tensile data on vulcanizates are conventionally obtained by stretching dumbbell-shaped specimens at some rate, this method has several major disadvantages. In the first place, it is difficult to determine the strain in the gage section of the specimen because the strain is not directly proportional to the crosshead displacement except when the strains remain less than about 200 or 300%. Thus, to determine strain, it is necessary to use an extensometer or to place bench marks on the specimen and to monitor either visually or photographically their separation during the test. Although such methods can be employed, it is difficult, if not impossible, to interpret in a basic manner the data obtained, because the strain rate varies during the test. During a test made at a constant crosshead speed, the rate of separation of two bench marks on a specimen often decreases by a factor of two or more, especially if the elongation at rupture is high, *e.g.*, 500-800%.

Perhaps the best and easiest way of overcoming the fundamental difficulties associated with testing dumbbell specimens is to use rubber rings as test specimens. Such rings can be cut from sheets of rubber and can be tested by placing them over hooks mounted on the Instron. (See Appendix III, Figs. III-2 to III-4.) However, some difficulties are



A-3659-19

FIG. IV-1 SKETCH OF RING-SPECIMEN STRETCHED OVER SUPPORTING HOOKS

connected with testing ring specimens, and thus certain questions must be considered before test data of known reliability can be obtained.

The primary disadvantage of using a ring for a tensile specimen is that the strain in a stretched ring is nonuniform; it is a maximum around the inner circumference of the ring and a minimum around the outer circumference. Likewise, the stress varies across a stretched ring. However, the nonuniformity of the stress and strain does not preclude the obtainment of reliable data, provided that the test results are analyzed in a proper manner.

The tensile stress in a stretched ring equals the retractive force divided by twice the cross-sectional area of the ring; twice the cross-sectional area is used because the force is supported by both sides of a stretched ring.

When a ring is tested, the average strain in the ring  $\epsilon_a$  is usually calculated from the crosshead displacement  $\Delta L$  by the equation:

$$\epsilon_a = \frac{2\Delta L}{\pi D_a} \quad (\text{IV-1})$$

where  $D_a$  is the average diameter of the unstretched ring. The strain around the inner circumference of the ring equals  $\epsilon_a(D_a/D_i)$ , where  $D_i$  is the inside diameter of the unstretched ring; likewise the strain around the outside circumference equals  $\epsilon_a(D_a/D_o)$ , where  $D_o$  is the outside diameter of the unstretched ring.

The above equation, although sufficiently accurate for most purposes, is not precisely correct. To see more clearly what occurs when a ring is stretched, let us consider the sketch in Fig. IV-1, which shows a ring stretched over two hooks. For this consideration, the following quantities are needed:

- $D_i$  = inside diameter of unstretched ring  
 $D_o$  = outside diameter of unstretched ring  
 $D_a$  =  $(D_i + D_o)/2$  = average diameter of unstretched ring  
 $d$  = diameter of hooks  
 $W^o$  = width of unstretched ring  
 $W$  = width of stretched ring  
 $T^o$  = thickness of unstretched ring  
 $T$  = thickness of stretched ring  
 $L^o$  = initial distance between centers of hooks  
 $L$  = distance between centers of hooks.

The average strain in the stretched ring equals

$$\epsilon_a = \frac{C_a}{C_a^o} - 1 \quad (\text{IV-2})$$

where  $C_a$  is the circumference measured along the line equidistant between the inside and outside circumference and  $C_a^o$  is the initial value which equals  $\pi D_a$ . The initial and final circumference can be written as follows:

$$C_a = 2L + \pi \left( d + \frac{W}{2} \right) \quad (\text{IV-3})$$

$$C_a^o = 2L^o + \pi \left( d + \frac{W^o}{2} \right) \quad (\text{IV-4})$$

Thus, the strain equals:

$$\epsilon_a = \frac{C_a - C_a^o}{C_a^o} = \frac{2L + \pi \left( d + \frac{W}{2} \right) - 2L^o - \pi \left( d + \frac{W^o}{2} \right)}{C_a^o} \quad (\text{IV-5})$$

$$= \frac{2\Delta L}{C_a^o} + \frac{\pi}{2} \left( \frac{W - W^o}{C_a^o} \right) \quad (\text{IV-6})$$

where  $\Delta L = L - L^o$  and is the crosshead displacement which produces the strain  $\epsilon_a$ . It is seen that Eq. (IV-6) is independent of the diameter of the hooks.

When a rubber is deformed in tension, the volume change which occurs is negligible for present purposes. Also, the fractional changes in the width and thickness are equal. Thus, we can write

$$1 = \frac{C_a WT}{C_a^o W^o T^o} = \frac{C_a}{C_a^o} \left( \frac{W}{W^o} \right)^2 = (\epsilon_a + 1) \left( \frac{W}{W^o} \right)^2 \quad (IV-7)$$

By rearranging Eq. (IV-7) we obtain

$$W - W^o = W^o \left[ \frac{1}{\sqrt{\epsilon_a + 1}} - 1 \right] \quad (IV-8)$$

Upon substituting Eq. (IV-8) in Eq. (IV-6) and replacing  $C_a^o$  with  $\pi D_a$ , we obtain the equation:

$$\epsilon_a = \frac{2\Delta L}{\pi D_a} - \frac{W^o}{2D_a} \left[ 1 - \frac{1}{\sqrt{\epsilon_a + 1}} \right] \quad (IV-9)$$

This equation differs from Eq. (IV-1), the one normally used, by a relatively small amount which depends on  $W^o/D_a$  and  $\epsilon_a$ .

To see the percentage error introduced by neglecting the second term in Eq. (IV-9), the equation can be written as follows:

$$\frac{\frac{2\Delta L}{\pi D_a} - \epsilon_a}{\epsilon_a} \times 100 = \frac{W^o}{2D_a \epsilon_a} \left( 1 - \frac{1}{\sqrt{\epsilon_a + 1}} \right) \times 100 \quad (IV-10)$$

The percentage error is greatest in the limit of zero strain and equals:

$$\% \text{ error} = \frac{1}{4} \frac{W^o}{D_a} \times 100 \quad (IV-11)$$

The quantity  $W^o/D_a$  can be written in terms of  $D_o/D_i$  and, if this is done, Eq. (IV-11) becomes

$$\% \text{ error} = 25 \left( \frac{D_o}{D_i} - 1 \right) \left( \frac{D_o}{D_i} + 1 \right) \quad (IV-12)$$

Thus, if the  $D_o/D_i$  ratio is 1.10, the maximum error introduced by neglecting the second term in Eq. (IV-9) is about 1.2%; if the  $D_o/D_i$  ratio is 1.30, the maximum error is about 3.2%. However, these errors are for the limit of zero strain, and with increasing strain the percentage error drops rapidly. For example, when the  $D_o/D_i$  ratio is 1.10 and the strain is 1.0, the error is 0.7%; when the strain is 5.0, the error is 0.28%. Because tests are normally made on rings having a  $D_o/D_i$  ratio of about 1.10, it was decided that the error introduced by the use of Eq. (IV-1) to relate crosshead displacement to strain is small and that the use of the more complex equation [Eq. (IV-9)] is not warranted.

As already pointed out, the strain around the inner circumference of a stretched ring is greater than the average strain. During a test, a ring will break when the strain around its inner circumference equals the ultimate strain  $\epsilon_b$ . Thus, to determine the strain at break  $\epsilon_b$  from the crosshead displacement which exists when rupture occurs, the following equation, which gives the strain around the inner circumference, should be used:

$$\epsilon_b = \frac{2\Delta L}{\pi D_i} \quad (IV-13)$$

To obtain a value for the stress at break (tensile strength), an extrapolation of the observed load-time curve (Instron trace) must be made. This extrapolation is needed because the force observed at break results from a specimen being under a strain which ranges from  $\epsilon_b$  to  $\epsilon_b D_i/D_o$ . What is desired is the load which would be observed if rupture would occur when the average strain  $\epsilon_a$  equals  $\epsilon_b$ .

To determine how far to extrapolate an observed force-time curve to obtain the correct value for the force at break, let us suppose that a test is made at a crosshead speed  $XHS$  and that the chart speed of the recorder is  $CS$ . If the crosshead displacement at rupture is  $(\Delta L)_b$ , then

the corresponding distance in inches along the time-axis of the recorder trace is

$$I_b = (\Delta L)_b \frac{(CS)}{(XHS)} = \frac{\pi D_i}{2} \frac{(CS)}{(XHS)} \epsilon_b \quad (IV-14)$$

If rupture had occurred when the  $\epsilon_a$  equalled  $\epsilon_b$ , then the corresponding distance ( $I'_b$ ) along the time axis would have been

$$I'_b = \frac{\pi D_o}{2} \frac{(CS)}{(XHS)} \epsilon_b \quad (IV-15)$$

Thus, the number of inches along the time-axis that the curve must be extrapolated is

$$I'_b - I_b = \frac{\pi \epsilon_b}{2} \frac{(CS)}{(XHS)} (D_o - D_i) \quad (IV-16)$$

But because

$$\frac{\pi \epsilon_b (CS)}{2(XHS)} = \frac{I_b}{D_i} \quad (IV-17)$$

we obtain the following equation:

$$I'_b - I_b = \Delta X = I_b \left( \frac{D_o}{D_i} - 1 \right) \quad (IV-18)$$

where  $\Delta X$  is the number of inches along the time-axis that the curve must be extrapolated. In terms of the  $D_o/D_i$  ratio, Eq. (IV-18) becomes

$$\Delta X = \frac{I_b}{2} \left( \frac{D_o}{D_i} - 1 \right) \quad (IV-19)$$

As an example, suppose that a test is conducted at a crosshead speed of 2.0 inches/minute and a chart speed of 5.0 inches/minute. If the inside diameter of the ring is 1.25 inches and the strain at rupture is about 8.0, then  $I_b = 39.4$  inches. Now, if  $D_o/D_i = 1.08$ , then the

number of inches to be extrapolated is about 1.58 inches. On the other hand, if  $D_o/D_i = 1.30$ , the corresponding number of inches is 5.9, which is a rather large distance to extrapolate a curve, especially if the force prior to the observed rupture point is changing rapidly with time.

#### B. EVALUATION OF DATA OBTAINED BY TESTING RING SPECIMENS

From the preceding theoretical discussion, it appeared that no basic reasons exist which might prevent the obtainment of accurate data, including ultimate property data, at a constant strain rate by testing ring-type specimens at a constant crosshead speed. However, from a practical standpoint, several potential problems could be envisioned. These are as follows:

- (a) Preparation of Rings. A method must be available for cutting rings to close tolerance from sheet rubber; otherwise a ring will stretch in a nonuniform and unknown manner during a test.
- (b) Dimensions of Rings. The dimensions of the prepared rings must be known precisely; otherwise accurate values of the stress and strain cannot be obtained from force-crosshead displacement data.
- (c) Slippage of Rings on Hooks. In the discussion in the preceding section, it was assumed that the strain around the circumference of a ring is uniform at all times during a test. This uniformity can exist only if a ring slips easily over the supporting hooks during a test. Otherwise, the strain and strain rate in those portions of the ring which contact the hooks will be less than in other portions of the ring.
- (d) Ultimate Properties. Although methods were proposed in the preceding section for obtaining values of tensile strength and ultimate strain by testing rings, such methods require evaluation to assure that values obtained are independent of the dimensions of a ring.
- (e) Stress-Strain Values. Because only average values of stress and strain are obtained from testing rings (the stress and strain vary across a ring), the reliability of such data needs to be checked. This verification is particularly required because the rubber in contact with the hooks is under a biaxial strain because of the contact pressure between the rubber and the hooks.

A systematic study has been made of the various problems mentioned above, and the results are discussed in the remaining portion of this Appendix.

## 1. PREPARATION AND DIMENSIONS OF RINGS

Two types of cutters, shown in Fig. IV-2, were constructed and evaluated for cutting rings from sheets of rubber. The "adjustable" cutter, shown on the left in Fig. IV-2, has blades which can be adjusted to cut rings having any desired inside and outside diameter. The cutting blades are of tool steel and are prepared by grinding. The cutter is used by mounting it in a drill press.

The three other cutters in Fig. IV-2 have fixed dimensions and were made from pieces of mild steel rods. These cutters are also mounted in a drill press for use and they were used to prepare the rings in series 3-8 listed in Table IV-1. (The adjustable cutter was used to prepare the other rings listed in Table IV-1.) Actually, the fixed cutters were prepared before satisfactory blades were prepared for the adjustable cutter. With the present blades in the adjustable cutter, rings can now be prepared which are as good as and probably somewhat better than those cut with the fixed cutters. Thus, the adjustable cutter was used in the work described in the main portion of this report.

Various methods were considered and tested for measuring the dimensions of rings. It was decided that the most reliable values could be obtained by calculating the dimensions from the weights of a ring and the disc coming from the inside of the ring, the thickness of the rubber sheet, and the density of the rubber. The following equations are used:

$$D_i = \left[ \frac{4W_d}{\pi T \rho} \right]^{1/2} \quad (\text{IV-20})$$

$$D_o = \left[ \frac{4(W_d + W_R)}{\pi T \rho} \right]^{1/2} \quad (\text{IV-21})$$

where  $D_i$  and  $D_o$  are the inside and outside diameters of a ring,  $W_d$  and  $W_R$  are the weights of the disc and the ring, and  $T$  and  $\rho$  are the thickness and density of the rubber sheet.

As a material to use in evaluating the method for preparing and testing rings, large sheets of a natural rubber vulcanizate were purchased from a local supplier. The rubber contained only a minor amount of filler and had a nominal thickness of  $1/16$  inch and a 30-40 Shore A hardness.



P-3859-28

FIG. IV-2 ADJUSTABLE AND FIXED CUTTERS FOR CUTTING RING SPECIMENS

Table IV-1  
 AVERAGE VALUES AND PERCENT STANDARD DEVIATION (% S. D.) OF VARIOUS QUANTITIES  
 USED TO CHARACTERIZE DIMENSIONS OF RINGS IN VARIOUS SERIES STUDIED

| SERIES<br>DESIG-<br>NATION | $W_R$<br>grams | %<br>S. D. | $W_D$<br>grams | %<br>S. D. | $D_o'$<br>inches | %<br>S. D. | $D_i'$<br>inches | %<br>S. D. | $D_e'$<br>inches | $10^3 A$<br>sq in. | $\frac{D_o}{D_i}$ | TYPE OF<br>CUTTER | METHOD OF<br>PREPARATION† |
|----------------------------|----------------|------------|----------------|------------|------------------|------------|------------------|------------|------------------|--------------------|-------------------|-------------------|---------------------------|
| 1                          | 0.2893         | 1.48       | 1.3222         | 0.9        | 1.4847           | 0.28       | 1.3412           | 0.29       | 1.4130           | 4.34               | 1.107             | Adjustable        | 1                         |
| 2                          | 0.2541         | 1.78       | 1.3174         | 0.6        | 1.4622           | 0.26       | 1.3387           | 0.22       | 1.4004           | 3.74               | 1.092             | Adjustable        | 2                         |
| 3                          | 0.2588         | 1.93       | 1.1972         | 1.3        | 1.4074           | 0.19       | 1.2762           | 0.16       | 1.3418           | 3.97               | 1.103             | Fixed             | 1                         |
| 4                          | 0.6325         | 1.04       | 0.8531         | 1.3        | 1.4216           | 0.45       | 1.0773           | 0.39       | 1.2494           | 10.42              | 1.320             | Fixed             | 1                         |
| 5                          | 0.7506         | 1.10       | 0.7162         | 0.7        | 1.4126           | 0.13       | 0.9871           | 0.38       | 1.1998           | 12.87              | 1.431             | Fixed             | 1                         |
| 6                          | 0.2656         | 3.87       | 1.2195         | 1.1        | 1.4214           | 0.13       | 1.2880           | 0.22       | 1.3547           | 4.04               | 1.104             | Fixed             | 2                         |
| 7                          | 0.6353         | 0.69       | 0.8782         | 1.0        | 1.4349           | 0.08       | 1.0930           | 0.25       | 1.2640           | 10.34              | 1.313             | Fixed             | 2                         |
| 8                          | 0.7392         | 0.63       | 0.7243         | 0.5        | 1.4110           | 0.10       | 0.9926           | 0.25       | 1.2018           | 12.66              | 1.422             | Fixed             | 2                         |
| a                          | 0.1835         | 1.80       | 0.7205         | 1.0        | 1.1070           | --         | 0.9883           | --         | 1.0480           | 3.604              | 1.120             | Adjustable        | 2                         |
| b                          | 0.2439         | 1.00       | 1.1353         | 0.2        | 1.3670           | --         | 1.2410           | --         | 1.3040           | 3.825              | 1.102             | Adjustable        | 2                         |
| c                          | 0.3316         | 1.00       | 1.6426         | 0.7        | 1.6360           | --         | 1.4920           | --         | 1.5640           | 4.372              | 1.097             | Adjustable        | 2                         |

\* Each series contained 10 rings.

† Method 1: Masking tape on both sides of rubber sheet.

Method 2: Masking tape on bottom of rubber sheet and metal template on top of rubber sheet.

$W_R$  is weight of ring

$W_D$  is weight of center disc

$D_o$  is outside diameter

$D_i$  is inside diameter

$$D_c = \frac{D_o + D_i}{2}$$

$A$  = cross-sectional area

Thickness of rubber sheet assumed to be 0.0605 in. (see text).

The evaluation involved the preparation and testing of over 120 rings as well as a number of dumbbell-shaped specimens.

Data used to characterize the dimensions of a number of series of rings are given in Table IV-1. Each series consists of ten rings each cut in the same manner. Rings comprising Series 1 and 2 and Series a, b, and c were cut by the adjustable cutter and those in Series 3-8 by the fixed cutters. Two methods were employed for holding the rubber while it was being cut. The first method consisted of placing masking tape on both surfaces of the rubber; the second method of placing masking tape only on the under surface and placing a metal plate having a hole in it on top of the rubber sheet. In cutting rings by both methods, soapy water was used to lubricate the cutting blades. The second method seemed to be preferable, although the data presented in this appendix showed no significant difference between the two methods.

Table IV-1 gives average values of  $W_R$  and  $W_D$  along with standard deviations expressed as percentage. As might be expected, the dispersion in the weights becomes less as the average weight increases. In the studies described in the main portion of this report, tests were made of rings whose dimensions are quite close to those in Series b; i.e.,  $D_i = 1.24$  in. and  $D_o/D_i = 1.10$ . The standard deviation of the weights of the rings in this series is about 1%. When a number of "identical" rings are cut, the deviation of the weight of a ring from the average value appears to be the best criterion to use in assessing the perfection of the ring, provided that the thickness of the rubber sheet is highly uniform.

The method for measuring the thickness of the disc cut from the center of each ring employs a precision dial gage (Ames Dial Indicator No. 312.5) which is graduated in units of 0.0001 inch. The gage has a foot which is a metal disc about 0.75 inch in diameter. For use, the gage is mounted above a large flat metal slab.

The gage was used to measure the thicknesses of the 30 discs from rings in Series a, b, and c. After thicknesses were measured once, they were measured again except that now the discs were measured in random order to minimize bias. This procedure was repeated five times. For each disc, the difference between individual values and the average of the five values was normally  $\pm 0.0001$  inch, although in several instances it was  $\pm 0.0002$  inch. It thus appears that if a disc is about 0.060 inch thick, its thickness can be measured with a precision of a few parts

in 600. However, the accuracy is uncertain because the degree to which the rubber is compressed while being measured is not known. It is believed, however, that the compression is slight.

The thicknesses of discs in Series a, b, and c ranged from 0.0594 to 0.0609 inch and the average value was 0.0605 inch. Although the variation observed is undoubtedly real, the average value was used in the calculation of ring dimensions. It was also necessary to use this average thickness to calculate the dimensions of the rings in Series 1-8 because the precision dial gage was not available when these rings were prepared.

Values of  $D_o$  and  $D_i$  for rings in Series 1-8 were calculated from individual values of  $W_R$  and  $W_D$ , a density of 0.944 g/cc for the rubber, and a thickness of 0.0605 inch. (The thickness of each ring was assumed to be the same.) The values given in Table IV-1 were obtained by averaging the individual values. In the calculation of  $D_o$  and  $D_i$  for rings in Series a, b, and c, average values of  $W_R$  and  $W_D$ , given in Table IV-1, were used.

No statistical analysis has been made to estimate the accuracy of ring dimensions calculated from  $W_R$ ,  $W_D$ ,  $T$ , and  $\rho$ . However, let us suppose that  $T$  and  $\rho$  are known precisely but that  $W_R$  and  $W_D$  are known only to 1%. Now, if  $D_i$  is about 1.0 inch and  $D_o/D_i$  is about 1.10, the cross-sectional area may be in error by up to 15%.

Although individual values of  $W_R$  and  $W_D$  can be obtained to within about 0.1%, it is difficult to estimate the accuracy of the thickness measurement. Further, the thickness at various points on a sheet of rubber can differ by several percent. To obtain the best values for ring dimensions, individual values of  $W_R$ ,  $W_D$ , and  $T$  instead of average values were used to obtain dimensions of the rings used in the studies of the gum vulcanizates discussed in this report. However, as already pointed out, this method was not used in obtaining the data presented in this appendix.

## 2. SLIPPAGE OF RINGS DURING TEST

Rings were tested by placing them over the hooks mounted on the Instron. The hooks were lubricated with a silicone grease to promote slippage of rings being tested. To determine whether or not slippage occurred in a uniform manner, bench marks were placed on rings and

photographs were taken periodically during a test. In most instances two bench marks were used, although four marks were used at times.

To analyze the results, the photographs were projected on paper mounted on a wall, and the positions of the bench marks were marked on the paper. The distances between the marks were measured by use of a Bensen-Lehner Oscar Model K. Plots were then made of distance against time. Figure IV-3 shows a typical plot. This plot shows that the strain in the ring increases linearly with time. From the slope of the line and the intercept on the ordinate, a strain rate of  $2.19 \text{ min}^{-1}$  was calculated. This value is in perfect agreement with the value  $2.19 \text{ min}^{-1}$  calculated from the crosshead speed and the average diameter of the ring.

A large number of similar tests were conducted, and in every instance the plot of distance between marks against time was linear throughout the test. Two tests made without lubricant on the hooks gave similar results. However, in obtaining the data discussed in the main portion of this

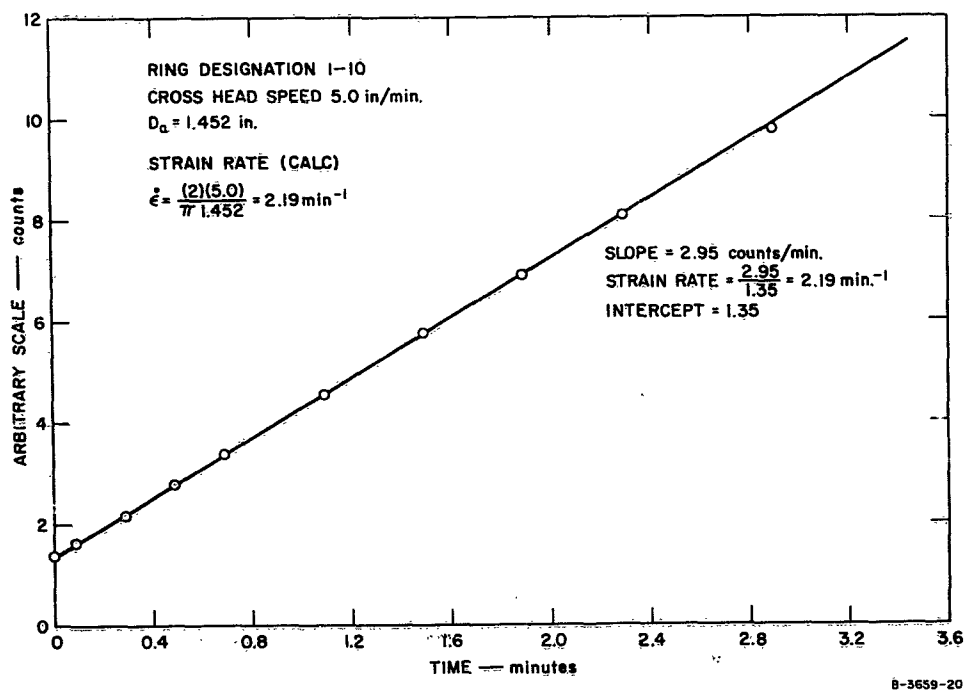


FIG. IV-3 VARIATION WITH TIME OF DISTANCE BETWEEN BENCH MARKS ON RING SPECIMEN

report, lubricant was used in conducting all tests. A silicone grease was used except at low test temperatures a DC-200 fluid was used.

Some of the results from the photographic studies are given in Table IV-2. For the first group of rings listed in the Table, the agreement between the experimental and calculated values of the strain

Table IV-2  
STRAIN RATE IN RING SPECIMENS  
TESTED AT CONSTANT  
CROSSHEAD SPEEDS

| DESIG-<br>NATION | XHS <sup>a</sup><br>in./min | STRAIN RATE,<br>MIN <sup>-1</sup> |                    |
|------------------|-----------------------------|-----------------------------------|--------------------|
|                  |                             | Exp. <sup>b</sup>                 | Calc. <sup>c</sup> |
| 1-8              | 5.0                         | 2.20                              | 2.19               |
| 1-9              | 5.0                         | 2.17                              | 2.19               |
| 1-10             | 5.0                         | 2.19                              | 2.19               |
| 2-7              | 5.0                         | 2.20                              | 2.20               |
| 2-8              | 5.0                         | 2.18                              | 2.20               |
| 2-9              | 5.0                         | 2.24                              | 2.20               |
| a-12             | 20.0                        | 13.3                              | 12.2               |
| b-12             | 20.0                        | 8.28                              | 9.75               |
| a-10             | 5.0                         | 3.23*                             | 3.04               |
| a-11             | 5.0                         | 3.21*                             | 3.04               |
| b-10             | 5.0                         | 2.53*                             | 2.44               |
| b-11             | 5.0                         | 2.42                              | 2.44               |
| c-10             | 5.0                         | 1.98                              | 2.04               |

<sup>a</sup> XHS = crosshead speed

<sup>b</sup> Strain rate from photographs of bench marks

<sup>c</sup> Strain rate calculated from XHS and  $D_o$ ;  $\dot{\epsilon} = [2(XHS)/\pi D_o]$

\* No lubricant used on hooks

rate is excellent. The poorer agreement for the second set of rings results, it is believed, from the use of a modified test procedure which made it difficult to establish zero time for each test. Without knowing zero time accurately, values of the intercept on plots like those shown in Fig. IV-3 are uncertain. However, because straight lines were always obtained, the strain rate is known to have been constant during each test and, unquestionably, the actual strain rate was the same as predicted from the crosshead speed and the average diameter of a ring. In addition to results shown in Table IV-2, tests were made at crosshead speeds of 2.0, 0.2, and 0.02 inch/min. Again, the results confirmed that the rings were subjected to a constant strain rate.

### 3. ULTIMATE TENSILE PROPERTIES

Average values of the ultimate tensile properties obtained from tests made on rings in Series 1-8 and Series a, b, and c at 5.0 inches/minute crosshead speed are given in Table IV-3 along with the percent standard deviation of some of the results. A major reason for conducting this work was to determine if values of the tensile strength and the ultimate strain can be obtained which are independent of ring dimensions. Thus, rings in Series 3-5 and in Series 6-8 have  $D_o/D_i$  ratios which increase from about 1.10 to 1.42. Rings in Series a, b, and c have a  $D_o/D_i$  ratio of about 1.1 but their average diameter increases from about 1.05 to 1.56 inches.

Table IV-3 gives values of  $\bar{\sigma}_b$ , the force observed at rupture divided by twice the cross-sectional area of the ring. This quantity depends markedly on the  $D_o/D_i$  ratio. For example, as the  $D_o/D_i$  ratio increases

Table IV-3

AVERAGE VALUES OF TENSILE STRENGTH (psi) AND ULTIMATE STRAIN AND PERCENT STANDARD DEVIATION. TESTS MADE AT 5.0 INCHES/MINUTE CROSSHEAD SPEED

| SERIES DESIGNATION | $\frac{D_o}{D_i}$ | $D_o$ , inches | $\bar{\sigma}_b$ | % S. D. | $\sigma_b$ | % S. D. | $\bar{\epsilon}_b$ | % S. D. | $\epsilon_b$ | STRAIN RATE, MIN <sup>-1</sup> |
|--------------------|-------------------|----------------|------------------|---------|------------|---------|--------------------|---------|--------------|--------------------------------|
| 1                  | 1.107             | 1.4130         | 2640             | 11.2    | 3318       | 11.6    | 7.74               | 1.9     | 8.14         | 2.26                           |
| 2                  | 1.092             | 1.4004         | 2680             | 16.6    | 3275       | 16.1    | 7.64               | 2.4     | 7.98         | 2.28                           |
| 3                  | 1.103             | 1.3418         | 2535             | 14.8    | 3171       | 14.6    | 7.60               | 3.2     | 8.00         | 2.37                           |
| 4                  | 1.320             | 1.2494         | 1920             | 7.0     | 3434       | 11.5    | 7.17               | 2.2     | 8.30         | 2.55                           |
| 5                  | 1.431             | 1.1998         | 1605             | 3.4     | 3229       | 4.3     | 6.82               | 0.7     | 8.30         | 2.66                           |
| 6                  | 1.104             | 1.3547         | 2700             | 8.0     | 3097       | 8.6     | 7.84               | 1.7     | 8.25         | 2.35                           |
| 7                  | 1.313             | 1.2640         | 1935             | 6.9     | 3292       | 6.8     | 7.16               | 1.6     | 8.30         | 2.52                           |
| 8                  | 1.422             | 1.2018         | 1513             | 16.9    | 3003       | 18.6    | 6.60               | 4.0     | 8.01         | 2.66                           |
| a                  | 1.120             | 1.048          | 2822             | 7.8     | 3646       | 8.3     | 7.59               | 1.8     | 8.05         | 3.04                           |
| b                  | 1.102             | 1.304          | 2961             | 10.8    | 3634       | 5.3     | 7.75               | 1.5     | 8.15         | 2.44                           |
| c                  | 1.097             | 1.564          | 2802             | 11.1    | 3388       | 11.6    | 7.63               | 2.4     | 7.99         | 2.04                           |

$\bar{\sigma}_b$  is the average stress when rupture occurred

$\sigma_b$  is the stress at break obtained by extrapolation procedure

$\bar{\epsilon}_b$  is the average strain when rupture occurred

$\epsilon_b$  is the ultimate strain; i.e., the strain based on inside diameter of ring.

$$\epsilon_b = \bar{\epsilon}_b D_o/D_i$$

from 1.10 to 1.42,  $\bar{\sigma}_b$  decreases from 2700 psi to 1513 psi. To correct this dependence, each force-time curve (Instron recorder trace) was extrapolated beyond the rupture point by the amount predicted by Eq. (IV-19). The extrapolations were made by use of a French curve; when extrapolations had to be made for several inches along the time axis, the results were perhaps not as precise as could have been obtained by other methods of extrapolating. However, values given in Table IV-3 for  $\sigma_b$  (extrapolated value) show no consistent trend with the  $D_o/D_i$  ratio.

Values for  $\bar{\sigma}_b$  and  $\sigma_b$  obtained for rings in Series a, b, and c appear to be somewhat higher than those for rings in the other series. No reason for the apparent difference can be given, although the strain rate at which Series a was tested was somewhat higher than for the other series. (The strain rate at which each series was tested was not the same because the average ring diameter was not the same.)

Table IV-3 also gives values of  $\bar{\epsilon}_b$  and  $\epsilon_b$ , where  $\bar{\epsilon}_b$  is the average value of the strain at rupture and  $\epsilon_b$  is the value based on the initial inside diameter of the rings. Again as expected, values of  $\bar{\epsilon}_b$  decrease as the  $D_o/D_i$  ratio increases. However, when values of  $\bar{\epsilon}_b$  are multiplied by  $D_o/D_i$ , the resulting values of  $\epsilon_b$  are independent of ring dimensions.

A number of dumbbell-shaped specimens were tested to obtain tensile data for comparison with the data obtained by testing rings. Dumbbells were cut which were 0.25 inch in width and had a 1.5-inch gage section. However, these specimens could not be broken because of the high elongation of the rubber and the limited crosshead travel of the Instron. Some tests were made on miniature dumbbells but difficulties were encountered in gripping these, as grips suitable for such specimens were not available. Thus, a special (and somewhat undesirable) technique was used to cut short specimens with the die having a 1.5-inch gage section. By placing the rubber over the edge of a block, cutting through the rubber once, rotating the rubber 180°, and cutting again, it was possible to prepare specimens having a gage section about or somewhat less than 1 inch. Thus, these specimens were not all of equal gage length and were not as precisely cut as perhaps desirable.

The dumbbell specimens were tested at 5.0 inch/min. crosshead speed. Bench marks on the specimens were photographed periodically during the test and the photographs were analyzed as described previously. Figure IV-4 is a typical plot which shows the variation of the extension ratio ( $\epsilon + 1$ ) with time during a test. It is seen that the strain rate is constant only as long as the elongation is between 0 and 300%. In

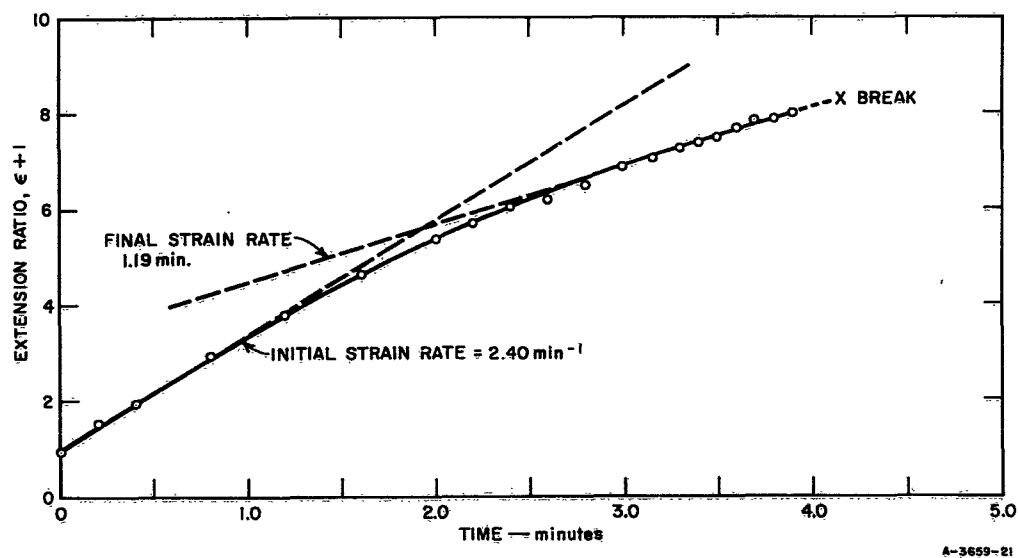


FIG. IV-4 VARIATION WITH TIME OF EXTENSION RATIO ( $\epsilon + 1$ ) OBTAINED FROM BENCH MARKS ON DUMBBELL-SHAPED SPECIMEN

this range, the strain rate is  $2.40 \text{ min}^{-1}$ , but the strain rate during the latter part of the test is  $1.19 \text{ min}^{-1}$ . (The strain rate is here defined as the slope of a plot of strain, or extension ratio, against time.)

Values of the ultimate properties obtained from tests on the dumbbells are given in Table IV-4 along with values of the initial and final strain rates. The precision of the data is reasonably good, especially considering the manner of specimen preparation. The values of the tensile strength, however, are appreciably lower than those obtained by testing rings at 5.0 inch/min crosshead speed (Table IV-3). However, the strain rates when the dumbbells broke are lower by a factor of two or more than the strain rates at which the rings were tested.

To see the effect of strain rate on the ultimate properties, rings having an average diameter of 1.299 inches and a  $D_o/D_i$  ratio of 1.08 were tested at crosshead speeds of 20.0, 2.0, 0.20, and 0.020 in./min. The results are given in Table IV-5. The values of  $\sigma_b$  were obtained by the extrapolation method and values of  $\epsilon_b$  are based on the inside diameter of the rings. It is seen that  $\epsilon_b$  decreases only a moderate amount with

Table IV-4

ULTIMATE TENSILE PROPERTIES OBTAINED  
BY TESTING DUMBBELL-SHAPED SPECIMENS

| DESIG-<br>NATION | $\sigma_b$ ,<br>psi | $\epsilon_b$ * | STRAIN RATE, <sup>*</sup><br>MIN <sup>-1</sup> |       |
|------------------|---------------------|----------------|------------------------------------------------|-------|
|                  |                     |                | Initial                                        | Final |
| d-1              | 2665                | 7.40           | 2.40                                           | 1.19  |
| d-4              | 2311                | 7.14           | 2.53                                           | 0.81  |
| d-7              | 2734                | 7.64           | 2.28                                           | 0.79  |
| d-9              | 2622                | 7.70           | 2.85                                           | 1.28  |
| d-11             | 2546                | 7.73           | 2.59                                           | 0.98  |
| d-12             | 2681                | 7.49           | 2.57                                           | 1.37  |
| d-13             | 2544                | 6.96           | 2.31                                           | 1.03  |
| d-14             | 2684                | 7.36           | 2.60                                           | 1.34  |
| d-15             | 2387                | 7.14           | 2.56                                           | 1.40  |
| d-16             | 2659                | 7.85           | 2.60                                           | 1.25  |
| Av.              | 2583                | 7.44           | 2.53                                           | 1.14  |

\* Values of strain and strain rate obtained from separation of bench marks on gage section of dumbbells

Table IV-5

EFFECT OF STRAIN RATE ON ULTIMATE  
TENSILE PROPERTIES

| RING<br>DESIG-<br>NATION | $\sigma_b$ ,<br>psi | $\epsilon_b$ | STRAIN RATE,<br>MIN <sup>-1</sup> |
|--------------------------|---------------------|--------------|-----------------------------------|
| 1-1-19                   | 3865                | 8.20         | 9.82                              |
| 1-1-20                   | 3832                | 8.18         |                                   |
| 1-1-21                   | 3932                | 8.29         |                                   |
| Av.                      | 3876                | 8.22         |                                   |
| 1-1-22                   | 3484                | 8.07         | 0.982                             |
| 1-1-23                   | 3517                | 8.03         |                                   |
| 1-1-24                   | 3434                | 8.01         |                                   |
| Av.                      | 3478                | 8.04         |                                   |
| 1-1-25                   | 2671                | 7.60         | 0.0982                            |
| 1-1-26                   | 1675                | 7.08         | 0.00982                           |

Values of  $\sigma_b$  obtained by extrapolation procedure.

Values of  $\epsilon_b$  based in inside diameter of ring.

Dimensions of rings are  $D_o = 1.348 \text{ in.}$ ;  $D_i = 1.249 \text{ in.}$ ;  $D_o = 1.299 \text{ in.}$ ;  $D_o/D_i = 1.08$ ;  $A = 0.003014 \text{ sq in.}$ ; and thickness =  $0.0609 \text{ in.}$

decreasing strain rate but that  $\sigma_b$  decreases by more than a factor of two as the strain rate is decreased from 0.98 to 0.0098  $\text{min}^{-1}$ . It is difficult to compare the data (Table IV-5) obtained by testing rings with those (Table IV-4) obtained by testing dumbbell specimens because in the latter instance the strain rate decreased during each test. However, when a ring was tested at 0.0982  $\text{min}^{-1}$ , values of  $\sigma_b$  and  $\epsilon_b$  were 2671 psi and 7.60, respectively, and these values are close to the average values ( $\sigma_b = 2583$  psi and  $\epsilon_b = 7.44$ ) obtained by testing dumbbell specimens.

#### 4. STRESS-STRAIN VALUES PRIOR TO RUPTURE

As a large number of rings were tested for various reasons, it was desirable to analyze the stress-strain curves prior to rupture to see (1) whether or not the data are independent of ring dimensions and (2) how closely the data agree with those obtained from testing dumbbells.

The initial portion of a stress-strain curve obtained from testing a ring is not as accurate as the latter portion. This condition occurs because the force-time curve (Instron recorder trace) has an initial "toe." This toe results from the slight force required to change the ring from its initial circular shape into the shape (Fig. IV-1) which exists during most of the test. (The toe is observed only if a sensitive load cell range is used while recording the initial portion of the curve.) Ideally, circular rings should not be tested but rings shaped like a normal rubber band should be used; these should be supported on hooks whose radius of curvature is the same as that at the two ends of the rubber band. However, the error introduced by testing circular rings is not appreciable except at low strain values. If accurate data at low strains are desired, they can be obtained readily and accurately by the use of conventional methods.

The toe on a force-time curve becomes large as the  $D_o/D_i$  ratio of the ring increases. However, a correction can be made for the toe by extrapolating the normal portion of the curve to the zero load axis and by using the point of intersection on the time axis as the point of zero time.

All curves obtained from testing rings in Series 1-8 and Series a, b, and c were analyzed. Values of stress were obtained at strains of 0.1, 0.2, 0.5, 1.5, 3.0, 5.0, and 6.5, and average values at these

strains are given in Table IV-6. Unfortunately, not all tests were made in an identical manner. In testing all 10 rings in Series 3 and the first six rings in Series 1 and 2, the rings were placed under a slight initial tension by moving the crosshead down slightly; the output from the Instron load cell was next adjusted to zero, and then the test started. The curves from these tests showed no toe. All rings in the other series were conducted by hanging the rings loosely over the hooks and then starting the crosshead. This latter procedure is the desirable one. The former method may fortuitously give the same results as obtained from the latter by correcting for the toe. Actually, both methods lead to a small error in the data; the percentage error is significant, however, only at low values of strain.

Table IV-6

AVERAGE VALUES OF STRESS  $\sigma$  (psi) AND PERCENT STANDARD DEVIATION AT VARIOUS VALUES OF STRAIN. TESTS MADE AT 5.0 INCHES/MINUTE CROSSHEAD SPEED

| SERIES DESIGNATION | $\frac{D_o}{D_i}$ | $D_o$ , inches | $\epsilon = 0.1$ |         | $\epsilon = 0.2$ |         | $\epsilon = 0.5$ |         | $\epsilon = 1.5$ |         | $\epsilon = 3.0$ |         | $\epsilon = 5.0$ |         | $\epsilon = 6.5$ |         | STRAIN RATE, MIN <sup>-1</sup> |
|--------------------|-------------------|----------------|------------------|---------|------------------|---------|------------------|---------|------------------|---------|------------------|---------|------------------|---------|------------------|---------|--------------------------------|
|                    |                   |                | $\sigma$         | % S. D. |                                |
| 1                  | 1.107             | 1.4130         | 14.2             | 14.69   | 29.5             | 6.51    | 58.2             | 2.20    | 113              | 1.88    | 199              | 1.15    | 445              | 1.57    | 1256             | 6.25    | 2.26                           |
| 2                  | 1.092             | 1.4004         | 14.0             | 18.56   | 29.4             | 10.64   | 60.0             | 3.10    | 116              | 1.64    | 204              | 1.29    | 458              | 1.25    | 1321             | 2.53    | 2.28                           |
| 3                  | 1.103             | 1.3418         | 14.5             | 13.92   | 30.8             | 4.41    | 59.3             | 4.05    | 117              | 2.98    | 209              | 1.69    | 468              | 2.36    | 1432             | 6.84    | 2.37                           |
| 4                  | 1.320             | 1.2494         | 13.2             | 9.17    | 27.2             | 7.43    | 59.1             | 3.11    | 117              | 1.84    | 207              | 2.00    | 436              | 3.21    | 1407             | 4.36    | 2.55                           |
| 5                  | 1.431             | 1.1998         | 10.3             | 24.75   | 22.9             | 15.12   | 55.7             | 4.55    | 115              | 1.48    | 204              | 2.72    | 496              | 2.96    | 1432             | 3.35    | 2.66                           |
| 6                  | 1.104             | 1.3547         | 15.3             | 5.96    | 29.6             | 2.99    | 59.4             | 1.83    | 117              | 1.23    | 205              | 1.73    | 434              | 8.38    | 1260             | 2.77    | 2.35                           |
| 7                  | 1.313             | 1.2640         | 11.5             | 25.55   | 25.9             | 17.27   | 59.0             | 4.87    | 118              | 2.73    | 209              | 1.37    | 482              | 2.90    | 1397             | 2.62    | 2.52                           |
| 8                  | 1.422             | 1.2018         | 9.8              | 20.39   | 22.5             | 12.61   | 56.7             | 3.59    | 118              | 2.34    | 209              | 2.03    | 518              | 2.23    | 1522             | 3.15    | 2.66                           |
| a                  | 1.120             | 1.0480         | 14.3             | 17.5    | 29.3             | 6.0     | 62.1             | 2.7     | 121              | 2.5     | 214              | 1.9     | 463              | 1.9     | 1311             | 3.3     | 3.04                           |
| b                  | 1.102             | 1.3040         | 14.5             | 8.5     | 30.5             | 3.7     | 61.2             | 1.4     | 119              | 1.7     | 210              | 1.4     | 462              | 1.8     | 1272             | 3.6     | 2.44                           |
| c                  | 1.097             | 1.5640         | 15.1             | 12.0    | 29.1             | 5.6     | 60.9             | 2.7     | 118              | 1.9     | 209              | 2.0     | 464              | 2.0     | 1294             | 3.2     | 2.04                           |
| Dumbbells*         |                   |                | --               | --      | --               | --      | 63.0             | --      | 121              | --      | 212              | --      | 442              | --      | 1057             | --      | 2.70†                          |

\* Results from test of three dumbbells (see text)

† Initial value of strain rate; value near end of test is considerably less (see text)

Table IV-6 shows that stress values at various values of strain are independent, or sensibly independent, of ring dimensions for strain greater than 0.5. At small strains, the stress seems to decrease as the  $D_o/D_i$  ratio increases. Also, at strains of 5.0 and 6.5, the stress varies more than desirable, but this is probably a result of the rapid increase of stress with strain during the final portion of the test.

A few dumbbell specimens were tested to obtain data for comparison. These dumbbells had a width of 0.25 inch and a nominal gage length of

1.5 inches. (As mentioned in the preceding discussion, these specimens could not be broken during tests at 5.0 in./min crosshead speed.) Bench marks placed on the specimens were photographed during each test. From an analysis of the photographs, the initial strain rate was found to be about  $2.7 \text{ min}^{-1}$ , although during the last portion of the test the strain rate was markedly lower. Values of stress at strains of 0.5, 1.5, 3.0, 5.0, and 6.5 are given in Table IV-6. These values agree closely with those obtained from testing rings, except for the value at a strain of 6.5. The low value is probably caused by the low strain rate which existed during the final portion of the tests made on dumbbells.

### C. SUMMARY REMARKS

An investigation was made of the preparation of rings, a method for obtaining their dimensions, and various factors which might influence test results. It is concluded that reliable stress-strain data, except possibly at low values of strain, can be obtained by testing rings. Further, the testing of ring specimens is the only known method which can be readily employed to obtain data at a strain rate which remains constant throughout a test. Because under many test conditions small changes in strain rate effect a marked change in the test results, it is necessary in conducting basic studies to obtain stress-strain data under precisely known test conditions.

*APPENDIX V*

**TABULATION OF ULTIMATE TENSILE PROPERTIES  
OF GUM VULCANIZATES**

APPENDIX V

TABULATION OF ULTIMATE TENSILE PROPERTIES  
OF GUM VULCANIZATES

Ultimate tensile property data of the five gum vulcanizates discussed in the main portion of this report are contained in the following tables. It should be noted that values of  $\log \sigma_b$  and  $\log \epsilon_b$  are given but that values of  $\log \sigma_b, 273/T$  were used in the analyses presented in Section IV.

Table V-1  
 ULTIMATE TENSILE PROPERTIES FOR  
 BUTYL GUM VULCANIZATE (SULFUR)

| CROSSHEAD<br>SPEED<br>(in./min) | 100°C          |                  | 70°C           |                  | 40°C           |                  | 25°C           |                  | 10°C           |                  |
|---------------------------------|----------------|------------------|----------------|------------------|----------------|------------------|----------------|------------------|----------------|------------------|
|                                 | log $\sigma_b$ | log $\epsilon_b$ |
| 20                              | 2.050          | 0.186            | 2.149          | 0.301            | 2.297          | 0.508            | 2.408          | 0.554            | 3.188          | 0.783            |
| 12                              | 2.058          | 0.213            | 2.153          | 0.315            | 2.254          | 0.474            | 2.271          | 0.500            | 2.401          | 0.596            |
| 10                              | 2.016          | 0.156            | 2.189          | 0.350            | 2.190          | 0.398            | 2.219          | 0.429            | 3.354          | 0.809            |
| 5                               | 2.120          | 0.262            | 2.130          | 0.310            | 2.130          | 0.355            | 2.315          | 0.538            | 2.391          | 0.575            |
| 2                               | 2.091          | 0.250            | 2.087          | 0.278            | 2.117          | 0.328            | 2.198          | 0.421            | 2.423          | 0.568            |
| 1                               | 2.091          | 0.258            | 2.113          | 0.305            | 2.124          | 0.314            | 2.177          | 0.370            | 2.429          | 0.577            |
| 0.5                             | 2.027          | 0.149            | 2.073          | 0.220            | 2.082          | 0.270            | 2.120          | 0.365            | 2.373          | 0.558            |
| 0.2                             | 2.014          | 0.127            | 2.128          | 0.298            | 2.048          | 0.233            | --             | --               | 3.252          | 0.794            |
| 0.1                             | 2.094          | 0.233            | 2.094          | 0.252            | 2.146          | 0.345            | 2.175          | 0.424            | 3.137          | 0.770            |
| 0.02                            | 1.944          | 0.035            | 2.038          | 0.187            | 1.996          | 0.156            | 1.931          | 0.076            | 2.954          | 0.754            |

| CROSSHEAD<br>SPEED<br>(in./min) | -5°C           |                  | -20°C          |                  | -35°C          |                  | -45°C          |                  |
|---------------------------------|----------------|------------------|----------------|------------------|----------------|------------------|----------------|------------------|
|                                 | log $\sigma_b$ | log $\epsilon_b$ |
| 20                              | 2.924          | 0.736            | 3.102          | 0.761            | 3.513          | 0.880            | 3.563          | 0.767            |
| 12                              | 3.460          | 0.812            | 3.074          | 0.771            | 3.356          | 0.786            | 3.468          | 0.758            |
| 10                              | 3.286          | 0.788            | 2.840          | 0.743            | 3.460          | 0.792            | 3.595          | 0.794            |
| 5                               | 3.508          | 0.802            | 2.861          | 0.720            | 3.437          | 0.783            | 3.571          | 0.778            |
| 2                               | 3.567          | 0.819            | 3.619          | 0.849            | 3.625          | 0.802            | 3.639          | 0.785            |
| 1                               | 3.436          | 0.788            | 3.641          | 0.863            | 3.644          | 0.815            | 3.611          | 0.787            |
| 0.5                             | 3.510          | 0.808            | 3.546          | 0.843            | 3.188          | 0.753            | 3.556          | 0.784            |
| 0.2                             | 3.441          | 0.787            | 3.586          | 0.836            | 3.523          | 0.828            | 3.161          | 0.745            |
| 0.1                             | 3.355          | 0.790            | 3.514          | 0.800            | 3.592          | 0.825            | 3.429          | 0.767            |
| 0.02                            | 3.388          | 0.790            | 3.383          | 0.824            | 3.404          | 0.798            | 3.648          | 0.801            |

Table V-2  
 ULTIMATE TENSILE PROPERTIES FOR  
 BUTYL GUM VULCANIZATE (RESIN)

| CROSSHEAD<br>SPEED<br>(in./min) | 140°C          |                  | 100°C          |                  | 70°C           |                  | 40°C           |                  | 25°C           |                  | 10°C           |                  |
|---------------------------------|----------------|------------------|----------------|------------------|----------------|------------------|----------------|------------------|----------------|------------------|----------------|------------------|
|                                 | log $\sigma_b$ | log $\epsilon_b$ |
| 20                              | 2.031          | 0.175            | 2.051          | 0.304            | 2.167          | 0.408            | 2.383          | 0.548            | 2.462          | 0.611            | 2.533          | 0.628            |
| 12                              | 2.001          | 0.116            | 2.070          | 0.302            | 2.047          | 0.261            | 2.279          | 0.497            | 2.342          | 0.551            | 2.652          | 0.686            |
| 10                              | 1.944          | 0.051            | 2.025          | 0.229            | 2.116          | 0.357            | 2.303          | 0.519            | 2.397          | 0.623            | 2.623          | 0.678            |
| 5                               | 1.981          | 0.133            | 2.008          | 0.244            | 2.014          | 0.212            | 2.216          | 0.462            | 2.281          | 0.537            | 2.466          | 0.596            |
| 2                               | 1.940          | 0.065            | 1.957          | 0.169            | 1.922          | 0.055            | 2.169          | 0.397            | 2.194          | 0.381            | 2.309          | 0.496            |
| 1                               | 1.932          | 0.060            | 1.968          | 0.165            | 2.057          | 0.252            | 2.075          | 0.283            | 2.134          | 0.303            | 2.418          | 0.600            |
| 0.5                             | 1.913          | 0.009            | 1.907          | 0.075            | 2.010          | 0.217            | 2.108          | 0.295            | 2.060          | 0.276            | 2.301          | 0.526            |
| 0.2                             | 1.890          | 0.013            | 1.949          | 0.154            | 1.833          | -0.019           | 2.079          | 0.318            | --             | --               | 2.426          | 0.621            |
| 0.1                             | 1.875          | 0.040            | 1.898          | 0.106            | 2.013          | 0.250            | 2.075          | 0.322            | 2.045          | 0.270            | 2.215          | 0.456            |
| 0.02                            | 1.834          | -0.157           | 1.909          | 0.086            | 1.954          | 0.161            | 1.911          | 0.096            | 2.051          | 0.229            | 2.122          | 0.407            |

| CROSSHEAD<br>SPEED<br>(in./min) | -5°C           |                  | -20°C          |                  | -35°C          |                  | -45°C          |                  |
|---------------------------------|----------------|------------------|----------------|------------------|----------------|------------------|----------------|------------------|
|                                 | log $\sigma_b$ | log $\epsilon_b$ |
| 20                              | 2.939          | 0.726            | 2.964          | 0.679            | 3.381          | 0.690            | 3.405          | 0.678            |
| 12                              | 2.979          | 0.739            | 3.140          | 0.733            | 3.246          | 0.665            | 3.445          | 0.661            |
| 10                              | 3.016          | 0.756            | 3.220          | 0.756            | 3.248          | 0.691            | 3.447          | 0.665            |
| 5                               | 2.912          | 0.739            | 2.951          | 0.680            | 3.404          | 0.728            | 3.434          | 0.659            |
| 2                               | 2.938          | 0.738            | 2.876          | 0.679            | 3.302          | 0.714            | 3.371          | 0.662            |
| 1                               | 2.738          | 0.686            | 3.302          | 0.744            | 3.400          | 0.768            | 3.520          | 0.701            |
| 0.5                             | 2.702          | 0.695            | 3.023          | 0.713            | 3.160          | 0.734            | 3.531          | 0.696            |
| 0.2                             | 2.498          | 0.617            | 2.760          | 0.672            | 3.309          | 0.753            | 3.307          | 0.714            |
| 0.1                             | 2.358          | 0.536            | 2.955          | 0.701            | 3.283          | 0.752            | 3.481          | 0.740            |
| 0.02                            | --             | --               | 2.469          | 0.559            | 3.213          | 0.751            | 3.401          | 0.761            |

Table V-3

## ULTIMATE TENSILE PROPERTIES FOR VITON B GUM VULCANIZATE

| CROSSHEAD<br>SPEED<br>(in./min) | 180°C          |                  | 140°C          |                  | 100°C          |                  | 70°C           |                  | 40°C           |                  | 25°C           |                  |
|---------------------------------|----------------|------------------|----------------|------------------|----------------|------------------|----------------|------------------|----------------|------------------|----------------|------------------|
|                                 | log $\sigma_b$ | log $\epsilon_b$ |
| 20                              | 1.884          | -0.247           | 2.109          | 0.051            | 2.214          | 0.283            | 2.532          | 0.442            | 2.871          | 0.587            | 3.071          | 0.633            |
| 12                              | 1.881          | -0.258           | 2.141          | 0.103            | 2.274          | 0.339            | 2.510          | 0.429            | 2.920          | 0.612            | 3.084          | 0.637            |
| 10                              | 1.828          | -0.332           | 2.158          | 0.119            | 2.261          | 0.334            | 2.539          | 0.449            | 2.917          | 0.602            | 2.990          | 0.612            |
| 5                               | 1.948          | -0.157           | 2.086          | 0.137            | 2.242          | 0.280            | 2.378          | 0.374            | 2.783          | 0.552            | 3.051          | 0.637            |
| 2                               | 2.064          | -0.037           | 2.107          | 0.171            | 2.178          | 0.235            | 2.347          | 0.366            | 2.616          | 0.516            | 3.024          | 0.629            |
| 1                               | 2.113          | 0.021            | 2.051          | 0.119            | 2.030          | 0.058            | 2.275          | 0.325            | 2.463          | 0.468            | 2.897          | 0.595            |
| 0.5                             | 2.157          | 0.081            | 2.098          | 0.179            | 2.118          | 0.180            | 2.215          | 0.298            | 2.567          | 0.523            | 2.859          | 0.598            |
| 0.2                             | 2.138          | 0.046            | 2.045          | 0.106            | 2.040          | 0.078            | 2.229          | 0.308            | 2.399          | 0.462            | --             | --               |
| 0.1                             | 2.126          | 0.023            | 2.015          | 0.073            | 2.123          | 0.196            | 2.131          | 0.221            | 2.505          | 0.496            | 2.825          | 0.594            |
| 0.02                            | 1.825          | -0.345           | 2.043          | 0.027            | 1.980          | 0.019            | 2.102          | 0.214            | 2.334          | 0.358            | 2.587          | 0.529            |

| CROSSHEAD<br>SPEED<br>(in./min) | 10°C           |                  | -5°C           |                  | -20°C          |                  |
|---------------------------------|----------------|------------------|----------------|------------------|----------------|------------------|
|                                 | log $\sigma_b$ | log $\epsilon_b$ | log $\sigma_b$ | log $\epsilon_b$ | log $\sigma_b$ | log $\epsilon_b$ |
| 20                              | 3.205          | 0.594            | 3.364          | 0.502            | 3.564          | 0.452            |
| 12                              | 3.327          | 0.639            | 3.357          | 0.519            | 3.574          | 0.386            |
| 10                              | 3.307          | 0.632            | 3.338          | 0.516            | 3.648          | 0.450            |
| 5                               | 3.439          | 0.665            | 3.375          | 0.525            | 3.624          | 0.411            |
| 2                               | 3.389          | 0.660            | 3.399          | 0.523            | 3.605          | 0.417            |
| 1                               | 3.471          | 0.676            | 3.334          | 0.556            | 3.605          | 0.461            |
| 0.5                             | 3.043          | 0.576            | 3.447          | 0.564            | 3.489          | 0.497            |
| 0.2                             | 2.717          | 0.468            | 3.376          | 0.558            | 3.561          | 0.457            |
| 0.1                             | 2.870          | 0.523            | 3.368          | 0.621            | 3.572          | 0.471            |
| 0.02                            | 3.089          | 0.634            | 3.339          | 0.605            | 3.519          | 0.490            |

Table V-4  
ULTIMATE TENSILE PROPERTIES FOR SILICONE GUM VULCANIZATE

| CROSSHEAD SPEED<br>(in./min) | 140°C          |                  | 100°C          |                  | 70°C           |                  | 40°C           |                  | 25°C           |                  | 10°C           |                  |
|------------------------------|----------------|------------------|----------------|------------------|----------------|------------------|----------------|------------------|----------------|------------------|----------------|------------------|
|                              | log $\sigma_b$ | log $\epsilon_b$ |
| 20                           | 1.826          | 0.346            | 1.889          | 0.440            | 1.920          | 0.481            | 1.925          | 0.526            | 1.878          | 0.471            | 1.827          | 0.459            |
| 12                           | 1.748          | 0.264            | 1.877          | 0.436            | 1.796          | 0.390            | 1.842          | 0.462            | 1.900          | 0.486            | 1.862          | 0.487            |
| 10                           | 1.785          | 0.300            | 1.890          | 0.456            | 1.924          | 0.506            | 1.901          | 0.498            | 1.885          | 0.481            | 1.838          | 0.472            |
| 5                            | 1.789          | 0.329            | 1.770          | 0.335            | 1.810          | 0.427            | 1.819          | 0.426            | 1.810          | 0.436            | 1.849          | 0.493            |
| 2                            | 1.678          | 0.210            | 1.842          | 0.416            | 1.878          | 0.487            | 1.793          | 0.412            | 1.819          | 0.454            | 1.876          | 0.514            |
| 1                            | 1.735          | 0.301            | 1.718          | 0.309            | 1.827          | 0.435            | 1.839          | 0.472            | 1.796          | 0.439            | 1.793          | 0.446            |
| 0.5                          | 1.684          | 0.213            | 1.674          | 0.257            | 1.778          | 0.422            | 1.740          | 0.404            | 1.750          | 0.380            | 1.764          | 0.418            |
| 0.2                          | 1.646          | 0.180            | 1.694          | 0.272            | 1.720          | 0.366            | 1.742          | 0.389            | --             | --               | 1.785          | 0.428            |
| 0.1                          | 1.626          | 0.180            | 1.742          | 0.332            | 1.688          | 0.311            | 1.720          | 0.380            | 1.671          | 0.302            | 1.649          | 0.322            |
| 0.02                         | 1.472          | -0.033           | 1.692          | 0.300            | 1.683          | 0.285            | 1.607          | 0.264            | 1.680          | 0.344            | 1.631          | 0.375            |

| CROSSHEAD SPEED<br>(in./min) | -5°C           |                  | -20°C          |                  | -35°C          |                  | -45°C          |                  | -55°C          |                  | -65°C          |                  |
|------------------------------|----------------|------------------|----------------|------------------|----------------|------------------|----------------|------------------|----------------|------------------|----------------|------------------|
|                              | log $\sigma_b$ | log $\epsilon_b$ |
| 20                           | 1.883          | 0.494            | 1.842          | 0.464            | 1.958          | 0.562            | 2.056          | 0.598            | 2.683          | 0.752            | 3.023          | 0.037            |
| 12                           | 1.941          | 0.474            | 1.831          | 0.469            | 2.000          | 0.583            | 2.121          | 0.630            | 2.799          | 0.709            | 3.049          | 0.562            |
| 10                           | 1.809          | 0.451            | 1.616          | 0.290            | 1.924          | 0.533            | 2.158          | 0.646            | 2.828          | 0.036            | 2.990          | -0.088           |
| 5                            | 1.829          | 0.472            | 1.867          | 0.504            | 1.906          | 0.520            | 2.285          | 0.695            | 2.923          | 0.780            | 2.799          | -0.510           |
| 2                            | 1.844          | 0.486            | 1.907          | 0.546            | 1.928          | 0.549            | 2.777          | 0.776            | 2.886          | 0.720            | 2.972          | -0.233           |
| 1                            | 1.831          | 0.493            | 1.944          | 0.569            | 1.981          | 0.589            | 2.800          | 0.776            | 2.823          | 0.647            | 2.959          | -0.200           |
| 0.5                          | 1.715          | 0.408            | 1.901          | 0.540            | 1.762          | 0.446            | 2.932          | 0.802            | --             | --               | --             | --               |
| 0.2                          | 1.685          | 0.403            | 1.763          | 0.455            | 1.741          | 0.427            | 2.861          | 0.798            | 2.799          | 0.709            | 3.062          | -0.161           |
| 0.1                          | 1.658          | 0.377            | 1.782          | 0.478            | 1.824          | 0.493            | 2.872          | 0.822            | --             | --               | 3.021          | -0.267           |
| 0.02                         | 1.532          | 0.205            | 1.537          | 0.244            | 1.586          | 0.307            | 2.865          | 0.805            | --             | --               | --             | --               |

Table V-5

## ULTIMATE TENSILE PROPERTIES FOR NATURAL RUBBER GUM VULCANIZATE

| CROSSHEAD<br>SPEED<br>(in./min) | 100°C          |                  | 80°C           |                  | 60°C           |                  | 40°C           |                  | 25°C           |                  | 10°C           |                  |
|---------------------------------|----------------|------------------|----------------|------------------|----------------|------------------|----------------|------------------|----------------|------------------|----------------|------------------|
|                                 | log $\sigma_b$ | log $\epsilon_b$ |
| 20                              | 3.377          | 0.967            | 3.511          | 0.972            | 3.510          | 0.947            | 3.355          | 0.908            | 3.475          | 0.909            | 3.462          | 0.880            |
| 12                              | 3.200          | 0.945            | 3.461          | 0.960            | 3.469          | 0.948            |                |                  | 3.419          | 0.889            | 3.530          | 0.904            |
| 10                              | 3.286          | 0.953            | 3.430          | 0.961            | 3.412          | 0.941            | 3.433          | 0.908            | 3.567          | 0.917            | 3.543          | 0.900            |
| 5                               | 3.261          | 0.954            | 3.378          | 0.958            | 3.464          | 0.930            | 3.459          | 0.927            | 3.562          | 0.920            | 3.534          | 0.887            |
| 2                               | 2.977          | 0.906            | 3.241          | 0.921            | 3.409          | 0.933            | 3.342          | 0.906            | 3.437          | 0.894            | 3.414          | 0.877            |
| 1                               | 2.890          | 0.868            | 3.328          | 0.937            | 3.422          | 0.930            | 3.405          | 0.919            | 3.493          | 0.913            | 3.472          | 0.885            |
| 0.5                             | 2.926          | 0.899            | 3.242          | 0.925            | 3.375          | 0.925            | 3.278          | 0.880            | 3.428          | 0.898            | 3.490          | 0.877            |
| 0.2                             | 2.730          | 0.822            | 3.224          | 0.934            | 3.351          | 0.927            | 3.372          | 0.896            | 3.372          | 0.898            | 3.342          | 0.837            |
| 0.1                             | 2.681          | 0.791            | 3.173          | 0.916            | 3.263          | 0.904            | 3.277          | 0.876            | 3.337          | 0.880            | 3.296          | 0.845            |
| 0.02                            | 2.302          | 0.577            | 2.911          | 0.871            | 3.148          | 0.899            | 3.120          | 0.853            | 3.171          | 0.850            | 3.199          | 0.813            |

| CROSSHEAD<br>SPEED<br>(in./min) | -5°C           |                  | -20°C          |                  | -35°C          |                  | -45°C          |                  | -55°C          |                  |
|---------------------------------|----------------|------------------|----------------|------------------|----------------|------------------|----------------|------------------|----------------|------------------|
|                                 | log $\sigma_b$ | log $\epsilon_b$ |
| 20                              | 3.332          | 0.816            | 3.545          | 0.867            | 3.545          | 0.869            | 3.601          | 0.865            |                |                  |
| 12                              |                |                  | 3.451          | 0.837            | 3.512          | 0.838            |                |                  |                |                  |
| 10                              | 3.549          | 0.896            | 3.559          | 0.870            | 3.551          | 0.859            | 3.555          | 0.859            | 3.606          | 0.781            |
| 5                               | 3.550          | 0.884            | 3.588          | 0.879            | 3.554          | 0.851            | 3.511          | 0.865            | 3.663          | 0.768            |
| 2                               | 3.497          | 0.883            | 3.575          | 0.865            | 3.633          | 0.863            | 3.695          | 0.874            | 3.748          | 0.791            |
| 1                               | 3.481          | 0.868            | 3.615          | 0.863            | 3.566          | 0.848            | 3.629          | 0.873            | 3.638          | 0.820            |
| 0.5                             | 3.494          | 0.858            | 3.589          | 0.859            | 3.576          | 0.850            | 3.451          | 0.827            | 3.721          | 0.846            |
| 0.2                             | 3.440          | 0.866            | 3.581          | 0.866            |                |                  | 3.317          | 0.790            | 3.492          | 0.822            |
| 0.1                             | 3.450          | 0.841            | 3.587          | 0.851            |                |                  | 3.402          | 0.805            | 3.564          | 0.832            |
| 0.02                            | 3.291          | 0.808            | 3.432          | 0.804            |                |                  | 3.517          | 0.829            | 3.364          | 0.810            |

## REFERENCES

1. A. Nadai, *Theory of Flow and Fracture of Solids*, Vol. I, Second Edition, McGraw-Hill Book Co., Inc., New York, 1950.
2. F. Schwarzl and A. J. Staverman, "Bruchspannung und Festigkeit von Hochpolymeren," in *Die Physik Der Hochpolymeren*, Vol. IV, (Chapter III), edited by H. A. Stuart. Springer, Berlin, 1956.
3. M. L. Williams, P. J. Blatz, and R. A. Schapery, *Fundamental Studies Relating to Systems Analysis of Solid Propellants*, Final Report—Galcit 101, February 1961. Guggenheim Aeronautical Laboratory, California Institute of Technology, Pasadena, California.
4. A. V. Tobolsky, *Properties and Structure of Polymers*, John Wiley and Sons, Inc., 1960.
5. M. L. Williams, R. F. Landel, and J. D. Ferry. *J. Am. Chem. Soc.* **77**, 3701 (1955). See also, J. D. Ferry, *Viscoelastic Properties of Polymers*. John Wiley and Sons, Inc., 1961.
6. T. L. Smith, *J. Polymer Sci.* **32**, 99 (1958).
7. T. L. Smith, *SPE JOURNAL*, Vol. 16, No. 11, p. 1, 1960.
8. T. L. Smith and A. B. Magnusson, *J. Polymer Sci.* **42**, 391 (1960); *J. Appl. Polymer Sci.* **5**, 218 (1961).
9. G. Fromandi, R. Ecker, and W. Heidemann, *Proceedings International Rubber Conference*, November 8-13, 1959, pp. 177-189. Papers preprinted for the Conference by the American Chemical Society.
10. R. F. Landel and T. L. Smith, *ARS Journal* **31**, 599 (1961).
11. T. L. Smith, preprint of paper given before the Division of Organic Coatings and Plastic Chemistry at the September 1961 Meeting of the American Chemical Society, Vol. 21, No. 2, pp. 168-183.
12. V. E. Gul, *Rubber Chem. and Tech.* **34**, 101 (1961). (Article translated from Russian.)
13. F. Bueche, *Rubber Chem. and Tech.* **32**, 1269 (1959).
14. A. M. Bueche, *J. Polymer Sci.* **19**, 275 (1956).
15. G. R. Taylor and S. R. Darin, *J. Polymer Sci.* **17**, 511 (1955).
16. F. Bueche, *J. Polymer Sci.* **24**, 189 (1957); **33**, 259 (1958).
17. L. M. Epstein and R. P. Smith, *Trans. Soc. Rheology* **2**, 219 (1958).
18. F. Bueche, *J. Appl. Phys.* **26**, 1133 (1955).
19. For a brief discussion and pertinent references, see A. V. Tobolsky, *Properties and Structure of Polymers*, John Wiley and Sons, Inc., 1960, pp. 260-262.
20. T. L. Smith, presented at the Annual Meeting of the Society of Rheology, Madison, Wisconsin, 1961. To be published in *Trans. Soc. Rheology*, Vol. VI, 1962.
21. E. Guth, P. E. Wack, and R. L. Anthony, *J. Appl. Phys.* **17**, 347 (1946).
22. A. V. Tobolsky and R. D. Andrews, *J. Chem. Phys.* **13**, 3 (1945); R. D. Andrews, N. Hofman-Bang, and A. V. Tobolsky, *J. Polymer Sci.* **3**, 669 (1948); also see, A. V. Tobolsky, *Properties and Structure of Polymers*, John Wiley and Sons, Inc., 1960.
23. T. Alfrey, Jr., *Mechanical Behavior of High Polymers*, Interscience Publishers, New York, 1948.
24. T. L. Smith, *J. Polymer Sci.* **20**, 89 (1956).
25. T. L. Smith, *J. Polymer Sci.* **32**, 99 (1958).

## REFERENCES

26. A. Ciferri and P. J. Flory, *J. Appl. Phys.* **30**, 1498 (1959).
27. L. A. Wood and F. L. Roth, *J. Appl. Phys.* **15**, 781 (1944).
28. P. J. Flory, C. A. J. Hoeve, and A. Ciferri, *J. Polymer Sci.* **34**, 337 (1959).
29. A. Ciferri, C. A. J. Hoeve, and P. J. Flory, *J. Am. Chem. Soc.* **83**, 1015 (1961).
30. T. L. Smith and P. J. Stedry, *J. Appl. Phys.* **31**, 1892 (1960).
31. J. D. Ferry, *Viscoelastic Properties of Polymers*, John Wiley and Sons, Inc., 1961.
32. C. E. Weir, W. H. Leser, and L. A. Wood, *J. Research National Bureau of Standards* **44**, 367 (1950).
33. D. J. Plazek, W. Dannhauser, and J. D. Ferry, *J. Colloid Sci.* **16**, 101 (1961).
34. S. M. Ohlberg, L. E. Alexander, and E. L. Warrick, *J. Polymer Sci.* **27**, 1 (1958).
35. E. L. Warrick, *J. Polymer Sci.* **27**, 19 (1958).
36. K. E. Polmanteer and M. J. Hunter, *J. Applied Polymer Sci.* **1**, 3 (1959).
37. C. M. Huggins, L. E. St. Pierre, and A. M. Bueche, *J. Phys. Chem.* **64**, 1304 (1960).
38. T. L. Smith, J. R. Smith, and H. J. Sang, *Viscoelastic Properties of Solid Propellants and Propellant Binders*, Quarterly Technical Summary Report No. 1, October 30, 1961. Prepared for Bureau of Naval Weapons on Contract No. NOW 61-1057-d.
39. T. L. Smith and J. R. Smith, *Viscoelastic Properties of Solid Propellants and Propellant Binders*, Quarterly Technical Summary Report No. 2, January 30, 1962. Prepared for Bureau of Naval Weapons on Contract No. NOW-61-1057-d.
40. N. Bekkedahl, *J. Research National Bureau of Standards*, **13**, 411 (1934).
41. A. R. Payne, "Temperature Frequency Relationships of Dielectric and Mechanical Properties of Polymers," *The Rheology of Elastomers*, edited by P. Mason and N. Wookey, Pergamon Press, New York, 1958.
42. N. Bekkedahl and L. A. Wood, *Ing. Eng. Chem.* **33**, 381 (1941).
43. T. L. Smith, *Measurement and Analysis of Small Deformation and Ultimate Tensile Properties of Amorphous Elastomers*, Application Series PC-5, Instron Engineering Corp., Canton, Massachusetts.

## ASD DISTRIBUTION LIST

|                             |                               |
|-----------------------------|-------------------------------|
| MCLRCA (3 Cys)              | ASRRL                         |
| ASRMC                       | ASRCNL (3 Cys)                |
| ASRMF                       | ASRCNP (3 Cys)                |
| ASRMG                       | ASRCNE (25 Cys)               |
| ASZDBP (Mr. Graham) (3 Cys) | ASRC (Dr. Lovelace)           |
| ASRNR                       | ASRCN                         |
| ASAPR                       | ASRCNC                        |
| ASAP                        | ASAPTT (Mr. Thomas)           |
| ASRD                        | ASRCFM-2 (Mrs. Ragen) (2 Cys) |
| ASRNE                       | ASEP                          |
| ASNE                        | ASNY                          |
| ASNV                        | ASNG                          |
| ASNL                        | ASNR                          |
| ASND                        | ASNN                          |
| ASNP                        | ASNC                          |
| ASNS                        | ASNX                          |
| ASRE                        | ASRO                          |
| ASRS                        | ASRC                          |
| ASRN                        | ASRM                          |
| MRO                         | ASO                           |
| AST                         | ASZ                           |
| ASN XO (M. G. Toll)         |                               |

|                                                                                                                                                                                                                                                                                                                                                                                                                                                                                                                                                                                                                                                                                                                                                                                                                                                                                                                                                                                                                                |                                                                                                                                                                                                                                                                                                                                                                                                                                                              |                                                                                                                                                                                                                                                                                                                                                                                                                                                                                                                                                                                                                                                                                                                                                                                                                                                                                                                                                                                                                                |                                                                                                                                                                                                                                                                                                                                                                                                                                                              |
|--------------------------------------------------------------------------------------------------------------------------------------------------------------------------------------------------------------------------------------------------------------------------------------------------------------------------------------------------------------------------------------------------------------------------------------------------------------------------------------------------------------------------------------------------------------------------------------------------------------------------------------------------------------------------------------------------------------------------------------------------------------------------------------------------------------------------------------------------------------------------------------------------------------------------------------------------------------------------------------------------------------------------------|--------------------------------------------------------------------------------------------------------------------------------------------------------------------------------------------------------------------------------------------------------------------------------------------------------------------------------------------------------------------------------------------------------------------------------------------------------------|--------------------------------------------------------------------------------------------------------------------------------------------------------------------------------------------------------------------------------------------------------------------------------------------------------------------------------------------------------------------------------------------------------------------------------------------------------------------------------------------------------------------------------------------------------------------------------------------------------------------------------------------------------------------------------------------------------------------------------------------------------------------------------------------------------------------------------------------------------------------------------------------------------------------------------------------------------------------------------------------------------------------------------|--------------------------------------------------------------------------------------------------------------------------------------------------------------------------------------------------------------------------------------------------------------------------------------------------------------------------------------------------------------------------------------------------------------------------------------------------------------|
| <p>Aeronautical Systems Division, Dir./Materials and Processes, Nonmetallic Materials Lab, Wright-Patterson AFB, Ohio<br/> <b>Rep Nr ASD-TDR-62-572. MECHANISMS OF REVERSIBLE AND IRREVERSIBLE LOSS OF MECHANICAL PROPERTIES OF ELASTOMERIC VULCANIZATES WHICH OCCUR AT ELEVATED TEMPERATURES.</b> Tech. Documentary Report, June 1962, 181 p incl illus, tables, and 43 refs.</p> <p>Unclassified Report</p> <p>Strength characteristics of five elastomeric gum vulcanizates were investigated over a wide range of evaluation conditions. Results from continuous and intermittent stress-relaxation evaluations made between 100 and 200°C showed that the thermal stabilities of the vulcanizates decrease in the following order: hydrofluorocarbon, resin-cured butyl, silicone, sulfur-cured butyl, and natural rubber. Tensile properties of each vulcanizate in the absence of thermal degradation were determined with an Instron tester at about 10 strain rates and 10 temperatures. Except for</p> <p>(over)</p> | <p>UNCLASSIFIED</p> <ol style="list-style-type: none"> <li>1. Natural rubber</li> <li>2. Synthetic rubber</li> <li>3. Mechanical properties</li> </ol> <ol style="list-style-type: none"> <li>I. AFSC Project 7342, Task 734202</li> <li>II. Contract AF 33(616)-8298</li> <li>III. Stanford Research Institute, Menlo Park, California</li> <li>IV. T. L. Smith</li> <li>V. Not aval fr OTS</li> <li>VI. In ASTIA collection</li> </ol> <p>UNCLASSIFIED</p> | <p>Aeronautical Systems Division, Dir./Materials and Processes, Nonmetallic Materials Lab, Wright-Patterson AFB, Ohio<br/> <b>Rep Nr ASD-TDR-62-572. MECHANISMS OF REVERSIBLE AND IRREVERSIBLE LOSS OF MECHANICAL PROPERTIES OF ELASTOMERIC VULCANIZATES WHICH OCCUR AT ELEVATED TEMPERATURES.</b> Tech. Documentary Report, June 1962, 181 p incl illus, tables, and 43 refs.</p> <p>Unclassified Report</p> <p>Strength characteristics of five elastomeric gum vulcanizates were investigated over a wide range of evaluation conditions. Results from continuous and intermittent stress-relaxation evaluations made between 100 and 200°C showed that the thermal stabilities of the vulcanizates decrease in the following order: hydrofluorocarbon, resin-cured butyl, silicone, sulfur-cured butyl, and natural rubber. Tensile properties of each vulcanizate in the absence of thermal degradation were determined with an Instron tester at about 10 strain rates and 10 temperatures. Except for</p> <p>(over)</p> | <p>UNCLASSIFIED</p> <ol style="list-style-type: none"> <li>1. Natural rubber</li> <li>2. Synthetic rubber</li> <li>3. Mechanical properties</li> </ol> <ol style="list-style-type: none"> <li>I. AFSC Project 7342, Task 734202</li> <li>II. Contract AF 33(616)-8298</li> <li>III. Stanford Research Institute, Menlo Park, California</li> <li>IV. T. L. Smith</li> <li>V. Not aval fr OTS</li> <li>VI. In ASTIA collection</li> </ol> <p>UNCLASSIFIED</p> |
| <p>Aeronautical Systems Division, Dir./Materials and Processes, Nonmetallic Materials Lab, Wright-Patterson AFB, Ohio<br/> <b>Rep Nr ASD-TDR-62-572. MECHANISMS OF REVERSIBLE AND IRREVERSIBLE LOSS OF MECHANICAL PROPERTIES OF ELASTOMERIC VULCANIZATES WHICH OCCUR AT ELEVATED TEMPERATURES.</b> Tech. Documentary Report, June 1962, 181 p incl illus, tables, and 43 refs.</p> <p>Unclassified Report</p> <p>Strength characteristics of five elastomeric gum vulcanizates were investigated over a wide range of evaluation conditions. Results from continuous and intermittent stress-relaxation evaluations made between 100 and 200°C showed that the thermal stabilities of the vulcanizates decrease in the following order: hydrofluorocarbon, resin-cured butyl, silicone, sulfur-cured butyl, and natural rubber. Tensile properties of each vulcanizate in the absence of thermal degradation were determined with an Instron tester at about 10 strain rates and 10 temperatures. Except for</p> <p>(over)</p> | <p>UNCLASSIFIED</p> <ol style="list-style-type: none"> <li>1. Natural rubber</li> <li>2. Synthetic rubber</li> <li>3. Mechanical properties</li> </ol> <ol style="list-style-type: none"> <li>I. AFSC Project 7342, Task 734202</li> <li>II. Contract AF 33(616)-8298</li> <li>III. Stanford Research Institute, Menlo Park, California</li> <li>IV. T. L. Smith</li> <li>V. Not aval fr OTS</li> <li>VI. In ASTIA collection</li> </ol> <p>UNCLASSIFIED</p> | <p>Aeronautical Systems Division, Dir./Materials and Processes, Nonmetallic Materials Lab, Wright-Patterson AFB, Ohio<br/> <b>Rep Nr ASD-TDR-62-572. MECHANISMS OF REVERSIBLE AND IRREVERSIBLE LOSS OF MECHANICAL PROPERTIES OF ELASTOMERIC VULCANIZATES WHICH OCCUR AT ELEVATED TEMPERATURES.</b> Tech. Documentary Report, June 1962, 181 p incl illus, tables, and 43 refs.</p> <p>Unclassified Report</p> <p>Strength characteristics of five elastomeric gum vulcanizates were investigated over a wide range of evaluation conditions. Results from continuous and intermittent stress-relaxation evaluations made between 100 and 200°C showed that the thermal stabilities of the vulcanizates decrease in the following order: hydrofluorocarbon, resin-cured butyl, silicone, sulfur-cured butyl, and natural rubber. Tensile properties of each vulcanizate in the absence of thermal degradation were determined with an Instron tester at about 10 strain rates and 10 temperatures. Except for</p> <p>(over)</p> | <p>UNCLASSIFIED</p> <ol style="list-style-type: none"> <li>1. Natural rubber</li> <li>2. Synthetic rubber</li> <li>3. Mechanical properties</li> </ol> <ol style="list-style-type: none"> <li>I. AFSC Project 7342, Task 734202</li> <li>II. Contract AF 33(616)-8298</li> <li>III. Stanford Research Institute, Menlo Park, California</li> <li>IV. T. L. Smith</li> <li>V. Not aval fr OTS</li> <li>VI. In ASTIA collection</li> </ol> <p>UNCLASSIFIED</p> |

|                                                                                                                                                                                                                                                                                                                                                                                                                                                                                                                                                                                                      |                     |                                                                                                                                                                                                                                                                                                                                                                                                                                                                                                                                                                                                                                              |
|------------------------------------------------------------------------------------------------------------------------------------------------------------------------------------------------------------------------------------------------------------------------------------------------------------------------------------------------------------------------------------------------------------------------------------------------------------------------------------------------------------------------------------------------------------------------------------------------------|---------------------|----------------------------------------------------------------------------------------------------------------------------------------------------------------------------------------------------------------------------------------------------------------------------------------------------------------------------------------------------------------------------------------------------------------------------------------------------------------------------------------------------------------------------------------------------------------------------------------------------------------------------------------------|
| <p>natural rubber, the ultimate tensile properties of each vulcanizate could be characterized by a time- and temperature-independent failure envelope which results from a plot of <math>\log \sigma_b 273/T</math> vs <math>\log \epsilon_b</math>, where <math>\sigma_b</math> is the tensile strength and <math>\epsilon_b</math> is the ultimate strain. Envelopes for the different vulcanizates are essentially identical in shape; their relative displacements result from difference in degree of crosslinking and probably from differences in their chemical and physical structures.</p> | <p>UNCLASSIFIED</p> | <p>UNCLASSIFIED</p> <p>natural rubber, the ultimate tensile properties of each vulcanizate could be characterized by a time- and temperature-independent failure envelope which results from a plot of <math>\log \sigma_b 273/T</math> vs <math>\log \epsilon_b</math>, where <math>\sigma_b</math> is the tensile strength and <math>\epsilon_b</math> is the ultimate strain. Envelopes for the different vulcanizates are essentially identical in shape; their relative displacements result from difference in degree of crosslinking and probably from differences in their chemical and physical structures.</p> <p>UNCLASSIFIED</p> |
| <p>natural rubber, the ultimate tensile properties of each vulcanizate could be characterized by a time- and temperature-independent failure envelope which results from a plot of <math>\log \sigma_b 273/T</math> vs <math>\log \epsilon_b</math>, where <math>\sigma_b</math> is the tensile strength and <math>\epsilon_b</math> is the ultimate strain. Envelopes for the different vulcanizates are essentially identical in shape; their relative displacements result from difference in degree of crosslinking and probably from differences in their chemical and physical structures.</p> | <p>UNCLASSIFIED</p> | <p>UNCLASSIFIED</p> <p>natural rubber, the ultimate tensile properties of each vulcanizate could be characterized by a time- and temperature-independent failure envelope which results from a plot of <math>\log \sigma_b 273/T</math> vs <math>\log \epsilon_b</math>, where <math>\sigma_b</math> is the tensile strength and <math>\epsilon_b</math> is the ultimate strain. Envelopes for the different vulcanizates are essentially identical in shape; their relative displacements result from difference in degree of crosslinking and probably from differences in their chemical and physical structures.</p> <p>UNCLASSIFIED</p> |